Universidad Politécnica de Cartagena

Departamento de Ingeniería Térmica y de Fluidos

CHARACTERISATION OF HEAT TRANSFER AND PRESSURE DROP IN CONDENSATION PROCESSES WITHIN MINI-CHANNEL TUBES WITH LAST GENERATION OF REFRIGERANT FLUIDS

Tesis Doctoral realizada por:

D. Alejandro López Belchí

Bajo la dirección de:

Dr. José Ramón García Cascales

Dr. Francisco Vera García

2014

DOCTORAL THESIS

with European Mention

CHARACTERISATION OF HEAT TRANSFER AND PRESSURE DROP IN CONDENSATION PROCESSES WITHIN MINI-CHANNEL TUBES WITH LAST GENERATION OF REFRIGERANT FLUIDS

Defended on October 28th, 2014 by:

Eng. Alejandro López Belchí

Under the supervision of:

Dr. José Ramón García Cascales

Dr. Francisco Vera García

DEFENSE COMMITTEE:

CHAIRMAN:	**Dr. José Gonzálvez Maciá**	*Universidad Politécnica de Valencia*
SECRETARY:	**Dr. Fernando Illán Gómez**	*Universidad Politécnica de Cartagena*
MEMBER:	**Dr. Alfonso William Mauro**	*Università degli Studi di Napoli Federico II*

ALTERNATE MEMBERS

Dr. José Miguel Corberán Salvador	*Universidad Politécnica de Valencia*
Dr. Juan Pedro Solano Fernández	*Universidad Politécnica de Cartagena*
Dr. Claudio Zilio	*Università degli Studi di Padova*

DISSERTATION READERS

Dr. Jocelyn Bonjour	*Centre d'Energétique et de Thermique de Lyon*
Dr. Stephan Colasson	*Commissariat à l'Énergie Atomique et aux Énergies Alternatives*

Universidad Politécnica de Cartagena

DT-16

CONFORMIDAD DE SOLICITUD DEAUTORIZACIÓN DE DEPÓSITO DE TESIS DOCTORAL POR EL/LA DIRECTOR/A DE LA TESIS

D. José Ramón García Cascales y D. Francisco Vera García, Directores de la Tesis doctoral "Characterization of heat transfer and pressure drop in condensation processes within mini-channel tubes with last generation of refrigerant fluids"

INFORMA:

Que la referida Tesis Doctoral, ha sido realizada por D. Alejandro López Belchí, dentro del programa de doctorado Energías Renovables, dando mi conformidad para que sea presentada ante la Comisión de Doctorado para ser autorizado su depósito.

La rama de conocimiento en la que esta tesis ha sido desarrollada es:

- ☐ Ciencias
- ☐ Ciencias Sociales y Jurídicas
- ✓ Ingeniería y Arquitectura

En Cartagena, a 5 de junio de 2014

LOS DIRECTORES DE LA TESIS

Fdo.: JOSÉ R. GARCÍA CASCALES

Fdo.: Francisco Vera García

COMISIÓN DE DOCTORADO

Universidad Politécnica de Cartagena

DT-17

CONFORMIDAD DE DEPÓSITO DE TESIS DOCTORAL POR LA COMISIÓN ACADÉMICA DEL PROGRAMA

D. Antonio Urbina Yeregui, Presidente/a de la Comisión Académica del Programa en Energías Renovables.

INFORMA:

Que la Tesis Doctoral titulada, "Characterisation of heat transfer and pressure drop in condensation processes within mini-channel tubes with last generation of refrigerant fluids", ha sido realizada, dentro del mencionado programa de doctorado, por D. Alejandro López Belchí, bajo la dirección y supervisión del Dr. José Ramón García Cascales y Dr. Francisco Vera García.

En reunión de la Comisión Académica de fecha 31 / 03 / 2014, visto que en la misma se acreditan los indicios de calidad correspondientes y la autorización del Director de la misma, se acordó dar la conformidad, con la finalidad de que sea autorizado su depósito por la Comisión de Doctorado.

La Rama de conocimiento por la que esta tesis ha sido desarrollada es:

- ☐ Ciencias
- ☐ Ciencias Sociales y Jurídicas
- ✓ Ingeniería y Arquitectura

En Cartagena, a 14 de 04 de 2014

EL PRESIDENTE DE LA COMISIÓN ACADÉMICA DEL PROGRAMA

Fdo:

COMISIÓN DE DOCTORADO

Abstract

Heat exchanger developments are driven by energetic efficiency increase and emission reduction. To reach the standards new system are required based on mini-channels.

Mini-channels can be described as tubes with one or more ports extruded in aluminium with hydraulic diameter are in the range of 0.2 to 3 mm. Its use in refrigeration systems for some years ago is a reality thanks to the human ability to made micro-scale systems. Some heat exchanger enterprises have some models developed specially for their use in automotive sector, cooling sector, and industrial refrigeration without having a deep knowledge of how these reduced geometries affect the most important parameters such as pressure drop and the heat transfer coefficient.

To respond to this objective, an exhaustive literature review of the last two decades has been performed to determinate the state of the research. Between all the publications, several models have been selected to check the predicting capacities of them because most of them were developed for single port mini-channel tubes. Experimental measurements of heat transfer coefficient and frictional pressure drop were recorded in an experimental installation built on purpose at the Technical University of Cartagena. Multiple variables are recorded in this installation in order to calculate local heat transfer coefficient in two-phase condensing flow within mini-channels.

Both pressure drop and heat transfer coefficient experimental measurements are compared to the previously mentioned models. Most of them capture the trend correctly but others fail predicting experimental data. These differences can be explained by the experimental parameters considered during the models development. In some cases the models found in the literature were developed specific conditions, consequently their predicting capacities are restricted.

As main contributions, this thesis provides new modelling tools for mini-channels condensing pressure drop and heat transfer coefficient calculation. A comparison of a recently developed refrigerant is also given in this thesis.

Acknowledgements

I wish these lines serve to express my deepest and most sincere thanks to all those who have collaborated with their help in the realisation of this work, especially Dr. José Ramón García Cascales and Dr. Francisco Vera García directors of this research, guidance, monitoring and supervision of it, but mostly for motivation, support and confidence received over the years.

I cannot overlook the great work done by Dr. Fernando Illán Gómez over the years of completion of this thesis, his experience and advices have been key to completion.

Dr. Antonio Villarejo Mañas, Dr. José Manuel Cano Izquierdo, Dr. Julio José Ibarrola Lacalle and Dr. Miguel Almonacid Kroeger deserve special recognition for their interest in my work and suggestions received in the early stages of research.

I would also like to acknowledge the help received by Mr. Juan Antonio Albaladejo López, a colleague and friend, for his tireless hours spent in making the necessary components.

I cannot go without thanking Dr. Stephan Colasson from CEA – "Commissariat à l'Énergie Atomique et aux Énergies Alternatives" (France) and Dr. Jocelyn Bonjour from CETHIL – "Centre d'Energétique et de Thermique de Lyon" (France) for their reports of my thesis to opt to the Doctor Degree with European Mention.

Finally, very special thanks are due to understanding, patience and encouragement received especially by my family and friends.

To everyone, thank you very much.

A mis padres y hermanos

INDEX

	Index	**i**
	Caption of tables	**v**
	Caption of figures	**vi**
	Nomenclature	**ix**
	Chapter 1: Introduction	**1**
1.1	Status	1
1.2	Objective	1
1.3	Methodology	2
1.4	PhD. Thesis Schema	4
	Chapter 2: State of the art	**7**
2.1	Introduction	7
2.2	State of the art	10
2.2.1	Heat transfer coefficient	10
2.2.2	Pressure drop	22
2.3	Conclusions	46
	Chapter 3: Models review	**59**
3.1	Void fraction	59
3.2	Two-phase flow pressure drop	60
3.2.1	Common channel correlations	60
3.2.1.1	Lockhart and Martinelli	60
3.2.1.2	Homogeneous model	61
3.2.1.3	Friedel	62
3.2.1.4	Müller-Steinhagen and Heck	62
3.2.2	Micro- and Mini-Channels	62
3.2.2.1	Mishima and Hibiki	63
3.2.2.2	Zhang and Webb	63
3.2.2.3	Garimella et al.	63
3.2.2.4	Cavallini et al	65
3.2.2.5	Cavallini et al.	66
3.2.2.6	Sun and Mishima	67
3.2.2.7	Kim and Mudawar	67
3.3	Heat transfer coefficient "HTC"	68
3.3.1	Common channels correlations	68
3.3.1.1	Haraguchi et al.	69
3.3.1.2	Dobson and Chato	69
3.3.1.3	Akers and Rosson	69
3.3.2	Correlations for mini-channels	70
3.3.2.1	Webb et al.	70
3.3.2.2	Wang et al.	71
3.3.2.3	Koyama et al.	71
3.3.2.4	Cavallini et al.	72
3.3.2.5	Garimella et al.	73
3.3.2.6	Bandhauer et al.	75

3.4	Conclusions	76
	Chapter 4: Experimental Installation description	**81**
4.1	Experimental installation description	81
4.2	Control system description	83
4.3	Test section	83
4.4	Measurement instruments and actuators	84
4.4.1	Temperature sensors	84
4.4.2	Mass flow meters	85
4.4.3	Electromagnetic volumetric flow meter	85
4.4.4	Pressure transmitters	85
4.4.5	Actuators	85
4.5	Acquisition system	85
4.6	Instrument calibration	86
4.7	Working fluids	86
4.8	Fluids chemical composition	87
4.9	Testing conditions	87
4.10	Conclusions	87
	Chapter 5: Experimental data analysis	**89**
5.1	Single-phase Nusselt number	89
5.2	Local two-phase heat transfer coefficient	93
5.3	Frictional pressure drop evaluation	95
5.3.1	Pressure drop in tube expansion and contractions	95
5.3.1.1	Single-phase flow	96
5.3.1.2	Two-phase flow	98
5.4	Calculation procedure	100
5.5	Uncertainty analysis	101
5.6	Conclusions	103
	Chapter 6: Experimental results	**105**
6.1	Two-phase flow heat transfer coefficient	105
6.1.1	HTC measurements of R134a	105
6.1.2	HTC measurements of R1234yf	106
6.1.3	HTC measurements of R290	107
6.1.4	HTC Measurements of R32	108
6.1.5	HTC Fluid behaviour discussion	109
6.2	Two-phase frictional pressure gradient	111
6.2.1	Pressure drop measurements of R134a	111
6.2.2	Pressure drop measurements of R1234yf	112
6.2.3	Pressure drop measurements of R290	112
6.2.4	Pressure drop measurements of R32	113
6.2.5	Pressure drop fluid comparison	114
6.3	Conclusions	117
	Chapter 7: Correlations comparison	**119**
7.1	Heat transfer coefficient	119
7.1.1	Models developed for macro-channels	119
7.1.1.1	Dobson and Chato	119
7.1.1.2	Haraguchi et al.	120

7.1.1.3	Akers et al.	121
7.1.2	Models developed for mini-channels	122
7.1.2.1	Koyama et al.	122
7.1.2.2	Webb et al.	123
7.1.2.3	Cavallini et al.	124
7.1.2.4	Wang et al.	125
7.1.2.5	Bandhauer et al.	126
7.2	Frictional pressure drop	129
7.2.1	Models developed for macro-channels	129
7.2.1.1	Homogeneous model	129
7.2.1.2	Friedel	130
7.2.1.3	Müller-Steinhagen and Heck	131
7.2.1.4	Souza and Pimenta	132
7.2.2	Models developed for mini-channels	133
7.2.2.1	Sun and Mushima	133
7.2.2.2	Zhang and Webb	134
7.2.2.3	Garimella et al.	135
7.2.2.4	Mishima and Hibiki	136
7.2.2.5	Cavallini et al	137
7.2.2.6	Kim and Mudawar	138
7.3	Conclusions	141
	Chapter 8: Experimental Correlation and Correction Factor	**143**
8.1	Two-phase flow heat transfer coefficient model adjustment	143
8.2	Two-phase frictional pressure gradient model development	145
8.3	Conclusions	148
	Chapter 9: Conclusions and Future Work	**149**
9.1	Conclusions	149
9.2	Future Work	152
	References	**155**

CAPTION OF TABLES

Table	Caption	Page
2.1	Transition geometries by some authors.	18
2.2	Heat transfer coefficient publications considered in this study.	19
2.3	Pressure drop publications considered in that study.	37
3.1	"C" values of Lokhart and Martinelli correlation.	61
3.2	Garimella et al. correlation coefficients.	64
3.3	Kim and Mudawar correlation coefficients.	68
4.1	Tube characteristics.	84
4.2	Measurements made with refrigerants	87
5.1	Summary of total uncertainty analysis for the experimental results.	102
6.1	Fluid properties at 40ºC.	110
7.1	MARD and MRD values for pressure drop prediction models.	128
7.2	MARD and MRD values for heat transfer coefficient prediction models.	140
8.1	HTC MARD and MRD values of HTC model adjustment.	145
8.2	HTC MARD and MRD values of frictional pressure drop model development.	148

CAPTION OF FIGURES

Figure	Caption	Page
1.1	Methodology block diagram	3
4.1	Experimental test rig.	82
4.2	Block diagram of programmed controllers.	83
4.3	Tested geometry, thermocouple location and water chase geometry.	84
4.4	Thermocouple location and tube lengths.	84
4.5	Installation Graphical User Interface.	86
5.1	Liquid Nusselt number of R134a.	91
5.2	Single-phase test local parameters obtained.	92
5.3	Water heat transfer coefficient profile at different refrigerant flow conditions.	93
5.4	Schematic view of local heat transfer coefficient calculation.	94
5.5	Expansion and contraction nomenclature	95
5.6	Expansion coefficient by Kays and London.	96
5.7	Contraction coefficients by Kays and London.	97
6.1	R134a HTC sorted by mass velocity at one saturation temperature.	106
6.2	R1234yf HTC sorted by mass velocity at two different saturation temperatures.	107
6.3	R290 HTC sorted by mass velocity at two different saturation temperatures.	108
6.4	R32 HTC sorted by mass velocity at two different saturation temperatures.	109
6.5	HTC comparison of R134a and R1234yf.	110
6.6	R134a frictional pressure gradient.	111
6.7	R1234yf frictional pressure gradient.	112
6.8	R290 frictional pressure gradient.	113
6.9	R32 frictional pressure gradient.	114
6.10	Frictional pressure gradient comparison at G = 810 kg $m^{-2}s^{-1}$.	115
6.11	Frictional pressure gradient comparison at G = 350 kg $m^{-2}s^{-1}$.	116
6.12	Frictional pressure gradient comparison at G = 350 kg $m^{-2}s^{-1}$.	116
6.13	Void fraction comparison	117
7.1	Dobson and Chato prediction.	120
7.2	Haraguchi et al. prediction	121
7.3	Akers et al. prediction	122
7.4	Koyama et al. prediction	123
7.5	Webb et al. prediction	123
7.6	Cavallini et al. prediction	124
7.7	Wang et al. prediction	125
7.8	Bandhauer et al. prediction	126
7.9	Homogeneous model prediction	130
7.10	Friedel model prediction	131

7.11	Müeller-Steinhagen and Heck model prediction	132
7.12	Souza and Pimenta model prediction	133
7.13	Sun and Mishima prediction	134
7.14	Zhang and Webb prediction	135
7.15	Garimella prediction	136
7.16	Mishima and Hibiki prediction.	137
7.17	Cavallini et al. (2009) prediction	138
7.18	Kim and Mudawar prediction.	138
8.1	Koyama et al. HTC model readjustment.	144
8.2	New frictional pressure drop model adjustment.	147

NOMENCLATURE

Acronyms

FC-72	Perfluorohexane
HTC	Heat transfer coefficient
MARD	Mean absolute relative deviation
MRD	Mean relative deviation
N_2	Nitrogen
ODP	Ozone depleting power
R11	Trichlorofluoromethane
R12	Dichlorofluoromethane
R22	Chlorodifluoromethane
R32	Difluoromethane
R113	1,1,2-trichloro-1,2,2-trifluoroethane
R123	2,2-dichloro-1,1,1-trifluoroethane
R125	Pentafluoroethane
R134a	1,1,1,2-tetrafluoroethane
R141b	1,1-dichloro-1-fluoroethane
R236ea	1,1,1,2,3,3-hexafluoropropane
R236fa	1,1,1,3,3,3-hexafluoropropane
R245fa	1,1,1,3,3-pentafluoropropane
R290	Propane
R404a	44% R125/4% R134a/52% R143a
R407C	23% R32/25% R125/52% R134a
R410A	50% R32/50% R125
R422D	65.1 % R125/ 31.5 % R134a/ 3.4% R600a
R600	Butane
R600a	Isobutane
R717 / NH_3	Ammonia
R744 / CO_2	Carbon dioxide
R1234yf	2,3,3,3-tetrafluoroprop-1-ene
R1234ze	trans-1,3,3,3-tetrafluoropropene
RAC	Refrigeration and Air Conditioning

Latin symbols

A	area	m^2
$Bo = \frac{\Delta\rho\ g\ L^2}{\sigma}$	Bond number	[-]
C	Chisholm parameter	[-]
C_c	vena contracta coefficient	[-]
C_p	specific heat	$J\ kg^{-1}\ K^{-1}$
D, d	diameter	mm

E	entrainment ratio	[-]
f	friction factor	[-]
$Fr = \frac{v}{c}$	Froude number	[-]
g	gravitational acceleration	m s^{-2}
G	mass velocity	kg $m^{-2}s^{-1}$
h	specific enthalpy	J kg^{-1}
j	superficial velocity	ms^{-1}
$La = \frac{\sigma \rho D}{\mu^2}$	Laplace number	[-]
$\dot{m}$	mass flow rate	kg s^{-1}
Nu	Nusselt number	[-]
p	pressure	Pa
$p_r = p/p_{crit}$	reduced pressure	[-]
$\dot{q}$	heat flux	W m^{-2}
$\dot{Q}$	heat transferred	W
Ra	roughness	mm
$Re = \frac{\rho v L}{\mu}$	Reynold number	[-]
$RR = \frac{2\ Ra}{D}$	relative roughness	[-]
t	thickness	m
T	temperature	K / ºC
u	velocity/uncertainty	m s^{-1}/[-]
$We = \frac{\rho v^2 L}{\sigma}$	Weber number	[-]
x	vapour quality	[-]
X	Martinelli parameter	[-]
z	length	m

Greek symbols

α	heat transfer coefficient	W $m^{-2}K^{-1}$
γ	area ratio	[-]
δ	liquid film thickness	M
ε	void fraction	[-]
λ	thermal conductivity	W $m^{-1}K^{-1}$
μ	dynamic viscosity	kg $m^{-1}s^{-1}$
σ	surface tension	N m^{-1}
ρ	density	kg m^{-3}
τ	shear stress	Pa
ϕ	multiplier	[-]
ψ	surface tension parameter	[-]
ω	kinematic viscosity	m^2s^{-1}

Subscripts and superscripts

Subscripts

acc	accessories
Al	aluminium
annul	annular
B	gravity driven
C	contraction / combined
convection	convection
crit	critical
E	expansion / expanded
eq	equivalent
evap	evaporator
F	forced
f	frictional
film	film
grav	gravitational
g	gas
gc	gas core
go	gas only
h	hydraulic
hom	homogeneous
in	inlet
inner	inner
j	index j
l	liquid
lo	liquid only
mom	momentum
out	outlet
ref	refrigerant
S	separated
strat	stratified
tp	two-phase
tran	transition
ts	test section
Tube	referred to test tube
w	water
wall	wall

Superscripts

+	non dimensional turbulent parameter
*	frictional parameter
$[Y]$	Evaluated at Y conditions

CHAPTER 1: Introduction

1.1. STATUS

Nowadays, micro and mini-channels are present in many applications ranging from different heat exchangers in process industry to automotive, electronics and domestic applications. Two-phase flow has been applied to a growing number of fields in recent years because of its higher energy efficiency in comparison with single-phase flow. Compactness is a synonym of charge reduction and this is very important in present day refrigeration systems and heat pumps because of the great contribution of HCFC and HFC refrigerants to the direct greenhouse effect. This reduction is also important for natural refrigerants such as hydrocarbons and ammonia for safety reasons [1].

One of the pioneers authors who studied the influence of reducing diameter in heat transfer coefficient were Kays and London [2]. From then on, the investigation on heat transfer in mini-channels has been one of the most researched topics in this field.

Condensers utilising mini/micro-channels are especially suited for applications demanding high heat dissipation in a limited volume as the more the tube diameter decreases, the more the ratio of area to volume increases, and the heat transfer increases.

These condensers maintain mostly annular or intermittent flow to take advantage of the large condensation heat transfer coefficients associated with these flow patterns. Decreasing channel diameter increases vapour velocity and the interfacial shear stress, which causes a thinning of the annular film and increases the condensation heat transfer coefficient. Unfortunately, while the heat transfer is empowered by reducing the tube diameter, a higher pressure drop is obtained, which may degrade the overall efficiency of the two-phase system. Therefore, the design of high performance mini-channel condensers requires accurate predictive tools for both pressure drop and condensation heat transfer coefficient.

1.2. OBJECTIVE

The main goal of this PhD thesis is to experimentally measure pressure drop and heat transfer coefficient in condensation processes inside mini-channel tubes with different refrigerants flowing inside to get a better knowledge of how heat transfer coefficient is affected by the design variables of commercial equipment such as saturation temperature, mass velocity, free flow area and tube diameter.

This investigation uses natural and new refrigerants in this reduced geometry kind of tubes and other non-ozone depleting refrigerants. There is few investigations working with these kinds of refrigerants and the use of mini-channels allows reducing equipment charge so it is an appealing combination.

Commercial software like IMST-Art or EVAP-COND, widely used for refrigerating systems, makes use of the available correlations in the literature in their calculations. So, accurate correlations must be developed to assist engineers in the designing process of industrial equipment.

1.3. METHODOLOGY

The main goal to achieve is to take accurate measurements of heat transfer coefficient and frictional pressure drop during condensation processes within mini-channel tubes. First of all, a large state of art was made and updated during this PhD thesis development in order to know the situation of the investigations on that subject. No publications were found dealing with heat transfer coefficient or pressure drop of propane or R32 in mini-channel multi-port tubes and only a few dealing with R1234yf.

To develop this experimental PhD thesis an installation built on purpose to work with flammable fluids was constructed at the Technical University of Cartagena. In this installation the refrigerant in two-phase flow conditions circulate inside the multi-port mini-channel tube that composes the test section. In this test section, the refrigerant condensates and pressure drop, local heat flux and wall temperature are measured to be able to perform frictional pressure drop and local heat transfer coefficient of the refrigerant.

As the correlations available in the literature were developed mostly for R134a, firstly some measurements were made with this refrigerant to validate the measuring technique. Steady state conditions were maintained during 1200 seconds for each measuring value with minimal variations of the measuring variables.

Several models were found to be able to predict the experimental measurements recorded in our experimental installation. After that, other fluids were experimentally tested under similar conditions and compared between them and against the available models in the literature. Some of these models are able to predict experimental data correctly and some others fail with some fluids. The data recorded during the experimental campaign will be used to develop predictive models for HTC and pressure drop.

The block diagram of the methodology followed can be seen in Fig. 1.1.

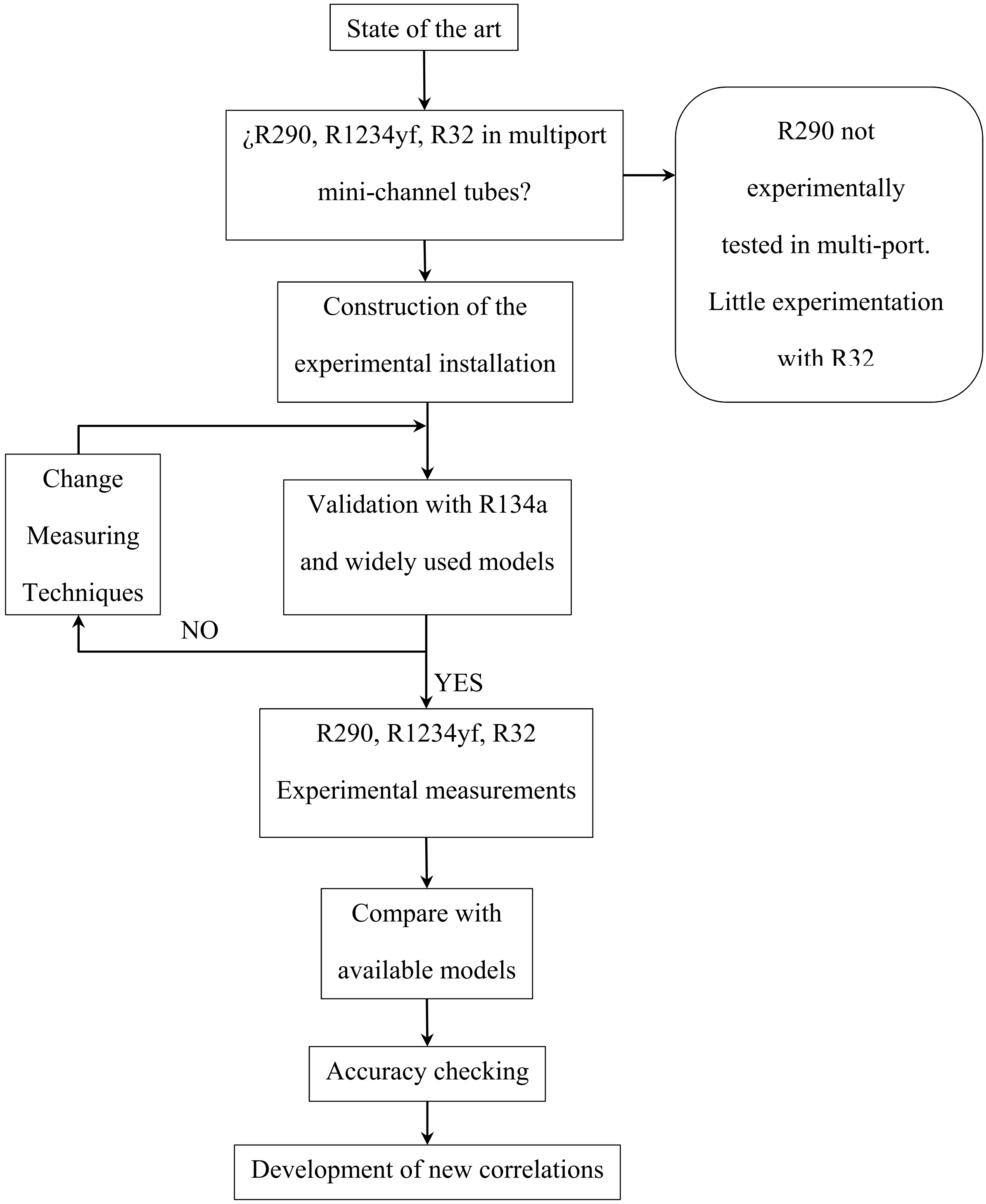

Fig. 1.1. Methodology block diagram.

1.4. PhD THESIS SCHEMA

This PhD thesis is composed of several chapters and a short summarise of all of them is given in the following lines.

In the first chapter objectives and the methodology followed in this PhD thesis are presented.

In Chapter 2, the state of the art of the investigations dealing with mini-channels with heat transfer coefficient or pressure drop measurements is presented. A huge amount of publications can be found about that subject but only a few working with natural refrigerants. The author did not find publications dealing with R290 in multiport mini-channel tubes. According to the state of the art, only one reference of R32 inside multi-port mini-channel tubes was found.

In Chapter 3, a review of some of the models available in the open literature is presented. These models are sorted by tube size, divided into two groups: models developed for macro-channels and specifically developed for mini-channels. This part deals with the models developed for heat transfer coefficient and pressure drop prediction.

Chapter 4 presents the experimental installation constructed on purpose to this PhD development. A complete description of the installation, control system, test section geometry and experimental campaign can be found in this chapter.

In Chapter 5 the experimental data analysis is reported. In this section the calculation process of the local heat transfer coefficient is presented. The expressions considered to calculate sudden expansion and contraction pressure drops are provided to understand the calculation process of frictional pressure gradient.

In Chapter 6 the experimental results are presented for both heat transfer coefficient and pressure drop. The graphical results are sorted by fluid and some comparisons between experimental measurements are commented.

The Chapter 7 shows the results presented in Chapter 6 compared with the models included in Chapter 3 sorted by author's correlation and separated by working fluid. This analysis is made for heat transfer coefficient and pressure drop separately for all the fluid experimentally tested.

In Chapter 8 two models to pressure drop and heat transfer coefficient calculations are provided. These models are developed thanks to the great quantity of frictional pressure drop and heat transfer coefficient measurements recorded during the realisation of this thesis.

Finally, in Chapter 9 some conclusions partially mentioned in previous chapters are summarised. Also a future work section is written in this chapter.

REFERENCES

[1] F. Poggi, H. Macchi-Tejeda, D. Leducq, and A. Bontemps, Refrigerant charge in refrigerating systems and strategies of charge reduction, International Journal of Refrigeration, 31 (2008) 353-370.

[2] W. M. Kays and A. L. London. Compact Heat Exchangers. McGraw-Hill. New York. Second Edition. 1964.

CHAPTER 2: State of the art

2.1. INTRODUCTION

Mini-channels can be described as tubes with one or more ports extruded in aluminium. They are mini-channels if its hydraulic diameter is in the range of 0.2 to 3 mm. Its use in refrigeration systems for some years ago is a reality thanks to the human ability to made micro-scale systems. Some heat exchanger enterprises have some models developed specially for their use in automotive sector, cooling sector, and industrial refrigeration.

Many profits can be obtained using this technology. In many cases, these heat exchangers have been used without having a wide knowledge of how the small geometriy affects physical processes. The augmentation of transport processes due to micro-scale dimensions has lots of profits and it is widely used in biolgical systems. The main advantages of these tubes are higher thermal efficiency; higher compactness and lower weigth compared with same thermal capacity finned tube heat exchangers.

In engineering systems, the main goal is to understand and cuantify how the use of this technology affects flow patterns and so heat transfer coefficient and mass transfer. In that way performance is maximised and cost, size and energy requirements are minimised.

Boiling and condensation phenomena inside mini-channels have lots of applications: in heat sinks or power electronics, temperature control in aerospace industry, refrigeration of fuel injection systems, boilers components in fuel cells, cooling the sections in contact with plasma in fusion reactors, condensing units of air conditioning equipments in cars, and so on.

The aim of using mini-channels in the design of compact heat exchangers in air conditioning and refrigeration is reducing refrigerant charge. This charge reduction is empowering the use of natural refrigerants and contributing to more efficient and greener equipments. At the present time, a quite big portion of the electricity produced is consumed in air conditioning equipments and so on the comsumption of fuel and their CO_2 emmisions associated. Refrigeration and Air Conditioning (RAC) are responsible for approximately 40 % of total energy consumption in the European Union [1] and related CO_2 emissions.

The use of these devices in air conditioning and refrigeration systems have been empowered in last years to get addecuate to new energy efficiency standars. The mixtures of refrigerants and use of additional heat exchange surfaces have been empowered as an alternative to hydrofluorocarbons that deplete the ozone layer.

In fact, it is a reality the incorporation of this technology to domestic air conditioning equipments in order to develop compact, cheaper and lower power equipments.

As mentioned above, a great number of international research equipments are foccused on the study of heat transfer and pressure losses in these systems. This research is focused on the condensation studies performed in the research group "Modelling of Thermal and Energy Systems".

Momentum and heat transfer processes are strongly influenced by flow patterns so any prediction of two-phase heat transfer coefficient must be based on existing flow patterns for that size. Flow patterns strongly affect flow and heat transfer laws. In addition, the correct desings of heat transfer exchangers with mini-channels should be based on proven calculion methods for heat transfer coefficient and pressure drop. These two parameters are influenced by gravity effects, inertial forces, viscous shear, and surface tensions which are affected with reducing size. So, it is dangerous to extrapolate calculus methods of macro-channles to mini-channles without an experimental validation of the models.

Pressure drop and heat transfer coefficient researches show that the validity of correlations is linked to tube diameter and mass velocity. As previously mentioned, attention must be paid to flow pattern structures in these tubes.

Single-phase flow in mini-channels is limited by the small temperature rise the fluid can experiment. Two-phase flow is much more interesting due to the exploitation of latent heat (phase change). Therefore, higher heat transfer coefficients are reached with two-phase flow with also higher pressure drop values.

The main reason why normal tubes should be distinguished from mini-channels is because of great differences between the fluid forces that take into account the following non-dimension numbers: Bond, Weber, Froude and Reynolds numbers.

Channel size compared with bubble size can be expresed in terms of Bond number. Bond number relates the importance of body forces (almost always gravitational forces) to surface tensión forces.

$$Bo = \frac{\Delta\rho\ g\ L^2}{\sigma} \tag{2.1}$$

A high value of Bond number shows that surface tension effects are negligible. A low value of this number shows that surface tension effects dominate.

Weber number is commonly used to analise flows with an interfase between two different fluids, specially for multi-phase flows or with highly curved surfaces.

$$We = \frac{\rho v^2 L}{\sigma} \tag{2.2}$$

It can be considered as a measure of the relative inportance of inertial forces versus surface tension forces.

Froude number is defined as the relation of a charateristic velocity versus the speed of gravitational waves. An equivalent definition could be the ratio between inercia to gravitational forces.

$$Fr = \frac{v}{c} \tag{2.3}$$

Reynolds number provides a measurement ratio of inertial forces to viscous forces. This number quantifies the relative importance of these forces for a given flow conditions.

$$Re = \frac{\rho v L}{\mu} \tag{2.4}$$

This dimensonless number plays an important role in flow pattern characterisation such as, turbulent or laminar. Laminar flows present Reynolds number with dominating viscous forces. On the other hand, turbulent flows take place at high Reynolds number values and inertial forces dominate.

In small diameter tubes, lower than 3 mm, vapour surface and shear tension dominate the flow pattern. Even being the mass velocity and vapour quality the main factors that affect flow pattern, thermophysical properties of fluid and tube diameter play a secondary role. Its influence is much more evident at intermediate mass velocities, 150 to 300 kg $m^{-2}s^{-1}$, where mass velocities are not high or low enough to let a regime prevail over the rest. The fluid properties that affect the most are: liquid and vapour densities, viscosity and surface tension. Much of the variations of fluid properties are related to reduced pressure.

Tube diameter also affects flow pattern transitions. As the diameter is being reduced, with a constant mass velocity, the flow transtition from to anular flow to wavy-anular and from wavy-annular to wavy flow, is being displaced to lower vapour quality values. At high mass velocities, most of vapour quality range is linked to anular flow and diameter effects are less pronounced.

In this research, heat exchangers are made of aluminium tubes that may have different geometries with rectangular, triangular or circular sections and hydraulic diameters of around 1 mm.

In view of this and considering that it is an emerging technology whose progress will make air conditioning systems manufacturing more efficient, an experimental installation for researching on condensation heat transfer coefficents and pressure drop was built at the Technical University of Cartagena.

This document contains a wide bibliographic review providing the actual situation of international research group publications about this subject. The installation for condensation processes, the tube geometries and process followed for the heat transfer coefficent and pressure drop calculationis described in Chapters 3 and 4.

2.2. STATE OF THE ART

2.2.1. Heat Transfer Coefficient

The state of the art of the actual researching situation about condensation heat transfer coefficient and pressure drop inside mini-channels is presented in the following section. Much of them are briefly commented and a summarising table is presented with the most important information. A first table collects the transition diameter from macro to mini-channels proposed by several authors. Author names, publication year, geometries tested, experimental defining parameters, mass fluxes, tube diameters and saturation temperatures are summarised in the Table 2.2.

Heat transfer characterisation and pressure drop inside mini-channels during condensation have been strongly researched for the last years. In macro-channels the process is dominated by vapour shear tension or gravitational forces. When shear tensions prevail in the condensation process over the gravitational forces, the prevailing flow pattern is annular flow. If the opposite happens, then, stratified, wavy and slug flow patterns prevail. Heat transfer correlations for pure or near azeotropic mixtures take that into account. If annular flow prevails, the heat transfer coefficient depends on mass flux, vapour quality, and saturation temperature.

If gravitational forces prevail, the heat transfer coefficient depends on the difference between tube wall and saturation temperature. Flow pattern influence is very strong in heat transfer processes and momentum. So pressure drop and heat transfer predictions must be based on existing pattern maps [2]. Therefore, special attention mus be paid to these correlations, in micro and mini-channels gravitational forces are negligible. Instead of them, surface tensions play the main role.

Most of researching articles present and compare experimental data of mini-channels with correlations developed for macro-tubes. Only in a few cases, a precise heat transfer correlation is proposed to fit experimental data. This state of the art investigation is focused on researches with tubes with hydraulic diameter about 1 to 3mm. A good revision of recent condensation heat transfer coefficient and pressure drop in tubes of small and large diameter can be found in English and Kandlikar [4].

Yang and Webb [4] studied R12 condensation in plain micro-finned multi-port struded tubes with hydraulic diameters of 2.637 and 1.564 mm. They compared against the correlations developed by Akers et al. [5] and Shah and London [6].They found that Akers et al. [5] correlation predicted well their experimental data for plain tubes. The authors also showed that high velocity data are over estimated.

Yang and Webb [7] proposed a correlation for heat transfer coefficient prediction in finned mini-channels. This correlation takes into account vapour shear tension and surface tension effects.They proved that at high mass velocities, heat transfer coefficient is controlled by vapour shear tension and the contribution of surface tension is quite small (it is much affected by fin geometry). These authors also proposed a separated asymptotic model for these two effects. Yang and Webb [7] validated the previous model analysing five different geometries (a single port tube and several multi-port tubes with and without fins) and two refrigerants, R12 and R134a.

Webb et al. [8] studied a circular copper tube with a hydraulic diameter of 3.55 mm and an aluminium multi-port tube of 2.13 mm. They checked their experimental results for R134a with those provided by Shah [6] and Moser et al. [9] correlations under similar conditions. They found good concordance between their data and both correlation predictions, at 65 ºC saturation temperature, they showed that Shah [6] correlation over-estimates their data. The authors attributed this difference to the reduced pressures. In their data, it was p_{red} = 0.47 while Shah [6] correlation was developed for $0.011 < p_r < 0.44$. Accordingly, round single port tubes and multi-port tubes are going to reach the same condensation performance.

Webb andKemal [10] studied the effect of hydraulic diameter size over heat transfer coefficient and pressure drop during R134a condensation. They used four different hydraulic diameter aluminium tubes of 0.44, 0.611, 1.33 and 1.564 mm. Webb and Kemal [10] showed a good agreement between experimental data and the correlations of Akers et al. [5] and Moser et al [9] correlation. They showed that Moser [9] correlation provides satisfactory results for big and small diameters. It is valid for condensation driven by shear stress. The authors recommend Yang and Webb [7] correlation to consider surface tension effects.

Yan and Lin. [11] studied R134a condensation in a matrix of small circulat tubes with a hydraulic diameter of 2 mm. They proposed correlations for heat transfer coefficient and pressure drop calculation. They observed higher heat transfer coefficient values at lower heat fluxes, lower saturation temperatures and mass fluxes.

Wang et al. [12] investigated the R134a condensation in an aluminium rectangular multi-port tube of 1.46 mm of hydraulic diameter. They showed that at low mass fluxes or vapour quality values, stratified flow and Nusselt film condensation phenomena dominate. They demonstrated the dependency of heat transfer coefficient with temperature difference. Since the mass flux or vapour quality grow, a annular film is created that provokes convection to dominate. A high dependency with mass flux, especially at high mass fluxes, and vapour quality values was observed. They viewed annular, wavy and slug flows.

Kim et al. [13] studied condensation of R22 and R410A in two rectangular multi-port tubes with and without micro-fins and with hydraulic diameters of 1.56 and 1.41 mm respectively. They compared their experimental data with the correlations developed by Webbet al. [8], Koyama [14], Shah [6], Akers et al. [5] and Yang and Webb [7]. The data showed the same effect as Webb et al. [8] regarding to Akers et al. [5] and Shah [6] correlations. According to Koyama et al. [14] and Kim et al. [13] correlations, they obtained under-estimation of their experimental data. They recommend the use of Webb et al. [8] and Moser et al. [9] correlations for smooth tubes and a modified version of Yang and Webb [4] correlation in the case of micro-finned tubes.They also showed a slightly higher heat transfer coefficient values of R410A compared with R22 under the same saturation conditions in smooth tubes.

Koyama et al. [15] studied R134a condensation in two rectangular multi-port tubes with hydraulic diameters of 0.8 and 1.11 mm. They showed that some correlations based on forced convection models such as [9], Dobson and Chato [16] under-estimate their values at low mass fluxes because these models neglect free convection effect. Haraguchi et al. [17] correlation prediction also disagrees with Koyama et al. [14], and in that case the authors claimed that this could be explained due to the use of homogeneous model for momentum pressure drop calculation. They proposed an asympthotic model that takes into account convetion forces, free convection and also the effects of surface tension effects. This is based on the correlation of Haraguchiet al. [17] and Mishima and Hibiki [18]. In opposition to the above mentioned investigations, Koyama et al. [15] correlated their data to develop a new correlation for two-phase flow pressure drop multiplier. To do that, they considered another two multi-port micro-finned tubes in addition to the two considered in the previous investigation. These correlations with the proposed by Wang et al. [12], consider heat transfer coefficient at low vapour quality values. Baird et al. [19] uses Seebeck effect to produce R123 and R11 condensation in passages with hydraulic diameters of 0.92 and 1.95 mm. The correlation proposed is valid for annular flow in which shear tension effects dominate. They showed a significant influence of heat flux at high vapour quality values. An increase in saturation pressure at a fixed mass flux leads to a decrease of heat transfer coefficient. Also, an increase of mass flux leads to an increase of heat transfer coefficient.

Cavallini et al. [2, 20, 21] studied the heat transfer coefficient during condensation of R236ea, R134a and R410A inside multi-port mini-channel tubes with thirteen parallel rectangular ports and a hydraulic diameter of 1.4 mm. They tested a huge range of reduced pressures. They also compared experimental results with some of the correlations available in the literature: Moser et al. [9], Cavallini et al. [22], Akers et al. [5], Koyama et al. [15] and Wang et al [12]. They showed that Moser et al. [9] and Cavallini et al. [23] under-estimate heat transfer coefficient at values of dimensionless gas velocity higher than ten. They claimed that for dimensionless gas velocity lower than 2.5, a deeper investigation in mini-channels with different diameters should be made in order to determine if heat transfer coefficients depends on the difference between saturation temperature and wall temperature. For the regime of free convection, Wang et al. [12] and Koyama et al. [15] correlation try to predict free convection.They also contributed with the analysis of Moser et al. [9] and Zhang and Webb [24] correlation for pressure drop prediction. These correlations correctly predict pressure drop and heat transfer coefficient in shear dominated regime if there are no droplets entraintment from the liquid film.

Bandhauer et al. [25] studied three multi-port tubes with circular geometry and different hydraulic diameters. Their model is assesed on a multi-region model that explains the mechanisms in each regimen found in condensation in the tubes with hydraulic diameters in the range 0.4 to 5 mm. Acordigly, the predominant regimes are intermittent, annular and mist flows. Garimella et al. [26] claimed that shear driven models for condensation are close and linked to pressure drop models which, sometimes, explain that some models fails on its heat transfer coefficient prediction when using a non accurate pressure drop model. The correlation proposed by the authors is based on the analysis of the boundary layer of Traviss et al. [27] andMoser et al. [9] but with a pressure drop model especially developed for mini-channles by Garimella et al. [26].

Wen et al. [28] studied local heat transfer coefficient during condensation inside a three step coil of 2.46 mm diameter working with R600, R290 and a mixture at 50% in weight of R600 and R290. Heat transfer coefficients are a 155 %, 124 % and 89 % higher for R600, R600/R290 and R290 than R134a under the same conditions. Dobson and Chato [16] correlation predicts the best heat transfer coefficient values for tested refrigerants with a standard deviation of 12.8 %.

Médéric et al. [29] analysed condensing R134a heat transfer coefficients based on flow patterns inside the mini-channel tube. As temperature difference was almost zero in the glass condenser, they used an image technique to calculate void fraction, assisted by an energy balance, they obtained global heat transfer coefficient. Heat transfer is almost constant in annular regime and is degraded in bubbly flows. These two flow patterns were the only observed in the test section.

Cavallini et al. [30] and Matkovic et al. [31] studied R32 and showed that Cavallini et al. [32] provides good results when it is compared with their data but over-estimate heat transfer coefficient in some cases. In contrast, the macro-tubes correlation developed by Cavallini et al. [2] provides better results.

Cheng et al. [33] made a bibliographic revision about supercritic CO_2 cooling in macro and micro-channels. He observed that the heat transfer coefficient in supercritical zone is quite different from the region of constant fluid properties. This is explained by the fact that in supercritical zone, fluid properties are quite different from those in the undercritical zone. To summarise experimental results, heat transfer coefficient grows up to near its maximum value with decreasing refrigerant temperature. The maximum value is reached near pseudo-critic zone due to the high variation of CO_2 properties. There is no correlation valid for all experimental data due to the high variation mentioned above. The authors suggested higher effort about that subject.

Cavallini et al. [34] studied condensation processes in a single-port mini-channel for R134a and R32. Heat transfer coefficient was obtained by wall and saturation temperature measurements. They compared the results with Moser et al. [9], Koyama et al. [15] and Cavallini et al. [2] correlations. They used Moser et al. correlation [9] for heat transfer coefficient calculation and Zhang and Webb [24] correlation for frictional pressure gradient in small channels. In that way the tendency of experimental data was captured but is also under-estimated. The under-estimation is much higher as the mass flux is reduced. This effect can be explained because the correlation was developed for annular flow conditions. Koyama et al. et al. [15] correlation predictions are not precisse because its predictions do not reflect experimental tendency related to mass flux. Thome et al. [35] correlation over-estimates heat transfer coefficient values but experimental data fit correctly. The last model, Cavallini et al. [2], predicts better results even having been developed for tubes with higher hydraulic diameters.

Park and Hrnjak [36] studied R744 condensation inside a mini-channel tube of 0.89 mm at saturation temperatures of -15 and -25 ºC for heat transfer coefficient and pressure drop measurements. The measurements of heat transfer coefficents were augmented with higher values of mass fluxes and vapour quialities. Heat transfer coefficient was not affected with changes with wall subcooling temperature. They remark that the condensation mechanism in the mini-channel is similar to a higher diameter tube and that several existing correlations predict correctly the pressure drop behaviour.

Wen and Ho [37] investigated the condensation of R290 and R600 with oil inside coils of 2.46 mm of inner diameter. They remarked that heat transfer coefficient increases with higher values of mass flux, vapour quality, and the number of coil elbows; and decreases with the oil concentration increase. Pressure drop measurements increases with higher mass fluxes, increasing number of elbows and oil concentration.

Agarwal et al. [38] studied condensation phenomena in six mini-channels with different geometry and non-circular section working with R134a. They used the thermic amplification technique for heat transfer coefficient calculation. The authors took into account tube transversal section to apply flow regime. Data was correlated with a modified version of annular flow model using the pressure drop model for non-circular mini-channels in the square, rectangular and barrel sections. There was good agreement. For the rest of geometries with sharp corners, the model used was based on mist flow for higher diameter tubes.

Cascales et al. [39] presented a model for compact heat exchanger analysis working as evaporators and condensers with mini-channel geometry and R134a and R410A as refrigerants.

Del Col et al. [40] investigated pressure drop and heat transfer coefficient during condensation of R1234yf inside a mini-channel circular single port tube with a diameter of 0.96 mm. They compared the data with the results obtained for R134a. This experiment was made in a special apparatus built to measure the cooling fluid profile. R1234yf has lower heat transfer coefficient values than R134a under the same opeating conditions. Cavallini et al. [2] predicts experimental data with an error of 15 %. Pressure drop meassurements with R1234yf are between 10 and 12 % lower than R134a values.

Bohdal et al. [41] experimentally studied heat transfer coefficient and pressure drop of R134a and R404A during condensation inside mini-channels. Experimental data was compared against correlations developed by other authors with good agreement by Akers et al. [5] and Shah et al. [6] correlation for heat transfer coefficient. The model that best fitted to pressure drop values were Friedel [42] and Garimella et al. [43] models. At the end, they proposed their own correlation for local heat transfer coefficient.

Oh and Son [44] studied the heat transfer coefficient of R22, R134a and R410Ain a single port circular mini-channel of 1.77 mm hydraulic diameter without oil. They obtained that heat transfer coefficient value in single-phase flow was greater than that obtained by using Gnielinski correlation. In two-phase flow, the heat transfer coefficient of R410A is higher than those given by R22 or R134a at the same value of mass flux. The measurements obtained for R22 and R134a show similar values.According to them, most of the correlations developed for bigger dimension tubes do not predict local heat transfer coefficient correctly. In addition, the correlation developed by Yan and Lin [11] for single port micro-tubes is not appropriate for the mini-channel studied so the authors claim for more investigation on that way.

Park et al. [45] compared the heat transfer coefficient of the new refrigerant R1234ze with R134a and R236fa in a mini-channel tube of 1.45 mm of hydraulic diameter vertically aligned. Heat transfer coefficient was not affected by flow pattern or by entrance conditions in the range studied. It was found that R1234ze heat transfer coefficient is lower than that provided by R134a in 15 and 25 % but it is similar to R236fa values. The comparisons with Bandhauer et al. [25], Cavallini et al. [2], Moser et al. [9], Koyama et al. [14], Thome et al. [35] correlations and Nusselt film theory gave them poor results. This is, high Nusselt numbers are over-estimated and under-estimated the lower values of it. A new correlation for the three fluid tested was developed with a good fitting over the conditions tested. The authors re-adjusted the existing model of Koyama et al. [14].

De Col et al. [46] measured the heat transfer coefficient in a square shape mini-channel. Its measurements were compared with previous data of a single mini-channel with circular section working with R134a, both of them with the same hydraulic diameter. In the square shape mini-channel, heat transfer coefficient augmented at low mass fluxes due to surface tension. At higher mass fluxes there is no increase because condensation is dominated by shear stress.

Zhao et al. [47] studied heat transfer coefficient and pressure drop of CO_2 mixed with oil at supercritical pressures inside horizontal tubes with inner diameters of 1.98 and 4.14 mm. In the tests without oil, the correlation proposed by Dang and Hihara [48] predicted the heat transfer coefficient and Petukhov [49] correlation for pressure drop, both correctly. Oil entrance decreases heat transfer coefficient values and increases pressure drop values. Heat transfer coefficient is strongly related with density and viscosity ratios of oil to CO_2. In addition, a new correlation was developed with experimental data recorded. The new correlation fits most of the data with a deviation lower than 20 %.

Cavallini et al. [50] studied local heat transfer coefficient during condensation of R32 and R245fa inside a circular mini-channel with a 0.96 mm hydraulic diameter at 40 ºC. At equal values of vapour quality and mass flow rate, almost the same values of heat transfer coefficient were measured. The R32 values are slightly higher.

Del Col et al. [46] measured the heat transfer coefficient inside a square shape mini-channel of 1.23 mm of hydraulic diameter. They compared the measurements with the data of a 0.96 mm diameter round mini-channel. They used R134a as working fluid at a saturation temperature of 40 ºC. Square shape tube has higher heat transfer coefficient at low mass flow rates mostly due to surface tension effects. At high value of mass flow rates, condensation phenomena are dominated by shear stress, no difference was found.

Kim and Mudawar [51] studied the heat transfer coefficient of FC-72 flowing through rectangular multi-port mini-channels with a hydraulic diameter of 1 mm. Heat transfer coefficient is higher at the entrance of the tube where liquid film thickness is lower. The heat transfer coefficient value decreases along the tube due to the increase of liquid film and the collapse of annular flow. The authors compare their data with the correlations for annular flow. Their results are better explained by the correlations developed for macro-tubes than those specifically developed for mini-channels. They propose a correlation that perfectly fits their data and other database for mini-channels.

Jige et al. [52] studied the condensation process of pure refrigerants R134a and R32 in a horizontal multi-port tube. The test tube is made of aluminium alloy with 0.85 mm in hydraulic diameter. The experiments were carried out in the mass velocity range of 100 to 400 kg $m^{-2}s^{-1}$ at saturation temperatures of 40 and 60 ºC. Then, the sectional average heat transfer coefficients were measured in eight subsections. In cases of high mass velocity, the heat transfer coefficient decreases monotonically with decrease of vapour quality; this corresponds to the decrease of vapour shear stress. On the other hand, in case of low mass velocity, the heat transfer coefficient is kept almost constant in a wide vapour quality range; it is inferred that the surface tension effect is dominant in this range. Based on these results, they developed a new heat transfer correlation considering both effects of vapour shear stress and surface tension.

Derby et al. [53] analised the heat transfer coefficient during condensation in mini-channels with triangular, square and semi-circular shape made on copper with R134a. Data were reported for R134a in 1 mm square, triangular, and semicircular multiple parallel minichannels cooled on three sides. A parametric study was conducted over a range of conditions for mass flux, average quality, saturation pressure, and heat flux. Mass flux and quality were determined to have significant effects on the condensation process, even at lower mass fluxes, while saturation pressure, heat flux, and channel shape had no significant effects. The lack of shape effects was attributed to the three-sided cooling boundary conditions as there was no significant surface tension enhancement. A strange effect over heat transfer coefficient was discovered due to non-uniform cooling boundary, only three faces were cooled. As the effect of surface tension is negligible, Shah et al. [53] correlation for macro-tubes predicts the best the data.

Charun [54] presented the results of his investigation with R404A condensing inside round and small diameter tubes in the range of 1.4 to 3.3 mm. Pressure drop results are reasonably well predicted by Friedel [42] and Garimella et al. [26,43] correlations. As final result, he proposed a new correlation to calculate heat transfer coefficient in condensation processes.

Zhang et al. [55] studied the heat transfer coefficient during condensation of three refrigerants; R22, R410A and R407C; inside two round tubes of 1.088 and 1.289 mm of hydraulic diameter at saturation temperatures of 30 and 40 ºC. The range of mass fluxes is between 300 and 600 kg $m^{-2}s^{-1}$. The experimental measurements were compared with correlations developed for tubes with diameter higher than 3 mm.

Goss Jr and Passos [56] published a study about local heat transfer coefficient in a multi-port tube with a hydraulic diameter of 0.77 mm working with R134a. Unlike most experimental installations, this makes the cooling process by means of thermo-electric Peltier modules. As conclussions they claim that there is no clear influence of saturation temperature and heat dissipated over the heat transfer coefficient value but it is affected by increasing mass flow rate.At intermediate vapour quality values, heat transfer coefficient tendency is to remain constant. Their data is best predicted by Cavallini et al. [2] correlation.

Zhang et al. [57] investigated two-phase flow heat transfer coefficient during CO_2 condensation inside a mini-channel condenser with a hydraulic diameter of 0.9 mm. The experiemtal measurements were made at saturation temperatrues from -5 ºC to 15 ºC and mass velocities of 180, 360 and 540 kg $m^{-2}s^{-1}$. Thome et al. [35] correlation presented the lower deviation, less than 30 %.

Al-Hajri et al. [58] experimentally studied two-phase condensing flows of R134a and R245fa in a single mini-channel of 0.7 mm diameter with high aspect ratio. Pressure drop is accurately predicted by Lockhart-Martinelli with deviation lower than 20 %. Heat transfer coefficient is predicted with errors lower to 20 % by Dobson and Chato correlation with a modified power of the Martinelli parameter.

Heo et al. [59] reported a study about in-tube condensation heat transfer characteristics of CO_2 in different mini-channels. Multi-port minichannels had hydraulic diameters of 1.5, 0.78 and 0.68 mm and they were tested from -5 to 5 ºC of saturation temperature. The model by Thome et al. [35] showed the lowest deviations.

Heo et al. [60] published a study about condensation heat transfer coefficient and pressure drop of CO_2 in a multiport mini-channel with a hydraulic diameter of 1.5 mm. Mas flux variation was from 400 to 100 kg $m^{-2}s^{-1}$ and saturation temperatures from -5 to 5 ºC. Heat transfer coefficient increases with decreasing saturation temperature and increasing mass flux. There was no model able to predict the experimental data correctly.

Liu et al. [61] experimentally investigated heat transfer and pressure drop during condensation of R152a in circular and square mini-channels with hydrauulic diameters of 1.152 and 0.952 mm, respectively. Heat transfer is correctly predicted by several author correlations. Channel geometry has much effect on heat transfer at low mass fluxes.

Sakamatapan et al. [62] published a study on condensation heat transfer with R134a flowing inside a multiport mini-channel tube of 1.1 mm of hydraulic diameter. The experiment was performed with mass fluxes of refrigerant between 340 and 680 kg $m^{-2}s^{-1}$, with 15, 20, and 25 kWm^{-2} heat fluxes, and saturation temperatures of 35– 45 ºC. It could be noted that the annular flow pattern existed for most of the experimental data. Results showed that the average heat transfer coefficient increased with the increase of vapour quality, mass flux, and heat flux, but decreased as saturation temperature rose. When compared with Koyama et al. [15] and Webb et al. [8] correlations obtained from condensation inside the multiport minichannels, the heat transfer coefficient could be predicted within an acceptable range.

Wang et al. [63] presented a short overwiew of the heat transfer performance of R1234yf versus R134a with previous published data. For in-tube condensation, it was found that the condensation heat transfer coefficients for R1234yf are inferior to those of R134a. These differences increase with the rise of vapour quality.

Table 2.2 summarises the different investigations related with heat transfer coefficient calculation in mini-channels considered in this document.Most of them use R134a as working fluid but there are some of them with R12, R22, R410A, R123 and R11. Only a few tests are available for R407C and R1234yf what sujects that a higher effort must be made with different refrigerants.

If Table 2.2 is carefully observed, it can be appreciated that most of the documents preferred to use R134a because is has been a widely used refrigerant from end 80s until now. After Montreal protocol, the air conditioning refrigerants in car AC, (old CFC clorofluorocarbons) were mostly substituted by R134a. This latter one is a HFC (hidrofluorocarbon); much less harmfull with ozone layer but it must be substituted in the near future too. As opposite, the global warming power (GWP) of R134a is 1300 instead of 3 of natural hydrocarbon R290 (propane) or 0 in the case of CO_2.

Table 2.1. Transition geometries by some authors.

(Mehendal et al. 2000)		(Kandlikar 2002)	
Micro-channel	1-100 μm	Micro-channels	50-600 μm
Meso-channels	100 μm – 1 mm	Mini-channels	600 μm – 3 mm
Macro-channels	1-6 mm	Normal channels	> 3 mm

Table 2.2. Heat transfer coefficient publications considered in this study.

Researchers	Year	Fluids		d_h (mm)	t_{sat} or p_{sat}	G (kg m^{-2}s^{-1})	HTC
Yang and Webb	1996	R12	MS MSmf	1.564, 2.637	65 ºC	400-1400	Local
Vardhan and Dunn.	1997	R-134a, R22, R407C	MC	1.494	51.7 ºC	400-1100	
Webb and Zhang	1998	R134a	C, MR	3.25, 2.13	40, 65 ºC	200-400-600-1000	Local
Yan and Lin	1999	R134a	C	2	25, 30, 40, 50 ºC	100 - 200	Local
Wang and Du.	1999	Water vapour	C	1.94, 2.80, 3.95, 4.98		11.3 - 94.5	Local
Wang	1999	R134a	MR	1.46	61-66.5 ºC	200-600	
Kim NH et al.	2000	R22	MR, MRmf	1.41, 1.56	45 ºC	200-699	Local
Garimella and Bandhauer	2001	R134a	MR	0.4 – 4.91	-	150 - 750	Local
Webb and Kemal	2001	R134a	MR, MRmf	0.44 - 1.56	65 ºC	300-1000	Local
Wang et al.	2002	R134a	MR	1.46	45-66 ºC	75-750	Local
Kim MH et al.	2003	R134a	C	0.691	40 ºC	100, 200, 400 and 600	Local
Baird et al.	2003	R123, R11	C.	0.92, 1.95	p_{sat} = 120-410 kPa	70-600	Local
Kim NH et al.	2003	R22, R410A	MR, MRmf	1.41, 1.56	45 ºC	200-600	Local
Koyama et al.	2003a	R134a	MR	0.807, 1.114	p_{sat} = 1700 kPa	100-700	Local
Koyama et al.	2003b	R134a	MR, MRmf	1.062, 0.807, 0.889 and 0.937 mf.	p_{sat} = 1700 kPa	100-700	Local
Shin and Kim.	2004	R134a	C	0.691	40 ºC	100 - 600	Local
Cavallini et al	2005	R134a R410a	MR	1.4	40 ºC	400-1000 600-1400	Local
Cavallini et al.	2005b, c, 2006	R236ea, R134a, R410A	MR	1.4	40 ºC p_{red}: 0.1-0.5	200 – 1000	Local

Researchers	Year	Fluids		d_h (mm)	t_{sat} or p_{sat}	G (kg m^{-2}s^{-1})	HTC
Bandhaueret al.	2006	R134a	MC	0.506 -1.524	-	150 - 750	Local
Wen et al.	2006	R-600, R600/R-290 (50%/50%), R-290	C - serpentine	2.46	40 ºC	205 - 510	Local
Médéric et al.	2006	R134a	C	0.56	40 ºC	3.4 – 13.8	Global
Cavallini et al.	2008	R134a, R32	C	0.96	40 ºC.	200, 400 and 600	Local
Matkovic et al.	2008	R32	C	0.96	40 ºC, 19-29 ºC	100-1200	Local
Cheng et al.	2008	CO_2 (R744)			Review of available literature		
Matkovic et al.	2009	R134a R32	C	0.96	40 ºC	100-1200 100-1200	Local
Park and Hrnjak	2009	CO_2 (R744)	MC	0.89	-15 ºC -25 ºC	200-400 600-800	Local
Wen and Ho	2009	R-290, R600a + oil	C	2.46 mm	40 ºC	300 - 600	Local
Agarwal et al.	2010	R134a	MS, MB, MT, MR MW, MN	0.424 - 0.839	55 ºC	150 - 750	Local
Cascales et al	2010	R134a. R410a	MR	0.96	p_{sat}= 1000 and 2500 kPa	200	Local
De Col et al	2010	R1234yf	C	0.96	40 ºC	200 - 1000	Local
Bohdal et al.	2011	R134a, R404a	C	0.31 to 3.30 mm	30 – 40 ºC	100 - 1300	Local
Oh and Son.	2011	R134a, R22, R410a	C	1.77 mm	40 ºC	450 - 1050	Local
Park et al.	2011	R134a, R236fa, R1234ze	MR	1.44 mm	25, 30, 55, 70 ºC	50 - 260	Local
Del Col et al.	2011	R134a	S	1.23	40 ºC	200 - 800	Local
Zhao et al.	2011	CO_2 (R744) + oil	-	1.98 - 4.14	8000-11000 kPa	400-1200	Local
Ma et al.	2011	Water	R	3.64	24 - 37.5 ºC	285 - 2320	Local
Cavallini et al.	2011	R32, R245fa	C	0.96	40 ºC	100 – 1200 100 - 500	Local
Del Col et al.	2011	R134a	S	1.23	40 ºC	200 - 800	Local

Researchers	Year	Fluids		d_h (mm)	t_{sat} or p_{sat}	G (kg m^{-2}s^{-1})	HTC
Kim S-M and Mudawar	2011	FC-72	MR	1	57.2, 62.3 ºC	68-367	Local
Jige et al.	2011	R134a, R32	MR	0.85	40, 60 ºC	100 - 400	Local
Derby et al.	2011	R134a	T	1	35-45 ºC	75-450	Local
Charun	2012	R404	C	1.4, 1.6, 1.94, 2.3, 3.3	20-40 ºC	100-1000	Local
Zhang et al.	2012	R22, R410A, R407C	C	1.088 and 1.289	30 and 40 ºC	300 - 600	Local
Derby et al.	2012	R134a	MT, MR, MSC	1	35 – 45 ºC	75 - 450	Local
Kim et al.	2012	FC72	MS	1	57.2 – 62.3 ºC	65 - 367	Local
Goss Jr and Passos.	2013	R134a	MC	0.77	730-970 kPa	230-445	Local
Zhang et al.	20133	R744	C	0.9	-5 – 15 ºC	180, 360, 540	Local
Al-Hajri et al.	2013	R134a, R245fa	S	0.7	30 – 70 ºC	50 - 500	Global/averaged
Heo et al.	2013	R744	MR	1.5, 0.78, 0.68	-5ºc – 5 ºC	400 - 800	Global
Heo et al.	2013	R744	MR	1.5	-5ºC – 5 ºC	400 - 1000	Global
Liu et al.	2013	R152a	C,S	1.152, 0.952	40, 50 ºC	200-800	Local
Sakamapatan et al.	2013	R134a	C	1.1	35-45 ºC	340-680	Local
Wang	2013	R1234yf vs. R134a			Short review of differences		

Cross sections: C: circular, S: square, MC: multi-port circular, MS: multi-port square, MR: multi-port rectangular, MB: multi-port barrel, MT: multi-port triangular, MW: multi-port W-shape, MN: multi-port N-shape, MRmf: multi-port rectangular micro-finned, MSmf: multi-port square micro-finned, MSC: multiport semi-circular.

2.2.2 Pressure Drop

Pressure drop characterisation is as important as heat transfer coefficient characterisation in compact heat exchanger design. Boiling and condensing pressure drop is given by:

$$-\left(\frac{dp}{dz}\right) = -\left(\frac{dp}{dz}\right)_f - \left(\frac{dp}{dz}\right)_{grav} - \left(\frac{dp}{dz}\right)_{mom} - \left(\frac{dp}{dz}\right)_{acc}$$

Where the left side term is the addition of: frictional component *(f)*, gravitational component *(grav),* which is null in horizontal tubes, momentum component *(mom)* and pressure drop in accessories *(acc)*.

For the last decades, many research studies have been developed to measure fluid pressure drop inside mini-channels with different refrigerants and geometries. Many authors relate two-phase pressure gradient with single-phase pressure gradient and an added multiplier. Different correlations are obtained by the authors if they try to include the refrigerant effects, thermodynamic conditions, the tube geometry, surface tension, and so on.

In the existing literature, the following researches maybe highlighted. Lazarek and Black [64] studied R113 pressure drop in a horizontal tube with a hydraulic diameter of 0.31 mm. The authors proposed an expression based on the Chisholm multiplier with a value of the *"C"* parameter. A value for $C=30$ was obtained after correlating their data. Mishima and Hibiki [18] studied two-phase pressure drop of water and air in an adiabatic flow through capilar tubes of glass or aluminium with hydraulic diameters in the range of 1 to 4 mm. They used the Chilsholm multiplier equation to characterise pressure drop and they obtained a modified Chisholm parameter as a function of tube diameter. They also compared it with other author's data and claimed that the correlation is valid to be used in capillary vertical or horizontal tubes. They included to the correlated data the previous test made with rectangular tubes, increasing the range of geometries which the correlation is valid for.

Tong et al. [65] studied the pressure drop in vertical circular tubes with a diameter range of 1.05 to 2.44 mm working with boiling water and reaching critical heat transfer coefficient values. They studied the effects of mass flow rate, entrance temperature, outlet pressure, tube diameter and the ratio diameter to tube length on pressure drop. They obtained that the pressure drop is proportional to mass flow rate and the relation of diameter to tube length ratio. In addition, they developed two correlations for single and two-phase pressure drop.

Yan and Lin [11] studied condensation pressure drop and heat transfer coefficient in a circular tube of 2 mm of diameter working with R134a. They investigated how pressure drop is affected by heat fluxes, mass flow rate, saturation temperature, and vapour quality. In condensation test, they obtained that pressure drop increases with higher values of mass flow rate and decreasing heat fluxes. They also developed a pressure drop correlation.

Triplett et al. [66] studied two-phase pressure drop with air and water in circular mini-channles of 1.1 and 1.5 mm and also in semi-triangular mini-channels with one rounded corner of 1.09 and 1.49 mm of hydraulic diameter. Bubbly and slug flow patterns, friction factor based on homogeneous mixture model with Friedel correlation [49] provided the best results. For annular flow, homogeneous model and widely used correlation under-estimate frictional pressure drop.

Tran et al. [67] proposed a pressure drop correlation based on the *"B"* coefficient developedby Chisholm; they developed a two-phase flow multiplier correlation. In a similar way, Ju Lee and Yong Lee [68] studied adiabatic pressure drop with air and water in a rectangular horizontal mini-channel. They proposed a Lochart-Martinelli form correlation for two-phase pressure drop with a *"C"* parameter including mass velocity and channel shape effects. The range of superficial velocity covered is in the range of 0.03 to 2.39 ms^{-1} for water and from 0.05 to 18.7 $ms^{-1}$for air.

Pettersen et al. [69] studied R744 (CO_2) boiling pressure drop inside multi-port mini-channel tubes with circular geometry and a hydraulic diameter of 0.79 mm. The test section had twenty five parallel ports and they varied mass flux in the range from 200 to 600 kg $m^{-2}s^{-}1$ with heat fluxes between 5 and 20 kWm^{-2}. Friedel correlation [49] fitted the best with an average deviation of 22 %. Premoli correlation was used for void fraction calculation as recommended by Thome et al. [70]. Experimental measurements do not fit quite well with correlations, especially at low void fraction values where deviations are much higher.

Zhang and Webb [24] measured two-phase flow pressure drop of R134a, R22, and R404A in adiabatic conditions. The authors studied two circular copper tubes with diameters of 3.25 and 6.2 mm and a circular multi-port tube with a hydraulic diameter of 2.13 mm. They showed that Friedel [49] correlation did not fit correctly to experimental data. They modified it and provided a two-phase flow multiplier expression based on reduced pressure. The authors recommend this correlation for tube diameters in the range between 1 to 7 mm and a reduced pressure higher than 0.2. They recommended the use of Blasius correlation for single-phase flows. The authors also compared their correlation with Tran et al. [67] one and the results for reduced pressured in the range between 0.04 and 0.2 are quite similar if vapour quality is lower than 0.5. For higher values of vapour quality, Tran et al. [67] correlation provides higher pressure gradient values.

Webb and Kemal [10] analised condensation pressure drop in a 0.44 mm diameter tube. The authors were pioneers in measuring in such a small diameter tube. They obtained that for a fixed value of mass flow rate, pressure drop gradient increases with a decreasing diameter values.

Agostini et al. [71] studied boiling pressure drop of R134a in a vertical eleven parallel ports mini-channel tube of 2.01 mm hydraulic diameter. They observed that frictional pressure drop is quite similar to those produced in normal tubes with higher diameters.

Kawahara et al. [72] investigated the pressure drop in a 0.1 mm diameter mini-channel with a mixture of water and nitrogen.The two-phase flow multiplier was over-estimated with homogeneous model with their experimental data but it was correctly predicted with separated flow model by Lockhart and Martinelli [73].

Koyama et al. [14] studied heat transfer coefficient and pressure drop with R134a. Pressure drop values were correctly predicted by Mishima and Hibiki correlation. Koyama et al. [15] included new experiments to their previous database. They included two new multi-port tubes and developed a pressure drop correlation for the aforementioned tubes. This correlation is also based on the calculation of a two-phase flow multiplier with R134a condensation. They showed that Friedel correlation worked correctly at higher velocities but it was not able to predict pressure drop at low velocities where free convection is important.

Garimella et al. [26, 43, 74, 75] researched in condensation pressure drop of R134a in horizontal tubes with circular and non-circular shape in finned and non-finned multi-port tubes. They considered the different flow regimes that take places during condensation; they provided an expression for annular regime and another for slug/intermittent flow taking into account a three zones model. In this latter case, pressure drop is divided into two parts: the first one assumes that the film flow is modelled by a combination of film/bubble zone pressure gradient and the shear effect of the interfase film/bubble; the second part considers the pressure drop that takes place in the liquid flow between the film and the slug. In these articles, the authors studied circular tubes: two tubes of 3.05 mm and one of 4.91 mm of hydraulic diameter and three multi-port tubes with hydraulic diameters of 0.506, 0.761 and 1.52 mm. They also experimented with non circular section tubes; they used rectangular and triangular section tubes with hydraulic diameters of 0.424, 0.536, 0.732, 0.762, 0.799 and 0.839 mm.

Yu et al. [76] studied the pressure drop of boiling water and ethylene glycol in circular tubes of 2.98 mm hydraulic diameter. The authors proposed a correlation for two-phase flow multiplier.They detected that the exponential parameter of Martinelli correlated well with their data. They showed that Lockhart and Martinelli [73] correlation over-estimates their data.

Choi et al. [77] studied the pressure drop of boiling R410A, R407C, and CO_2 in horizontal mini-channles with hydraulic diameters of 1.5 and 3 mm. They proposed a correlation for liquid only two-phase flow multiplier that considers gravitational and surface tension effects with Froude and Weber non-dimensionless numbers. They observed an increase in pressure gradient at low vapour quality values and a decrease at vapour quality values higher than 0.6. They claimed that it could be due to initial dry out zone. The authors compared with typical correlations developed for higher diameter values. They also showed that Tran et al. [67] correlation developed for small diameter tubes predicted their data with lower deviation values than the average of the rest. After that, the same authors in Choi et al. [78] developed a correlation for R410A using the same tubes. In that case, the Chisholm parameter in the Lockhart and Martinelli correlation was fitted as a function of dimensionless numbers of Reynolds and Weber. The fit was made taking into account the effect of mass flow rate and surface tension on two-phase pressure.

Cavallini et al. [79] researched in two-phase flow pressure drop inside a rectangular multi-port mini-channel tube of 1.4 mm hydraulic diameter in adiabtatic conditions with R134a and R410A. Pressure drop measurement was made by saturation temperature measurement. The results showed that R134a pressure drop was correctly predicted with the available models. R410A pressure drop was not correctly predicted by existing models, all of them trended to over-estimate pressure drop values presenting Zhang and Webb correlation the lowest deviation values.

Garimella et al. [43] studied R134a condensation pressure drop in circular and multi-port tubes in the range of hydraulic diamters from 0.5 to 4.91 mm. He developed an experimentally validated multi-regime model for pressure drop prediction in circular horizontal tubes working with R134a.

Yue et al. [80] presented pressure drop characteristics of two-phase flows through two T-type rectangular microchannel mixers with hydraulic diameters of 528 and 333µm, respectively. The obtained pressure drop data of N_2–water two-phase flow in micromixers are analysed and compared with existing flow pattern-independent models. The Lockhart–Martinelli method was found to generally underpredict the frictional pressuredrop. Thereafter, a modified correlation of *"C"* value in the Chisholm's equation based on linear regression of experimental data is proposed to provide a better prediction of the two-phase frictional pressure drop. Also among the homogeneous flow models investigated, the viscosity correlation of McAdams indicates the best performance in correlating the frictional pressure drop data (mean deviations within ±20 % for two micromixers both). Finally, it is suggested that systematic studies are still required to accurately predict two-phase frictional performance in microchannels.

Cavallini et al. [20] studied the adiabatic pressure gradient of R236ea, R134a and R410A inside multi-port mini-channel tubes with thirteen parallel rectangular ports and a hydraulic diameter of 1.4 mm. They found out that Friedel [42], Zhang and Webb [24], Mishima and Hibiki [18] and Müller-Steinhagen and Heck [81] correlations fitted well with their R134a experimental data. They also showed that only Müller-Steinhagen and Heck [81] correlation deviation was the lowest when the data included R236ea experiments. They concluded that most of the correlations were not accurate when comparing R410A experimental data because they over-estimate experimental data. They provided that Zhang and Webb [24] correlation, previously mentioned, had the lowest average deviation 32 %.

Yun et al. [82] studied single circular shape and multi-port tubes with CO_2 and R410A respectively. They considered single-port tubes with hydraulic diameters of 0.98 and 2 mm and multi-port tubes with hydraulic diamters from 1.08 to 1.54 mm. They based their investigation in Lochart and Martinelli liquid two-phase flow multiplier. They derived expressions of *"C"* Chisholm parameter as functions of hydraulic diameter and provided different expressions for round and multi-port tubes. The models developed for higher diameter tubes under-estimate their experimental data. Only Tran et al. [67] correlation provides good results. Mishima and Hibiki model [18] under-estimate their data. In Yun et al. [82], the authors checked out that the correlations developed for CO_2 predicts quite well the experimental results of R410A.

Pehlivan et al. [83] studied two-phase flow pressure drop in horizontal circular mini-channels of 0.8, 1 and 3 mm diameter with a mixture of air and water. They compared experimental pressure drop with theorical, homogeneous, Friedel [42] and Chisholm models [84]. They found that homogeneous and Chisholm models [84] predictions were quite similar to experimental test for 1 and 0.8 mm diameter tubes. Therefore, the error standard deviation increased as diameter decreased pointing out that homogeneous model is not as accurate as it is in the range of macro-channels. Friedel model [42] trends to over-estimate experimental pressure drop data meanwhile Chisholm model [84] trends to under-estimate them.

Wen et al. [28] studied condensation pressure drop in a 2.46 mm diameter coil of three steps working with R600, R290 and a mixture at 50 % in weight of both of them. Pressure drops are a 59 %, 58 % and 36 % higher for R600, R600/R290 and R290 than R134a working under the same conditions. Experimental data are correctly predicted by Friedel correlation with an average deviation of 15.3 %.

English and Kandlikar [3] obtained a new model for two-phase flow pressure drop in a square tube of 1.018 mm hydraulic diameter in adiabatic conditions. Their investigations were made with mixtures of air and water in the range of 0.5-21.6 kg $m^{-2}s^{-1}$ and 4.0 - 12.0 kg $m^{-2}s^{-1}$ respectively. The tests were repeated adding a surfactant that modifies water surface tension and claimed for the importance of this effect in two-phase flow pressure drop.

Ribatski et al. [85] analysed the pressure drop in mini and micro-channels from published data. The database covers adiabatic and diabatic flows with eight different fluids. The overall mass velocity range goes from 23 up to 6000 kg $m^{-2}s^{-1}$. They checked out twelve pressure drop models, also some for macro-channels. Müller-Steinhagen and Heck [81], Mishima and Hibiki [18] and the homogeneous models with Cicchitti definition of two-phase flow viscosity provide the most acqurate presults.

Médéric et al. [29] studied condensation pressure drop inside a 100 mm length and 0.56 mm diameter tube made of borosilicate. They concluded that the two-phase flow pressure drop depends only on mass flow rate.

Jassim and Newell [86] developed a pressure drop model and void fraction map for 6-port micro-channels in order to provide a more accurate and common means of predicting void fraction and pressure drop. The models were developed for R134a, R410A, and air–water in six ports micro-channel at 10 ºC saturation temperature, qualities from 0 to 1, and mass fluxes varying from 50 to 300 kg $m^{-2}s^{-1}$. The probabilistic flow map models are found to accurately predict void fraction and pressure drop for the entire quality range and for all three fluids.

Revellin and Thome [87] experimentally investigated the pressure drop in mini-channels of 0.509 and 0.790 mm diameter under adiabatic conditions with R134a and R245fa. According to them, laminar to turbulent transitions is not predicted correctly by any model. Turbulent zone is better predicted by Müller-Steinhagen and Heck model [81]. In addition, a new two-phase homogeneous pressure drop correlation with a limited applicability range is proposed.

Field and Hrnjak [88] studied adiabatic pressure drop inside a rectangular shape mini-channel with a hydraulic diameter of 0.148 mm with several refrigerants. They proposed a new correlation for *"C"* Chisholm parameter based on vapour Reynolds number that relates viscous forces to surface tension effects. This correlation takes into account variable fluid properties of different refrigerants. Flow pattern effect is taken into account with Weber number based on the criteria of flow pattern map transition of Akbar et al. [89].

Qi et al. [90] analised liquid nitrogen boiling in mini-channels with diamters of 0.531, 0.834, 1.042 and 1.931 mm in diabatic and adiabatic conditions. Opposite to normal channels, the homogeneous model predicts two-phase flow pressure drop correctly meanwhile Lockhart and Martinelli, Friedel and the *"B"* Chisholm coefficient models diverge. This may be explained because the rate liquid to vapour density for nitrogen is very low and are well mixed at high mass velocities inside mini-channels due to the low liquid viscosity, so the behaviour is more similar to a homogeneous model.

Wen and Ho [37] researched on R290 and R600a condensation mixed with lubricating oil inside a 2.46 mm diameter coil. Inlet oil condentration was varied from 0 to 5 %. They observed that pressure drop increases with increasing mass flow rate, number of coil elbows and oil concentration.

Rosato et al. [91] studied adiabatic pressure gradient of R422D, substitute of R22 with a null ozone depletion power. R422D is a mixture of R125, R134a and R600a (65.1 % /31.5 % /3.4 % in weight). The investigations were made with a 3 mm diameter tube under usual working conditions of dry boilers. The model was developed for other refrigerants so the experimental data were compared with the phenomelogic method of Moreno-Quibèn and Thome [92] and the empirical models of Friedel [42], Grönnerud [93], Müller-Steinaghen and Heck [81] and Jung and Rademacher [94]. The conclusion was that Moreno-Quibèn and Thome method showed the best results.

Cavallini et al. [30] presented an adiabatic and condensing pressure drop model based on their own and other authors' experimental data.

Cheng et al. [95] presented a new flow pattern map and a new pressure drop correlation inside mini-channels with diameters in the range from 0.6 to 10 mm in the case of CO_2 boiling. The experimental conditions range for mass flux vary between 50 and 1500 kg $m^{-2}s^{-1}$, heat fluxes from 1.8 to 46 $kWm^{-2}$and saturation temperatures from -28 to 25 ºC. The authors compared their database of CO_2 boiling with multiple pressure drop correlations with poor predicting behaviours. So, they developed a new two-phase pressure drop model by modifying Moreno-Quiben and Thome model [92] and using an updated flow pattern map. A good predicition was obtained.

Cheng et al. [96] made a bibliographic revision about supercritical CO_2 cooling in micro and macro-channels. Blasius correlation predicts correctly frictional pressure drop, however it is recommended further research on that field because results differ so much. Oil concentration negatively affects pressure drop values increasing this value with higher oil concentrations.

Choi et al [78] investigated convective boiling pressure drop experiments in horizontal minichannels with a binary mixture refrigerant, R-410A. The test section was made of stainless steel tubes with inner diameters of 1.5 mm and 3.0 mm and uniformly heated by applying electric current directly to the tubes. Experiments were performed at inlet saturation temperature of 10 ºC, mass flux ranges from 300 to 600 $kgm^{-2}s^{-1}$ and heat flux ranges from 10 to 40 kWm^{-2}. The homogeneous model predicted well the experimental pressure drop, generally. A new pressure drop prediction method based on the Lockhart–Martinelli method was developed with 4.02 % mean deviation.

Pamitran et al. [97] used the same installation as Choi et al. [78] to study R744 (CO_2) under similar conditions. Experiments were performed at inlet saturation temperatures of -10, -5 and 10 ºC, mass flux ranges from 200 to 600 kg $m^{-2}s^{-1}$ and heat flux ranges from 10 to 30 kWm^{-2}. Finally, a new pressure drop prediction method based on the Lockhart–Martinelli method was developed with 9.41 % mean deviation.

Choi et al. [98] examined the two-phase flow boiling pressure drop and heat transfer for propane in horizontal minichannels. The pressure drop and local heat transfer coefficients were obtained for heat fluxes ranging from 5–20 kWm^{-2}, mass fluxes ranging from 50 - 400 kg $m^{-2}s^{-1}$, saturation temperatures of 10, 5 and 0 ºC, and vapour quality up to 1.0. The test section was the same as in Pamitran et al. [97] and Choi et al. [78]. This study showed the effect of mass flux, heat flux, inner tube diameter and saturation temperature on pressure drop and heat transfer coefficient. New correlations of pressure drop and boiling heat transfer coefficient were developed.

Jang et al. [99] studied the heat transfer and pressure drop characteristics of FC72 in small channel heat sinks, which were designed for liquid cooling of electronic components, by varying the mass flux, saturation temperature, and vapour quality. The small channels had circular cross-sections with diameters of 2 and 4 mm and length of 100 mm. The heat flux provided by the heaters in the copper block ranged from 0.5 to 3.0 Wcm^{-2}. Based on data comparisons, the existing pressure drop correlations were modified by introducing the effective viscosity including wall effects of the fluid in the small channel. The modified homogeneous pressure drop model yielded the best predictions in average. The measured heat transfer coefficient was also compared with the predictions obtained by using existing heat transfer correlations.

Saisorn and Wongwises [100] investigated adiabatic two-phase air–water flow characteristics, including the two-phase flow pattern as well as the void fraction and two-phase frictional pressure drop, in a circular micro-channel A fused silica channel, with an inside diameter of 0.53 mm is used as the test section. The test runs are done at superficial velocity of gas and liquid ranging between 0.37 – 16 and 0.005 – 3.04 ms^{-1}, respectively. The two-phase pressure drops are also used to calculate the frictional multiplier. The multiplier data show a dependence on flow pattern as well as mass flux. Finally a new correlation of two-phase frictional multiplier is also proposed for practical application.

Agarwal and Garimella [101] published a multi-flow model for pressure drop calculation with R134a condensation in horizontal mini-channels. They measured in two circular and six non circular tubes with diameters in the range from 0.41 to 0.8 mm. Mass flow rate studied are in the range from 150 to 750 kg $m^{-2}s^{-1}$ with vapour quality over the whole range from 0 to 1.The combined model presented predicts the 80 % of the data over whole range of flow conditions and tube geometries with a ±25 %.

Cavallini et al. [34] presented a pressure drop calculus model in single port mini-channels considering surface rougness. They observed that surface rougness affects single phase pressure drop in turbulent flow. The single phase measurements are correctly predicted by the existing models for macro-channles and their model correctly predicts two-phase flow pressure drop with a parameter of surface roughness.

Sun and Mishima [102] proposed a modification of Chisholm correlation [84] after studying two thousand and ninety two experiments from eighteen different publications. They checked that their last update works better than the correlations studied with an average relative error of only 29 % in the turbulent zone. The new correlation and Müller-Steinhagen and Heck correlation [81] present similar values and better prediction for refrigerants only.

Park and Hrnjak [36] analised adiabatic pressure drop of R744 inside multi-port circular mini-channels. The two-phase flow pressure drop of R744 increases with increasing values of mass flow rate, vapour quality, and decreasing values of saturation temperature. McAdams et al. correlation, based on a homogeneous model flow predicts pressure drop very accurate. On their investigation, the correlations which are based on homogeneous models for high diameter tubes values are very sharp and provide better predictions than those based on separated flow models. Mishima and Hibiki [18] provides the best results.

Cioncolini et al. [103] studied frictional pressure drop in adiabatic annular flows over the range macro to micro-scale. They compared twenty four experimental correlations against the database made from the investigation of twenty two tubes with three thousand nine hundred and eight tests for eigth gases. The diameter range covers from 0.517 to 31.7 mm. The models that fit the best are Lombardi [104], Friedel [42] and Barozcy [105] for macro-tubes; Lombardi [104], Müller-Steinhagen and Heck [81] for micro-tubes and the homogeneous model for two-phase flow viscosity calculation defined by Cicchitti. The authors also proposed a new correlation for macro-channels and the extension to micro-channels that provides the best results.

Hamdar et al. [106] investigated boiling pressure drop of HFC-152a in a horizontal square mini-channel of 1 mm in diameter. Tests were performed at a nearly constant system pressure of 600 kPa for mass flux ranging from 200 to 600 kg $m^{-2}s^{-1}$ and for heat flux ranging from 10 to 60 kWm^{-2}. The correlation of Müller-Steinhagen and Heck [81] was found to give a good agreement for prediction of mini-channel frictional pressure losses.

Pamitran et al. [107] presented a new publication with an experimental investigation on the characteristics of two-phase flow pattern transitions and pressure drop of R22, R134a, R410A, R290 and R744 in horizontal small stainless steel tubes of 0.5, 1.5, and 3.0 mm inner diameters. Experimental data were obtained over a heat flux range of 5 – 40 kWm^{-2}, mass flux range of 50 – 600 kg $m^{-2}s^{-1}$, saturation temperature range of 0 – 15 ºC, and quality up to 1.0. The experimental pressure drop was compared with the predictions from some existing correlations. A new two-phase pressure drop model based on a superposition model for two-phase flow boiling of refrigerants in small tubes is presented.

Del Col et al. [40] studied adiabatic pressure drop with R1234yf and compared the results with R134a [34]. They obtained the R1234yf pressure drop was between a 10 to 12 % lower compared with R134a under the same conditions. The authors explain this behaviour by the fact that R1234yf reduced pressure is about a 20 % higher than R134a in the tested conditions. From that point of view, R1234yf behaviour is better than R134a.

Ma et al. [108] researched on two-phase flow pressure drop with water, ethanol, n-propanol, and air flowing inside. The authors observed that pressure drop was severely affected by capillarity number that takes into account the ratio of viscous forces and liquid-gas interface tension. They obtained a modified *"C"* Chisholm parameter to correctly predict experimental data. They included aspect ratio and surface tension to the new *"C"* correlation as no correlation predicted correctly the whole database.

Li and Wu [209] developed a new correlation for pressure drop in mini and micro-channel with a database from open literature and diverse conditions and fluids. A particular trend was observed with the Bond number that distinguished the data in three ranges, indicating the relative importance of surface tension.

Saisorn et al. [110] investigated R134a pressure drop in a circular steel tube of 1.75 mm diameter with heat fluxes from 1 to 83 kWm^{-2}. Mass flow rate range was from 200 to 1000 kg m^{-2}s^{-1}.Pressure drop is obtained substracting momentum pressure drop to the measurement read by the differential pressure transmitter.

Ducoulombier et al. [111] investigated two-phase pressure drops in a single horizontal stainless steel micro-tube having a 0.529 mm inner diameter. Experiments were carried out in adiabatic conditions at four saturation temperatures of -10; -5; 0; 5 ºC and mass fluxes ranging from 200 to 1400 kg m^{-2}s^{-1}, for inlet qualities up to unity. Measurements have been compared to the predictions of well-known methods. The Müller-Steinhagen and Heck correlation [81] and the Friedel correlation [42] gave the best fit as well as the homogeneous model when the liquid viscosity is used to represent the apparent two-phase viscosity. The apparent viscosity of the two-phase mixture was found larger than the liquid viscosity at low vapour qualities, namely at the lowest temperatures. Hence, a new expression to determine the equivalent viscosity was suggested as a function of the reduced pressure. Lastly, the Chisholm parameter from the Lockhart–Martinelli correlation was found lower than expected and mainly dependent on the saturation temperature.

Bohdal et al. [41] analised condensing R134a and R404A pressure drop in mini-channels. They concluded that the pressure drop of these refrigerants was correctly predicted with Friedel [42] and Garimella correlations [26]. In addition, they proposed a new pressure drop correlation. The range of validity is described in the publication.

Zhao et al. [47] studied CO_2 pressure drop mixed with lubricating oil at super-critical pressures inside horizontal tubes with inner diameters of 1.98 and 4.14 mm. The authors observed that Petukhov [49] correlation predicted reasonably well the data without oil. The entrance of lubricating oil increases pressure drop values.

Phan et al. [112] investigated water boiling pressure drop inside mini-channels with different contact angles between liquid and walls. They concluded that the influence of contact angle affects severely the two-phase flow pressure drop value reaching differences up to 170 % between wet and dry surfaces. The Lockhart and Martinelli [73] method gives out the best predictions of experimental values, the second position is the Bankoff [113] method and thirdly the Müller-Steinhagen and Heck [81] model. The authors proposed a new procedure to calculate pressure drop by means of a "wet pressure drop". The "wet pressure drop" can be calculated as the difference between two-phase flow experimental, frictional and momentum pressure drops obtained with Lockhart and Martinelli [73] model.

Donaldson et al. [114] analised the two-phase flow pressure drop of a mixture of air and water flowing inside a straight tube and a coil, both with inner diameter of 1 mm. They investigated the influence of bubble/slug length, curve radius and flow pattern transition over pressure gradient in the coil. The pressure drop model proposed by Kreutzer et al. [115] for straight channels predicted the coil data with the use of a multiplier as happened with the straight channel. In addition, they obtained empirical correlations for friction factor for each flow region.

Choi et al. [116] experimented with water and nitrogen flowing in a rectangular mini-channel. Decreasing values of hydraulic diameter makes *"C"* value of Lockhart and Martinelly to decrease. This behaviour represents that the weak interaction between the two phases. Zhang and Webb [24] correlation correctly predicts the pressure drop in rectangular mini-channels. The value of *"C"* parameter in bubbly flow is higher than in annular flow, which means that bubly flow is much more important than annular flow in pressure drop value.

Cavallini et al. [50] studied R32 and R245fa pressure drop in a 0.96 mm mini-channel. The tested refrigerants are quite different to the classic R134a; in addition the R32 is classified as high pressure refrigerant and R245fa as low pressure fluid. The authors used these two fluids by their different thermodynamic properties and in that way to be able to check the useness of the existing models. As expected, the pressure drop values of R245fa are quite higher.

Choi and Kim [117] analised the two-phase flow pressure drop in mini-channels with a mixture of water and nitrogen under adiabatic conditions. They proposed new correlations for homogeneous and separated flow models.

Foroughi and Kawaji [118] published an investigation about pressure drop of a mixture of water and silicon oil in a mini-channel of 0.25 mm diameter.At the beginning of the investigation, the mini-channel was filled with oil, a little film of this oils remained on the walls with dispersed water flowing in the core. The total pressure drop is a linear contribution of water and oil pressure drop.

Wu et al. [119] studied CO_2 boiling pressure drop inside a stainless steel mini-channel. The test section has a hydraulic diameter of 1.42 mm and 300 mm lenght. The range of mass fluxes from 300 to 600 kg $m^{-2}s^{-1}$ with heat fluxes from 7.5 to 29.8 kWm^{-2}. Experimental tests were performed at saturation temperatures from -40ºC to 0ºC. The authors compared the results with Cheng et al. [33] model with good prediction behaviour. In adittion, they proposed a modification of friction factor for mist flow. They claimed that pressure drop increases with increasing mass fluxes and decreasing saturation temperature due to thermodynamic properties change.

Jige et al. [52] studied the condensation process of pure refrigerants R134a and R32 in a horizontal multi-port tube. The test tube is made of aluminium alloy with 0.85 mm in hydraulic diameter. The experiments were carried out in the mass velocity range of 100 to 400 kg $m^{-2}s^{-1}$ at saturation temperatures of 40 and 60 ºC. They experimentally measured heat transfer coefficient and pressure drop.

Fang et al. [120] analised frictional pressure drop inside mini-channel tubes at super-critical pressures. Their analysis showed that none of the correlations is able to predict pressure drop satisfactorily. They proposed a new correlation for frictional pressure drop based on other author's experimental data available in the literature. They obtained an improvement of 10 % from the best fitting correlation published by then.

Zhao et al. [47] described the heat transfer and the pressure drop characteristics of CO_2 mixed with small amounts of compatible lubricating oil at super-critical pressures inside horizontal tubes with inner diameters of 1.98 mm and 4.14 mm during cooling. The heat transfer coefficients and pressure drops were measured. The results show that for the oil-free cases, the correlation proposed by Dang and Hihara accurately predicted the heat transfer coefficients and Petukhov's correlation was found to predict the frictional pressure drops reasonably. Entrainment of the lubricating oil reduced the heat transfer coefficients and increased the pressure drops. Their analysis showed that the heat transfer coefficients of the CO_2/oil mixture are strongly related to the density and viscosity ratios of the oil to the CO_2. An empirical correlation was developed based on the measured data, which predicts most of the experimental data within a deviation of 20%.

Park et al. [121] analised boiling pressure drop of FC72 in micro-channels of 0.061 and 0.278 mm with the following range of mass fluxes, from 188 to 1539 kg $m^{-2}s^{-1}$and heat fluxes from 0.6 to 45.1 kWm^{-2}. This refrigerant is only used in power electronic components because it is not corrosive, very stable, not toxic and has not high saturation pressures.The authors compared their experimental results with those provided by models available for usual refrigerants in mini-channels reaching a good prediction of experimental data. Macro-tube correlations can not be used for pressure drop predictions.

Kaew-on et al [122] investigated boiling pressure drop in multi-port mini-channel tubes with R134a with hydraulic diameters of 1.1 and 1.2 mm. In their inverstigation, experimental measurements were compared against nine widely accepted pressure drop correlations for mini and macro-channels. The authors performed the vaporisation of the refrigerants thanks to a hot water external chase. The range of mass fluxes tested was from 350 to 980 kg $m^{-2}s^{-1}$, heat fluxes from 18 to 80 kWm^{-2} and the studied saturation pressures that correspond to 4, 5 and 6 bars. The inlet vapour quality value is constant along the tests with a value of 0.05. Finally, they presented a comparison with some existing correlations. Friedel correlation [42] fitted the best with their experimental data.

Kim et al. [51] studied multi-port mini-channel pressure drop working with FC2. They provided a detailed model for pressure drop calculation. They also analised the experimental frictional pressure drop measurements with the existing correlations available in the open literature for homogeneous and separated flow.

Sur and Liu [123] studied adiabatic frictional pressure drop of mixtures of air and water inside mini-channels of 0.1, 0.18 and 0.324 mm hydraulic diameters. The authors analysed the influence of channel dimensions and superficial velocities over pressure drop. The results showed that frictional two-phase pressure drop is predicted more accurately by the models based on flow patterns than those based on homogeneous or separated flow models.

Kim and Mudawar [124] published an approach for two-phase pressure drop under adiabatic and condensing conditions in mini and micro-channels. They collected 7115 data for pressure drop from thirty six publications with seenteen different fluids. The diameter ranges tested go from 0.0695 to 6.22 mm, mass velocities from 4 to 8528 kg $m^{-2}s^{-1}$. The model proposed provides excellent predictions for the entire database with uniform accuracy being able to predict pressure drop for single and multi-port tubes.

Son and Oh [125] investigated condensation pressure drop of R22, R134a, and R410A in a single tube of 1.22 m length and an inner diameter of 1.77 mm. The measurements were made with mass fluxes from 450 to 1050 kg $m^{-2}s^{-1}$and a saturation temperature of 40 ºC. The authors analised the behaviour of the three different refrigerants and they also compared experimental values with fourteen two-phase flow pressure drop correlations. Finally, they provided a new pressure drop model based on the superposition of several models of pressure drop.

Bohdal et al. [126] analised the condensing R134a, R404a and R407C pressure drop in mini-channel tubes with hydraulic diameter in the range, 0.31 to 3.30mm. Experimental data are correctly predicted by Garimella and Friedel correlations. In adittion, the authors porposed a new correlation for pressure drop calculation.

Xu et al. [127] reviewed twenty nine correlations for two-phase flow pressure drop with three thousand, four hundred and eighty experimental data with hydraulic diameters from 0.0695 to 14 mm and mass fluxes from 8 to 6000 kg $m^{-2}s^{-1}$. The authors compared the correlations and experimental data and discussed the effects of channel shape, mass flux, and fluid properties.

Zhang et al. [55] studied R22, R410A and R407C condensation pressure drop inside two circular tubes of 1.088 and 1.289 mm diameter at saturation temperatures of 30 and 40 ºC. The mass fluxes studied went from 300 to 600 kg $m^{-2}s^{-1}$. The experimental data were compared with correlations developed for tubes with diameter higher than 3 mm.

Kim and Mudawar [128] developed a method to predict boiling flow pressure drop in mini-channel heat sinks. Their model captures the tendencies of pressure drop with different fluids, HFE7100, water, and R134a, independently of single or two phase flow. The hydraulic diameter corresponds to values between 0.1757 mm and 0.4159 mm with a test lenght of 10 mm.

Harirchian and Garimella [129] investigated local heat transfer coefficients and pressure drops during boiling of the dielectric liquid fluorinert FC-77 in parallel microchannels. A regime-based prediction of pressure drop in microchannels is presented by computing the pressure drop during each flow regime that occurs along the microchannel length. The results of this study reveal the promise of flow regime-based modelling efforts for predicting heat transfer and pressure drop in microchannel boiling.

Saraceno et al. [130] performed different tests for a fluorinert fluid FC-72 as coolant. The test section consists of a horizontal 1 mm inner diameter stainless steel tube having a heated length (Joule effect) of approximately 60 mm. The mass flux range is between 1000 and 2000 kg $m^{-2}s^{-1}$ while the applied heat flux is between 10 and 150 kWm^{-2}. By means of a preheater, the coolant inlet temperature is changed setting the operating pressure in a range between 3 and 7 bars, a broad spectrum of subcooling degree at inlet test section was achieved. The local heat transfer coefficients were evaluated for both subcooled and saturated flow boiling regimes. The experimental data show an increase of local heat transfer coefficient for increasing values of heat flux, with a weak dependence on the vapour quality. The experimental values obtained were compared with those from the adoption of one of the main heat transfer correlations in the literature. A substantial independence of heat transfer coefficient from vapour quality is highlighted in the saturated boiling region. The Liu and Winterton [131] correlation seems to predict the experimental datawell.

Kim et al. [51] performed experimental investigation on condensation of FC72 in a square mini-channel of 1 mm hydraulic dyameter. A detailed pressure model is presented which includes all components of pressure drop across the micro-channel. Different sub-models for the frictional and accelerational pressure gradients are examined using the homogeneous equilibrium model (with different two-phase friction factor relations) as well as previous macro-channel and mini/micro-channel separated flow correlations. Unexpectedly, the homogenous flow model provided far more accurate predictions of pressure drop than the separated flow models. Among the separated flow models, better predictions were achieved with those for adiabatic and mini/micro-channels than those for flow boiling and macro-channels.

Xu and Fang [132] developed a new correlation of two-phase frictional pressure drop for evaporating flow in pipes. They used a database for mini and macro-channels with hydraulic diameters from 0.81 to 19.1 mm and mass flux from 25.4 to 1150 kg $m^{-2}s^{-1}$. The new correlation has lower mean absolute relative deviation than the best correlation studied.

Zhang et al. [57] investigated two-phase pressure drop during CO_2 condensation inside a mini-channel condenser with a hydraulic diameter of 0.9 mm. The experimental measurements were made at saturation temperatures from -5ºC to 15 ºC and mass velocities of 180, 360 and 540 kg $m^{-2}s^{-1}$. Friedel´s correlation [42] could be applied within relative errors of 30 %.

Zhu et al. [133] experimentally measured the flow frictional resistance characteristics of kerosene RP-3 in a horizontal isothermal tube with an inner diameter of 1.78 mm al supercritical pressures. Frictional pressure drop and friction factor were investigated under the pressures of 3-6 MPa, temperatures from 329 to 810 K and mass velocities of 803.71 to 1607.4 kg $m^{-2}s^{-1}$. The experimental friction factors were compared with the calculated results via the Blasius and Filonenko correlations. Based on the experiment data, a new friction factor correlation was proposed, which showed much less deviation of friction factor for sub- and super-critical kerosene RP-3.

Al-Hajri et al. [58] experimentally studied two-phase condensing flows of R134a and R245fa in a single mini-channel of 0.7 mm diameter with high aspect ratio. Pressure drop is accurately predicted by Lockhart-Martinelli with deviation lower than 20 %.

Copetti et al. [134] experimentally measured R600a pressure drop in a 2.6 mm tube. In comparison with R134a, R600a has higher pressure drops. For frictional pressure drops, deviations from results obtained by usual correlations were quite large.

Dang et al. [135] experimentally investigated pressure drop of R744 with different oil concentrations in tubes with hydraulic diameter of 2, 4 and 6 mm at mass fluxes of 360 to 1440 kg $m^{-2}s^{-1}$ at 15 ºC. The effect of oil is negative due to larger measured pressure drops.

Del Col et al. [136] investigated frictional pressure drop during adiabatic liquid-vapour flow inside mini-channels with hydraulic diameter ranging from 0.96 to 2 mm. They updated the friction pressure drop model presented by Cavallini et al. [34, 137] and compared with other correlations.

Vakili-Farahani et al. [138]experimentally tested upward flow boiling pressure drop in a multipor mini-channel tuve of 1.4 mm of hydraulic diameter with R1234ze and R245fa.

Heo et al. [59] reported a study about in-tube condensation heat transfer characteristics and pressure drop of CO_2 in different mini-channels. Multi-port minichannels had hydraulic diameters of 1.5, 0.78 and 0.68 mm and they were tested from -5 to 5 ºC of saturation temperatures. The model of Mishima and Hibiki [18] showed the lowest deviations.

Heo et al. [60] published a study about condensation heat transfer coefficient and pressure drop of CO_2 in a multiport mini-channel with a hydraulic diameter of 1.5 mm. Mass flux variation was from 400 to 100 kg $m^{-2}s^{-1}$ and saturation temperatures from -5 to 5 ºC. The Mishima and Hibiki [18] model showed mean deviation of 29.1 %.

Li et al. [139] experimentally measured flow boiling pressure drop of R1234yf, R32 and their mixtures with different mass fractions (80/20 and 50/50) in a smooth horizontal tube of 2 mm of inner diameter. Several models for pressure drop were compared with experimental measurements but Müller-Steinhagen and Heck [81] outperformed the rest of models.

Liu et al. [61] experimentally investigated heat transfer and pressure drop during condensation of R152a in circular and square mini-channels with hydraulic diameters of 1.152 and 0.952 mm, respectively. They analysed their data with those provided by other correlations. In particular, Koyama et al. [15] underestimated the data for both micro-channels while Agarwal and Garimella [101] overestimated the data for the square microchannel. Predictions of Cavallini et al. [137] showed large root-mean-square errors for data in both circular and square micro-channels.

Maqbool et al. [140] reported the flow boiling heat transfer and pressure drop results of propane in a vertical circular stainless steel minichannel having an internal diameter of 1.70 mm and a heated length of 245 mm. Two phase heat transfer and pressure drop experiments were performed at saturation temperaturesof 23, 33 and 43 ºC. Heat flux was varied from 5 to 280 kWm^{-2} and mass flux wasvaried from 100 to 500 kg $m^{-2}s^{-1}$. The results showed that the two phase frictional pressure drops, as expected, increase with the increase of mass flux, vapour qualities, and with the decrease of saturation temperature. After incipient dryout, the authors observed a decrease in heat transfer coefficient and pressure drop, especially at higher mass fluxes. The two-phase frictional pressure drop correlations of Müller-Steinhagen and Heck [81], Friedel [42] and two phase flow heat transfer correlations of Cooper and Liu and Winterton [131] predicted the experimental results well.

Xu and Fang [141] published a new correlation of two-phase frictional pressure drop for condensing flow in pipes. In this paper, an overall survey of correlations and experimental investigations of two-phasefrictional pressure drop was carried out. The 525 experimental data points of 9 refrigerants were gathered from literature, with hydraulic diameter from 0.1 to 10.07 mm, mass flux from 20 to 800 kg $m^{-2}s^{-1}$, and heat flux from 2 to 55.3 kWm^{-2}. The 29 correlations considered were evaluated against the experimental database, among which the best one has a mean absolute relative deviation (MARD) of 25.2%. Based on all theexperimental data, a new correlation which has an MARD of 19.4% was proposed, improving significantlythe prediction of two-phase frictional pressure drop for pipe condensing flow.

Table 2.3 summarises the different research studies of frictional pressure drop considered in previos paragraphs. Many of them are related with heat transfer coefficients publications because in the same experiment both measurements can be recorded.

Table 2.3. Pressure drop publications considered in that study.

Researchers	Year	Fluid	Geometry	d_h (mm)	q (kW/m^2)	t_{sat} or p_{sat}	Mass velocity, (kg m^{-2}s^{-1})
Lazarek and Black	1982	R113	C	3.1	14-380 (boiling)	p_{sat} = 130-410 kPa	125-750
Ungar and Cornwell	1992	R717	C	1.46, 1.78, 2.58			
Mishima and Hibiki	1996	Air and water	C	-	Adiabatic	-	--
Tong et al.	1997	Air	C	1.05 – 2.44	Boiling (50000 – 80000)	22 - 66ºC 400-1600 kPa	25 - 45
Yan and Lin	1999	R134a	C	2	Condensation	25-30 ºC 4050 kPa	100-200
Yan and Lin	1999	R134a	C	2	5 - 31 5 - 20 (boiling)		50-200
Triplett et al.	1999	Air and water	MC, MST	1.09, 1.1 1.45, 1.49	Adiabatic	Atmospheric at exit	LV: 0.02 to 8 m/s. GV: 0.02 to 80 m/s
Tran et al.	2000	R134a, R22, R113	C, R	2.46, 2.92 y 4.06x1.7 mm	~4-32 (boiling)	p_{sat} = 138-856 kPa	Up to 500
Pettersen et al.	2000	R-744	MC	0.79	5-20 (boiling)	0-20 ºC	200 - 600
Zhang and Webb	2001	R134a, R22, R404A	C, MC	3.25, 2.13	Adiabatic	25-65 ºC	200, 400, 600, 1000
Ju Lee and Yong Lee	2001	Air and water	R	0.78,1.91,3.64,6.67	Adiabatic	Atmospheric pressure	LV: 0.03 to 2.39 m/s. GV: 0.05 to 18.7 m/s
Webb and Kemal	2001	R134a	MR, MRmf	0.44 - 1.56	Condensation	65 ºC	300-1000
Zhao and Bi	2001	Air and water	T	0.866,1.443,2.886			

Researchers	Year	Fluid	Geometry	d_h (mm)	q (kW/m^2)	t_{sat} or p_{sat}	Mass velocity, (kg m^{-2}s^{-1})
Niño et al.	2001	Air and water, R-134a, R410A	M	1.02, 1.54		10, 20, 35 ºC	55-280
Yu et al.	2002	Water	C	2.98	~75-300 (boiling)	p_{sat} = 200 kPa	50-200
Agostini et al.	2002	R134a	MR	2.01	0.84 - 22 (boiling)	p_{sat} = 2000 kPa	28 – 800
Kawahara et al.	2002	Air and nitrogen	C	0.1 mm	Adiabatic	p_{sat} = 200, 1374, 3435, 13740 kPa	LV: 0.02 to 4 m/s. GV: 0.1 to 60 m/s
Garimella et al.	2002, 2003, 2005	R134a	C, MC, MS, MR, MT	0.424-4.91	With and without condensation	-	150 – 750
Koyama et al.	2003a	R134a	MR	0.8, 1.11	Condensation	p_{sat} = 1700 kPa	100-700
Koyama et al.	2003b	R134a	MR, MRmf	1.062, 0.807, 0.889 and 0.937 mf.	Condensation	p_{sat} = 1700 kPa	100-700
Cavallini	2004	R134a, R410a	MS	1.4	Adiabatic	40ºC	400-1000 600-1400
Garimella	2004	R134a	C	0.5-4.91	Condensation	52.3 ºC(1396 kPa)	150 – 750
Yue	2004	Water + N_2	R	0.528, 0.333	Adiabatic		0-30ml/s

Researchers	Year	Fluid	Geometry	d_h (mm)	q (kW/m^2)	t_{sat} or p_{sat}	Mass velocity, (kg m^{-2}s^{-1})
Yun et al.	2005	CO_2	C, MC	0,98, 2 (C) 1.08, 1.54 (MC)	7-48 5-20 (boiling)	0, 5 and 10 ºC	500 3570 100-400
Choi et al.	2005	R410A, R407C, CO_2	C	1.5, 3	5-20 (boiling)	10 ºC	200-600
Cavallini et al.	2005a, 2006a	R236ea, R134a, R410A	MR	1.4	Adiabatic	40ºC p_{red}= 0.1-0.5	200-1000
Yun et al	2006	R410A	MC	1.36, 1.44	10-20 (boiling)	0, 5, 10 ºC	200-400
Pehlivan et al.	2006	Air and water	C	0.8, 1, 3	Adiabatic		LV: 0.02 to 1 m/s. GV: 10 to 100 m/s
Wen et al.	2006	R-600, R600/R-290 (50%/50%), R-290	C - coil	2.46	5.2 - Condensation	40 ºC	205 - 510
English and Kandlikar	2006	Air and water	S	1	Adiabatic		LV:0.005-0.022 m/s. GV: 3.19-10.06 m/s
Ribatski et al.	2006	R134a,R113, R12, R11, R123, R141b, CO2, R407C, R410A,R22, water	C, R	0.4 – 3.6	5 to 180 boiling	0 to 105 ºC	100 - 800
Médéric et al.	2006	R134a	C	0.56	Condensation	40 ºC	3.4 – 13.8
Jassim and Newell	2006	R134a, R410A, air+water	MC	1.54	Adiabatic	10 ºC	50-300

Researchers	Year	Fluid	Geometry	d_h (mm)	q (kW/m^2)	t_{sat} or p_{sat}	Mass velocity, (kg m^{-2}s^{-1})
Revellin and Thome	2007	R134a R245fa	C	0.509, 0.790	Adiabatic	26, 30, 35 ºC	210 – 2094
Field and Hrnjak	2007	R134a, R410a, R290, R717	R	0.148 mm	Adiabatic	22 to 25 ºC	300 – 700
Qi et al.	2007	Nitrogen		0.531, 0.834, 1.042, 1.931 mm	5.09 to 21.39 (boiling) Diabatic and adiabatic	78.2 to 79.8 K	440 to 3000
Cheng et al.	2008	CO_2	C	0.6-10 mm	Boiling 1.8-46 kW/m^2	-28 a 25 ºC	50-1500
Choi et al.	2008	R410A	C	1.5, 3	10-40 (boiling)	10 ºC	-
Cavallini et al	2008	R134a, R236ea,R410, R22, R404a, R744	Calculation model with other authors data. MS, MC, C	0.51-3.25	Adiabatic	0 - 65 ºC	150-1400
Cheng et al.	2008	CO_2 (R744)			Review of available literature		
Jang et al.	2008	FC72	C	2, 4	5-30 boiling	45, 55, 65, 75 ºC	265 - 440
Cheng et al.	2008	CO_2 (R744)	C	0.6 - 10	1.8 – 46 boiling	-28 - +25 ºC	50 - 1500
Saisorn and Wongwises	2008	Air + water	C	0.53	Adiabatic		J_l=0.37-16; J_g=0.005-3.04m/s
Choi et al.	2008	R410A	C	1.5, 3.0	Boiling 10 - 40	10 ºC	300 - 600
Pamitran et al.	2008	R744	C	1.5, 3.0	Boiling 10 - 30	-10, -5, +10 ºC	200 - 600
Agarwal and Garimella	2008	R134a	MC, MS, MB, MT, MN	0,42 – 0,,8	Condensation	52,3 ºC	150 - 750
Choi et al.	2009	R290	C	1.5, 3.0	Boiling 5 - 20	10, 5, 0 ºC	50 - 400
Cavallini et al	2009	R134a, R32	C	0.96	Adiabatic	39-41 ºC	200-1000

Researchers	Year	Fluid	Geometry	d_h (mm)	q (kW/m^2)	t_{sat} or p_{sat}	Mass velocity, (kg m^{-2}s^{-1})
Wen and Ho	2009	R-290, R600a + oil	C	2.46 mm	Condensation	40 ºC	300 – 600
Rosato et al.	2009	R422D	C	3.00	Adiabatic	-9.2 to 11.8 ºC (400 to 780 kPa)	198-350
Sun and Mishima	2009	R22, R123, R134a, R236ea, R245fa, R404a, R407C, R410a, CO_2, agua + aire, agua	Single and multi-port	0.509 - 6	Adiabatic and diabatic	Several	50 - 2000
Park and Hrnjak	2009	CO_2 (R744)	MC	0.89	Adiabatic	-15 ºC -25 ºC	200-400 600-800
Cioncolini et al.	2009	Water- (vapour, argon, nitrogen, air) R134a, R245fa		0.517 a 31.7	Adiabatic		184-4398
Hamdar et al.	2010	HFC-152a	S	1.0	Boiling 16 - 60	600 kPa	200 - 600
Pamitran et al.	2010	R22, R134, R410A, R290, R744	C	1.5, 3.0	5 - 40	0 – 15 ºC	50 - 600
Del Col et al	2010	R1234yf	C	0.96	Adiabatic	40 ºC	400 - 600 – 800

Researchers	Year	Fluid	Geometry	d_h (mm)	q (kW/m^2)	t_{sat} or p_{sat}	Mass velocity, (kg m^{-2}s^{-1})
Ma et al.	2010	Air+water, Air + ethanol, Air + n-propanol	R	100 µm x(200,400,800,200) µm	Adiabatic	298.15K	20 – 300
Li and Wu	2010	Data base with 12 fluids	Several	Several	Adiabatic	Several	Several
Saisorn et al.	2010	R-134a	C	1.75mm	Boiling 1-83kW/m^2	800, 1000, 1300 kPa	200-1000
Ducolombier et al.	2011	R744	C	0.529	Adiabatic	-10 to 5 ºC	200 – 1400
Bohdal et al.	2011	R134a, R404a	C	0.31 to 3.30 mm	Condensation	30 – 40 ºC	100 to 1300
Oh and Son	2011	R134a, R22, R410a	C	1.77 mm	Condensation	40 ºC	450 – 1050
Zhao et al.	2011	CO_2 (R744) + oil	-	1.98 - 4.14	Condensation	8000-11000 kPa	400-1200
Phan et al.	2011	Water	R	0.96	Condensation	Atmospheric pressure	100 to 120
Donaldson et al.	2011	Water, air + water	C - Serpentine	1	Adiabatic		LF: 180-95 ml/min GV: 10-15 ml/min
Choi et al.	2011	Water and nitrogen	R	0.49, 0.322, 0.143	Adiabatic		LV: 0.06-1. GV 0.06-71
Cavallini et al.	2011	R32, R245fa	C	0.96	Adiabatic	40 ºC	100 - 1200
Yong Park et al.	2011	FC-72	MS	0.006 0.258	Boling 0.6-45.1 kW/m^2	52.8, 84.4 ºC	188 - 1539

Researchers	Year	Fluid	Geometry	d_h (mm)	q (kW/m^2)	t_{sat} or p_{sat}	Mass velocity, (kg m^{-2}s^{-1})
Kaew-On et al.	2011	R134a	MR	1.1 1.2	Boiling	4,5,6 ºC	350 - 980
Kim S-M and Mudawar	2011	Fc-72	MS	1	Condensation	57.2, 62.3 ºC	68-367
Choi and Kim	2011	Water and nitrogen	R	0.141, 0.143, 0.304, 0.322, 0.490	Adiabatic		LV: 0.06/1 GV: 0.06/72
Foroughi and Kawaji	2011	Water and oil	C	0.25	Adiabatic	Atmospheric	Water:2 to 2200µL/min Oil: 3 to 57µL/min
Wu et al.	2011	R744	C	1.42	Boiling	-40ºC, 0 ºC	300 - 600
Phan et al.	2011	Water	R	0,91	Boiling	Atmospheric	100-120
Sur and Liu	2011	Water	C	0.1, 0.18, 0.324	Adiabatic		LV: 0.002.3.498 GV 0.0021-192.232
Wu et al.	2011	CO_2	C	1.42	Boiling. 4-28 kW/m^{2}K	-40 a 0 ºC	300-600
Fang et al.	2011	R410, R404, R22, R744,	Calculation model with others autor data C, MC	0,5 – 7,75	Boiling	20 – 72 ºC	200-1200
Jige et al.	2011	R134a, R32	MR	0.85	Condensation	40, 60 ºC	100 - 400
Zhao et al.	2011	R744/ R744+oil	C	1.98, 4.14	Condensation	8000 – 11000 kPa. 20 – 100 ºC	400 - 1200
Kaew-On	2012	R134a	MS	1.1, 1.2	Boiling 18-80	400, 500, 600 kPa	350-980

Researchers	Year	Fluid	Geometry	d_h (mm)	q (kW/m^2)	t_{sat} or p_{sat}	Mass velocity, (kg m^{-2}s^{-1})
Kim and Mudawar	2012	Multiple	Several	0.0695 a 6.22	Adiabatic and condensation	Multiple	4 a 8528
Son and Oh	2012	R134a, R410A, R22	C	1.77	5-30	40 ºC	450 - 1050
Bohdal et al.	2012	R134a, R404a and R407C	C	0.31 – 3.30	0 - 100	20 - 50 ºC	0 - 1300
Xu et al.	2012	Multiple	Several	0.0695 a 14	2-150 – Boiling and condensation	Several	8 to 6000
Zhang et al.	2012	R22, R410A, R407C	C	1.088 and 1.289	Condensation	30, 40 ºC	300 a 600
Kim and Mudawar	2012	HFC 7100, water and R134a	MR	0.1757 – 0.4159	Boiling	-30 ºC	670 - 5550
Harirchian and Garimella	2012	FC77	R	severals	25 - 380		225 - 1420
Saraceno et al.	2012	FC72	C	1	10 - 150	300 – 700 kPa	1000 - 2000
Kim et al.	2012	FC72	MS	1	Condensation	57.2 – 62.3 ºC	65 - 367
Xu and Fang	2012	Database		0.81 – 19.1	0.6 - 150	Several	24.4 - 1150
Xu et al.	2012	Database		0.0695 - 14	Database	Several	8 - 6000
Zhang et al.	2013	R744	C	0.9	Condensation	-5 – 15 ºC	180, 360, 540
Al-Hajri et al.	2013	R134a, R245fa	S	0.7	Condensation	30 – 70 ºC	50 - 500
Copetti et al.	2013	R-600a	C	2.6	44-95 Boiling	22 ºC	240 - 440
Dang et al.	2013	R744	C	2, 4, 6	4.5-36 Boiling	15 ºC	360-1440
Del Col et al.	2013	R134a, R1234yf, R32, R245fa	C,S,T, irregular	0.96 - 2	Adiabatic	26-50 ºC	200 - 1000
Vakili-Farahani	2013	R1234ze, R245fa	MS	1.4	3 - 107	30 - 70 ºC	50 - 400
Heo et al.	2013	R744	MR	1.5, 0.78, 0.68	Condensation	-5 – 5 ºC	400 - 800
Heo et al.	2013	R744	MR	1.5	Condensation	-5ºC – 5 ºC	400 - 1000

Researchers	Year	Fluid	Geometry	d_h (mm)	q (kW/m^2)	t_{sat} or p_{sat}	Mass velocity, (kg m^{-2}s^{-1})
Kim and Mudawar	2013	H20, R717, FC72, CO2, R134a, R235fa,CO2, R22, R410A	Several from database. From 0.349 up to 5.35 mm. Circular single tuve and multiport rectangular.		Boiling	Several	33 - 2738
Li et al.	2013	R1234yf, R32, mixture 50/50 and 80/20	C	2.0	Boiling 6-24	15 ºC	100-400
Liu et al.	2013	R152a	C, S	1.152, 0.952	Condensation	40, 50 ºC	200-800
Maqbool et al.	2013	R290	C	1.7	Boiling 5 - 280	23, 33, 43 ºC	100 - 500
Xu and Fang	2013	R134a, R22, R410A, R236ea, R125, R32, R290, R600a, R717	C, S	0.1-10.07	Condensation. 2-55.3	Several - database	20-800

Cross sections: C: circular, R: rectangular, MB: multi-port barrel, MC: multi-port circular, MN: multi-port N-shape, MS: multi-port square, MST: multi-port half-triangular (one corner rounded) MR: multi-port rectangular, MRmf: multi-pot rectangular microfinned MT: multi-port triangular.LF: Liquid fluid, GF: Gas fluid, LV: Liquid velocity, GV: Gas velocity.

2.3. CONCLUSIONS

In this chapter the state of the art is reviewed. Most of the publications found deal with circular single port tubes and little investigation have been reported about R1234yf inside multi-port tubes. According to the state of the art made, no article was found dealing with R290 inside multiport mini-channel tubes and only one published paper in the case of R32.

A high percentage of the publications summarised in the previous state of art are focussed on refrigeration of electronic equipments and the use of carbon dioxide as working fluid. Most of the articled revised deals with HTC and pressure drop at the same time, little of them deal only with one subject because they are both highly related.

All the articled reviewed in this section come from the las fifteen years and some classical articles have also been included due to their good predicting behaviour.

At present days the industry is manufacturing more equipment with multiport mini-channel tube but using general correlations developed mostly with R134a to predict HTC and pressure drop. The numerical models used in commercial software such as IMSTArt or CoolPack are highly dependant of the correlations programmed.

REFERENCES

[1] Directive 2010/31/EU of the European Parliament and of the Council of 19 May 2010 on the energy performance of buildings (recast). Official Journal of the European Union, 18/6/2010.

[2] A. Cavallini, L. Doretti, M. Matkovic, and L. Rossetto, Update on Condensation Heat Transfer and Pressure Drop inside Minichannels, Heat Transfer Engineering, 27 (2006) 74-87.

[3] N.J. English and S.G. Kandlikar, An Experimental Investigation into the Effect of Surfactants on Air-Water Two-Phase Flow in Minichannels, Heat Transfer Engineering, 27 (2006) 99-109.

[4] C.Y. Yang and R.L. Webb, Condensation of R-12 in small hydraulic diameter extruded aluminum tubes with and without micro-fins, International Journal of Heat and Mass Transfer, 39 (1996) 791-800.

[5] W.W. Akers, H.A. Deans, and O.K. Crosser, Condensing heat transfer within horizontal tubes, Chem. Eng. Progr., 54 (1958).

[6] R.K. Shah, Laminar Flow Forced Convection in Ducts, Advances in Heat Transfer, (1978).

[7] C.Y. Yang and R.L. Webb, A Predictive Model for Condensation in Small Hydraulic Diameter Tubes Having Axial Micro-Fins, Journal of Heat Transfer, 119 (1997) 776-782.

[8] R.L. Webb, M. Zhang, and R. Narayanamurthy, Condensation heat transfer in small diameter tubes, *Heat Transfer,* 1998, pp. 403-408.

[9] K.W. Moser, B. Na, and R.L. Webb, A New Equivalent Reynolds Number Model for Condensation in Smooth Tubes, Journal of Heat Transfer, 120 (1998) 410-417.

[10] R.L. Webb and E. Kemal, Effect of Hydraulic Diameter on Condensation of R-134A in Flat Extruded Aluminum Tubes, Journal of Enhanced Heat Transfer, 8 (2001) 77-90.

[11] Y.Y. Yan and T.F. Lin, Condensation heat transfer and pressure drop of refrigerant R-134a in a small pipe, International Journal of Heat and Mass Transfer, 42 (1999) 697-708.

[12] W.W. William Wang, T.D. Radcliff, and R.N. Christensen, A condensation heat transfer correlation for millimeter-scale tubing with flow regime transition, Experimental Thermal and Fluid Science, 26 (2002) 473-485.

[13] M.H. Kim, J.S. Shin, C. Huh, T.J. Kim, and K.W. Seo, A study of condensation heat transfer in a single mini-tube and a review of Korean micro- and mini-channel studies, *First International Conference on Microchannels and Minichannels,* 2003.

[14] S. Koyama, K. Kuwahara, and K. Nakashita, Condensation of refrigerant in a multi-port channel, *First International Conference on Microchannels and Minichannels,* 2003, pp. 193-205.

[15] S. Koyama, K. Kuwahara, K. Nakashita, and K. Yamamoto, An experimental study on condensation of refrigerant R134a in a multi-port extruded tube, International Journal of Refrigeration, 26 (2003) 425-432.

[16] M.K. Dobson and J.C. Chato, Condensation in smooth horizontal tubes, Journal of Heat Transfer, 120 (1998) 193-213.

[17] H. Haraguchi, S. Koyama, and T. Fujii, Condensation of refrigerants HCFC 22, HFC 134a and HCFC 123 in a horizontal smooth tube, Trans. JSME (B), 60 (1994) 245-252.

[18] K. Mishima and T. Hibiki, Some characteristics of air-water two-phase flow in small diameter vertical tubes, International Journal of Multiphase Flow, 22 (1996) 703-712.

[19] J.R. Baird, D.F. Fletcher, B.S. Haynes, Local condensation heat transfer rates in fine passages,International Journal of Heat and Mass Transfer,46(2003), 4453–4466. http://dx.doi.org/10.1016/S0017-9310(03)00287-4

[20] A. Cavallini, D. Del Col, L. Doretti, M. Matkovic, L. Rossetto, and C. Zilio, Two-phase frictional pressure gradient of R236ea, R134a and R410A inside multi-port mini-channels, Experimental Thermal and Fluid Science, 29 (2005) 861-870.

[21] A. Cavallini, D. Del Col, L. Doretti, M. Matkovic, L. Rossetto, and C. Zilio, Condensation Heat Transfer and Pressure Gradient Inside Multiport Minichannels, Heat Transfer Engineering, 26 (2005) 45-55.

[22] A. Cavallini, G. Censi, D. Del Col, L. Doretti, G.A. Longo, L. Rossetto, and C. Zilio, Condensation inside and outside smooth and enhanced tubes – a review of recent research, International Journal of Refrigeration, 26 (2003) 373-392.

[23] A. Cavallini, G. Censi, D. Del Col, L. Doretti, G.A. Longo, and L. Rossetto, Experimental investigation on condensation heat transfer and pressure drop of new HFC refrigerants (R134a, R125, R32, R410A, R236ea) in a horizontal smooth tube, International Journal of Refrigeration, 24 (2001) 73-87.

[24] M. Zhang and R.L. Webb, Correlation of two-phase friction for refrigerants in small-diameter tubes, Experimental Thermal and Fluid Science, 25 (2001) 131-139.

[25] T.M. Bandhauer, A. Agarwal, and S. Garimella, Measurement and Modeling of Condensation Heat Transfer Coefficients in Circular Microchannels, Journal of Heat Transfer, 128 (2006) 1050-1059.

[26] S. Garimella, A. Agarwal, and J.D. Killion, Condensation Pressure Drop in Circular Microchannels, Heat Transfer Engineering, 26 (2006) 28-35.

[27] D.P. Traviss, W.M. Rohsenow, and A.B. Baron, Forced Convection Condensation in tubes: A heat Transfer Correlation for condenser design, ASHRAE Transactions, 79 (1973) 157-165.

[28] M.Y. Wen, C.Y. Ho, and J.M. Hsieh, Condensation heat transfer and pressure drop characteristics of R-290 (propane), R-600 (butane), and a mixture of R-290/R-600 in the serpentine small-tube bank, Applied Thermal Engineering, 26 (2006) 2045-2053.

[29] B. Médéric, P. Lavieille, and M. Miscevic, Heat transfer analysis according to condensation flow structures in a minichannel, Experimental Thermal and Fluid Science, 30 (2006) 785-793.

[30] A. Cavallini, S. Bortolin, D. Del Col, M. Matkovic, and L. Rossetto, Condensation and vaporization of halogenated refrigerants inside a circular minichannel, 2008.

[31] M. Matkovic, A. Cavallini, S. Bortolin, D. Del Col, and L. Rossetto, Heat transfer coefficient during condensation of a high pressure refrigerant inside a circular minichannel, *5th European Thermal-Sciences Conference, The Netherlands, ,* 2008.

[32] A. Cavallini, L. Doretti, M. Matkovic, and L. Rossetto, Update on condensation heat transfer and pressure drop inside minichannels, 2005.

[33] L. Cheng, G. Ribatski, J.s. Moreno Quibén, and J.R. Thome, New prediction methods for CO_2 evaporation inside tubes: Part I - A two-phase flow pattern map and a flow pattern based phenomenological model for two-phase flow frictional pressure drops, International Journal of Heat and Mass Transfer, 51 (2008) 111-124.

[34] A. Cavallini, D. Del Col, M. Matkovic, and L. Rossetto, Pressure Drop During Two-Phase Flow of R134a and R32 in a Single Minichannel, Journal of Heat Transfer, 131 (2009) 033107.

[35] J.R. Thome, J. El Hajal, and A. Cavallini, Condensation in horizontal tubes, part 2: new heat transfer model based on flow regimes, International Journal of Heat and Mass Transfer, 46 (2003) 3365-3387.

[36] C.Y. Park and P. Hrnjak, CO_2 flow condensation heat transfer and pressure drop in multi-port microchannels at low temperatures, International Journal of Refrigeration, 32 (2009) 1129-1139.

[37] M.Y. Wen and C.Y. Ho, Condensation heat-transfer and pressure drop characteristics of refrigerant R-290/R-600a oil mixtures in serpentine small-diameter U-tubes, Applied Thermal Engineering, 29 (2009) 2460-2467.

[38] A. Agarwal, T.M. Bandhauer, and S. Garimella, Measurement and modeling of condensation heat transfer in non-circular microchannels, International Journal of Refrigeration, 33 (2010) 1169-1179.

[39] J.R. Garcia-Cascales, F. Vera-Garcia, J. Gonzalvez-Macia, J.M. Corberan-Salvador, M.W. Johnson, and G.T. Kohler, Compact heat exchangers modeling: Condensation, International Journal of Refrigeration, 33 (2010) 135-147.

[40] D. Del Col, D. Torresin, and A. Cavallini, Heat transfer and pressure drop during condensation of the low GWP refrigerant R1234yf, International Journal of Refrigeration, 33 (2010) 1307-1318.

[41] T. Bohdal, H. Charun, and M. Sikora, Comparative investigations of the condensation of R134a and R404A refrigerants in pipe minichannels, International Journal of Heat and Mass Transfer, 54 (2011) 1963-1974.

[42] L. Friedel, Improved Friction Pressure Drop Correlations for Horizontal and Vertical Two Phase Pipe Flow. European Two Phase Flow Group Meeting. Paper E 2. Ispra, Italy, 1979.

[43] S. Garimella, Condensation flow mechanisms, pressure drop and heat transfer in microchannels, Microscale Heat Transfer, (2004) 273-290.

[44] H.K. Oh and C.H. Son, Condensation heat transfer characteristics of R-22, R-134a and R-410A in a single circular microtube, Experimental Thermal and Fluid Science, 35 (2011) 706-716.

[45] J.E. Park, F. Vakili-Farahani, L. Consolini, and J.R. Thome, Experimental study on condensation heat transfer in vertical minichannels for new refrigerant R1234ze(E) versus R134a and R236fa, Experimental Thermal and Fluid Science, 35 (2011) 442-454.

[46] D. Del Col, S. Bortolin, A. Cavallini, and M. Matkovic, Effect of cross sectional shape during condensation in a single square minichannel, International Journal of Heat and Mass Transfer, 54 (2011) 3909-3920.

[47] C.R. Zhao, P.X. Jiang, and Y.W. Zhang, Flow and convection heat transfer characteristics of CO2 mixed with lubricating oil at super-critical pressures in small tube during cooling, International Journal of Refrigeration, 34 (2011) 29-39.

[48] D. Chaobin ,E. Hihara.In-tube cooling heat transfer of supercritical carbon dioxide. Part 1: Experimental measurement. International Journal of efrigeration, 27, (2004), 736-747. http://dx.doi.org/10.1016/j.ijrefrig.2004.04.018

[49] B. S. Petukhov. Heat Transfer and Frictionin Turbulent Pipe Flow withVariable Physical Properties. High Temperature Institute. Academy of Science of the USSR. Moscow. USSR. (1970).

[50] A. Cavallini, S. Bortolin, D. Del Col, M. Matkovic, and L. Rossetto, Condensation Heat Transfer and Pressure Losses of High- and Low-Pressure Refrigerants Flowing in a Single Circular Minichannel, Heat Transfer Engineering, 32 (2011) 90-98.

[51] S.M. Kim, J. Kim, and I. Mudawar, Flow condensation in parallel micro-channels: Part 1: Experimental results and assessment of pressure drop correlations, International Journal of Heat and Mass Transfer, 55 (2012) 971-983.

[52] D. Jige, S. Koyama, and M. Mino, An experimental study on condensation of pure refrigerants in horizontal rectangular mini-channels, 2011.

[52] M. Derby, H.J. Lee, Y. Peles, and M.K. Jensen, Condensation heat transfer in square, triangular, and semi-circular mini-channels, International Journal of Heat and Mass Transfer, 55 (2012) 187-197.

[53] M. M. Shah."An Improved and Extended General Correlation for Heat Transfer During Condensation in Plain Tubes," HVAC&R Research, 15(2009), pp. 889-913.

[54] H. Charun, Thermal and flow characteristics of the condensation of R404A refrigerant in pipe minichannels, International Journal of Heat and Mass Transfer, 55 (2012) 2692-2701.

[55] H.Y. Zhang, J.M. Li, N. Liu, and B.X. Wang, Experimental investigation of condensation heat transfer and pressure drop of R22, R410A and R407C in mini-tubes, International Journal of Heat and Mass Transfer, 55 (2012) 3522-3532.

[56] J. Goss and J.C. Passos, Heat transfer during the condensation of R134a inside eight parallel microchannels, International Journal of Heat and Mass Transfer, 59 (2013) 9-19.

[57] Z. Zhang, Z.L. Weng, T.X. Li, Z.C. Huang, X.H. Sun, Z.H. He, J. van Es, A. Pauw, E. Laudi, and R. Battiston, CO2 condensation heat transfer coefficient and pressure drop in a mini-channel space condenser, Experimental Thermal and Fluid Science, 44 (2013) 356-363.

[58] E. Al-Hajri, A.H. Shooshtari, S. Dessiatoun, and M.M. Ohadi, Performance characterization of R134a and R245fa in a high aspect ratio microchannel condenser, International Journal of Refrigeration, 36 (2013) 588-600.

[59] J. Heo, H. Park, and R. Yun, Condensation heat transfer and pressure drop characteristics of CO2 in a microchannel, International Journal of Refrigeration, 36 (2013) 1657-1668.

[60] J. Heo, H. Park, and R. Yun, Comparison of condensation heat transfer and pressure drop of CO2 in rectangular microchannels, International Journal of Heat and Mass Transfer, 65 (2013) 719-726.

[61] N. Liu, J.M. Li, J. Sun, and H.S. Wang, Heat transfer and pressure drop during condensation of R152a in circular and square microchannels, Experimental Thermal and Fluid Science, 47 (2013) 60-67.

[62] K. Sakamatapan, J. Kaew-On, A.S. Dalkilic, O. Mahian, and S. Wongwises, Condensation heat transfer characteristics of R-134a flowing inside the multiport minichannels, International Journal of Heat and Mass Transfer, 64 (2013) 976-985.

[63] C.C. Wang, An overview for the heat transfer performance of HFO-1234yf, Renewable and Sustainable Energy Reviews, 19 (2013) 444-453.

[64] G.M. Lazarek and S.H. Black, Evaporative heat transfer, pressure drop and critical heat flux in a small vertical tube with R-113, International Journal of Heat and Mass Transfer, 25 (1982) 945-960.

[65] W. Tong, A.E. Bergles, and M.K. Jensen, Pressure drop with highly subcooled flow boiling in small-diameter tubes, Experimental Thermal and Fluid Science, 15 (1997) 202-212.

[66] K.A. Triplett, S.M. Ghiaasiaan, S.I. Abdel-Khalik, A. LeMouel, and B.N. McCord, Gas-liquid two-phase flow in microchannels: Part II: void fraction and pressure drop, International Journal of Multiphase Flow, 25 (1999) 395-410.

[67] T.N. Tran, M.C. Chyu, M.W. Wambsganss, and D.M. France, Two-phase pressure drop of refrigerants during flow boiling in small channels: an experimental investigation and correlation development, International Journal of Multiphase Flow, 26 (2000) 1739-1754.

[68] H. Ju Lee and S. Yong Lee, Pressure drop correlations for two-phase flow within horizontal rectangular channels with small heights, International Journal of Multiphase Flow, 27 (2001) 783-796.

[69] J. Pettersen, R. Rieberer,S.T. Munkejord, Heat transfer and pressure drop characteristics of evaporating carbon dioxide in microchannels tubes, (2000).

[70] Thome, J.R., 1997, Refrigeration Heat Transfer, Course notes, GRETh/CEA, Grenoble, France.VDI, 1994, VDI-Wärmeatlas, Düsseldorf, Germany, VDI-Verlag.

[71] B. Agostini, B. Watel, A. Bontemps, and B. Thonon, Friction factor and heat transfer coefficient of R134a liquid flow in mini-channels, Applied Thermal Engineering, 22 (2002) 1821-1834.

[72] A. Kawahara, P.M.Y. Chung, and M. Kawaji, Investigation of two-phase flow pattern, void fraction and pressure drop in a microchannel, International Journal of Multiphase Flow, 28 (2002) 1411-1435.

[73] R.W. Lockhart and R.C. Martinelli, Proposed correlation of data for isothermal two-phase, two-component flow in pipes, Chem. Eng. Prog, 45 (1949) 39-48.

[74] S. Garimella, J.D. Killion, and J.W. Coleman, An Expermentally Validated Model for Two-Phase Pressure Drop in the Intermittent Flow Regime for Noncircular Microchannels, Journal of Fluids Engineering, 125 (2003) 887-894.

[75] S. Garimella, Condensation Flow Mechanisms in Microchannels: Basis for Pressure Drop and Heat Transfer Models, Heat Transfer Engineering, 25 (2004) 104-116.

[76] W. Yu, D.M. France, M.W. Wambsganss, and J.R. Hull, Two-phase pressure drop, boiling heat transfer, and critical heat flux to water in a small-diameter horizontal tube, International Journal of Multiphase Flow, 28 (2002) 927-941.

[77] K.I. Choi, A.S. Pamitran, J.T. Oh, and H.K. Oh, Effect on boiling heat transfer of horizontal smooth minichannel for R-410A and R-407C, J Mech Sci Technol, 19 (2005) 156-163.

[78] K.I. Choi, A.S. Pamitran, C.Y. Oh, and J.T. Oh, Two-phase pressure drop of R-410A in horizontal smooth minichannels, International Journal of Refrigeration, 31 (2008) 119-129.

[79] A. Cavallini, D. Del Col, L. Doretti, M. Matkovic, L. Rossetto, and C. Zilio, Measurement of pressure gradient during two-phase flow inside multi-port mini-channels, 2004.

[80] J. Yue, G. Chen, and Q. Yuan, Pressure drops of single and two-phase flows through T-type microchannel mixers, Chemical Engineering Journal, 102 (2004) 11-24.

[81] H. Muller-Steinhagen and K. Heck, A simple friction pressure drop correlation for two-phase flow in pipes, Chemical Engineering and Processing: Process Intensification, 20 (1986) 297-308.

[82] R. Yun, Y. Kim, and M. Soo Kim, Flow boiling heat transfer of carbon dioxide in horizontal mini tubes, International Journal of Heat and Fluid Flow, 26 (2005)

[83] K. Pehlivan, I. Hassan, and M. Vaillancourt, Experimental study on two-phase flow and pressure drop in millimeter-size channels, Applied Thermal Engineering, 26 (2006) 1506-1514.

[84] D. Chisholm, A theoretical basis for the Lockhart-Martinelli correlation for two-phase flow, International Journal of Heat and Mass Transfer, 10 (1967) 1767-1778.

[85] G. Ribatski, L. Wojtan, and J.R. Thome, An analysis of experimental data and prediction methods for two-phase frictional pressure drop and flow boiling heat transfer in micro-scale channels, Experimental Thermal and Fluid Science, 31 (2006) 1-19.

[86] E.W. Jassim, T.A. Newell, and J.C. Chato, Probabilistic Flow Regime Map Modeling of Two-Phase Flow. 2006. Air Conditioning and Refrigeration Center. University of Illinois at Urbana-Champaign.

[87] R. Revellin and J.R. Thome, Experimental investigation of R-134a and R-245fa two-phase flow in microchannels for different flow conditions, International Journal of Heat and Fluid Flow, 28 (2007) 63-71.

[88] B.S. Field and P. Hrnjak, Adiabatic Two-Phase Pressure Drop of Refrigerants in Small Channels, Heat Transfer Engineering, 28 (2007) 704-712.

[89] M.K. Akbar, D.A. Plummer, S.M. Ghiaasiaan. On gas–liquid two-phase flow regimes in microchannels.International Journal of Multiphase Flow, 29 (2003) 855 - 865.

[90] S.L. Qi, P. Zhang, R.Z. Wang, and L.X. Xu, Flow boiling of liquid nitrogen in micro-tubes: Part I – The onset of nucleate boiling, two-phase flow instability

and two-phase flow pressure drop, International Journal of Heat and Mass Transfer, 50 (2007) 4999-5016.

[91] A. Rosato, A.W. Mauro, R. Mastrullo, and G.P. Vanoli, Experiments during flow boiling of a R22 drop-in: R422D adiabatic pressure gradients, Energy Conversion and Management, 50 (2009) 2613-2621.

[92] J. Moreno Quibén, .J R. Thome.Flow pattern based two-phase frictional pressure drop model for horizontal tubes, Part II: New phenomenological model. International Journal of Heat and Fluid Flow 28 (2007) 1060-1072.

[93] Grönnerud, R., 1972. "Investigation in Liquid Holdup, Flow Resistance and Heat Transfer in Circular Type Evaporators, Part IV: Two-Phase Resistance in Boiling Refrigerants", Bulletin de l'Inst.du Froid, Annexe 1972-1.

[94] D. Jung, R. Rademacher. Prediction of pressure drop during horizontal, annular flow boiling of pure and mixed refrigerants. International Journal of Heat and Mass Transfer 32 (1989) 24435-2446

[95] L. Cheng, G. Ribatski, and J.R. Thome, New prediction methods for CO2 evaporation inside tubes: Part II - An updated general flow boiling heat transfer model based on flow patterns, International Journal of Heat and Mass Transfer, 51 (2008) 125-135

[96] L. Cheng, G. Ribatski, and J.R. Thome, Analysis of supercritical CO2 cooling in macro- and micro-channels, International Journal of Refrigeration, 31 (2008) 1301-1316.

[97] A.S. Pamitran, K.I. Choi, J.T. Oh, and H.K. Oh, Two-phase pressure drop during CO2 vaporization in horizontal smooth minichannels, International Journal of Refrigeration, 31 (2008) 1375-1383.

[98] K.I. Choi, A.S. Pamitran, J.T. Oh, and K. Saito, Pressure drop and heat transfer during two-phase flow vaporization of propane in horizontal smooth minichannels, International Journal of Refrigeration, 32 (2009) 837-845.

[99] Y. Jang, C. Park, Y. Lee, and Y. Kim, Flow boiling heat transfer coefficients and pressure drops of FC-72 in small channel heat sinks, International Journal of Refrigeration, 31 (2008) 1033-1041.

[100] S. Saisorn and S. Wongwises, Flow pattern, void fraction and pressure drop of two-phase airΓÇôwater flow in a horizontal circular micro-channel, Experimental Thermal and Fluid Science, 32 (2008) 748-760.

[101] A. Agarwal and S. Garimella, Modeling of Pressure Drop During Condensation in Circular and Noncircular Microchannels, Journal of Fluids Engineering, 131 (2008) 011302.

[102] L. Sun and K. Mishima, Evaluation analysis of prediction methods for two-phase flow pressure drop in mini-channels, International Journal of Multiphase Flow, 35 (2009) 47-54.

[103] A. Cioncolini, J.R. Thome, and C. Lombardi, Unified macro-to-microscale method to predict two-phase frictional pressure drops of annular flows, International Journal of Multiphase Flow, 35 (2009) 1138-1148.

[104] E. Lombardi, E. Pedrocchi, A pressure drop correlation in two-phase flow, Energy Nuclear.MiIan, 19 (1972) 91-99.

[105] C. J. Barozcy.A systematic correlation for two-phase pressure drop. Chemical Engineering Project Symposium, 62 (1966), 232-249.

[106] M. Hamdar, A. Zoughaib, D. Clodic. Flow boiling heat transfer and pressure drop of pure HFC-152a in a horizontal mini-channel. International Journal of Refrigeration, 33 (2010), 566–577

[107] A.S. Pamitran, K.I. Choi, J.T. Oh, and P. Hrnjak, Characteristics of two-phase flow pattern transitions and pressure drop of five refrigerants in horizontal circular small tubes, International Journal of Refrigeration, 33 (2010) 578-588.

[108] Y. Ma, X. Ji, D. Wang, T. Fu, and C. Zhu, Measurement and Correlation of Pressure Drop for Gas-Liquid Two-phase Flow in Rectangular Microchannels, Chinese Journal of Chemical Engineering, 18 (2010) 940-947.

[109] W. Li and Z. Wu, A general correlation for adiabatic two-phase pressure drop in micro/mini-channels, International Journal of Heat and Mass Transfer, 53 (2010) 2732-2739.

[110] S. Saisorn, J. Kaew-On, and S. Wongwises, Flow pattern and heat transfer characteristics of R-134a refrigerant during flow boiling in a horizontal circular mini-channel, International Journal of Heat and Mass Transfer, 53 (2010) 4023-4038.

[111] M. Ducoulombier, S.p. Colasson, J. Bonjour, and P. Haberschill, Carbon dioxide flow boiling in a single microchannel – Part I: Pressure drops, Experimental Thermal and Fluid Science, 35 (2011) 581-596.

[112] H. Trieu Phan, N. Caney, P. Marty, S.P. Colasson, and J. Gavillet, Flow boiling of water in a minichannel: The effects of surface wettability on two-phase pressure drop, Applied Thermal Engineering, 31 (2011) 1894-1905.

[113] S. G. Bankoff. A Variable Density Single-Fluid Model for Two-Phase Flow With Particular Reference to Steam-Water Flow. *J. Heat Transfer* 82 (1960), 265-272

[114] A.A. Donaldson, D.M. Kirpalani, and A. Macchi, Single and two-phase pressure drop in serpentine mini-channels, Chemical Engineering and Processing: Process Intensification, 50 (2011) 877-884.

[115] Michiel T. Kreutzer, Freek Kapteijn, Jacob A. Moulijn, Chris R.Kleijn, Johan J. Heiszwolf. Inertial and interfacial effects on pressure drop of Taylor flow in capillaries. AIChE Journal51 (2005), 2428-2440

[116] C.W. Choi, D.I. Yu, and M.H. Kim, Adiabatic two-phase flow in rectangular microchannels with different aspect ratios: Part I - Flow pattern, pressure drop and void fraction, International Journal of Heat and Mass Transfer, 54 (2011) 616-624.

[117] C. Choi and M. Kim, Flow pattern based correlations of two-phase pressure drop in rectangular microchannels, International Journal of Heat and Fluid Flow, 32 (2011) 1199-1207.

[118] H. Foroughi and M. Kawaji, Viscous oil–water flows in a microchannel initially saturated with oil: Flow patterns and pressure drop characteristics, International Journal of Multiphase Flow, 37 (2011) 1147-1155.

[119] J. Wu, T. Koettig, C. Franke, D. Helmer, T. Eisel, F. Haug, and J. Bremer, Investigation of heat transfer and pressure drop of CO2 two-phase flow in a horizontal minichannel, International Journal of Heat and Mass Transfer, 54 (2011) 2154-2162.

[120] X. Fang, Y. Xu, and Z. Zhou, New correlations of single-phase friction factor for turbulent pipe flow and evaluation of existing single-phase friction factor correlations, Nuclear Engineering and Design, 241 (2011) 897-902.

[121] C.Y. Park, Y. Jang, B. Kim, and Y. Kim, Flow boiling heat transfer coefficients and pressure drop of FC-72 in microchannels, International Journal of Multiphase Flow, 39 (2012) 45-54.

[122] J. Kaew-On and S. Wongwises, New proposed two-phase multiplier and evaporation heat transfer coefficient correlations for R134a flowing at low mass flux in a multiport minichannel, International Communications in Heat and Mass Transfer, 39 (2012) 853-860.

[123] A. Sur and D. Liu, Adiabatic air/water two-phase flow in circular microchannels, International Journal of Thermal Sciences, 53 (2012) 18-34.

[124] S.M. Kim and I. Mudawar, Universal approach to predicting two-phase frictional pressure drop for adiabatic and condensing mini/micro-channel flows, International Journal of Heat and Mass Transfer, 55 (2012) 3246-3261.

[125] C.H. Son and H.K. Oh, Condensation pressure drop of R22, R134a and R410A in a single circular microtube, Heat Mass Transfer, 48 (2012) 1437-1450.

[126] T. Bohdal, H. Charun, and M. Sikora, Pressure drop during condensation of refrigerants in pipe minichannels, Archives of Thermodynamics, 33 (2012) 87-106.

[127] Y. Xu, X. Fang, X. Su, Z. Zhou, and W. Chen, Evaluation of frictional pressure drop correlations for two-phase flow in pipes, Nuclear Engineering and Design, 253 (2012) 86-97.

[128] S.M. Kim and I. Mudawar, Consolidated method to predicting pressure drop and heat transfer coefficient for both subcooled and saturated flow boiling in micro-channel heat sinks, International Journal of Heat and Mass Transfer, 55 (2012) 3720-3731.

[129] T. Harirchian and S.V. Garimella, Flow regime-based modeling of heat transfer and pressure drop in microchannel flow boiling, International Journal of Heat and Mass Transfer, 55 (2012) 1246-1260.

[130] L. Saraceno, G.P. Celata, M. Furrer, A. Mariani, and G. Zummo, Flow boiling heat transfer of refrigerant FC-72 in microchannels, International Journal of Thermal Sciences, 53 (2012) 35-41.

[131] Z. Liu and R.H.S. Winterton, A general correlation for saturated and subcooled flow boiling in tubes and annuli, based on a nucleate pool boiling equation, International Journal of Heat and Mass Transfer, 34 (1991) 2759-2766.

[132] Y. Xu and X. Fang, A new correlation of two-phase frictional pressure drop for evaporating flow in pipes, International Journal of Refrigeration, 35 (2012) 2039-2050.

[133] K. Zhu, G.Q. Xu, Z. Tao, H.W. Deng, Z.H. Ran, and C.B. Zhang, Flow frictional resistance characteristics of kerosene RP-3 in horizontal circular tube at supercritical pressure, Experimental Thermal and Fluid Science, 44 (2013) 245-252.

[134] J.B. Copetti, M.H. Macagnan, and F. Zinani, Experimental study on R-600a boiling in 2.6-ámm tube, International Journal of Refrigeration, 36 (2013) 325-334.

[135] C. Dang, N. Haraguchi, T. Yamada, M. Li, and E. Hihara, Effect of lubricating oil on flow boiling heat transfer of carbon dioxide, International Journal of Refrigeration, 36 (2013) 136-144.

[136] D. Del Col, A. Bisetto, M. Bortolato, D. Torresin, and L. Rossetto, Experiments and updated model for two phase frictional pressure drop inside minichannels, International Journal of Heat and Mass Transfer, 67 (2013) 326-337.

[137] A. Cavallini, D. Del Col, M. Matkovic, and L. Rossetto, Frictional pressure drop during vapour – liquid flow in minichannels: Modelling and experimental evaluation, International Journal of Heat and Fluid Flow, 30 (2009) 131-139.

[138] F. Vakili-Farahani, B. Agostini, and J.R. Thome, Experimental study on flow boiling heat transfer of-ámultiport tubes with R245fa and R1234ze(E), International Journal of Refrigeration, 36 (2013) 335-352.

[139] M. Li, C. Dang, and E. Hihara, Flow boiling heat transfer of HFO1234yf and HFC32 refrigerant mixtures in a smooth horizontal tube: Part II. Prediction method, International Journal of Heat and Mass Transfer, 64 (2013) 591-608.

[140] M.H. Maqbool, B. Palm, and R. Khodabandeh, Investigation of two phase heat transfer and pressure drop of propane in a vertical circular minichannel, Experimental Thermal and Fluid Science, 46 (2013) 120-130.

[141] Y. Xu and X. Fang, A new correlation of two-phase frictional pressure drop for condensing flow in pipes, Nuclear Engineering and Design, 263 (2013) 87-96.

CHAPTER 3: Models review

A bibliography research was made to get the models available to calculate heat transfer coefficients and frictional pressure drop values in two-phase flow conditions.

First of all, several correlations widely used for void fraction calculation are presented because of the importance of this parameter to characterise two-phase flow pattern and its use in heat transfer coefficient and pressure drop calculation. Heat transfer coefficient and pressure drop correlations research is divided into classical correlations developed for macro-channels and new correlations developed for reduced flow area channels.

The models described below can be found in detail in the articles cited in the bibliography at the end of this chapter.

3.1. VOID FRACTION

Void fraction "ε" is one of most important parameters used to characterise two-phase flow pattern. This physical parameter is the key to get other important parameters such as biphasic density and viscosity in order to calculate relative average flow velocity between the two phases. This velocity is basic to use in the models developed to predict flow patterns, heat transfer coefficient and pressure drop in two-phase flows.

Many authors developed correlations for void fraction calculation; between them the following stand out:

Homogeneous model
$$\varepsilon = \frac{1}{1 + \frac{1-x}{x}\frac{\rho_g}{\rho_l}} \tag{3.1}$$

Zivi [1]
$$\varepsilon = \frac{1}{1 + \frac{1-x}{x}\left(\frac{\rho_g}{\rho_l}\right)^{2/3}} \tag{3.2}$$

Smith [2]
$$\varepsilon = \frac{1}{1 + \frac{\rho_g}{\rho_l}K\left(\frac{1}{x} - 1\right) + \frac{\rho_g}{\rho_l}(1-K)\left(\frac{1}{x} - 1\right)\frac{\frac{\rho_g}{\rho_l} + K\left(\frac{1}{x}-1\right)}{1 + K\left(\frac{1}{x}-1\right)}}, \tag{3.3}$$

$$K = 0.4$$

Baroczy [3]
$$\varepsilon = \frac{1}{1 + \left(\frac{1-x}{x}\right)^{0.74}\left(\frac{\rho_g}{\rho_l}\right)^{0.65}\left(\frac{\mu_q}{\mu_g}\right)^{0.13}} \tag{3.4}$$

Chisholm [4]
$$\varepsilon = \frac{1}{1 + \frac{1-x}{x}\frac{\rho_g}{\rho_l}S}, S = \sqrt{1 - x\frac{x\rho_l}{\rho_g}} \tag{3.5}$$

Chen [5]	$\varepsilon = \dfrac{1}{1+0.18\left(\frac{1-x}{x}\right)^{0.6}\left(\frac{\rho_g}{\rho_l}\right)^{0.33}\left(\frac{\mu_l}{\mu_g}\right)^{0.07}}$	(3.6)
Lockhart – Martinelli [6]	$\dfrac{1-\varepsilon}{\varepsilon} = 0.28\left(\dfrac{1-x}{x}\right)^{0.64}\left(\dfrac{\rho_g}{\rho_l}\right)^{0.36}\left(\dfrac{\mu_l}{\mu_g}\right)^{0.07}$	(3.7)

3.2. TWO-PHASE PRESSURE DROP

Two-phase flow pressure drop inside tubes is a very important variable to take into account in the designing process of a heat exchanger. Pressure gradient has been widely studied because of its importance and many models and correlations have been proposed to calculate it. In the following sections several models and correlations for its calculation are summarised. First, a few for common tubes are presented and after some of the correlations introduced above are described.

3.2.1 Common Channel Correlations

3.2.1.1 Lockhart and Martinelli [6]

This correlation is based in a separated flow model. These authors were the first of all to perform this analysis and then followed by many others. The authors provide the following equation for two-phase frictional pressure gradient calculation based on a liquid phase multiplier, ϕ.

$$\left(\frac{dp}{dz}\right)_{tp} = \phi_l^2\left(\frac{dp}{dz}\right)_l \tag{3.8}$$

Where Chisholm provided the following correlation to calculate the two-phase multiplier based on liquid phase pressure drop:

$$\phi_l^2 = 1 + \frac{C}{X} + \frac{1}{X^2} \tag{3.9}$$

"C" value depends of liquid and vapour flow regime and the Martinelli parameter; *"X"* is given by:

$$X^2 = \frac{\left(\frac{dp}{dz}\right)_l}{\left(\frac{dp}{dz}\right)_g} \tag{3.10}$$

with

$$\left(\frac{dp}{dz}\right)_l = f_l \frac{G^2(1-x)^2}{2D\rho_l} \tag{3.11}$$

and

$$\left(\frac{dp}{dz}\right)_g = f_g \frac{G^2 x^2}{2D\rho_g} \tag{3.12}$$

where *f,* ρ, *x, G* and *D* are the friction factor, density, vapour quality value, mass velocity and hydraulic diameter of the tube. The subscripts *g* and *l*denote gas and liquid phases respectively.

The value of "*C"* in Eq. 3.9 depends on the regimes of the liquid and vapour. The appropriate values to use are listed in Table 3.1. The correlation of Lockhart and Martinelli is applicable to the vapour quality range of $0 < x \leq 1$.

Table 3.1. C values of Lockhart and Martinelli correlation.

Liquid	Gas	C
Turbulent	Turbulent	20
Laminar	Turbulent	12
Turbulent	Laminar	10
Laminar	Laminar	5

3.2.1.2 Homogeneous model

There is no author information about the homogeneous model described below. This model uses a pseudo-fluid that obeys the conventional design equations for single-phase fluids and is characterised by suitably averaged properties of the liquid and vapour phase.

$$\left(\frac{dp}{dz}\right)_{tp} = \frac{2 f_{tp} G^2}{D\rho_{tp}} \tag{3.13}$$

$$f_{tp} = \frac{16}{Re_{tp}} \; if \; Re_{tp} < 2000 \tag{3.14}$$

$$f_{tp} = 0.079 Re_{tp}^{-0.25} \; if \; Re_{tp} > 2000 \tag{3.15}$$

where the subscript *"tp"* denotes two-phase. Two-phase density comes from the equation:

$$\rho_{tp} = \frac{1}{\frac{x}{\rho_g} + \frac{1-x}{\rho_l}} \tag{3.16}$$

3.2.1.3 Friedel [7]

The correlation method of Friedel utilises a two-phase multiplier. This model is a separate flow model

$$\left(\frac{dp}{dz}\right)_{tp} = \phi_{lo}^{2}\left(\frac{dp}{dz}\right)_{lo} \tag{3.17}$$

$$\phi_{lo}^{2} = E + \frac{3.24FX}{F_r^{\,0.045}We_l^{\,0.035}} \tag{3.18}$$

where

$$F_r = \frac{G^2}{gD\rho_{tp}^2}, F = x^{0.78}(1-x)^{0.224}, We_l = \frac{G^2 D}{\sigma\rho_l} \tag{3.19}$$

$$X = \left(\frac{\rho_l}{\rho_g}\right)^{0.91}\left(\frac{\mu_g}{\mu_l}\right)^{0.19}\left(1-\frac{\mu_g}{\mu_l}\right)^{0.7} \tag{3.20}$$

$$E = (1-x)^2 + x^2\frac{\rho_l f_{go}}{\rho_g f_{lo}} \tag{3.21}$$

This method is typically recommended when the ratio of (μ_l/μ_g) is lower than 1000 and is applicable to vapour qualities from $0 \leq x \leq 1$.

3.2.1.4 Müller-Steinhagen and Heck [8]

The authors proposed a new correlation for two-phase flow calculation based on an interpolation of single gas and liquid phase pressure drop values related with vapour quality values.

$$\left(\frac{dp}{dz}\right)_{tp} = F(1-x)^{1/3} + \left(\frac{dp}{dz}\right)_{lo}x^3 \tag{3.22}$$

where

$$F = \left(\frac{dp}{dz}\right)_{lo} + 2\left[\left(\frac{dp}{dz}\right)_{go} - \left(\frac{dp}{dz}\right)_{lo}\right]x \tag{3.23}$$

3.2.2 Micro- and Mini-Channels Correlations

There exist many correlations specially developed for micro- and mini-channels. The following correlations are generally used to calculate frictional pressure drop in micro and mini-channels.

3.2.2.1 Mishima and Hibiki [9]

The model proposed by these authors utilises a single-phase flow multiplier based on liquid phase. The model was adjusted with data of water and air mixtures. This model uses Lockhart and Martinelli parameter with *"C"* parameter of Eq. (3.9) modified as a dependable function of tube diameter:

$$C = 21(1 - e^{-319D}) \text{ with } D \text{ in } mm \tag{3.24}$$

3.2.2.2 Zhang and Webb [10]

The authors developed this model with single-phase and adiabatic two-phase flow measurements for R134a, R22 and R404A flowing in a multi-port extruded aluminium tube with hydraulic diameter of 2.13 mm and in two copper tubes having inside diameters of 6.25 and 3.25 mm. This new model is a modification of Friedel correlation [7] because the original model was not able to predict two-phase data accurately. The multi-port tube data considered was recorded by an external author with circular ports shape.

This model utilises a liquid only multiplier function of reduced pressure and vapour quality value only.

$$\left(\frac{dp}{dz}\right)_{tp} = \left(\frac{dp}{dz}\right)_{lo} \phi_{lo}^2 \tag{3.25}$$

$$\phi_{lo}^2 = (1-x)^2 + 2.87x^2\left(\frac{p}{p_{crit}}\right)^{-1} + 1.68x^{0.25}(1-x)^2\left(\frac{p}{p_{crit}}\right)^{-1.64} \tag{3.26}$$

3.2.2.3 Garimella et al. [11]

The authors presented this multiple flow-regime model for pressure drop during the condensation of the refrigerant R134a in horizontal mini-channels. Two-phase pressure drops were measured in five circular channels ranging in hydraulic diameter from 0.5 mm to 4.91 mm. The range of vapour qualities studies was from 0 to 1. The authors used previous work information on flow mechanism to assign the applicable flow regime to the data points.

For Annular/Mist and disperse flow:

$$\left(\frac{dp}{dz}\right)_{tp} = \frac{1}{2} f_i \rho_g u_g^2 \frac{1}{D} = \frac{1}{2} f_i \frac{G^2 x^2}{\rho_g \varepsilon^{2.5}} \frac{1}{D} \tag{3.27}$$

The Martinelli parameter *"X"* comes from:

$$X = \sqrt{\frac{(dp/dz)_l}{(dp/dz)_g}} \tag{3.28}$$

and void fraction is calculated by means of Baroczy [3], Eq (3.4).

In this model, liquid phase Reynolds number used in the two preceding equations is defined in terms of occupied area of the liquid phase in annular flow:

$$Re_l = \frac{GD(1-x)}{\left(1+\sqrt{\varepsilon}\right)\mu_l} \tag{3.29}$$

In a similar way, Reynolds number required in Martinelli parameter for pressure drop calculation due to gas core can be calculated as:

$$Re_l = \frac{GDx}{\sqrt{\varepsilon}\mu_g} \tag{3.30}$$

The non-dimensional parameter that takes into account the effect of surface tension by Ju Lee and Yong Lee [12]:

$$\psi = \frac{j_l \mu_l}{\sigma} \tag{3.31}$$

where

$$j_l = \frac{G(1-x)}{\rho_l(1-\varepsilon)} \tag{3.32}$$

is the liquid superficial velocity. The interface frictional ratio and liquid phase friction factor ratio is correlated by the Martinelli parameter, liquid phase Reynolds number and surface tension parameter:

$$\frac{f_i}{f_l} = A\, X^a Re_l^b \psi^c \tag{3.33}$$

The friction factor required for single phase pressure drop calculation is the one proposed by Churchill [13]

$$\begin{cases} f = \dfrac{64}{Re} & if\ Re < 2100 \\ f = 0.316 Re^{-0.25} & if\ Re > 3400 \end{cases} \tag{3.34}$$

Table 3.2. Garimella et al. correlation coefficients.

Laminar region (Re<2100)	A=1.308·10^{-3}; a=0.427; b=0.930; c=-0.121
Turbulent region(Re>3400)	A=25.64; a=0.532; b=-0.327; c=0.021
Transition region (2100<Re<3400)	Interpolation based on “*G*” and “*x*”

3.2.2.4 Cavallini et al. [14, 15]

The authors presented a frictional pressure drop model with data of R410A, R134a and R136ea in mini-channels of different cross-section geometries and with hydraulic diameters ranging from 0.4 to 3 mm. The authors attempt to take into account the effect of the entrainment rate of droplets from the liquid film with Paleev and Filippovich equation. This latter equation was experimentally obtained with macro-channels flowing in vertical with R113 but can be applied to horizontal mini-channels, as the gravitational settling of the drops can be neglected in annular flow in horizontal mini-channels.

The model proposed is an interpolated model of Coleman [16], Zhang [17] and Cavallini et al. [18] models.

For adiabatic flow conditions and $\mathrm{J_G} > 2.5$

$$\left(\frac{\mathrm{d}p}{dz}\right)_{tp} = \phi_{lo}^2\left(\frac{dp}{dz}\right)_{lo} = 2\ \phi_{lo}^2 f_{lo}{}^{*}\frac{G^2}{\rho_{liq}D} \tag{3.35}$$

$$f_{lo} = 0.046{Re_{lo}}^{-0.2} = 0.046\left(\frac{GD}{\mu_l}\right)^{-0.2}\quad for\ any\ value\ of\ Re_{lo} \tag{3.36}$$

$$\phi_{lo}^2 = Z + 3.595FH(1-E)^W \tag{3.37}$$

$$W = 1.398p_g \tag{3.38}$$

$$F = x^{0.9525}(1-x)^{0.414} \tag{3.39}$$

$$Z = (1-x)^2 + x^2\frac{\rho_l}{\rho_g}\left(\frac{\mu_g}{\mu_l}\right)^{0.2} \tag{3.40}$$

$$H = \left(\frac{\rho_l}{\rho_g}\right)^{1.132}\left(\frac{\mu_g}{\mu_l}\right)^{0.44}\left(1-\frac{\mu_g}{\mu_l}\right)^{3.542} \tag{3.41}$$

The Paleev y Fillippovich [19] entrainment ratio *"E"*:

$$E = 0.015 + 0.44\ log\left[\left(\frac{\rho_{gc}}{\rho_l}\right)\left(\frac{\mu_l j_g}{\sigma}\right)^2 10^4\right] \tag{3.42}$$

$$if\begin{cases} E \geq 0.95\ then\ E = 0.95 \\ E \leq 0\ \ then\ E = 0 \end{cases} \tag{3.43}$$

where gas core density is defined by:

$$\rho_{gc} = \left(\frac{x+(1-x)E}{\frac{x}{\rho_g}+\frac{(1-x)E}{\rho_l}}\right) \tag{3.44}$$

$$\rho_{gc} \cong \rho_g\left(1+\frac{(1-x)E}{x}\right)\ for\ \rho_l \gg \rho_g \tag{3.45}$$

This model for frictional pressure gradient can be extended to lower vapour quality values and mass velocities ($J_G < 2.5$), under the restriction of considering the highest value of $(dp/dz)_f$ of the previous equations and liquid only frictional pressure drop$(dp/dz)_{f,lo}$ for the channel geometry considered.

$$\left(\frac{dp}{dz}\right)_{lo} = 2\, f_{lo} \frac{G^2}{\rho_l D} \tag{3.46}$$

$$if \begin{cases} Re_{lo} > 2000\ then\ f_{lo=}0.046\left(GD/\mu_{liq}\right)^{-0.2} \\ Re_{lo} < 2000\ then\ f_{lo} = C/\left(GD/\mu_{liq}\right) \end{cases} \tag{3.47}$$

with $C = 16$ for circular section and $C = 14.3$ for square shape section.

Taking on that gas core and liquid entrainment have the same velocity as suggested by Hewitt and Hall-Taylor [20], the density of the mixture of liquid and vapour in the core has a density value ρ_{GC} and a velocity value, u_{GC}

$$u_{gc} = \frac{G[x + (1-x)E]}{(1-\varepsilon)\rho_{gc}} \tag{3.48}$$

The differential pressure gain due to momentum variation is the addition of the terms due to film liquid on the tube wall the quantity due to the mixture of liquid-vapour in the core. It can be expressed as:

$$(-dp)_{mom} = G^2\left[\frac{(1-x)^2(1-E)^2}{\varepsilon\,\rho_l} + \frac{[x+(1-x)E]^2}{(1-\varepsilon)\rho_{gc}}\right] \tag{3.49}$$

$$\begin{aligned}(-dp)_{mom} = {} & G^2\left[\frac{(1-x_{in})^2(1-E_{in})^2}{\varepsilon_{in}\,\rho_{liq}} + \frac{[x_{in}+(1-x_{in})E_{in}]^2}{(1-\varepsilon_{in})\rho_{gc,in}}\right] \\ & - G^2\left[\frac{(1-x_{out})^2(1-E_{out})^2}{\varepsilon_{out}\,\rho_{liq}} + \frac{[x_{out}+(1-x_{out})E_{out}]^2}{(1-\varepsilon_{out})\rho_{gc,out}}\right]\end{aligned} \tag{3.50}$$

3.2.2.5 Cavallini et al. [21]

This correlation is an improvement of previous Cavallini et al. correlation. This update includes the effect of tube roughness which modifies friction factor when film thickness is lower than roughness profile.

$$f_{lo}^{*} = 0.046\, Re_{lo}^{-0.2} + 0.7\, RR \quad para\ RR < 0.0027 \tag{3.51}$$

$$RR = \frac{2Ra}{D} \tag{3.52}$$

with "Ra" the roughness profile mean arithmetic deviation measured following ISO 4287:1997.

3.2.2.6 Sun and Mishima [22]

This model is based on 2092 experimental data points of R123, R134a, R22, R236ea, R245fa, R404A, R407C, R410A, R507, CO_2, water and air in 0.506 – 12 mm tubes. The authors proposed a modified Chisholm correlation [4] with better behaviour in turbulent region.

$$\left(\frac{\mathrm{d}p}{dz}\right)_{tp} = \phi_l^2 \left(\frac{dp}{dz}\right)_l \tag{3.53}$$

For viscous flow:

$$C = 26\left(1 + \frac{Re_l}{1000}\right)\left[1 - exp\left(\frac{-0.153}{0.8 + 0.27La}\right)\right] \tag{3.54}$$

For turbulent flow:

$$\phi_l^2 = 1 + \frac{C}{X^{1.19}} + \frac{1}{X^2} \tag{3.55}$$

$$C = 1.79\left(\frac{Re_l}{Re_g}\right)^{0.4}\sqrt{\frac{1-x}{x}} \tag{3.56}$$

$$Re_l = \frac{G(1-x)D}{\mu_l} \tag{3.57}$$

$$Re_g = \frac{GxD}{\mu_g} \tag{3.58}$$

3.2.2.7 Kim and Mudawar [23]

The authors proposed a universal approach based on an adjustment of 7115 data collected from thirty six sources with different fluids, diameters and tube geometries. The model presented is a Lockhart and Martinelli [6] type correlation based on liquid phase multiplier. Different *"C"* Chisholm parameter were adjusted based on liquid and gas phase conditions according to the following equations.

$$\left(\frac{dp}{dz}\right)_{tp} = \phi_l^2 \left(\frac{dp}{dz}\right)_l \tag{3.59}$$

where

$$\phi_l^2 = 1 + \frac{C}{X} + \frac{1}{X^2} \tag{3.60}$$

$$X^2 = \frac{(dp/dz)_l}{(dp/dz)_g} \tag{3.61}$$

$$-\left(\frac{dp}{dz}\right)_l = \frac{2f_l G^2 (1-x)^2}{\rho_l D} \tag{3.62}$$

$$-\left(\frac{dp}{dz}\right)_g = \frac{2f_g G^2 x^2}{\rho_g D} \tag{3.63}$$

$$\begin{cases} f_k = 16Re_k^{-1}\ for\ Re_k < 2000 \\ f_k = 0.079Re_k^{-0.25}\ for\ 2000 \leq Re_k < 20000 \\ f_k = 0.046Re_k^{-0.2}\ for\ 20000 \leq Re_k \end{cases} \tag{3.64}$$

subscripts k denotes *liq* or *gas* for liquid and vapour phases respectively.

$$Re_l = \frac{G(1-x)D}{\mu_l} \tag{3.65}$$

$$Re_g = \frac{GxD}{\mu_g} \tag{3.66}$$

$$Re_{lo} = \frac{GD}{\mu_l} \tag{3.67}$$

$$Su_{go} = \frac{\sigma \rho_g D}{{\mu_g}^2} \tag{3.68}$$

Table 3.3. Kim and Mudawar correlation coefficients.

Liquid	Vapour	C
Turbulen	Turbulent	$0.39Re_{lo}^{0.03}Su_{go}^{0.10}\left(\frac{\rho_l}{\rho_g}\right)^{0.35}$
Turbulent	Laminar	$8.7\cdot 10^{-4}Re_{lo}^{0.17}Su_{go}^{0.50}\left(\frac{\rho_l}{\rho_g}\right)^{0.14}$
Laminar	Turbulent	$0.0015Re_{lo}^{0.59}Su_{go}^{0.19}\left(\frac{\rho_l}{\rho_g}\right)^{0.36}$
Laminar	Laminar	$3.5\cdot 10^{-5}Re_{lo}^{0.44}Su_{go}^{0.50}\left(\frac{\rho_l}{\rho_g}\right)^{0.48}$

(3.69)

3.3 HEAT TRANSFER COEFFICIENT“HTC”

The second most important parameter is the heat transfer coefficient (HTC). There are many correlations for its calculation. In the following paragraphs the more important correlations are briefly described. This description goes from normal channel to mini-channels

3.3.1 Common Channel Correlations

Heat transfer calculation has been widely studied in macro-channels for a long time. There are several discrepancies with mini-channels in terms of dimensions, shear stresses and so on. The most relevant models for HTC calculation in macro-channels are described below.

3.3.1.1 Haraguchi et al. [24]

These authors measured condensation HTC of R22, R134a and R123 in a horizontal smooth tube. Based on the turbulent liquid film theory and Nusselt´s theory, they proposed an empirical equation for HTC in terms of the vapour shear stress (Nu_F) and gravity force (Nu_B).

This model takes into account Galilei and Prandtl dimensionless numbers. Galilei number relates gravity and viscous forces. This number is used in viscous flow and thermal expansion calculations. Prandtl dimensionless number relates momentum diffusivity to thermal diffusivity. It must point out that Prandtl number contains no length scale in its definition and is dependent only on the fluid and the fluid state.

$$\alpha = \frac{Nu\lambda_L}{D} \tag{3.70}$$

$$Nu = (Nu_F^2 + Nu_B^2)^{1/2} \tag{3.71}$$

$$Nu_F = 0.0152\left(1 + 0.6Pr_{liq}^{0.8}\right)\frac{\phi_g}{X}Re_l^{0.77} \tag{3.72}$$

$$Nu_B = 0.725H(\varepsilon)\left(\frac{GaPr_l}{H_l}\right)^{0.25} \tag{3.73}$$

$$\phi_g = 1 + 0.5\left[\frac{G}{\sqrt{gd\rho_g\left(\rho_l - \rho_g\right)}}\right]^{0.75} X^{0.35} \tag{3.74}$$

$$H(\varepsilon) = \varepsilon + \{10[(1-e)^{0.1} - 1] + 1.7\cdot 10^{-4}Re\}\sqrt{\varepsilon}\left(1 - \sqrt{\varepsilon}\right) \tag{3.75}$$

The void fraction is calculated by means of the Smith expression [2], Eq. (3.3).

3.3.1.2 Dobson and Chato [24]

These authors developed a two-phase HTC correlation based on Martinelli parameter. They correlated the two-phase HTC to liquid phase HTC. This correlation was developed for macro-tubes.

$$\frac{\alpha}{\alpha_l} = 1 + \frac{2.22}{X^{0.89}} \tag{3.76}$$

$$\alpha_l = 0.023Re_l^{0.8}Pr_l^{0.4}\frac{\lambda_l}{D} \tag{3.77}$$

3.3.1.3 Akers and Rosson [25]

These authors developed a two-phase multiplier-based correlation that became known as the “equivalent Reynolds number” model. This model defines the all-liquid mass flow rate that provides the same heat transfer coefficient as an annular condensing flow:

$$Nu = C_1 Pr_l^{1/3} \left(\frac{h_{fg}}{c_{p\,l}(T_{sat} - T_{wall})} \right)^{1/4} Re_g^{C_2} \tag{3.78}$$

$$Re_g = \left(\frac{G_{eq}\, D\, x}{\mu_l} \right) \left(\frac{\rho_l}{\rho_g} \right)^{1/2} \tag{3.79}$$

$$G_{eq} = G_l + G_g \left(\frac{\rho_l}{\rho_g} \right)^{1/2} \tag{3.80}$$

$$\begin{cases} 1000 < Re_{gas} < 20000\ then\ C_1 = 13.8\ and\ C_2 = 0.2 \\ 20000 < Re_{gas} < 30000\ then\ C_1 = 0.1\ and\ C_2 = 2/3 \end{cases} \tag{3.81}$$

Thus, there is nothing in this criterion about the flow instability when passing from an annular flow to a stratified-wavy flow.

3.3.2 Correlations For Mini-Channels

In recent years, several authors have investigated and developed new correlations for HTC calculation in reduced flow area tubes. Some of the most important correlations are presented below.

3.3.2.1 Webb et al. [26]

The authors presented a model applicable for a wide range of tube geometries including copper tubes and multi-port extruded aluminium tubes. The heat transfer coefficient proposed by this author has the following form:

$$\alpha = \alpha_l \left[1.31\, Pr_l^{-0.815} (R^+)^A Re_l^B \right] \tag{3.82}$$

where

$$R^+ = 0.0994 Re_{eq}^{\frac{7}{8}},\ \ A = 0.126 Pr_l^{-0.448},\ \ B = -0.113 Pr_l^{-0.563} \tag{3.83}$$

and

$$Re_{eq} = \left[0.5 \frac{D^3}{f_{l,eq}} \frac{\rho_l}{\mu_l^2} \left(\frac{dp}{dz} \right)_{liq} \right]^{0.5} \quad and \quad f_{l,eq} = 0.079 Re_{eq}^{-0.25} \tag{3.84}$$

α_l comes from Mosser et al.[27] expression.

$$Nu = \frac{\alpha_l D}{\lambda_l} = \frac{0.0994^{C_1} Re_l^{C_2} {Re_{eq}}^{1+0.875 C_1} {Pr_l}^{0.815}}{\left(1.58 \ln Re_{eq} - 3.28\right)\left(2.58 \ln Re_{eq} + 13.7\, Pr_l^{2/3} - 19.1\right)} \tag{3.85}$$

with

$$\begin{aligned} C_1 &= \quad 0.126\, Pr_l^{-0.448} \\ C_2 &= -0.113\, Pr_l^{-0.563} \end{aligned} \tag{3.86}$$

3.3.2.2 Wang et al. [28]

Wang et al. proposed an expression for heat transfer coefficient that is a combination of annular and stratified flow contribution.

$$Nu = \frac{\lambda_l}{D}(f_1 Nu_{annul} + (1 - f_1)Nu_{strat}) \tag{3.87}$$

where

$$f_1 = (x_{in} - x_{tran})/(x_{in} - x_{out}) \tag{3.88}$$

takes into account the proportional part of the test section which is under annular flow regime. The stratified flow part contribution is calculated with:

$$Nu_{strat} = \varepsilon Nu_{film} + (1 - \varepsilon)Nu_{convection} \tag{3.89}$$

and void fraction, ε is calculated with Zivi`s equation [1], Eq. (3.2):

$$Nu_{film} = 0.555\left(\frac{\rho_l(\rho_l - \rho_g)g\, h_{l-g}}{\lambda_l \mu_l (T_{sat} - T_{wall})}\right)^{1/4} \tag{3.90}$$

$$Nu_{convection} = 0.023 Re_l^{0.8} Pr_l^{0.4} \tag{3.91}$$

That is the Dittus-Boelter correlation [29] and,

$$Nu_{annul} = 0.0274 Pr_l Re_l^{0.6792} x^{0.2208}\left(\frac{1.376 + 8X^{1.655}}{X^2}\right)^{0.5} \tag{3.92}$$

where the Martinelli parameter, *X,* is given by:

$$X = \left(\frac{\mu_l}{\mu_g}\right)^{0.1}\left(\frac{1 - x}{x}\right)^{0.9}\left(\frac{\rho_g}{\rho_l}\right)^{0.5} \tag{3.93}$$

and finally:

$$\alpha = \frac{Nu\, D}{\lambda_l} \tag{3.94}$$

3.3.2.3 Koyama et al. [30]

The authors proposed an asymptotic expression with the form:

$$\alpha = \frac{\lambda_l}{D} \quad Nu = \frac{\lambda_l}{D}\sqrt{Nu_F^2 + Nu_B^2} \tag{3.95}$$

where

$$Nu_F = 0.0112 Pr_l^{1.37}\left(\frac{\phi_g}{X}\right) Re_l^{0.7} \tag{3.96}$$

$$Re_l = \frac{G(1-x)D}{\mu_l} \tag{3.97}$$

$$Nu_B = 0.725\left(1 - e^{-0.85\sqrt{Bo}}\right) H(\varepsilon)\left(\frac{Ga_l Pr_l}{Ph_l}\right)^{1/4} \tag{3.98}$$

with

$$H(\varepsilon) = \varepsilon + [10(1-\varepsilon)^{0.1} - 8.9]\sqrt{\varepsilon}\left(1 - \sqrt{\varepsilon}\right) \tag{3.99}$$

The Galilei number is,

$$Ga = \frac{g\rho_l^2 D^3}{\mu_l^2} \tag{3.100}$$

$$Ph_l = \frac{Cp_l\left(T_{ref} - T_{wall}\right)}{h_{l-g}} \tag{3.101}$$

and Bond number is,

$$Bo = \frac{D^2 g\left(\rho_l - \rho_g\right)}{\sigma} \tag{3.102}$$

The void fraction value is calculated with Smith´s correlation [2], Eq. (3.3).

And the two-phase gas flow multiplier, ϕ_g^2 is calculated with the equation introduced by Koyama et al. [31]

$$\phi_g^2 = 1 + 21(1 - e^{-0.319D})X + X^2 \tag{3.103}$$

3.3.2.4 Cavallini et al. [32-36]

The authors proposed the following expression for heat transfer coefficient in shear dominated regime.

$$\alpha = \frac{\rho_l Cp_l}{T^+}\left(\frac{\tau}{\rho_l}\right)^{0.5} \tag{3.104}$$

where

$$T^+ = \begin{cases} \delta^+ Pr_l & for\ Re_l \le 1145 \\ 0.0504 {Re_l}^{7/8} & for\ Re_l > 1145 \end{cases} \tag{3.105}$$

$$Re_l = G(1-x)(1-E)\frac{D}{\mu_l} \tag{3.106}$$

and

$$\tau = \left(\frac{dp}{dz}\right)_f \frac{D}{4} \tag{3.107}$$

$\left(\frac{dp}{dz}\right)_f$ is calculated with the correlation introduced by Cavallini et al. [32] and the liquid entrainment ratio "E" comes from Paleev and Filipovich equation [19]:

$$E = 0.015 + 0.44\, ln\left[\left(\frac{\rho_{gc}}{\rho_l}\right)\left(\frac{\mu_l j_g}{\sigma}\right)^2\right] \tag{3.108}$$

$$\rho_{gc} = \rho_g\left(1 + \frac{(1-x)E}{x}\right) \tag{3.109}$$

under the restriction:

$$E = 0.95\ if\ E \ge 0.95 \tag{3.110}$$

$$j_g = \frac{xG}{\left[gD\rho_g(\rho_l - \rho_g)\right]^{0.5}} \tag{3.111}$$

The heat transfer coefficient in free convection can be obtained using the correlations of Koyama et al. [30] or Wang et al. [28].

3.3.2.5 Garimella et al. [37]

During condensation process, the flow pattern changes from mist flow (where applicable) to annular flow and after that to intermittent flow pattern with high overlaps. Since the border between flow patterns is not clear, there exits transition flows (intermittent/annular, intermittent/annular/mist and annular/mist).

The following turbulent parameters are defined:

$$u^+ = \frac{u}{u^*} \tag{3.112}$$

$$y^+ = \frac{y\, \rho_l u^*}{\mu_l} \tag{3.113}$$

$$R^+ = \frac{R\, \rho_l u^*}{\mu_l} \tag{3.114}$$

Where frictional velocity is given by:

$$u^* = \sqrt{\tau_i / \rho_l} \tag{3.115}$$

In the previous equation, commonly used wall shear stress has been replaced by interfase shear stress. The last one models improve the two-phase situation introduced by Garimella et al. [37]

$$T^+ = \frac{\rho_l C p_l u^*}{q''}(T_i - T_{wall}) \tag{3.116}$$

Shear stress and heat flux written in commonly used expressions:

$$\tau = (\mu + \rho \omega_{mom})\frac{du}{dy} \tag{3.117}$$

$$q'' = -(\lambda + \omega\, \rho\, Cp)\frac{dT}{dy} \tag{3.118}$$

Assuming that the interface temperature is equal to the saturation temperature.

$$\alpha = \frac{q''}{T_{sat} - T_{wall}} = \frac{\rho_l C p_l u^*}{T^+} \tag{3.119}$$

$$\frac{dT^+}{dy^+} = \left(\frac{1}{Pr_l} + \frac{\rho_l \omega_h}{\mu_l}\right)^{-1} \tag{3.120}$$

The liquid film thickness is obtained with Baroczy [3] void fraction model as suggested below:

$$\delta = \left(1 - \sqrt{\varepsilon}\right)\frac{D}{2} \tag{3.121}$$

The non-dimensional turbulent liquid film thickness is defined as:

$$\delta^+ = \frac{\delta\, \rho_l u^*}{\mu_l} \tag{3.122}$$

$$\frac{\rho_l \omega_{mom}}{\mu_l} = \frac{1 - {y^+}/{R^+}}{{du^+}/{dy^+}} - 1 \tag{3.123}$$

$$T^+ = 5Pr_l + 5\, ln\left[Pr_l\left(\frac{\delta^+}{5} - 1\right) + 1\right]\ if\ Re_l < 2100 \tag{3.124}$$

$$T^+ = 5Pr_l + 5\, ln[5Pr_l + 1] + \int_{30}^{\delta^+} \frac{dy^+}{\left(\frac{1}{Pr_l} - 1\right) + \frac{y^+}{5}\left(1 - \frac{y^+}{R^+}\right)}\ if\ Re_l > 2100 \tag{3.125}$$

Using Agarwal et al. [39], pressure drop can be calculated and then:

$$\tau = \left(\frac{dp}{dz}\right)_f \frac{D}{4} \tag{3.126}$$

In order to get the heat transfer coefficient, the interfacial shear stress is calculated using the pressure drop model and the previous equation. With that result, frictional velocity can be calculated u^*, δ^+, $T^+$and finally α.

3.3.2.6 Bandhauer et al. [40]

The authors presented a model for predicting heat transfer during condensation of R134a in horizontal mini-channels. The model was developed for the entire vapour-liquid dome. The measurements were carried out with three different circular multi-port tubes.

The heat transfer coefficient in the refrigerant side is given by:

$$\alpha = \frac{\rho_l c_{p\,l} u^*}{T^+} \tag{3.127}$$

$$x_{tran} = \frac{a}{G + b} \tag{3.128}$$

where

$$a = 60.57 + 22.60e^{0.259D} \tag{3.129}$$

$$b = 59.99 + 176.8e^{0.383D} \tag{3.130}$$

$$T^+ = 5Pr_l + 5\ ln\left[Pr_l\left(\frac{\delta^+}{5} - 1\right) + 1\right]\ if\ Re_{liq} < 2100 \tag{3.131}$$

$$T^+ = 5Pr_l + 5\ ln[5Pr_l + 1] + \int_{30}^{\delta^+} \frac{dy^+}{\left(\frac{1}{Pr_l} - 1\right) + \frac{y^+}{5}\left(1 - \frac{y^+}{R^+}\right)}\ if\ Re_l > 2100 \tag{3.132}$$

where

$$u^* = \sqrt{\frac{\tau}{\rho_l}},\quad \tau = \left(\frac{dp}{dz}\right)_f \frac{D}{4} \tag{3.133}$$

$$Re_l = \frac{GD_h(1 - x)}{(1 + \sqrt{\varepsilon})\mu_l} \tag{3.134}$$

With $\left(\frac{dp}{dz}\right)_f$ being evaluated with the expression proposed by Agarwal et al. [39].

3.4. CONCLUSIONS

In this chapter several of the most widely used models used are summarised. Some classical models and other specially developed to be used with mini-channels are presented.

To correctly predict HTC an accurate correlation for pressure drop prediction must be used in order to calculate saturation condition of the refrigerant. Several models use the void fraction parameter to predict pressure drop so the order chosen to present this chapter was void fraction, pressure drop models and finally HTC models.

REFERENCES

[1] S.M. Zivi, Estimation of steady-state steam void-fraction by means of the principle of minimum entropy production, Journal of Heat Transfer, 86 (1964) 247.

[2] S.L. Smith, Void Fractions in Two-Phase Flow: A correlation Based upon an Equal Velocity Head Model, 1969, pp. 647-664.

[3] C.J. Baroczy, A systematic correlation for two phase pressure drop, 1966, pp. 232-249.

[4] D. Chisholm, A theoretical basis for the Lockhart-Martinelli correlation for two-phase flow, International Journal of Heat and Mass Transfer, 10 (1967) 1767-1778.

[5] J.J.J. Chen, A further examination of void fraction in annular two-phase flow, International Journal of Heat and Mass Transfer, 29 (1986) 1760-1763.

[6] R.W. Lockhart and R.C. Martinelli, Proposed correlation of data for isothermal two-phase, two-component flow in pipes, Chem. Eng. Prog, 45 (1949) 39-48.

[7] L. Friedel, Improved Friction Pressure Drop Correlations for Horizontal and Vertical Two Phase Pipe Flow. European Two Phase Flow Group Meeting. Paper E 2. Ispra, Italy, 1979.

[8] H. Muller-Steinhagen and K. Heck, A simple friction pressure drop correlation for two-phase flow in pipes, Chemical Engineering and Processing: Process Intensification, 20 (1986) 297-308.

[9] K. Mishima and T. Hibiki, Some characteristics of air-water two-phase flow in small diameter vertical tubes, International Journal of Multiphase Flow, 22 (1996) 703-712.

[10] M. Zhang and R.L. Webb, Correlation of two-phase friction for refrigerants in small-diameter tubes, Experimental Thermal and Fluid Science, 25 (2001) 131-139.

[11] S. Garimella, A. Agarwal, and J.D. Killion, Condensation Pressure Drop in Circular Microchannels, Heat Transfer Engineering, 26 (2006) 28-35.

[12] H. Ju Lee and S. Yong Lee, Pressure drop correlations for two-phase flow within horizontal rectangular channels with small heights, International Journal of Multiphase Flow, 27 (2001) 783-796.

[13] S.W. Churchill, Friction-factor equation spans all fluid-flow regimes, ChemEng (New York), 84 (1977) 91-92.

[14] Cavallini, D. Del Col, L. Doretti, M. Matkovic, L. Rossetto, and C. Zilio, Two-phase frictional pressure gradient of R236ea, R134a and R410A inside multi-port mini-channels, Experimental Thermal and Fluid Science, 29 (2005) 861-870.

[15] Cavallini, L. Doretti, M. Matkovic, and L. Rossetto, Update on Condensation Heat Transfer and Pressure Drop inside Minichannels, Heat Transfer Engineering, 27 (2006) 74-87.

[16] J. W. Coleman, , Flow Visualization and Pressure Drop for Refrigerant Phase Change and Air-Water Flow in Small Hydraulic Diameter Geometries, Ph.D. thesis, Iowa State University, Ames, Iowa, 2000.

[17] M. Zhang, A New Equivalent Reynolds Number Model for Vapor shear-controlled Condensation inside Smooth and Micro-Fin Tubes. Ph.D. thesis, The Pennsylvania State University, 1998.

[18] A. Cavallini, D. Del Col, L. Doretti, M. Matkovic, L. Rossetto, and C. Zilio, Measurement of Pressure Gradient During Two- Phase Flow inside Multi-Port Mini-Channels, 3rd Int. Symposium on Two-Phase Flow Modelling and Experimentation, Pisa, September 22–24, 2004.]

[19] I.I. Paleev and B.S. Filippovich, Phenomena of liquid transfer in two-phase dispersed annular flow, International Journal of Heat and Mass Transfer, 9 (1966) 1089-1093.

[20] G.F. Hewitt and N.S. Hall-Taylor, Annular two-phase flow, Pergamon, 1970.

[21] A. Cavallini, D. Del Col, M. Matkovic, and L. Rossetto, Frictional pressure drop during vapourliquid flow in minichannels: Modelling and experimental evaluation, International Journal of Heat and Fluid Flow, 30 (2009) 131-139.

[22] L. Sun and K. Mishima, Evaluation analysis of prediction methods for two-phase flow pressure drop in mini-channels, International Journal of Multiphase Flow, 35 (2009) 47-54.

[23] S.M. Kim and I. Mudawar, Universal approach to predicting two-phase frictional pressure drop for adiabatic and condensing mini/micro-channel flows, International Journal of Heat and Mass Transfer, 55 (2012) 3246-3261.

[24] H. Haraguchi, S. Koyama, and T. Fujii, Condensation of refrigerants HCFC 22, HFC 134a and HCFC 123 in a horizontal smooth tube, Trans. JSME (B), 60 (1994) 245-252.

[24] M.K. Dobson and J.C. Chato, Condensation in smooth horizontal tubes, Journal of Heat Transfer, 120 (1998) 193-213.

[25] Akers, W. W., &Rosson, H. F. Condensation Inside a Horizontal Tube. Chemical Engineering Progress Symposium Series, 50 (1960). 145–149

[26] R.L. Webb, M. Zhang, and R. Narayanamurthy, Condensation heat transfer in small diameter tubes, Heat Transfer, 1998, pp. 403-408.

[27] K.W. Moser, B. Na, and R.L. Webb, A New Equivalent Reynolds Number Model for Condensation in Smooth Tubes, Journal of Heat Transfer, 120 (1998) 410-417.

[28] W.W. William Wang, T.D. Radcliff, and R.N. Christensen, A condensation heat transfer correlation for millimeter-scale tubing with flow regime transition, Experimental Thermal and Fluid Science, 26 (2002) 473-485.

[29] P. W. Dittus, and L. M. K. Boelter. Univ. Calif. Pub. Eng., Vol. 2, No. 13, pp. 443-461 (1930), reprinted in Int. Comm. Heat Mass Transfer, Vol. 12, pp. 3-22 (1985).

[30] S. Koyama, K. Kuwahara, K. Nakashita, and K. Yamamoto, An experimental study on condensation of refrigerant R134a in a multi-port extruded tube, International Journal of Refrigeration, 26 (2003) 425-432.

[31] S. Koyama, K. Kuwahara, and K. Nakashita, Condensation of refrigerant in a multi-port channel, First International Conference on Microchannels and Minichannels, 2003, pp. 193-205.

[32] Cavallini, D. Del Col, L. Doretti, M. Matkovic, L. Rossetto, and C. Zilio, Two-phase frictional pressure gradient of R236ea, R134a and R410A inside multi-port mini-channels, Experimental Thermal and Fluid Science, 29 (2005) 861-870.

[33] A. Cavallini, D. Del Col, L. Doretti, M. Matkovic, L. Rossetto, and C. Zilio, Condensation Heat Transfer and Pressure Gradient Inside Multiport Minichannels, Heat Transfer Engineering, 26 (2005) 45-55.

[34] A. Cavallini, L. Rossetto, M. Matkovic, and D. Del Col, A model for frictional pressure drop during vapour-liquid flow in minichannels, International Institute of Refrigeration (IIR) - International Conference on Thermophysical properties and transfer processes of refrigerants, 2005.

[35] A. Cavallini, D. Del Col, L. Doretti, M. Matkovic, L. Rossetto, and C. Zilio, A model for condensation inside minichannels. ASME Summer Heat Transfer Conference. ASME Summer Heat Transfer Conference, 2005.

[36] Cavallini, L. Doretti, M. Matkovic, and L. Rossetto, Update on Condensation Heat Transfer and Pressure Drop inside Minichannels, Heat Transfer Engineering, 27 (2006) 74-87.

[37] S. Garimella, Condensation Flow Mechanisms in Microchannels: Basis for Pressure Drop and Heat Transfer Models, Heat Transfer Engineering, 25 (2004) 104-116.

[38] S. Garimella, J.D. Killion, and J.W. Coleman, An Experimentally Validated Model for Two-Phase Pressure Drop in the Intermittent Flow Regime for Circular Microchannels, Journal of Fluids Engineering, 124 (2001) 205-214.

[39] A. Agarwal and S. Garimella, Modeling of Pressure Drop During Condensation in Circular and Noncircular Microchannels, Journal of Fluids Engineering, 131 (2008) 011302.

[40] T.M. Bandhauer, A. Agarwal, and S. Garimella, Measurement and Modeling of Condensation Heat Transfer Coefficients in Circular Microchannels, Journal of Heat Transfer, 128 (2006) 1050-1059.

CHAPTER 4: Experimental Installation Description

The following paragraphs describe the installation in which experimental data were registered. The installation is placed in the Thermal and Fluid Engineering Department at the Technical University of Cartagena, Spain.

The main purpose of this installation is to measure heat transfer coefficient and pressure drop in condensation tests in a mini-channel multiport tube. This installation was upgraded along the development of this PhD and it has allowed us to record an important amount of experimental measurements of heat transfer coefficient and pressure drop of condensing refrigerants inside mini-channel multi-port tubes. New and traditional fluids were tested, during condensation process.

4.1 EXPERIMENTAL INSTALLATION DESCRIPTION

The experimental installation used for the tests developed is shown in Fig. 4.1. The test rig consists of the primary (refrigerant) loop and three auxiliary loops: two cooling water loops and one heating water loop.

The test section is the main component of the primary loop. It is made with a multiport mini-channel tube with a condensation measuring section of 259 mm length. The multiport tube studied in this thesis has a hydraulic diameter of 1.16 mm.

In order to control the vapour quality at the inlet of the test section, the refrigerant is previously pumped to an evaporator where it is total or partially evaporated up to a predetermined value of the vapour quality. The temperature of the refrigerant at the inlet of the evaporator is measured by a resistive temperature detector (RTD). After passing through the evaporator, the two-phase mixture flows through a ten centimetre copper tube to the inlet header. Uniform two-phase flow is assumed to be developed in the copper section before entering to the measuring section through the inlet header. This is an approximation but it is a common practice (e.g.: [1-4]). These references show experimental test sections similar to the section tested.

Then, the refrigerant flows through the test section where it is partially condensed. The measuring section has an external casing so it is shaped as a counter-current heat exchanger. The cold water provided by the first cooling water loop flows through the external casing whereas the condensing fluid flows inside the mini-channel. The temperature of the water at the inlet and the outlet of the test section is measured by two RTDs. Mass flow rate is also measured. Wall temperature of the test section is measured in nine equally separated points by means of thermocouples soldered to the tube wall. The temperature of the refrigerant at the inlet and the outlet of the test section are measured by RTDs. No flow disturbance on water case was detected due to the reduced diameter of the wires employed. Another flow meter is used to measure the refrigerant mass flow rate in the primary loop. The pressure measurements are obtained through two pressure transducers, connected to the inlet and the outlet of the test section.

Finally, the two phase mixture that leaves the test section is completely condensed in another heat exchanger thanks to the cold water provided by the second cooling water loop. The sub cooled refrigerant from the condenser is then returned to a small vessel from which the cycle will be repeated again. There is a controlled gear pump connected to this vessel, magnetically coupled to its variable speed electric motor. A control system guarantees steady state conditions and ensures that measurements are properly made.

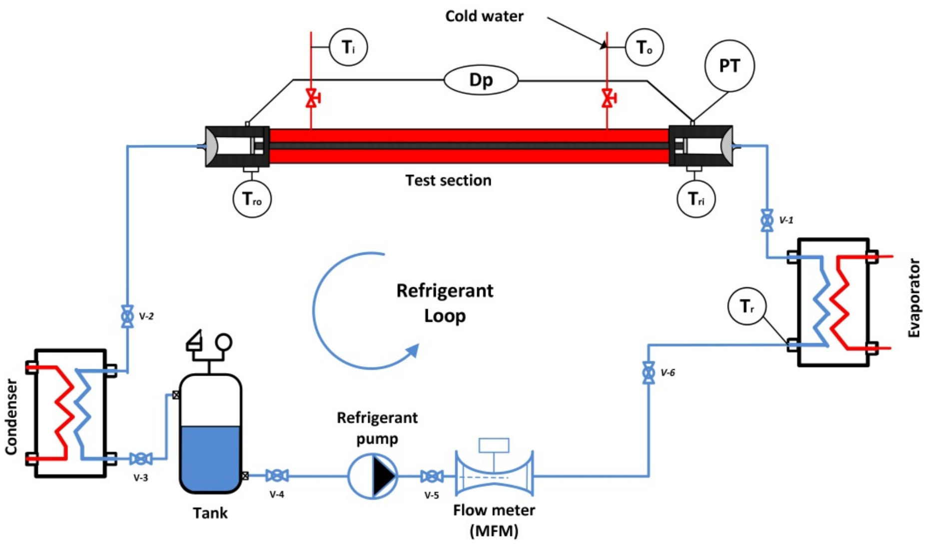

Fig. 4.1. Experimental test rig.

The tube studied is soldered to two headers that have two main roles. Firstly they are used to hydraulically connect the measuring section to the test rig. Secondly they have machined two ports each one to connect measuring instruments.

The presence of both temperature and pressure sensors at the inlet of the measuring sector allows a double check of the saturation temperature.

4.2 CONTROL SYSTEM DESCRIPTION

The control system of the above described installation is made with an acquisition card connected in a personal computer. The control software was developed in Matlab®.

Three different PID controllers are used in this installation. All of them vary frequency converter signals to modify actuator state. The first one controls the mass flow rate of the test section with the volumetric displacement pump and Coriolis effect measuring sensor. The second one regulates the thermal power exchanged in the evaporator in order to increase refrigerant vapour quality up to a desired value. The last control loop regulates the thermal power exchanged in the condenser in order to keep the system pressure controlled.

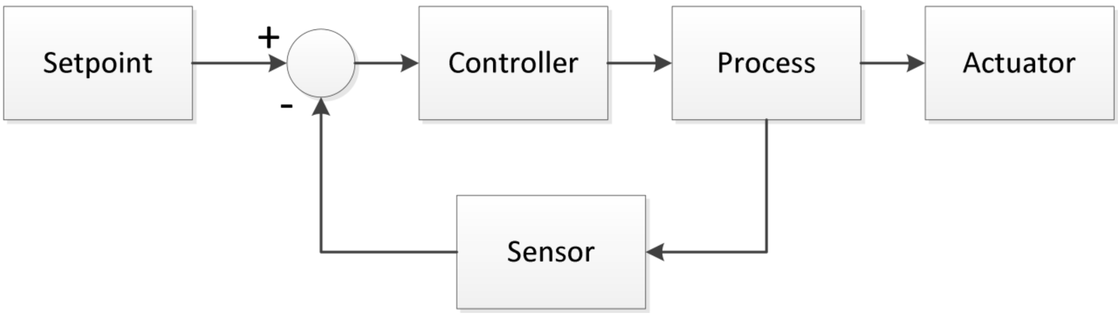

Figure 4.2. Block diagram of programmed controllers.

There are three commercial controllers to regulate secondary loops in addition to the previous controllers. These secondary loops controls the two mixing valves, placed at the inlet of the test section and condenser, and the hot water temperature.

4.3 TEST SECTION

The test section is made from a multiport mini-channel tube with a condensation measuring section of 259 mm length and two adiabatic sectors of 23.5 mm inside the headers. The multiport tube considered in this study has a hydraulic diameter of 1.16 mm. Its main characteristics are summarised in Table 4.1. Cross section and water chase is illustrated in Figure 4.3. The multi-port extruded aluminium tube was provided by Modine Manufacturing Company ©.

The measuring section has an external casing so it is shaped as a counter-current heat exchanger with the cooling water flowing outside and the condensing fluid inside the mini-channel. Wall temperature of the test section is measured in nine equally separated points by means of thermocouples soldered to the tube. The locations of thermocouples can be seen in Figure 4.4. The geometry of the test section was measured with an optical microscope getting accurate values of inner, outer areas and perimeters. Surface roughness was measured with a Scanning Electron Microscope (SEM) at the Research Technology Support Service of the Technical University of Cartagena.

The presence of both temperature and pressure sensors at the inlet of the measuring sector allows a double check of the saturation temperature.

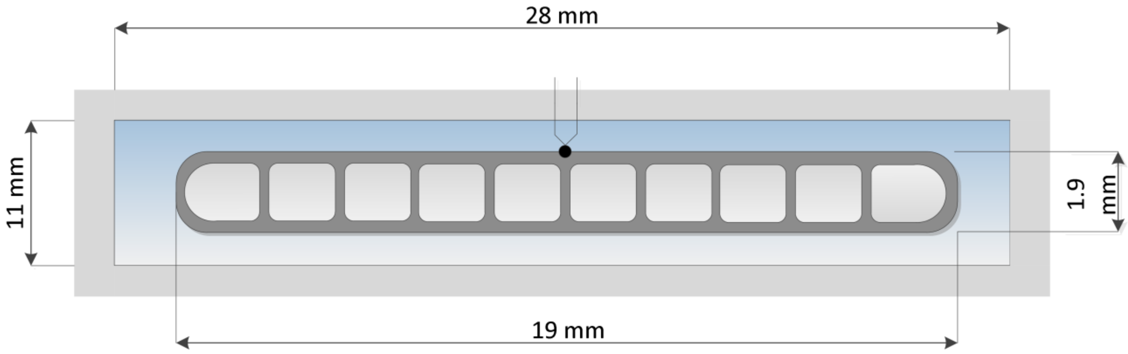

Figure 4.3. Tested geometry, thermocouple location and water chase geometry.

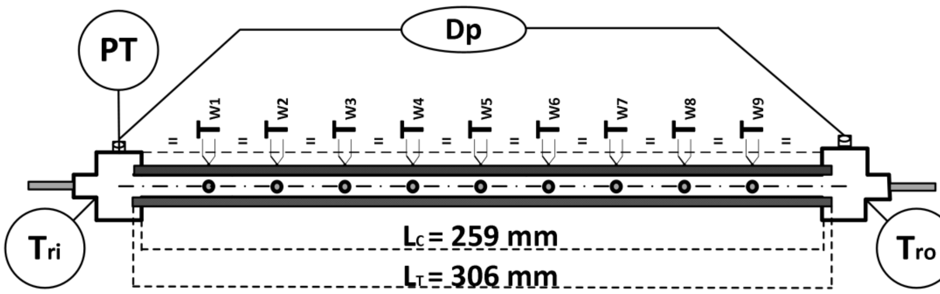

Figure 4.4. Thermocouple location and tube lengths.

Table 4.1. Tube characteristics.

Tube model	Flow area (mm^2)	Outer perimeter (mm)	Inner perimeter (mm)	Ports	D_h (mm)	Ra (µm)	RR (−)
Square ports	12.54	40.17	43.22	10	1.16	0.226	$3.89 \cdot 10^{-4}$

4.4 MEASUREMENT INSTRUMENTS AND ACTUATORS

4.4.1 Temperature sensors

There are two different types of temperature sensors in this experimental installation. T-type thermocouples and RTD100 sensors. T-type thermocouples are soldered to tube wall to measure tube wall temperature and RTD100 sensors are used to measure bulk temperature of the two different fluids, see Figure 4.1.

The base accuracy provided by the manufacturer of RTD sensors is 0.03 K and 0.5 K for T-type thermocouples.

4.4.2 Mass flow meters

There are two Coriolis Effect mass flow meters in the installation to measure refrigerant and cooling test section water mass flows. The electronic transmitter coupled with measuring element, both of them have a base accuracy of 0.05 % of measurement.

4.4.3 Electromagnetic volumetric flow meter

There are two electromagnetic flow meters placed on the condenser and hot water loop. The one placed on the condenser loop allows checking the whole energy balance of the experimental installation. The flow meter installed in the hot water loop is used to calculate the thermal input to the installation. Both of them have a base accuracy of 0.25 %.

4.4.4 Pressure transmitters

There are three sensors in the experimental installation, two absolute and one differential pressure transmitters. The absolute transmitters are connected to the vessel and to the inlet of the test section to get the pressure measurement on these places. The differential pressure transmitter gets the differential pressure across the test section as the refrigerant condensates. The range of the two absolute transmitters goes up to 58 bars and the differential up to 1 bar. The base accuracy is lower than 0.009 % for the differential one and 0.008 % for the both absolute.

4.4.5 Actuators

The control system acts on three different frequency converters that regulate the rotating speed of three pumps installed and on a three way mixing valve.

- The refrigerant gears pump to achieve the desired mass flow rate.
- The hot water pump to regulate the thermal input to the installation and the pump that feeds the condenser after the test section which controls the pressure of the system.
- The test section water temperature is varied with a recirculating valve for each refrigerant saturation pressure to get small vapour quality variations.

4.5 ACQUISITION SYSTEM

The signals provided by sensor elements and measurement equipment are connected to an Agilent Technologies multimeter, model 34970A with three 20 channel armature multiplexer model 34901A because of its accuracy. The software used to register the signal values is Benchlink Data Logger v3 provided by the manufacturer.

The control was specially programed with Matlab and it uses a National Instruments card installed on a personal computer that controls the installation. The Graphical User Interface was also developed with Matlab Guide Tool. The appearance is depicted in Figure 4.5.

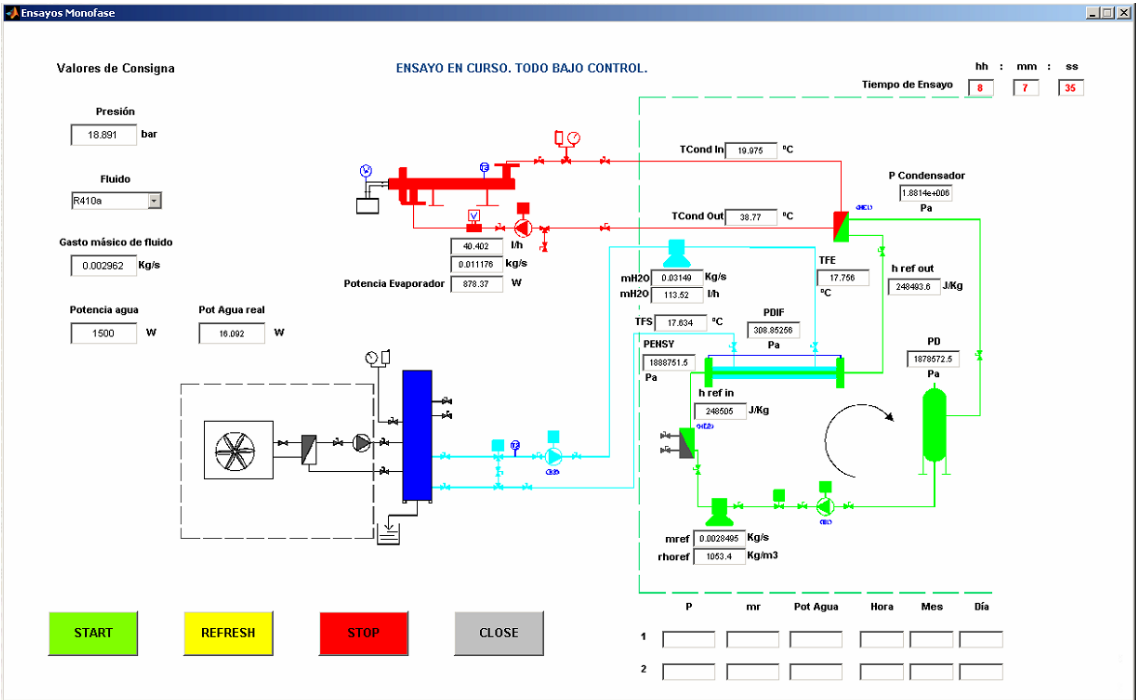

Figure 4.5. Installation Graphical User Interface.

4.6 INSTRUMENT CALIBRATION

All the sensor elements connected in this installation were calibrated by the manufacturer over the entire ranges and all of them were acquired with calibration certificate.

Thermocouples measurements were checked after soldering process in special tests against thermo-resistor measurements.

4.7 WORKING FLUIDS

The fluids tested were R134a, R1234yf, R290 and R32. The refrigerant R134a is a widely tested refrigerant and it has no interest except for installation validation. Several tests were made over a wide range of conditions of mass flux, vapour quality and saturation pressures. A good agreement was found between measured and modelled data by several author models.

Also the main substitute of R134a, the R1234yf was experimentally tested in the installation. Other refrigerants such as R290 (propane) and R32 were considered due to its naturally and none ozone depleting power.

The charge/discharge process of highly flammable refrigerants is a delicate process. Doubled checked processes were used in order not to provoke fire.

4.8 FLUIDS CHEMICAL COMPOSITION

All testing fluids were acquired to prestigious companies with fluid purity composition certificate. No leaks were discovered in the installation so fluid volume was conserved and no chemical composition variation was expected.

4.9 TESTING CONDITIONS

The different conditions tested for each refrigerant can be seen in Table 4.2. A total quantity of 582 tests were made for all refrigerants.

Table 4.2. Measurements made with refrigerants

Refrigerant	Saturation temperatures (°C)	Saturation pressures (kPa)	Mass velocities ($kg\ m^{-2}s^{-1}$)	Heat flux ($kW\ m^{-2}$)	Number of tests
R134a	40	1016.8	350 - 945	5.08 – 20.75	46
R1234yf	30 to 55	682.6 – 1464.7	350 - 945	4.37 – 42.45	189
R290	30 to 55	952.1 - 1907.2	150 - 350	4.98 – 36.25	189
R32	30 to 55	1689.6 – 3519.8	350 - 845	6.69 – 70.00	158

The highest values of heat fluxes correspond with some pressure drop experiments done to check the accuracy of the predicting correlation for momentum pressure gradient.

4.10 CONCLUSIONS

In this chapter the experimental installation constructed on purpose is described. It is a particular installation because it was designed to test flammable refrigerants so ATEX equipment and safety barriers were installed in order to prevent a possible risk of fire.

The experimental testing conditions used try to cover the highest range of conditions that can be present in refrigeration systems. The classical refrigerant R134a was used to validate the experimental installation and the measurement process. Other refrigerants such the new R1234yf, R32 potential substitute of R410A and natural hydrocarbon R290 were also experimentally tested.

REFERENCES

[1] M. Zhang and R.L. Webb, Correlation of two-phase friction for refrigerants in small-diameter tubes, Experimental Thermal and Fluid Science, 25 (2001) 131-139.

[2] S. Koyama, K. Kuwahara, K. Nakashita, and K. Yamamoto, An experimental study on condensation of refrigerant R134a in a multi-port extruded tube, International Journal of Refrigeration, 26 (2003) 425-432.

[3] A. Agarwal, T.M. Bandhauer, and S. Garimella, Measurement and modeling of condensation heat transfer in non-circular microchannels, International Journal of Refrigeration, 33 (2010) 1169-1179.

[4] K. Sakamatapan, J. Kaew-On, A.S. Dalkilic, O. Mahian, and S. Wongwises, Condensation heat transfer characteristics of R-134a flowing inside the multiport minichannels, International Journal of Heat and Mass Transfer, 64 (2013) 976-985.

CHAPTER 5: Experimental Data Analysis

In this chapter the experimental data analysis made of experimental measurements is explained. The analysis procedure is the same for the four refrigerants tested.

To make a full analysis of the experimental data, a program written in Fortran programming language was made. Heat transfer coefficients and frictional pressure drop values were automatically obtained with experimental data. The variation profile of heat transfer coefficient along the tube versus local properties such as vapour quality, saturation pressure and so on was also obtained.

The program was developed for any fluid and any test section. As cited in previous chapters, wall temperature is measured with nine thermocouples so the tube is divided into nine equal cells where heat transfer coefficient is calculated. Pressure drop is assumed linear due to the small saturation temperature variation in the tests and fluid properties are calculated with Refprop® v6 [1].

5.1 SINGLE-PHASE NUSSELT NUMBER

In order to validate the experimental setup and to obtain the HTC value in water side, a series of single-phase tests were developed following the method developed by Park et al. [2]. Average single-phase Nusselt number for the refrigerant flow can be obtained as:

$$\overline{Nu}_{ref} = \frac{\dot{q}D}{k_{ref}\left(\bar{T}_{ref} - \bar{T}_{wall\ inner}\right)} \tag{5.1}$$

where:

$$\dot{q} = \frac{\dot{m}_w Cp_w (T_{w\ out} - T_{w\ in})}{A} = \frac{\dot{m}_{ref} Cp_{ref}\left(T_{ref\ out} - T_{ref\ in}\right)}{A} = \lambda_{Al}\frac{\bar{T}_{wall\ outer} - \bar{T}_{wall\ inner}}{t} \tag{5.2}$$

$$\bar{T}_{wall\ inner} = \bar{T}_{wall\ outer} - \frac{\dot{q}\cdot t}{\lambda_{Al}} \tag{5.3}$$

$$\bar{T}_{wall\ outer} = \frac{1}{9}\sum_{j=1}^{9} T_{wall\ outer_j} \tag{5.4}$$

If refrigerant Nusselt number is calculated as explained above and compared with classical correlations such as Gnielinski, the results depicted in Fig. 5.1. are obtained.

Since during single-phase tests the fluid properties do not change appreciably along the tube, Reynolds number was considered practically constant and the local Nusselt number of the refrigerant flow is also expected to follow the Gnielinski correlation for turbulent flow:

$$Nu_{ref} = \frac{f/8\,(Re - 1000)Pr}{1 + 12.7\sqrt{f/8}\,(Pr^{2/3} - 1)} \tag{5.5}$$

The friction factor in turbulent region is obtained by means of eq. (5.7), that was verified to be the most accurate single-phase friction factor equation flow in smooth tubes by Fang et al [3,4] and Brkic [5].

$$f = \frac{64}{Re}\; for\; Re \leq 2000 \tag{5.6}$$

$$f = 0.25\left[log\left(\frac{150.39}{Re^{0.98865}} - \frac{152.66}{Re}\right)\right]^{-2} \; for\; Re \geq 3000 \tag{5.7}$$

$$f = (1.1525Re + 895) \cdot 10^{-5}\; for\; 2000 < Re < 3000 \tag{5.8}$$

The equation for the transition zone (eq. 5.8) was obtained by linear interpolation in Xu and Fang [6].

Taking into consideration the previous explanation, the local heat flux in each position "*j*" was calculated from wall temperature measurements and refrigerant temperature calculation using eq. (5.9):

$$\dot{q}_{ref,j} = Nu_{ref,j}\frac{\lambda_{ref,j}}{D_h}\left(T_{ref,j} - T_{wall\, inner,j}\right) \tag{5.9}$$

Refrigerant temperature in each position *"j"* was obtained from the temperature in the position *"j-1"* using eq. (5.10):

$$T_{ref,j} = T_{ref,j-1} - \left(\frac{\dot{q}_{ref,j-1} + \dot{q}_{ref,j}}{2\dot{m}_{ref}Cp_{ref}}\right) \tag{5.10}$$

For the first position eq. (5.10) becomes:

$$T_{ref,1} = T_{ref,in} - \frac{\dot{q}_{ref,1}}{\dot{m}_{ref}Cp_{ref}} \tag{5.11}$$

Since fluid properties depend on fluid temperature, the process is iterative and starts assuming linear evolution of refrigerant temperature, converging quickly to differences between two successive iterations lower than 0.5 %.

Fig.5.2. shows local heat flux and water side heat transfer coefficient profiles computed from single-phase experiments using Eqs. (5.7 to 5.11).

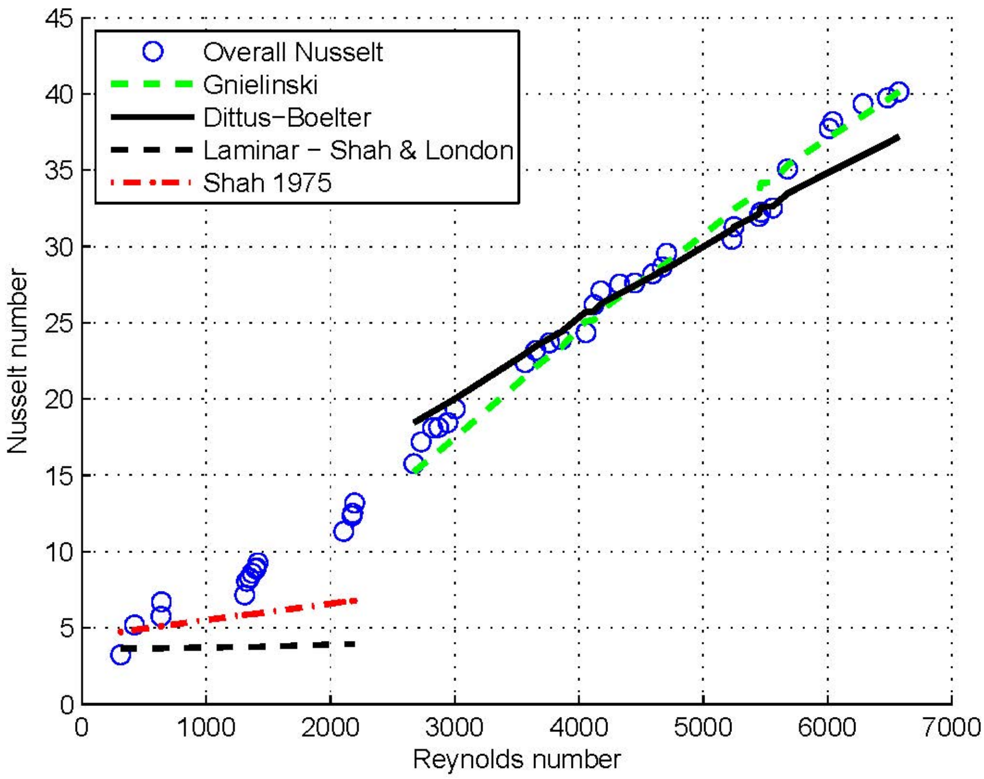

Figure 5.1. Liquid Nusselt number of R134a.

Once the local heat flux was calculated, a similar procedure was followed to obtain local HTC profile for the cooling water. Since all tests were carried out under steady-state conditions, there were no effects of energy accumulation in the tube walls and therefore the amount of heat flowing from the refrigerant to the inner wall must equals the heat flowing from the outer wall to the cooling water:

$$\dot{q}_{ref,j} = \dot{q}_{w,j} \tag{5.12}$$

$$T_{w,j} = T_{w,j-1} + \left(\frac{\dot{q}_{w,j-1} + \dot{q}_{w,j}}{2\dot{m}_w Cp_w}\right) \tag{5.13}$$

Since water properties depend on its temperature, water temperature profile was obtained from eq. (5.13) using an iterative process that begins assuming linear evolution of water temperature and quickly converges to differences between two successive iterations lower than 0.5 %.

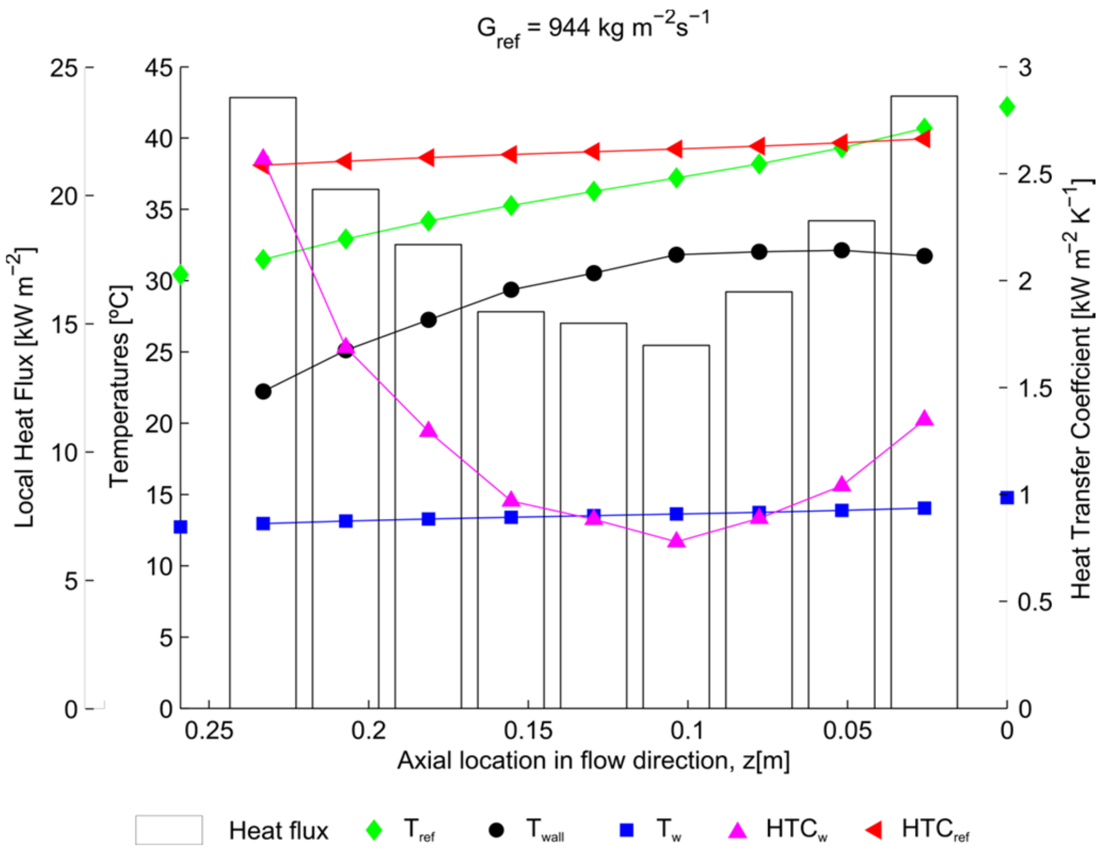

Figure 5.2. Single-phase test local parameters obtained.

Once the water temperature profile was obtained, the HTC profile of the cooling water was easily obtained applying eq. (5.14):

$$HTC_{w,j} = \frac{\dot{q}_{w,j}}{\left(T_{wall\ outer,j} - T_{w,j}\right)} \tag{5.14}$$

Fig. 5.2.shows the results obtained for the local HTC of the water following this procedure. According to this figure, a clear increase in the local heat flux was recorded at the inlet and the outlet of the test section. As test section is configured as a counter current heat exchanger, according to X axis, refrigerant enters by 0 coordinate while water flow exits in that position.

From the refrigerant side point of view, the HTC remains nearly constant and the increase in heat flow can be explained by the increase in the temperature difference between refrigerant and tube wall recorded at the inlet and the outlet of the test section. From the water side point of view, the temperature difference between water and tube wall is lower at the inlet and the outlet sections of the water jacket, but this effect is compensated by the increase in water HTC recorded. This can be explained by the impinging effects at the inlet and the acceleration effects at the outlet sections of the water casing.

Several tests were made at different temperature levels with similar results and therefore it can be concluded that: the local Nusselt number of the water at each location is the same regardless of the Reynolds number of the refrigerant flow or its saturation temperature when the water maintains the same flow condition or Reynolds number. Fig. 5.3. shows several water HTC profiles obtained at different refrigerant saturation temperatures and mass flow rates.

Only at low refrigerant Reynolds number the profiles obtained show a slightly different behaviour and have not been plotted in this figure. The blue line shows its averaged value.

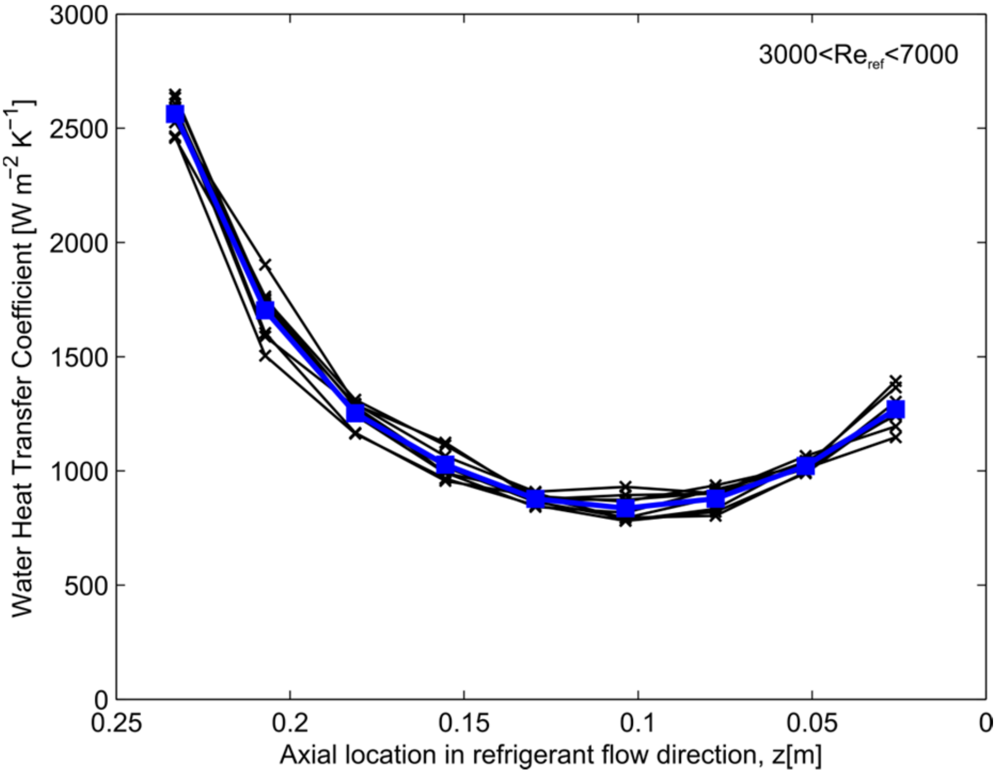

Figure 5.3. Water heat transfer coefficient profile at different refrigerant flow conditions.

5.2 LOCAL TWO-PHASE HEAT TRANSFER COEFFICIENT

Since single-phase tests were designed so that the total heat flow would be quite similar to the value of the total heat flow in two-phase flow. Single-phase test results have proved that the water HTC is almost independent of refrigerant conditions; it was assumed that the HTC of water side in refrigerant two-phase flow tests is similar to the HTC registered in turbulent single-phase tests.

The refrigerant local heat transfer coefficient $HTC_{ref,j}$ of each thermocouple location was determined by calculating the ratio of the heat flux $\dot{q}_j$ to the temperature difference between saturation temperature $T_{ref,j}$ and inner wall temperature $T_{wall\,inner}$ as follows:

$$HTC_{ref,j} = \frac{\dot{q}_j}{T_{ref,j} - (T_{wall\,inner})_j} \tag{5.15}$$

The heat flux $\dot{q}_j$ and water temperature at each thermocouple location were determined from the imposed water HTC profile obtained in single-phase tests, solving the two equations system formed by Eq. (5.13) and Eq. (5.16):

$$\dot{q}_{w,j} = HTC_{w,j}\left(T_{w,j} - T_{wall\ outer,j}\right) \tag{5.16}$$

Where, similarly to the procedure followed in single-phase tests, since water properties depend on its temperature, the water temperature at each point location, $T_{w,j}$, was calculated by an iterative process that begins assuming linear evolution of water temperature and quickly converges to differences between two successive iterations lower than 0.5 %.

The inner wall temperature $T_{wall\ inner}$ of the multi-port tube was derived from the measured outer wall temperature $T_{wall\ outer}$ and the heat flux:

$$(T_{wall\ inner})_j = (T_{wall\ outer})_j - \frac{\dot{q}_j \cdot t}{\lambda_{Al}} \tag{5.17}$$

The refrigerant temperature at each thermocouple location, $T_{ref,j}$, was calculated from the corresponding saturation pressure, assuming saturated state. Small pressure drop values were recorded between the inlet and the outlet of the test section. A new correlation for frictional pressure drop prediction was developed in order to calculate saturation conditions on each thermocouple location. The local process is schematically depicted in Fig. 5.4.

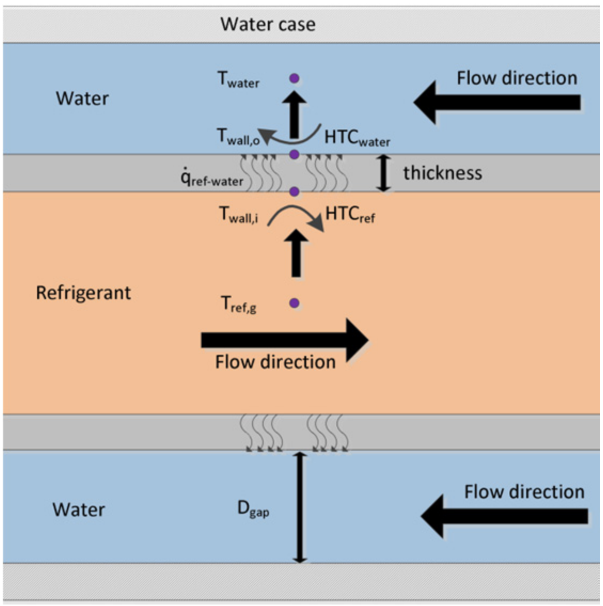

Figure 5.4. Schematic view of local heat transfer coefficient calculation.

5.3 FRICTIONAL PRESSURE DROP EVALUATION

Two-phase pressure gradient is composed by momentum, accessories, gravitational and frictional pressure gradient. Momentum pressure gradient is estimated by Eqs. (5.18 to 5.20); gravitational pressure gradient is zero due to horizontal flow. Two-phase frictional pressure gradient is calculated subtracting momentum pressure gradient and the pressure drop due to accessories to the experimental pressure gradient.

$$-\left(\frac{dp}{dz}\right)_{tp} = -\left(\frac{dp}{dz}\right)_{mom} - \left(\frac{dp}{dz}\right)_{acc} - \left(\frac{dp}{dz}\right)_{\mathrm{g}} - \left(\frac{dp}{dz}\right)_{\mathrm{f}} \tag{5.18}$$

Momentum pressure gradient for condensing flows is calculated as

$$-\left(\frac{dp}{dz}\right)_{mom} = G^2 \cdot \frac{d}{dz}\left[\frac{x^2}{\alpha \cdot \rho_v} + \frac{(1-x)^2}{(1-\alpha) \cdot \rho_l}\right] \tag{5.19}$$

where α is void fraction. Many correlations have been used to calculate void fraction, one of the most widely used is Zivi [7] correlation:

$$\alpha = \left[1 + \left(\frac{1-x}{x}\right) \cdot \left(\frac{\rho_g}{\rho_l}\right)^{2/3}\right]^{-1} \tag{5.20}$$

Other expressions may be found in the existing literature, extensive reviews of void fraction correlations were reported by Dalkilic and Wongwises [8] and Winkler et al. [9].

Pressure gradient in accessories is evaluated as explained below.

5.3.1 Pressure drop in tube expansion and contractions

During the calculation procedure the pressure drop in the headers should be taken into account, in addition to the tube pressure drop. For its calculation, both the expansion and the contraction processes which take place in the headers should be considered. The fluid state encountered in the header may be: vapour, liquid (single-phase) or a mixture (two-phase flow). The correlations studied in this work to calculate this pressure drop are described below. The nomenclature used in what follows is included in Figure 5.5.

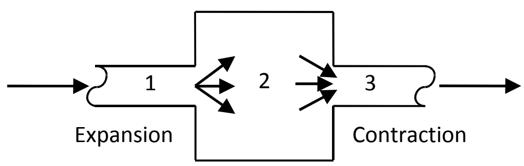

Figure 5.5. Expansion and contraction nomenclature

$$dp_{\text{channel}} = dp_{meas} - (dp_c + dp_e) \tag{5.21}$$

5.3.1.1 *Single-phase flow*

Kays and London [10] characterised the pressure drop through an abrupt change of section by introducing expansion and contraction coefficients for the pressure drop which can be calculated by means of the curves they provided in their book (Figure 5.6 and 5.7)

Thus, the pressure drop in the case of expansion is given by

$$dp_e = \frac{1}{2}u_1^2\rho_1 k_e - \frac{1}{2}\cdot u_1^2 \cdot \rho_1 \cdot (1-\gamma^2) \tag{5.22}$$

$\gamma = A_1/A_2$ and subscript 1 and 2 refers to the inlet and outlet section

The pressure drop in the case of a contraction is given by

$$\mathrm{d}p_c = \frac{1}{2}u_3^2\rho_3 k_c - \frac{1}{2}u_3^2\rho_3(1-\gamma^2) \tag{5.23}$$

where u_3 , is the velocity at the outlet, ρ_3 is the density of the fluid at the inlet, $\gamma = A_2/A_3$ in this case, andk_e and$k_c$are the expansion and contraction coefficients respectively.

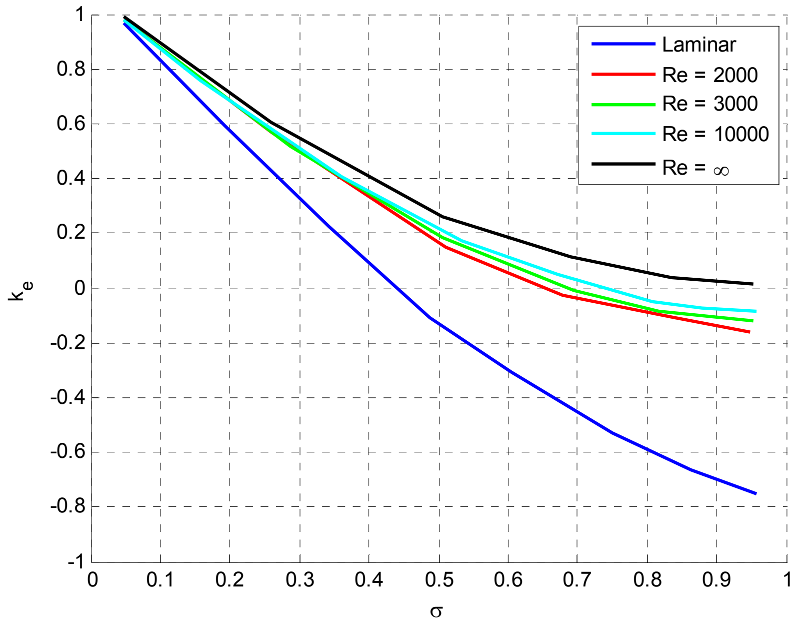

Figure 5.6. Expansion coefficient by Kays and London.

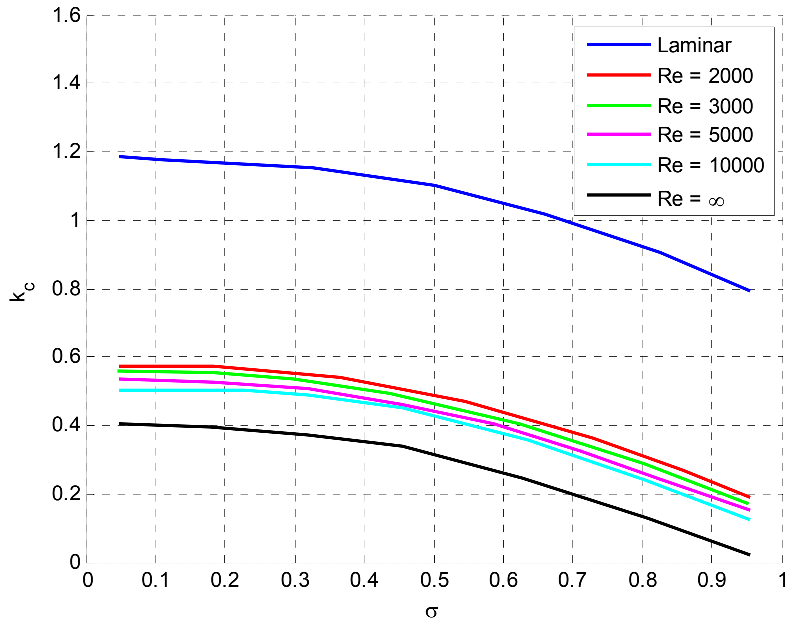

Figure 5.7. Contraction coefficients by Kays and London.

The equations of these coefficients depending on the Re number are:

$$k_e = \begin{cases} 0.009\gamma^2 - 0.288\gamma + 1.269 \; if laminar \\ 0.009\gamma^2 - 0.227\gamma + 1.202 \; if Re = 2000 \\ 0.009\gamma^2 - 0.224\gamma + 1.203 \; if Re = 3000 \\ 0.009\gamma^2 - 0.224\gamma + 1.198 \; if Re = 5000 \end{cases} \tag{5.24}$$

$$k_c = \begin{cases} -0.004\gamma^2 + 0.012\gamma + 1.172 \; if laminar \\ -0.004\gamma^2 + 0.014\gamma + 0.559 \; if Re = 2000 \\ -0.004\gamma^2 + 0.013\gamma + 0.541 \; if Re = 3000 \\ -0.004\gamma^2 + 0.010\gamma + 0.529 \; if Re = 5000 \end{cases} \tag{5.25}$$

In our implementation, the value of k_e or k_c is obtained by a linear interpolation as function of the Reynolds number.

Abdelall et al. [11] performed single-phase experiments studying the pressure drop caused by abrupt flow area changes; they proposed a general equation for flow area expansion:

$$dp_e = \frac{1}{2} u_1^2 \rho_1 k_e - \frac{1}{2} \cdot u_1^2 \cdot \rho_1 \cdot (1 - \gamma^2) \tag{5.26}$$

Where the expansion coefficient is given by $k_e = (1 - \gamma)^2$, the area ratio is $\gamma = A_1/A_2$ and u is the inlet velocity. Subscripts 1 and 2 stand for inlet and outlet respectively.

For a flow area contraction they suggested

$$\mathrm{d}p_c = \frac{u_3^2}{2}\rho_3\left[\left(1-\frac{1}{C_c}\right)^2 + (1-\gamma^2)\right] \tag{5.27}$$

Where u_3 is the outlet velocity, the vena contracta coefficient, C_c is given by

$$C_c = 1 - \frac{1-\gamma}{2.08(1-\gamma)+0.5371} \tag{5.28}$$

and $\gamma = A_2/A_3$. Subscripts 2 and 3 stand for the inlet and outlet respectively.

5.3.1.2 *Two-phase flow*

Different models may be found in the existing literature. Among them, we can standout several.

Hewitt et al. [12] correlation stated that the homogeneous model predicts the experimental data for sudden contractions better than the separated-flow model does. The opposite happens for sudden expansions.

Thus, for sudden expansions they proposed:

$$dp_e = \frac{G^2\gamma(1-\gamma)}{\rho_l}\phi_S \tag{5.29}$$

where the separated multiplier ϕ_S is given by

$$\phi_S = \frac{(1-x)^2}{(1-\alpha_g)} + \frac{\rho_l x^2}{\rho_g \alpha} \tag{5.30}$$

And for sudden contractions:

$$dp_c = \frac{G^2}{2\rho_l}\left[\left(\frac{1}{C_c}-1\right)^2 + (1-\frac{1}{\gamma^2})\right]\phi_H \tag{5.31}$$

where $\gamma = A_1/A_2$, C_c is the coefficient of contraction given by Chisholm as

$$C_c = \frac{1}{0.639[1-\gamma]^{1/2}+1} \tag{5.32}$$

and the homogeneous multiplier, ϕ_H given by

$$\phi_H = \left[1 + x\left(\frac{\rho_l}{\rho_g}-1\right)\right] \tag{5.33}$$

Kandlikar proposed same expression for the contraction model but for the expansion he proposed $dp_e = G^2\gamma(1-\gamma)\phi'_S$ with the following multiplier

$$\phi_S = 1 + \left(\frac{\rho_l}{\rho_g} - 1\right)[0.25x(1-x)+x^2] \tag{5.34}$$

An alternative expression for ϕ_S was also proposed by Chisholm on Hewitt [12].

Coleman and Krause [13] showed, that these expressions commonly used for estimating two-phase pressure losses, under-predict the pressure losses found in micro-channel tube headers. Furthermore, they point out that the recovery of pressure after the expansion is less than 5% of the total pressure variation and it was neglected. They say that this is typical for area ratios lower than 0.1. In the case of sudden contraction, they modified the correlation proposed by Schmidt and Friedel [14] so that the pressure drop is given by

$$dp_c = \frac{G_{vc}^2}{2\rho_{tp}}[(1-\gamma^2 C_c^2) - 2C_c(1-C_c)] \tag{5.35}$$

Where$\gamma\ = A_2/A_3$ and the vena contracta coefficient is given by

$$C_c = 1 - \frac{1-\gamma}{2.08(1-\gamma)+0.5371} \tag{5.36}$$

The two-phase density ρ_{tp} may be evaluated by using Eq. 5.37.

$$\frac{1}{\rho_{tp}} = \frac{x}{\rho_g} + \frac{(1-x)}{\rho_l} \tag{5.37}$$

And the mass velocity, G_{vc} is given by an expression adjusted by Coleman and Krause [13] $G_{vc} = CG_{tube}$ with $C = 2.08$. The values of the different thermodynamic variables have been calculated at inlet conditions.

In our case, the Schmidt and Friedel correlation [14] is used for sudden expansion in two-phase flow.

$$dp_e = \frac{G\left[\frac{\gamma_{1,2}}{\rho_{eff,1}} - \frac{\gamma_{1,2}^2}{\rho_{eff,2}} - f_{Exp}\rho_{eff,1}\left(\frac{x}{\rho_{g,1}\eta_1} - \frac{1-x}{\rho_{l,1}(1-\eta_1)}\right)^2 (1-\sqrt{\gamma_{1,2}})^2\right]}{1-\Gamma_{\mathrm{Exp}}(1-\gamma_{1,2})} \tag{5.38}$$

where

$$\frac{1}{\rho_{eff}} = \frac{x^2}{\rho_g \eta} + \frac{(1-x)^2}{\rho_l(1-\alpha)} + \rho_f(1-\varepsilon)\left(\frac{\alpha_E}{1-\alpha_E}\right)\left[\frac{x}{\rho_g\eta} - \frac{1-x}{\rho_l(1-\eta)}\right]^2 \tag{5.39}$$

$$\eta = 1 - \frac{2(1-x)^2}{1-2x+\sqrt{1+4x(1-x)\left(\frac{\rho_l}{\rho_g}-1\right)}} \tag{5.40}$$

$$\eta_E = 1/S\,[1 - \frac{1-x}{\left(1-x\left(1-0.05\mathrm{We}^{0.27}\mathrm{Re}^{0.05}\right)\right)}] \tag{5.41}$$

$$S = \frac{x}{1-x}\frac{1-\eta}{\eta}\frac{\rho_l}{\rho_g} \tag{5.42}$$

$$\mathrm{We} = Gx^2\frac{\mathrm{D}}{\rho_g\sigma}\frac{(\rho_l - \rho_g)}{\rho_g} \tag{5.43}$$

$$\mathrm{Re} = \frac{G(1-x)d}{\mu_l} \tag{5.44}$$

$$\Gamma_{\mathrm{Exp}} = 1 - \gamma_{2,3}^{0.25} \tag{5.45}$$

$$f_{Exp} = 4.9\times 10^{-3}x^2(1-x)^2\left(\frac{\mu_{l,1}}{\mu_{g,1}}\right)^{0.7} \tag{5.46}$$

A review of other expressions for the evaluation of pressure recovery in sudden expansions can be found in Ahmed et al. [15]. They compared different models. Zhang and Webb [16] recommended the use of the equations proposed by Collier and Thome [17].

5.4. CALCULATION PROCEDURE

The liquid enthalpy of the refrigerant is calculated with its bulk temperature and liquid density. The density is provided by the Coriolis-effect mass flow meter installed in the refrigerant loop. An RTD sensor gives fluid temperature reading prior entering the evaporator. In the evaporator, the heat transferred from water to the refrigerant is calculated with secondary fluid measurements. Hot water volumetric flow rate and inlet and outlet temperatures are used to calculate exchanged heat power. The entire installation has several layers of insulating foam so heat losses are negligible.

$$h_{ref\ liq} = h_{ref\ evap\ in} = h[T_{ref\ liq}, \rho_{ref\ liq}] \tag{5.47}$$

$$\dot{Q}_{evap} = \dot{m}_{ref}(h_{ref\ evap\ out} - h_{ref\ evap\ in}) \tag{5.48}$$

$$\dot{Q}_{evap} = \dot{v}_{hw}\rho_{hw}[T_{hw\ out}, T_{hw\ in}]c_{p\ hw}[T_{hw\ out}, T_{hw\ in}](T_{hw\ out} - T_{hw\ in}) \tag{5.49}$$

and therefore

$$h_{ref\ evap\ out} = h_{ref\ evap\ in} + \frac{\dot{Q}_{evap}}{\dot{m}_{ref}} \tag{5.50}$$

$$h_{tube\ in} \approx h_{ref\ evap\ out} = x_{tube\ in}h_{gas}[p_{tube\ in}] + (1 - x_{tube\ in})h_{liq}[p_{tube\ in}] \tag{5.51}$$

and re-arranging

$$x_{tube\ in} = \frac{h_{tube\ in} - h_{liq}[p_{tube\ in}]}{h_{liq-gas}[p_{tube\ in}]} \tag{5.52}$$

with enthalpy values evaluated at inlet section saturation pressure.

Since the refrigerant is condensed with water in the test section, cooling water measurements are used for heat transfer calculation. Inlet and outlet water temperatures in the condensation test, as well as mass flow meter are recorded. With the power transferred from refrigerant to the cooling water, exit refrigerant vapour quality can be calculated as follows.

$$\dot{Q}_{ts} = \dot{m}_w c_{pw}[T_{w\,out}, T_{w\,in}](T_{w\,out} - T_{w\,in}) \tag{5.53}$$

As

$$\dot{Q}_{ts} = \dot{m}_{ref}(h_{tube\,in} - h_{tube\,out}) \tag{5.54}$$

outlet enthalpy is

$$h_{tube\,out} = h_{tube\,in} - \frac{\dot{Q}_{ts}}{\dot{m}_{ref}} \tag{5.55}$$

HTC calculation is performed locally so

$$h_{tube,j} = h_{tube\,in} - \sum_{i=1}^{9} \frac{\dot{q}_{ts,j}}{\dot{m}_{ref}} A_j \tag{5.56}$$

And finally,

$$h_{tube\,out} = x_{tube\,out} \cdot h_{gas}[p_{tube\,out}] + (1 - x_{tube\,out}) \cdot h_{liq}[p_{tube\,out}] \tag{5.57}$$

The vapour quality at any location can be obtained as:

$$x_{tube,i} = \frac{h_{tube,j} - h_{liq}\left[p_{tube,j}\right]}{h_{liq-gas}\left[p_{tube,j}\right]} \tag{5.58}$$

$$x_{ave} = \frac{x_{tube,i} + x_{tube,o}}{2} \tag{5.59}$$

5.5 UNCERTAINTY ANALYSIS

The experiments were made over a wide range of test conditions. The influence of different parameters on the pressure drop was investigated. The mass flow rate, the vapour quality, the saturation temperature, and the condensing heat flux parameters were varied.

Following the rules reported in [18] for the expression of uncertainty in measurements, the "Type A" and "Type B" uncertainties were calculated for each parameter. The resulting *u* of each parameter *x* is obtained as:

$$u(x) = \sqrt{\left(u_A(x)\right)^2 + \left(u_B(x)\right)^2} \tag{5.60}$$

The standard uncertainty of the result of a measurement, when this is obtained from the values of a number of other quantities is called combined standard uncertainty, u_c, and it is calculated by combining the standard uncertainties of the measured quantities $x_1, \ldots, x_N$, through a functional relationship *f*.

$$y = f(x_1, \ldots, x_N) \tag{5.61}$$

$$u_C = \sqrt{\sum_{j=1}^{N} \left(\frac{\partial f}{\partial x_i}\right)^2 u^2(x_j)} \tag{5.62}$$

The expanded uncertainty u_E is calculated by multiplying the combined uncertainty by a coverage factor of $k = 2$ with a level of confidence about 95 %.

$$u_E = k \cdot u_C \tag{5.63}$$

The uncertainty analysis of frictional pressure drop can be carried out from the basic equation of frictional pressure drop calculation as presented in Eq. 5.18. The procedure to calculate average vapour quality value is explained in the paragraphs above, the basic equation to calculate its uncertainty is presented in Eq. 5.65. A similar procedure can be followed to get the uncertainty expression of heat transfer coefficient presented in Eq. 5.66.

$$u_{dp\,f} = \sqrt{\left(\frac{\partial dp_f}{\partial dp_{meas}}\right)^2 u_{dp\,meas}^2 + \left(\frac{\partial dp_f}{\partial dp_{exp}}\right)^2 u_{dp\,exp}^2 + \left(\frac{\partial dp_f}{\partial dp_{cont}}\right)^2 u_{dp\,cont}^2 + \left(\frac{\partial dp_f}{d\partial p_{mom}}\right)^2 u_{dp\,mom}^2} \tag{5.64}$$

$$u_{x\,ave} = \sqrt{\left(\frac{\partial x_{ave}}{\partial x_{in}}\right)^2 u_{x_{in}}^2 + \left(\frac{\partial x_{ave}}{\partial x_{out}}\right)^2 u_{x_{out}}^2} \tag{5.65}$$

$$u_{HTC,i} = \sqrt{\left(\frac{\partial HTC_{ref,i}}{\partial q_i}\right)^2 u_{q_i}^2 + \left(\frac{\partial HTC_{ref,i}}{\partial T_{ref,i}}\right)^2 u_{T_{ref,i}}^2 + \left(\frac{\partial HTC_{ref,i}}{\partial T_{wall\,inner_i}}\right)^2 u_{T_{wall\,inner_i}}^2} \tag{5.66}$$

Each term represents the contribution of each variable to the whole uncertainty value. The uncertainty of expansion and contraction expressions has conservatively been estimated to be lower than 5%.

The uncertainty ranges for the variables of interest of this study can be seen in Table 5.1.

Table 5.1. Summary of total uncertainty analysis for the experimental results.

Parameter	Total uncertainty (%)
Heat Flux	3.4 – 4.5
Vapour quality	2.2 – 12.5
Heat transfer coefficient	5.6 – 21.7
Inlet saturation pressure	1.6 – 3.3
Frictional pressure drop	2.2 – 11.9

5.6 CONCLUSIONS

This chapter presents the calculation procedure followed to determine the heat transfer coefficient and frictional pressure drop experimentally measured. The expressions used in sudden area expansions and contractions are included in this chapter.

Firstly single phase HTC measurements are presented and these are used to calculate water HTC profile used later in two-phase flow tests. Single-phase flow test correlates very well with several classical correlations widely accepted by the scientific community.

The procedure to calculate the uncertainty of measurements is also reported. The highest uncertainty in HTC comes from the measurement of the temperature difference between the bulk refrigerant and tube wall temperature.

REFERENCES

[1] E.W. Lemmon, M.L. Huber, and M.O. McLinden, NIST Standard Reference Database: Reference Fluid Thermodynamic and Transport Properties-REFPROP. 6.0, (1999).

[2] J.E. Park, F. Vakili-Farahani, L. Consolini, and J.R. Thome, Experimental study on condensation heat transfer in vertical minichannels for new refrigerant R1234ze(E) versus R134a and R236fa, Experimental Thermal and Fluid Science, 35 (2011) 442-454.

[3] X. Fang, Y. Xu, and Z. Zhou, New correlations of single-phase friction factor for turbulent pipe flow and evaluation of existing single-phase friction factor correlations, Nuclear Engineering and Design, 241 (2011) 897-902.

[4] X. Fang, H. Zhang, Y. Xu, and X. Su, Evaluation of using two-phase frictional pressure drop correlations for normal gravity to microgravity and reduced gravity, Advances in Space Research, 49 (2012) 351-364.

[5] D. Brkic, New explicit correlations for turbulent flow friction factor, Nuclear Engineering and Design, 241 (2011) 4055-4059.

[6] Y. Xu and X. Fang, A new correlation of two-phase frictional pressure drop for condensing flow in pipes, Nuclear Engineering and Design, 263 (2013) 87-96.

[7] S.M. Zivi, Estimation of steady-state steam void-fraction by means of the principle of minimum entropy production, Journal of Heat Transfer, 86 (1964) 247.

[8] A.S. Dalkilic and S. Wongwises, Intensive literature review of condensation inside smooth and enhanced tubes, International Journal of Heat and Mass Transfer, 52 (2009) 3409-3426.

[9] J. Winkler, J. Killion, S. Garimella, and B.M. Fronk, Void fractions for condensing refrigerant flow in small channels: Part I literature review, International Journal of Refrigeration, 35 (2012) 219-245.

[10] W.M. Kays and A.L. London, Compact heat exchangers, (1984).

[11] F.F. Abdelall, G. Hahn, S.M. Ghiaasiaan, S.I. Abdel-Khalik, S.S. Jeter, M. Yoda, and D.L. Sadowski, Pressure drop caused by abrupt flow area changes in small channels, Experimental Thermal and Fluid Science, 29 (2005) 425-434.

[12] G.F. Hewitt, G.L. Shires, and T.R. Bott, Process heat transfer, CRC press London, 1994.

[13] J.W. Coleman and P.E. Krause, Two phase pressure losses of R134a in microchannel tube headers with large free flow area ratios, Experimental Thermal and Fluid Science, 28 (2004) 123-130.

[14] J. Schmidt and L. Friedel, Two-phase pressure drop across sudden contractions in duct areas, International Journal of Multiphase Flow, 23 (1997) 283-299.

[15] W.H. Ahmed, C.Y. Ching, and M. Shoukri, Pressure recovery of two-phase flow across sudden expansions, International Journal of Multiphase Flow, 33 (2007) 575-594.

[16] M. Zhang and R.L. Webb, Correlation of two-phase friction for refrigerants in small-diameter tubes, Experimental Thermal and Fluid Science, 25 (2001) 131-139.

[17] J.G. Collier and J.R. Thome, Convective boiling and condensation, Oxford University Press, 1994.

[18] B.N. Taylor, Guidelines for Evaluating and Expressing the Uncertainty of NIST Measurement Results. DIANE Publishing, 2009.

CHAPTER 6: Experimental Results

In this chapter the experimental results obtained in the framework of this PhD. thesis are presented. The fluids and the conditions studied were also mentioned in Chapter 4. Heat transfer coefficients and frictional pressure drop values were calculated following the process described in Chapter 5. The data are plotted sorted by refrigerant and results are also commented.

6.1 TWO-PHASE FLOW HEAT TRANSFER COEFFICIENT

The experiments were made over a wide range of test conditions. The influence of different parameters on the heat transfer coefficient was investigated. The mass velocity, the inlet vapour quality, the inlet saturation temperature, and the condensing heat flux parameters were varied. Only two-phase flow data with vapour quality values higher than 0.1 are considered.

The uncertainty of measurements is also provided on each figure presenting experimental data.

6.1.1 HTC measurements of R134a

This refrigerant was the first one tested. As shown in the literature review, this has been intensively studied by other authors for many mini-channel geometries and these experimental results were used for the validation of the installation.

The mass velocity values studied correspond with values of 945, 810, 710, 590, 475, 355 kg $m^{-2}s^{-1}$ at one saturation temperature of 40 ºC. These analyses have covered values of heat flux ranging from 5.08 to 20.75 kWm^{-2}. In Fig 6.1, HTC is depicted versus vapour quality at two different mass velocities and one saturation temperature.

The reader can observe the effect of varying mass velocity, HTC increases with increasing mass velocity. This effect is important at low qualities. The range of vapour quality tested goes from 0.1 up to 0.9. High vapour quality values were not reached for all mass velocities. From general theory, it is expected that HTC values fall after higher vapour quality values than 0.9, in that situation the liquid film almost disappears and the flow is more similar to single vapour flow with a decrease in HTC.

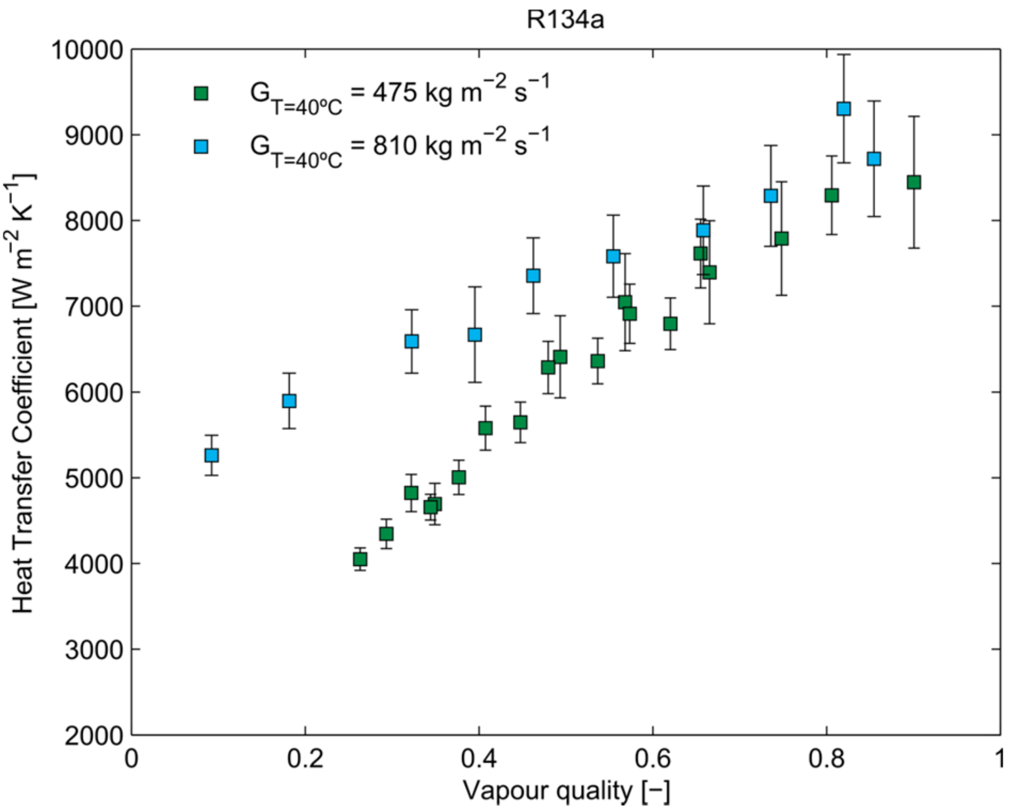

Figure 6.1. R134a HTC sorted by mass velocity at one saturation temperature.

6.1.2 HTC measurements of R1234yf

This refrigerant is one of the potential substitutes of R134a. It is being used in new mobile air conditioning equipment. Some car manufacturers claims that R1234yf is not safe because of its high flammability compared with R134a [1]. Their lower and upper flammability limits, in standard conditions of temperature and pressure, are 6.2 and 12.3 %.

The mass velocity values studied correspond with values of 945, 810, 710, 590, 475 and 355 kg $m^{-2}s^{-1}$ at the saturation temperatures of 30, 35, 40, 45, 50 and 55 ºC. These analyses have covered values of heat flux ranging from 4.37 to 20.52 kWm^{-2}.

In Fig. 6.2 the reader can observe the HTC behaviour of this refrigerant depicted versus vapour quality values. The data is sorted by saturation temperature and mass velocity. The same values of mass velocities as plotted in Fig 6.1 are kept. HTC increases with decreasing saturation temperature and increasing mass velocity.

The range of vapour quality values experimentally tested goes from nearly 0.1 to 0.9.

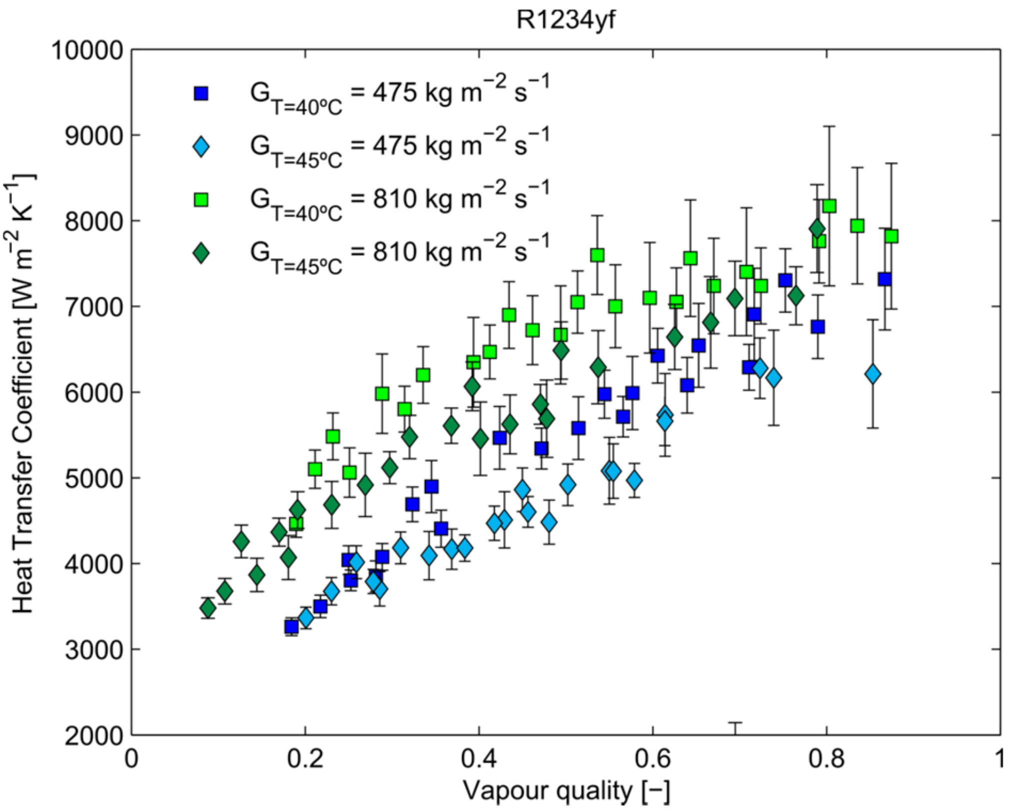

Figure 6.2. R1234yf HTC sorted by mass velocity at two different saturation temperatures.

6.1.3 HTC measurements of R290

This refrigerant is one of the potential substitutes of R22. It is a natural refrigerant with none Ozone Depleting Power (ODP). Their lower and upper flammability limits, in standard conditions of temperature and pressure, are 2.37 and 9.5 %.

So far, only a few research groups have studied the behaviour of this fluid in mini-channels. The liquid density of this refrigerant is mostly a half of R134a so mass velocities in commercial equipment are also lowers. Bearing this in mind, the values proposed to study are 175, 240, 300 and 350 kg m^{-2}s^{-1}. The saturation temperatures studies correspond with values of 30, 35, 40, 45, 50 and 55 ºC. The heat flux range covered goes from 4.98 to 21.52 kWm^{-2}.

Fig. 6.3 shows HTC of propane versus vapour quality values at two different saturation temperatures and mass velocities. The mass velocities shown in this figure are lower than for the aforementioned. There is a difference of 20 ºC between the two saturation temperatures depicted so the reader can appreciate the effect of this variable in HTC measurements. As in previous figures, the increase of saturation temperature causes a decrease in HTC. An increase of mass velocity causes an increase in HTC values.

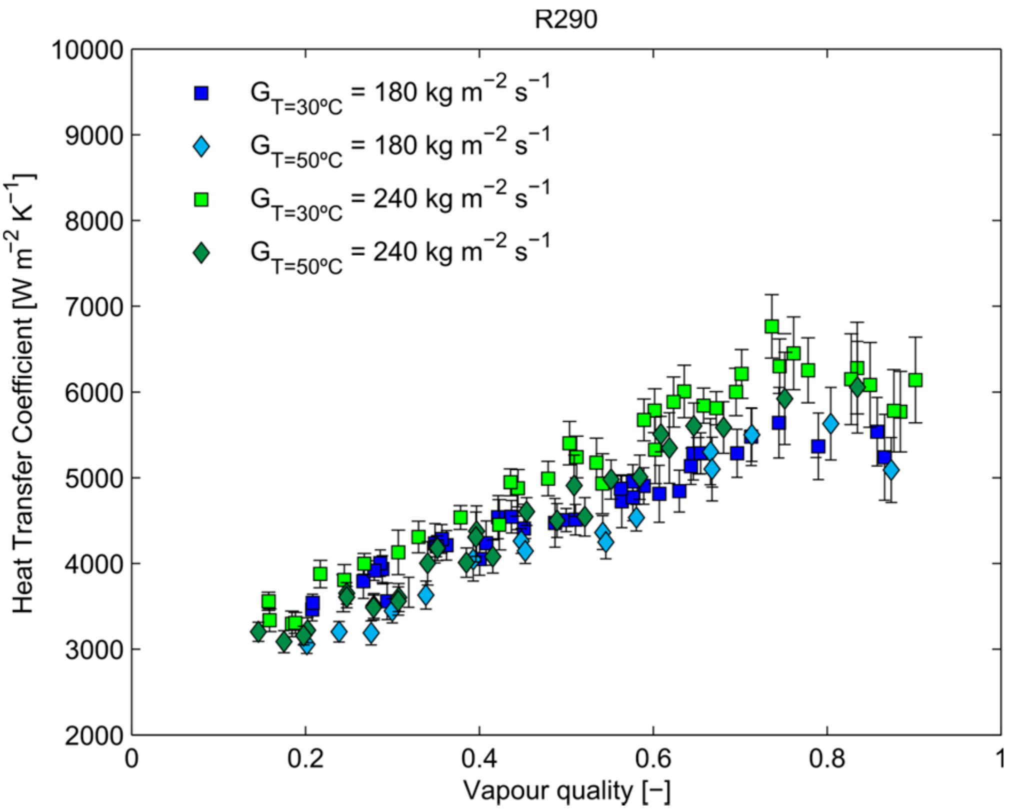

Figure 6.3. R290 HTC sorted by mass velocity at two different saturation temperatures.

6.1.4 HTC measurements of R32

This refrigerant is one of the potential substitutes of R410A and it is actually used by one of the main manufacturers of air conditioning equipment. Their lower and upper flammability limits, in standard conditions of temperature and pressure, are 14 and 31 %.

This refrigerant has null ODP. In this case, the mass velocity values studied are 350, 475, 600, 710, 795 and 825 kg $m^{-2}s^{-1}$ at the saturation temperature of 30, 35, 40, 45, 50 and 55 ºC. The analyses have covered values of heat flux ranging from 6.69 to 27.05 kWm^{-2}.

HTC is depicted versus vapour quality for two mass velocities and saturation temperatures. The reader can observe how an increase of mass velocity or decreases of saturation temperature yield to higher values of HTC.

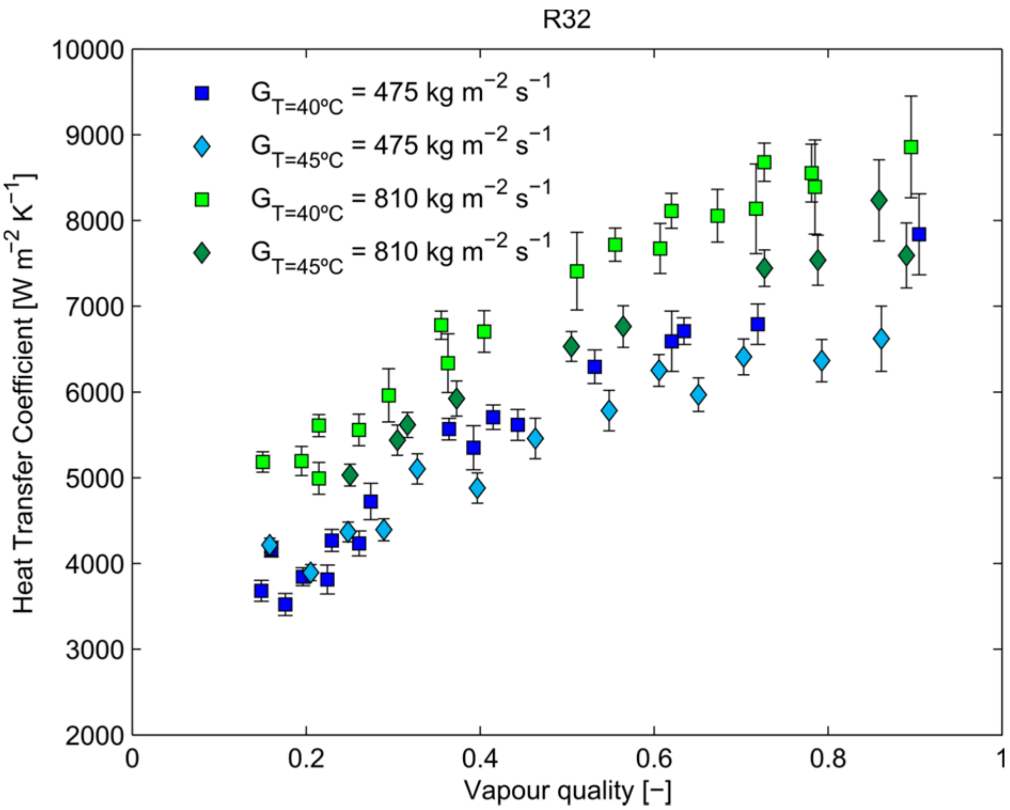

Figure 6.4. R32 HTC sorted by mass velocity at two different saturation temperatures.

6.1.5 HTC Fluid behaviour discussion

A comparison of HTC values at a fixed value of saturation temperature and mass velocity is shown in Fig. 6.5. In Fig. 6.5 HTC is plotted vs. vapour quality for a given mass flux of 810 kg $m^{-2}s^{-1}$ at a saturation temperature of 40 ºC for R32, R134a and R1234yf. Data of R134a, R1234yf, and R32 are only plotted because the mass velocity of 810 kg/m^2s was not experimentally tested for R290. Experimental measurements of three fluids are compared. The uncertainties of measurements do not allow being assertive but under similar conditions, experimental measurements points out that R32 has the highest values of HTC. From the two remaining fluids, R134a present higher HTC values than R1234yf. This behaviour may be explained by liquid thermal conductivity. Since the flow pattern in mini-channels is almost annular or intermittent, the liquid film around the gas core in the mini-channel increases the heat transfer in comparison with other flow patterns. So, higher liquid conductivities lead to higher HTC values.

In Table 6.1 the reader can see the most important thermo-physical properties for the plotted conditions included in Fig. 6.5.

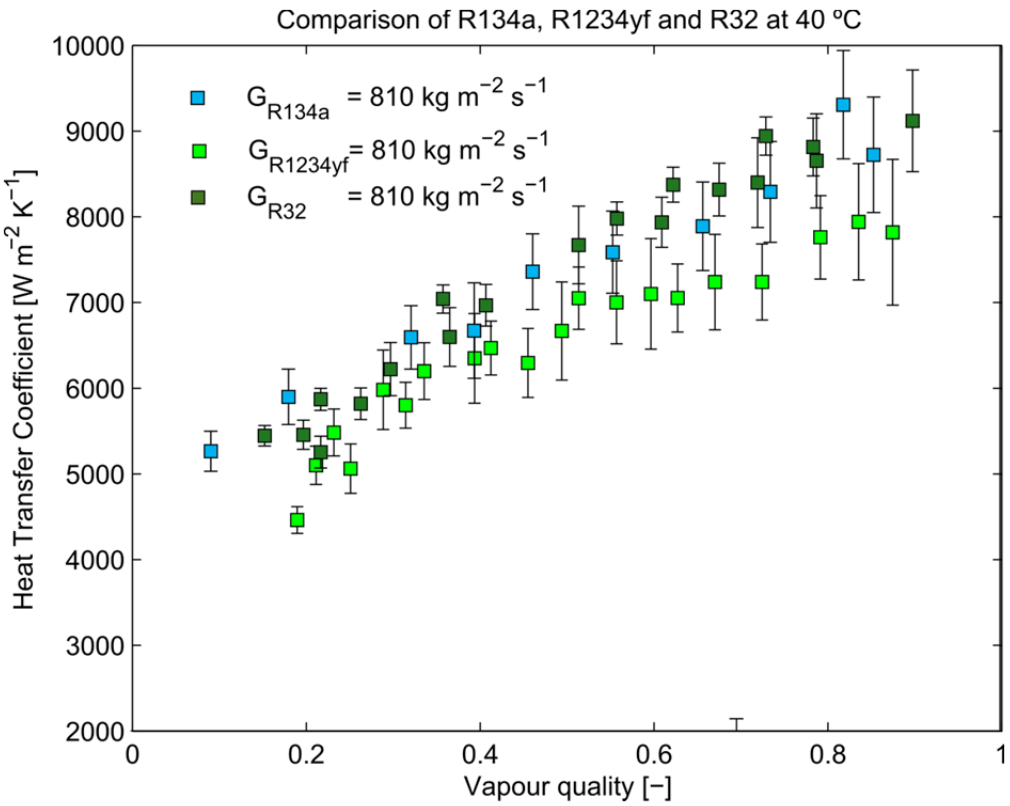

Figure 6.5.HTC comparison of R134a and R1234yf.

Table 6.1. Fluid properties at 40ºC.

Properties	R134a	R1234yf	R290	R32
Temperature [ºC]	40	40	40	40
Critical pressure [kPa]	4059.28	3382.20	4251.20	5782.10
Saturation pressure [kPa]	1016.86	1018.65	1369.73	2478.91
Reduced pressure	0.25	0.30	0.32	0.43
Liquid density [kg m^{-3}]	1446.69	1033.73	467.44	892.99
Vapour density [kg m^{-3}]	50.10	57.77	30.17	73.28
Liquid density/Vapour density	28.87	17.89	15.49	12.18
Liquid thermal conductivity [mWm^{-1}K^{-1}]	74.71	58.99	86.91	114.56
Liquid viscosity [µPa s]	161.42	129.98	82.83	94.97
Vapour viscosity [µPa s]	12.37	13.15	8.89	13.83

6.2 TWO-PHASE FRICTIONAL PRESSURE GRADIENT

Frictional two-phase flow pressure gradient is depicted in the following paragraphs sorted by refrigerant and mass velocity. On each Figure, frictional pressure gradient is plotted versus reduced pressure. The colour intensity of each marker corresponds to the colour scale on the right side of each picture.

Also a classical graph of vapour quality vs. frictional pressure drop is depicted under the same conditions of saturation temperature for all refrigerants tested. Each point is plotted with its uncertainty values on Fig. 6.10.

Frictional pressure drop of the fluids tested is plotted vs. average vapour quality values. Frictional pressure drop increases with increasing values of vapour quality and mass velocities.

6.2.1 Pressure drop measurements of R134a

In this paragraph, experimental pressure drop measurements are presented for R134a. The mass velocities studied correspond with 235, 475, 710 and 945 kg $m^{-2}s^{-1}$ at saturation temperature values of 30, 35, 40, 45, 50, and 55 ºC.

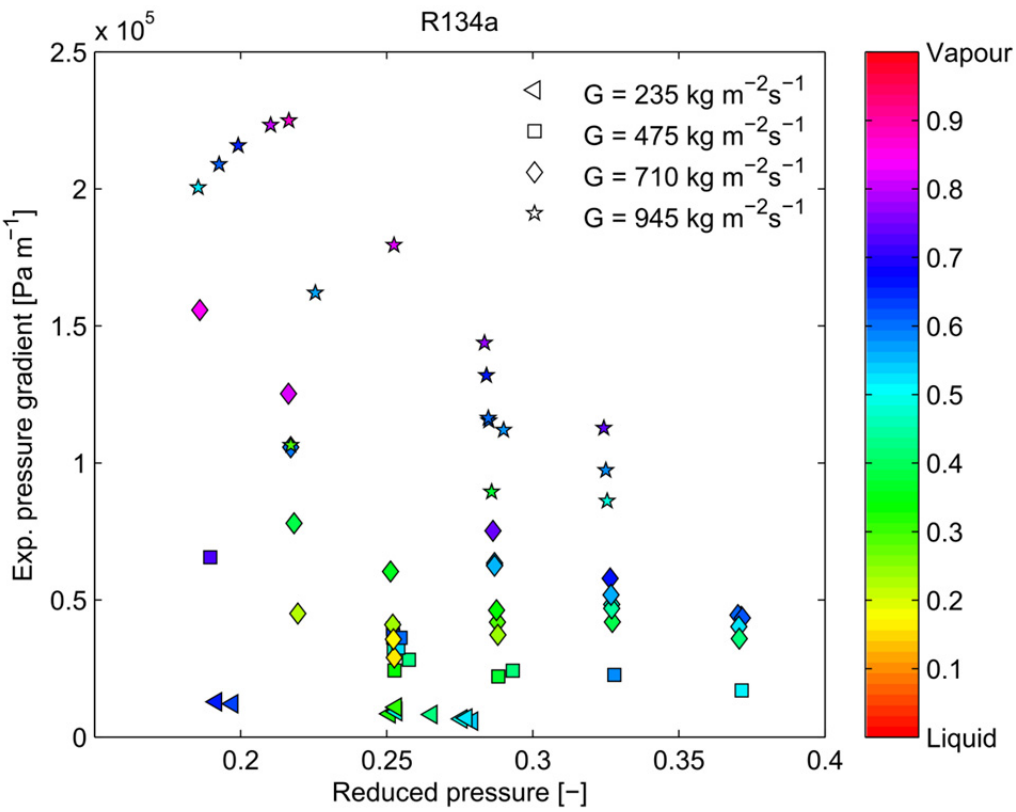

Figure 6.6. R134a frictional pressure gradient.

6.2.2 Pressure drop measurements of R1234yf

In this section R1234yf experimental pressure drop measurements are presented. The mass velocities studied correspond with 350, 475, 590, 710, 810 and 945 kg $m^{-2}s^{-1}$ at saturation temperature values of 30, 35, 40, 45, 50, and 55 ºC.

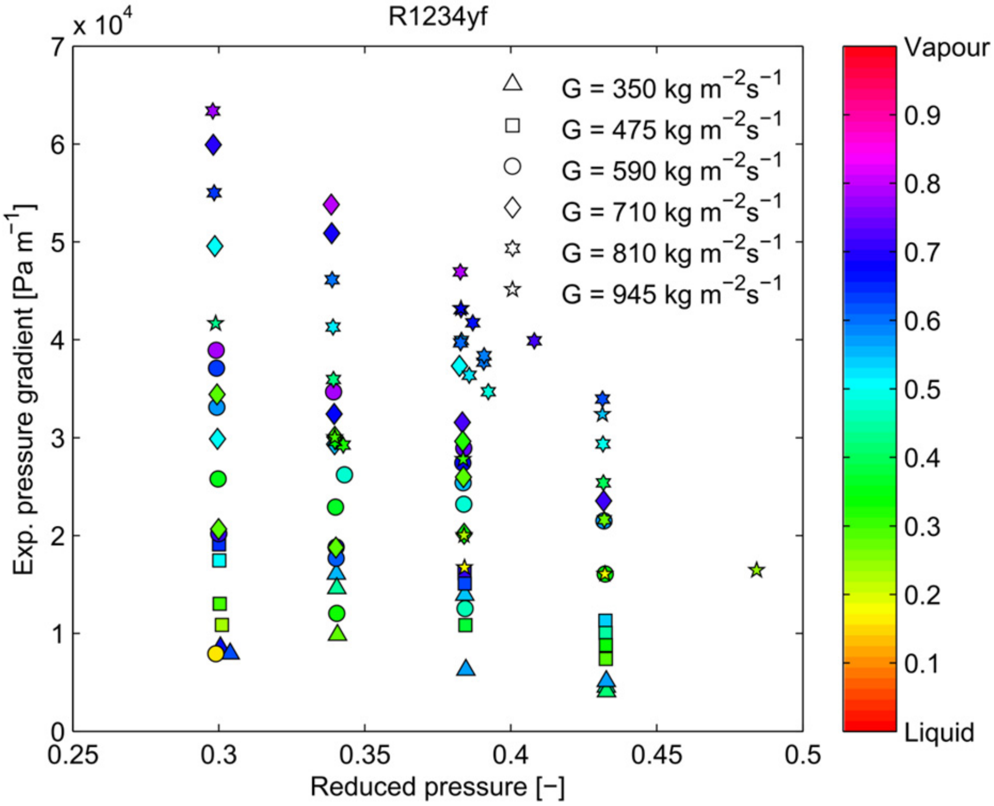

Figure 6.7. R1234yf frictional pressure gradient.

6.2.3 Pressure drop measurements of R290

In the following lines R290 experimental pressure drop measurements are presented. The mass velocities studied correspond with 175, 240, 300 and 350 kg $m^{-2}s^{-1}$ at saturation temperature values of 30, 35, 40, 45, 50, and 55 ºC.

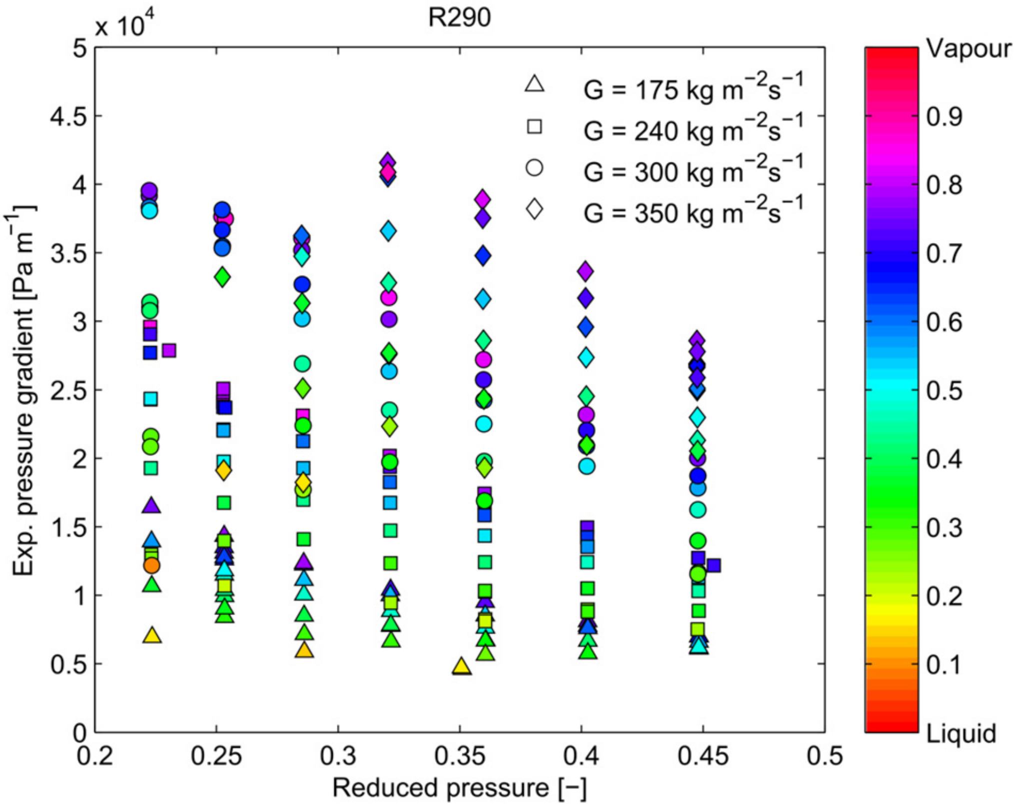

Figure 6.8. R290 frictional pressure gradient.

6.2.4 Pressure drop measurements of R32

In this last section R32 experimental pressure drop measurements are presented. The mass velocities studied correspond with 350, 475, 600, 710, 795 and 825 kg $m^{-2}s^{-1}$ at saturation temperature values of 30, 35, 40, 45, 50, and 55 ºC.

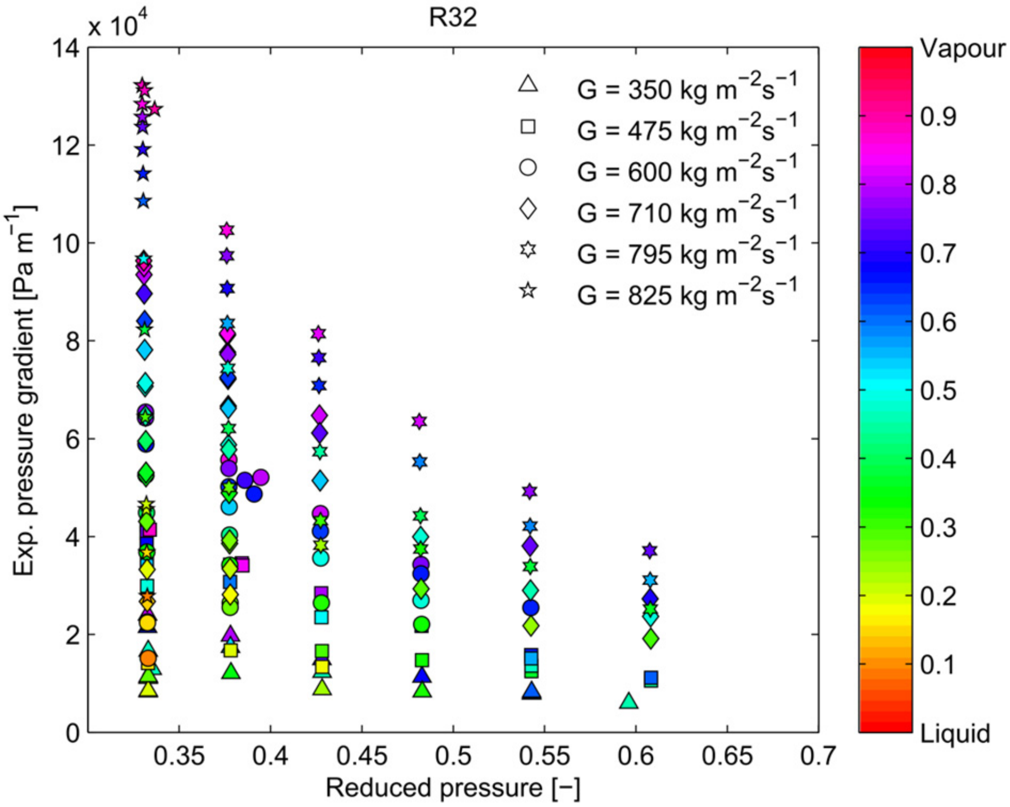

Figure 6.9. R32 frictional pressure gradient.

6.2.5 Pressure drop fluid comparison

In this section the fluid behaviour of each one of the four fluids tested is discussed based on frictional pressure drop measurements.

Firstly, R134a, R1234yf and R32 are plotted for a same value of mass velocity at the saturation temperature of 40 ºC on Fig. 6.10. Propane data is not depicted in this latter figure because the maximum mass velocity tested was 350 kg $m^{-2}s^{-1}$. Frictional pressure drop is depicted for each fluid. Under similar conditions, R134a has higher frictional pressure drop than R1234yf and this latter higher than R32. These differences became smaller as vapour quality decreases.

Because of the limitation of the installation, mass velocities lower than 350 kg $m^{-2}s^{-1}$ was not performed. So Fig. 6.11 plots the comparison of all tested fluids at this reduced value of mass velocity. On Fig. 6.11 the reader can observe that the previous tendency captured at higher mass velocities on Fig. 6.10 is kept. Interesting information must be pointed out; under similar conditions the frictional pressure drop of propane is much higher than the rest of refrigerants. This is a quite impressive behaviour because some authors explain these differences in their tendencies by the values of the fluid reduced pressure [2] but Fig. 6.11 is not explained by looking at reduced pressure vales of Table 6.1. This explanation may be valid if fluids have similar thermo physical properties. In this case, propane is a bit strange because it density is less than half of R134a and there are also big differences in dynamic viscosity.

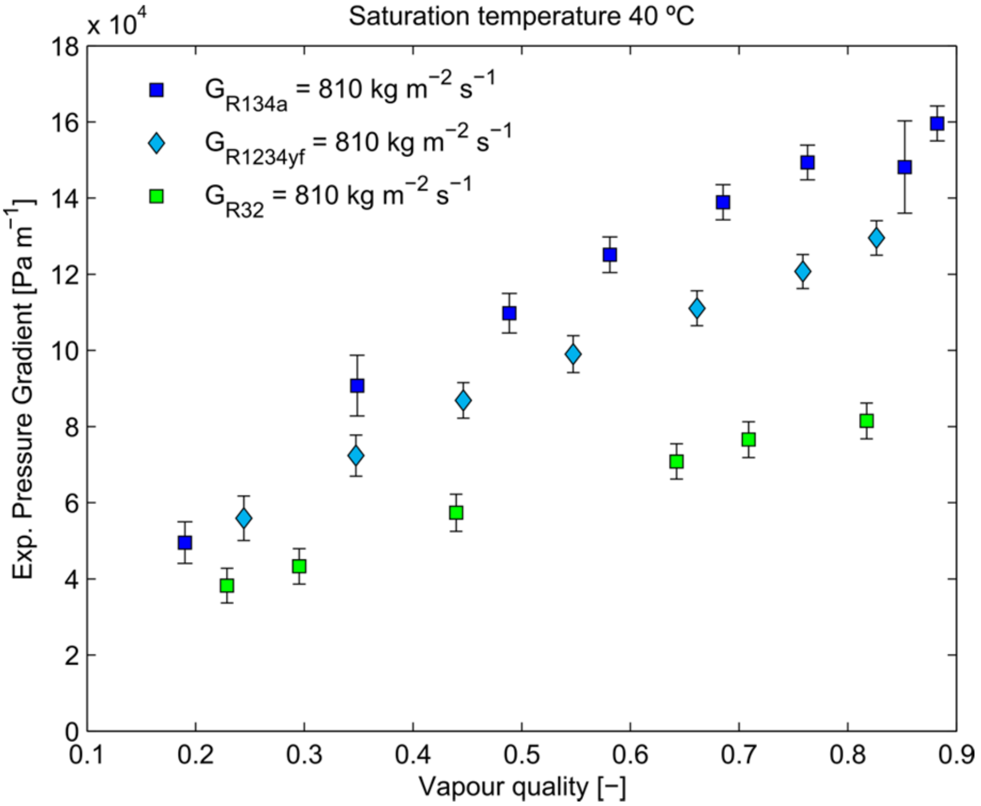

Figure 6.10. Frictional pressure gradient comparison at G = 810 kg $m^{-2}s^{-1}$.

A valid explanation can be reached observing Fig. 6.12 and 6.13. On Fig. 6.12 the reader can observe liquid and vapour pressure drop plotted versus vapour quality. Liquid phase pressure drop is depicted with squares and vapour phase with diamonds. The fluid conditions are the same as shown in Fig. 6.11. The four fluids liquid and vapour pressure drops are plotted at mass velocity of 350 kg $m^{-2}s^{-1}$. On that figure the reader can see how liquid and vapour frictional pressure drop of propane are the highest compared with the rest of fluids. It must be pointed that liquid pressure drop is about one tenth of vapour phase pressure drop.

Fig. 6.13 plots Zivi´s void fraction versus vapour quality. Looking at this figure, the reader can observe that at vapour quality values higher than 0.4 around 80% of the tube is occupied by vapour phase. At this value of vapour quality, liquid and vapour frictional pressure drops of Fig. 6.11 reach approximately the same value. At higher values of this crossing value of vapour quality, vapour pressure drop is dominant and rules over frictional pressure drop being rejected liquid pressure drop to a second place.

At null values of vapour quality, propane liquid pressure drop is also highest. This effect may be explained because of it low value of fluid density and viscosity that leads to higher values of Reynolds number and thus to frictional pressure drops.

The ranges of uncertainty values of the experimentally measured values and the proceeding followed to their calculation are provided in Chapter 4.

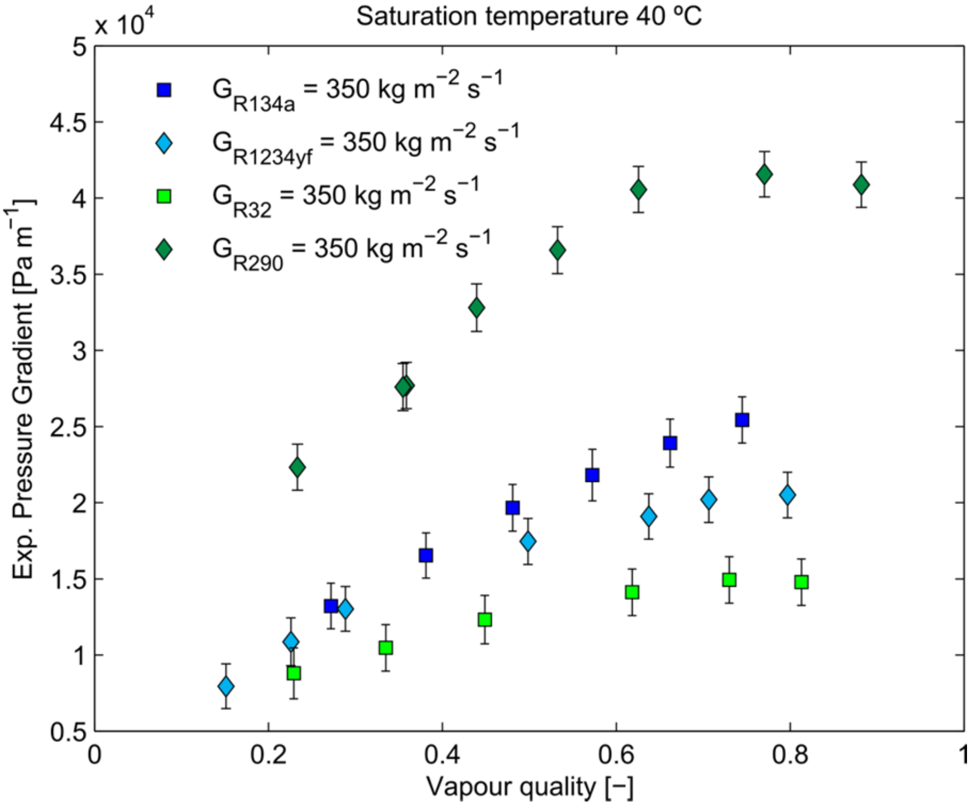

Figure 6.11. Frictional pressure gradient comparison at G = 350 kg $m^{-2}s^{-1}$

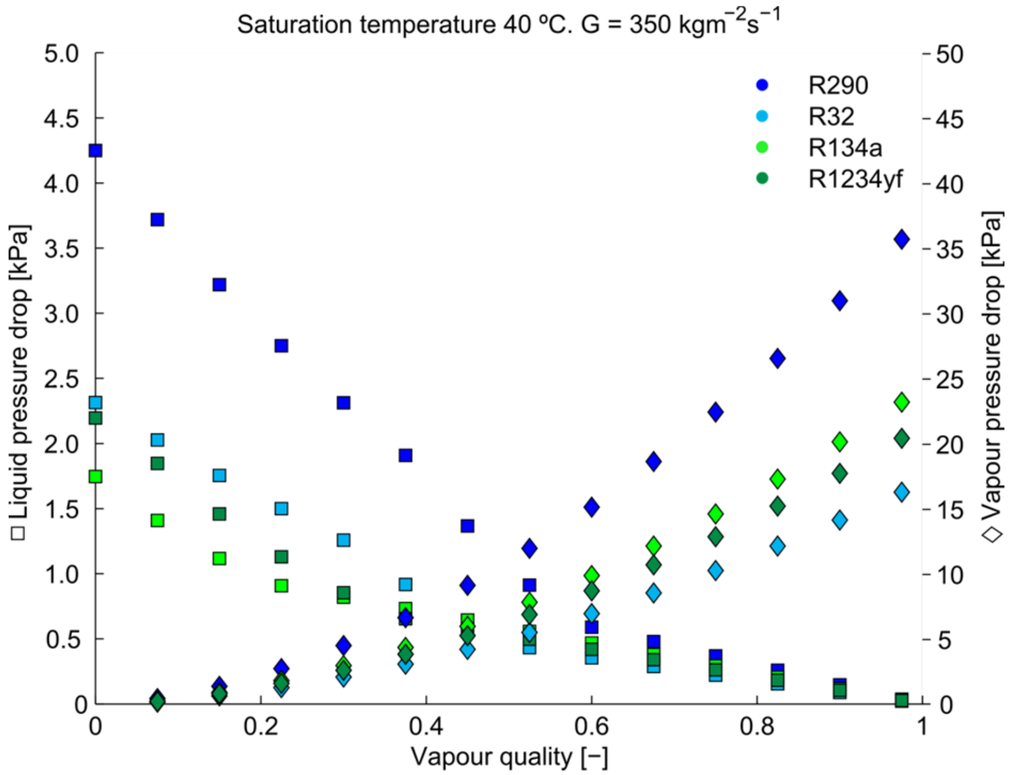

Figure 6.12. Frictional pressure gradient comparison at G = 350 kg $m^{-2}s^{-1}$

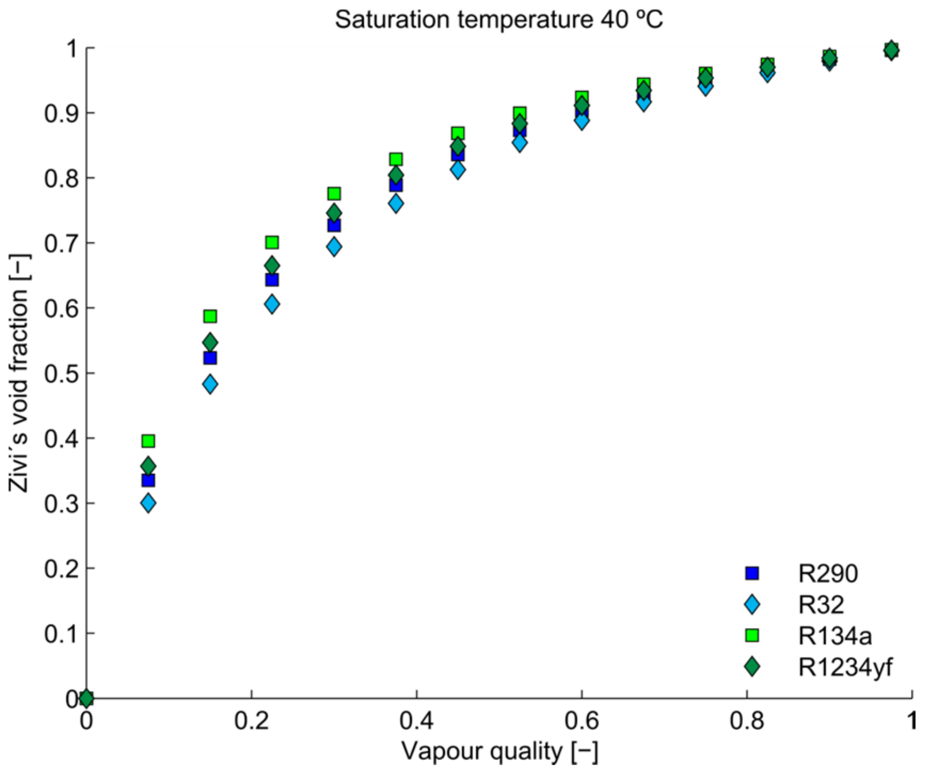

Figure 6.13. Void fraction comparison.

Measurements of frictional pressure drop during two-phase flow in condensation have been performed at 350 kg $m^{-2}s^{-1}$ to compare the behaviour of the four fluids. R32 performs the best followed by R1234yf, R134a and R290. This order is imposed by fluid properties such as density and viscosity both included in Reynolds number. So lower vapour viscosities lead higher Reynolds number and thus higher frictional pressure drop.

6.3 CONCLUSIONS

Several condensation experiments have been carried out in a horizontal mini-channel multi-port tube with an inner hydraulic diameter of 1.16 mm at mass velocities ranging of 150 to 945 kg $m^{-2}s^{-1}$ and saturation temperatures of 30, 35, 40, 45 and 50 °C using different refrigerants such as R134a, R1234y, R32 and R290. Experimental measurements of two-phase flow pressure drop and heat transfer coefficient were recorded during the experimental campaign.

Experimental measurements have been compared between them although not all the refrigerants can be compared with the others. Only R134a and R1234yf can be compared directly, in addition R1234yf is one of the potential substitutes of R134a. R22 and R290 can be compared but no experimental data of R22 in multiport tubes was found in the literature. Also, R32 and R410A can directly being compared but this latter refrigerant has not been tested experimentally yet.

Experimental data analysis suggests that R134a has higher heat transfer coefficient than its potential substitute R1234yf. R1234yf displays lower heat transfer coefficients than R134a at the same operating conditions, with heat transfer penalisation from 5 % at low mass flux and vapour quality values up to 25% at high values of both variables. R290 presents good heat transfer coefficient values even at low mass velocities; R32 heat transfer coefficient values are similar to those recorded with R134a.

The heat transfer coefficient behaviour recorded is similar to the theoretical expected. Heat transfer coefficient increase with increasing mass velocity and vapour quality values and decreasing values of saturation pressure.

Regarding to frictional pressure drop measurements, R32 performs the best. After that, R1234yf performs slightly better than R134a, since the pressure drop is by 5-7 % lower. Similar conclusion can be found in [2]. Lastly, R290 has the highest frictional pressure drop of all fluids tested.

Frictional pressure drop differences are explained in [3] by reduced pressure differences but this explanation is not valid in the case of R290 because of the high differences of density and viscosity. The frictional pressure drop of the four fluids is correctly explained by density and viscosity values of them.

In all cases, frictional pressure drop values increase with increasing values of mass velocity and vapour quality and decreasing values of reduced pressure. Frictional pressure drop under similar conditions have also been discussed.

The experimental heat transfer coefficient has been compared with several heat transfer coefficient correlations (Chapter 7).

REFERENCES

[1] S.A. Mercedes-Benz España, Mercedes-Benz considera que su evaluación de riesgos con respecto al uso del nuevo refrigerante R1234yf están confirmados. Press release. 9-8-2013.

Ref Type: Online Source

[2] D. Del Col, D. Torresin, and A. Cavallini, Heat transfer and pressure drop during condensation of the low GWP refrigerant R1234yf, International Journal of Refrigeration, 33 (2010) 1307-1318.

[3] A. López-Belchí, F. Illán-Gómez, F. Vera-García, and J.R. García-Cascales, Experimental condensing two-phase frictional pressure drop inside mini-channels. Comparisons and new model development, International Journal of Heat and Mass Transfer, 75 (2014) 581-591.

CHAPTER 7: Correlations comparison

In the following chapter the experimental data is compared against available models in the open literature. The comparison section is divided into two parts. The first part compares the frictional pressure drop data versus different author models. In the second part, the same procedure is used to compare heat transfer coefficient data.

The quantity of HTC experimental data is nine times higher than pressure drop measurements because HTC is measured locally at nine positions along the test section while pressure drop measurements consider the average value over the entire tube.

7.1 HEAT TRANSFER COEFFICIENT

In this section experimental values of heat transfer coefficient are predicted by means of the correlations presented in Chapter 3. The experimental data are plotted sorted by author models and also by model type (macro or mini-channels). In each Figure, the prediction of local heat transfer coefficient for each model for the four different fluids is plotted. These figures are also plotted in double-logarithmic axes so the reader can appreciate better small differences in heat transfer coefficient tendencies. Table 7.1 summarises mean absolute relative deviations "MARD" and mean relative deviations "MRD" at the end of this section.

7.1.1 Models developed for macro-channels

The following models were developed specifically for macro-channels heat transfer coefficient prediction.

7.1.1.1. Dobson & Chato. [1]

Dobson and Chato model is the first one analysed. This model was developed by the authors to predict HTC values. Dobson and Chato proposed a vast improvement of the Chato [2] correlation that includes both a stratified-wavy flow method with film condensation from the top towards the bottom of the tube and an annular flow correlation. The model clearly overestimates HTC over the whole range studied (Figure 7.1).

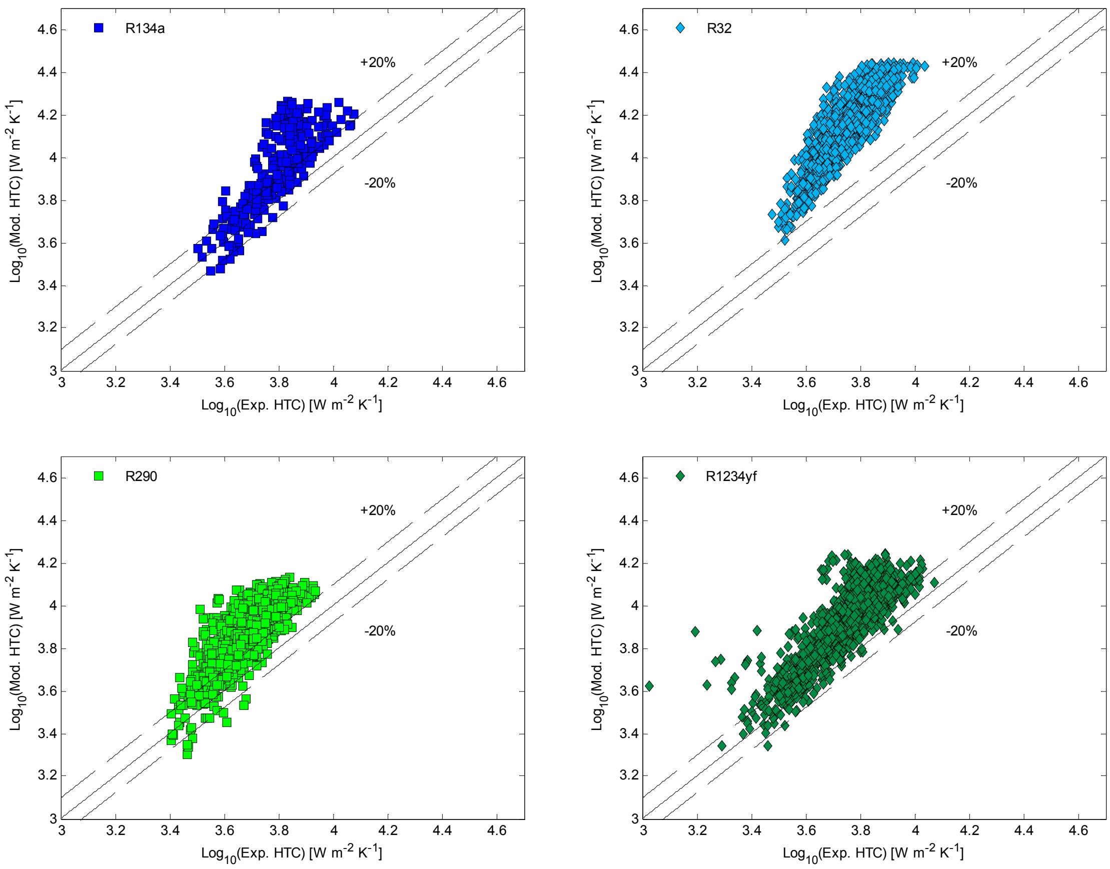

Figure 7.1. Dobson & Chato prediction

7.1.1.2. Haraguchi et al. [3]

Haraguchi et al. model was developed for condensation heat transfer coefficient prediction in smooth tubes. The model obtained a good agreement with many experimental results. The author studied the heat transfer coefficient and pressure drop during condensation using R22, R134a and R123 in an 8.4 mm hydraulic diameter horizontal smooth tube. On the basis of the turbulent liquid film theory (Travis et al, [4]) and Nusselt`s theory; they proposed an empirical asymptotic equation with the power of 2 for predicting the local Nusselt number. This model takes into account free and forced convection. The discrepancy between predicted and experimental data may be explained by the important differences between the diameter studied by the authors and that studied in the present study. Other, fluids/refrigerants different from those mentioned above with also different thermo-physical properties may be responsible for differences shown in Figure 7.2.

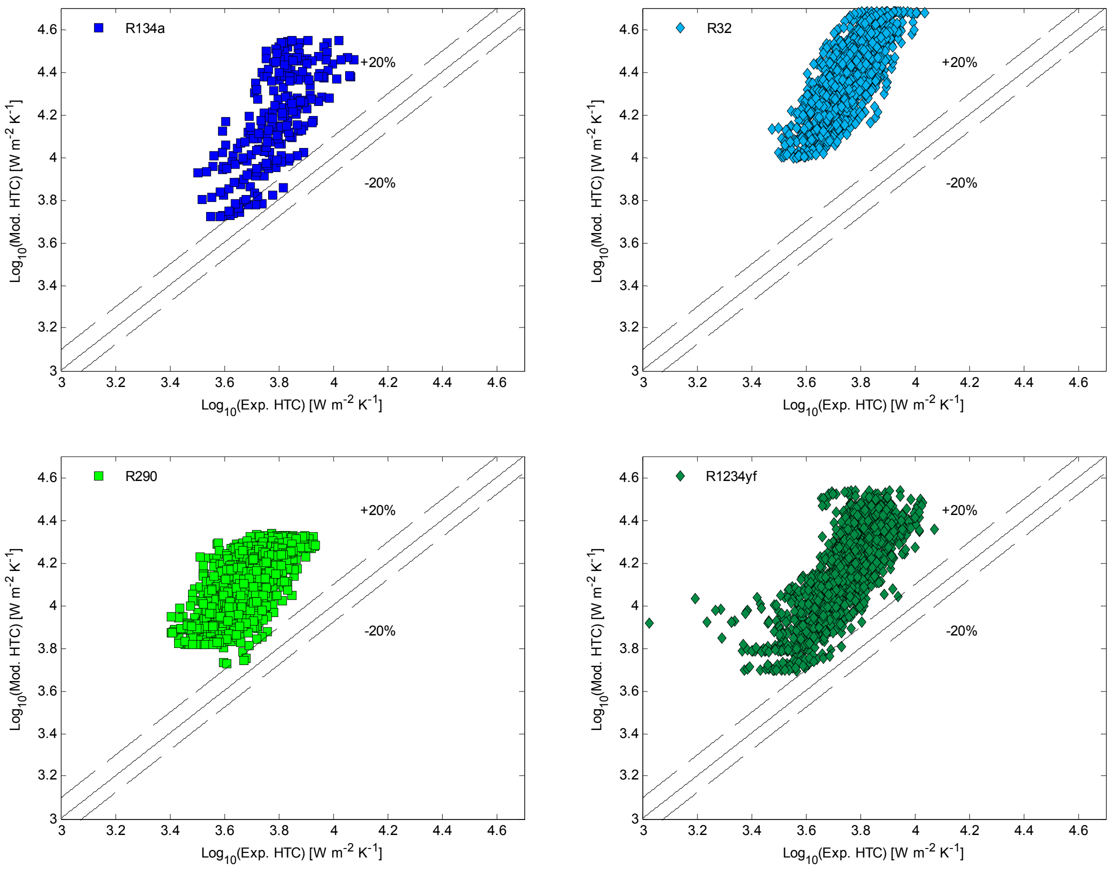

Figure 7.2. Haraguchi et al. prediction.

7.1.1.3. Akers et al. [5]

Akers et al. developed a two-phase multiplier-based correlation that became known as the “equivalent Reynolds number” model. This model defines the all-liquid mass flow rate that provides the same heat transfer coefficient as an annular condensing flow. The refrigerants tested were R12, propane and methanol in annular flow.

Figure 7.3 shows that Akers et al. model tendency does not fit to experimental data. This model underestimates HTC at low mass velocities and overestimates measured data at high mass velocities.

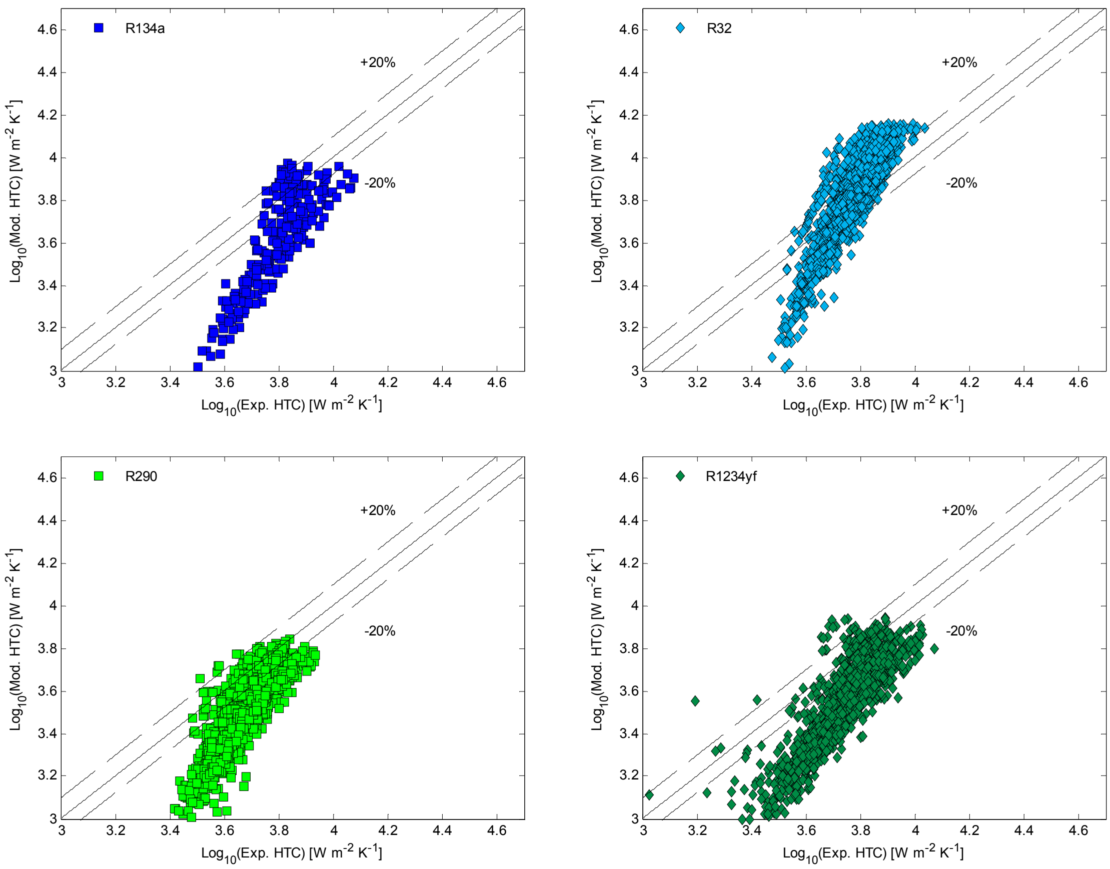

Figure 7.3. Akers et al. prediction.

7.1.2 Models developed for mini-channels

The following models were especially developed for mini-channels because of the increase of importance of shear stress.

7.1.2.1 Koyama et al. [6]

Koyama et al. model was developed in 2003 with multi-port mini-channel tubes of around 1 mm diameter and R134a. Their condensation heat transfer coefficient in terms of Nusselt number is expressed as a combination of forced convection condensation and gravity controlled convection condensation terms. Since the tube is in horizontal configuration the term that represents gravity controlled convection is null.

For the data obtained in this work, the model correctly estimates experimental HTC values with low deviation values as shown in Figure 7.4. Differences are more noticeable at low vapour quality values and mass velocities.

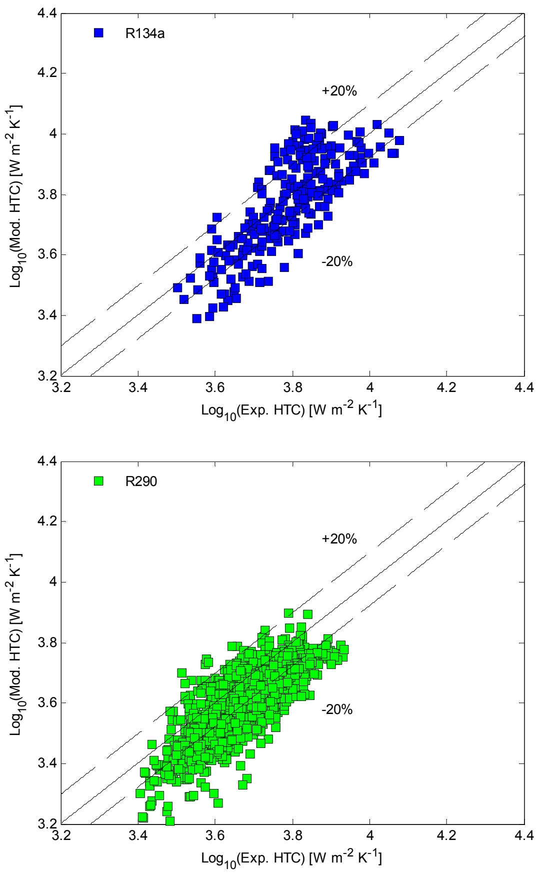

Figure 7.4. Koyama et al. prediction.

7.1.2.2. Webb et al. [7]

The model published by Webb et al. was developed with experimental measurements of R134a in multi-port mini-channel tubes with hydraulic diameters in the range 0.44 to 1.53 mm. Figure 7.4 shows a clear overestimation of experimental data at high mass velocities and vapour quality values which may be explained by the differences between the tubes. These authors also used tubes with micro-fins at the refrigerants side which may affect HTC.

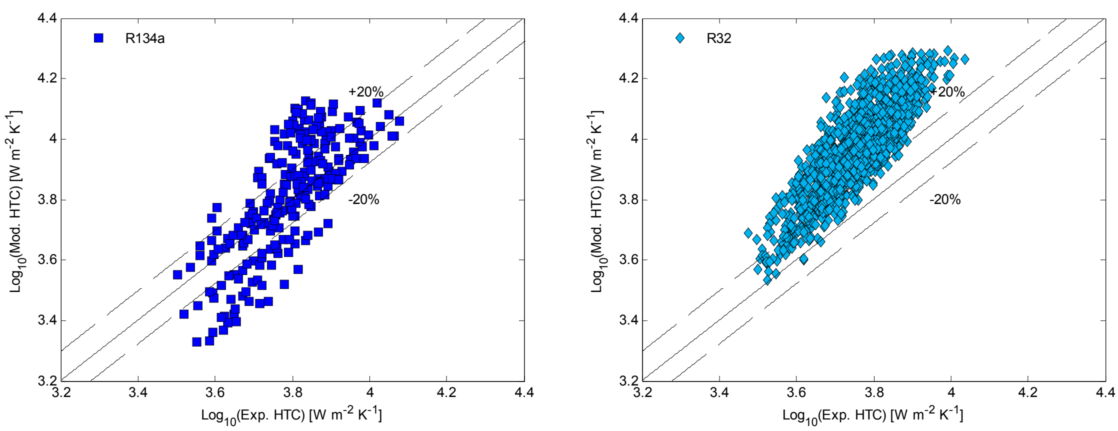

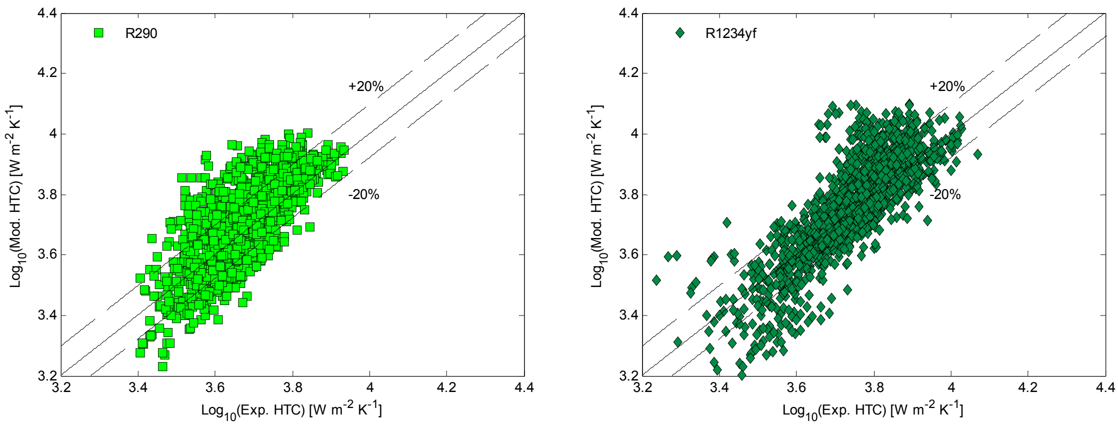

Figure 7.5. Webb et al. prediction.

7.1.2.3. Cavallini et al. [8]

The results presented in Figure 7.6 show that HTC model developed by Cavallini et al. overestimates the experimental measurements of HTC obtained for R32 and R290. The prediction of R134a and R1234yf are more accurate instead. As was presented in Chapter 3, this model depends on frictional pressure drop calculation. The frictional pressure drop model that this HTC model uses agrees quite well with the experimental results as is presented in the following section after HTC models discussion. A discrepancy of pressure drop evaluation would surely affect fluid thermo-physical properties, so the HTC predictions could not be as accurate as desired.

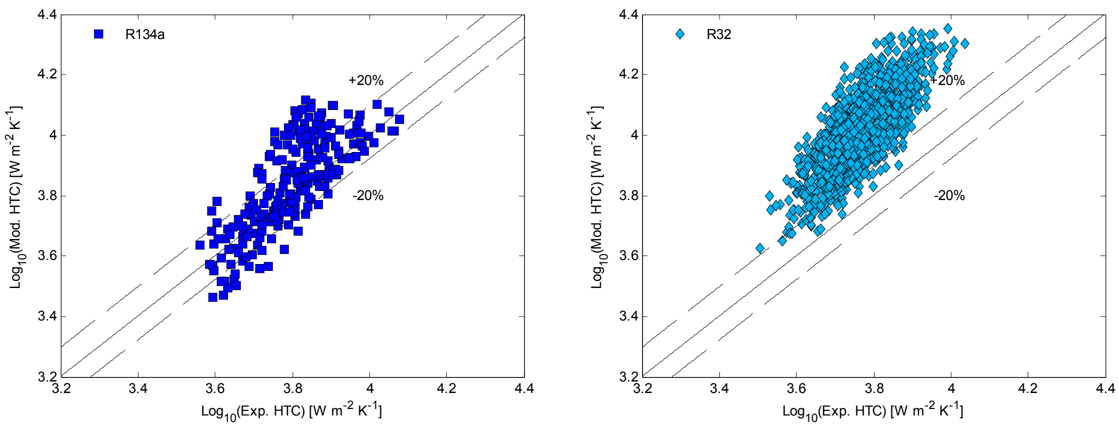

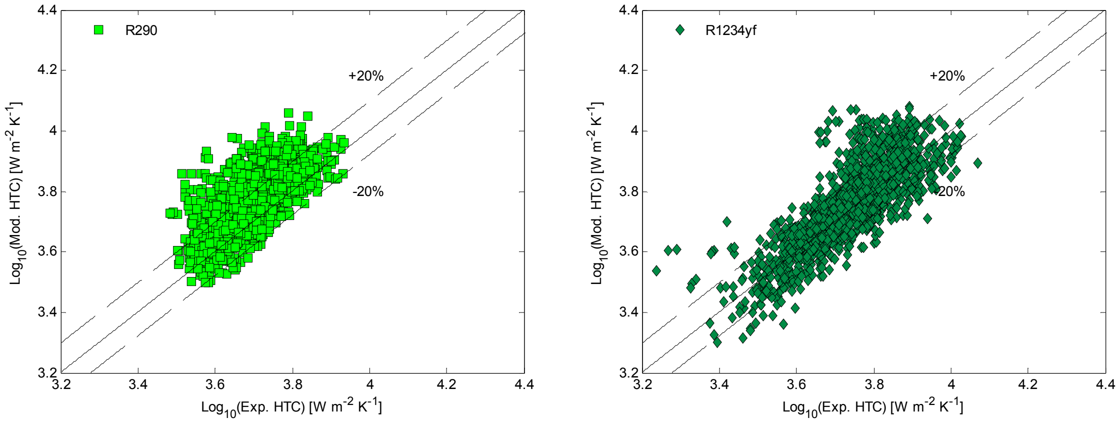

Figure 7.6. Cavallini et al. prediction.

7.1.2.4. Wang et al. [9]

Figure 7.7 shows that Wang et al. model slightly underestimates the experimental values of HTC at low mass velocities and vapour qualities and overestimates high heat transfer coefficients which correspond to higher values of mass velocities and vapour qualities. This model was developed with R134a as working fluid and for similar tubes to the tubes experimentally tested.

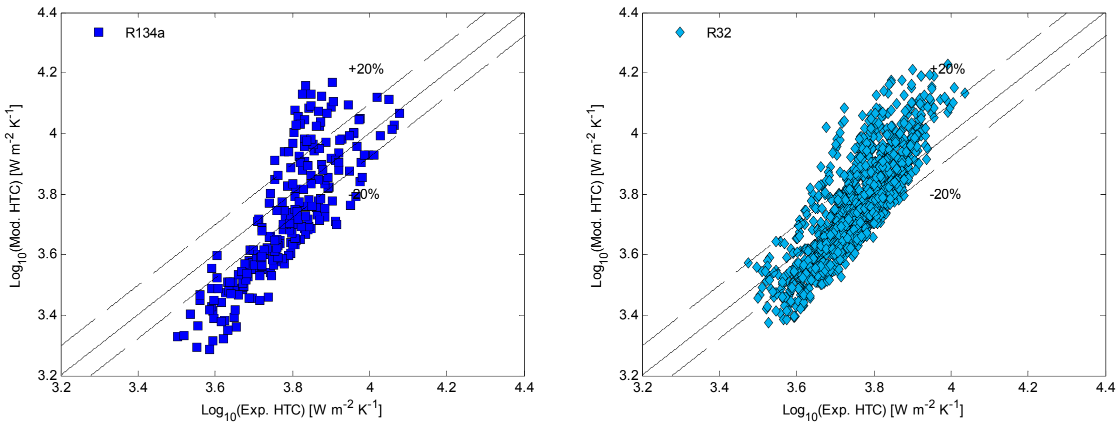

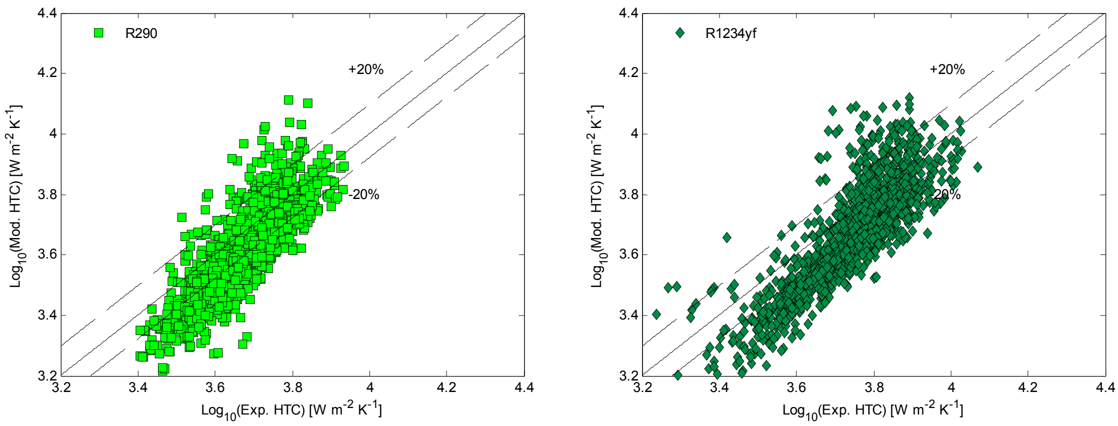

Figure 7.7. Wang et al. prediction.

7.1.2.5. Bandhauer et al. [10]

Bandhauer and Garimella model uses the correlation of Garimella et al. [11] for frictional pressure drop calculation. The underestimation of pressure drop at high values of frictional pressure gradient shown below may lead this model to overestimate HTC at high mass velocities. As commented previously, the discrepancies of pressure drop evaluation surely affects fluid thermo-physical properties, so the HTC predictions are not as accurate as desired (Figure 7.8).

The prediction for R32 is not as good as in the rest of fluids. This can be explained by the high different fluid properties of this fluid compared to those used for the model development.

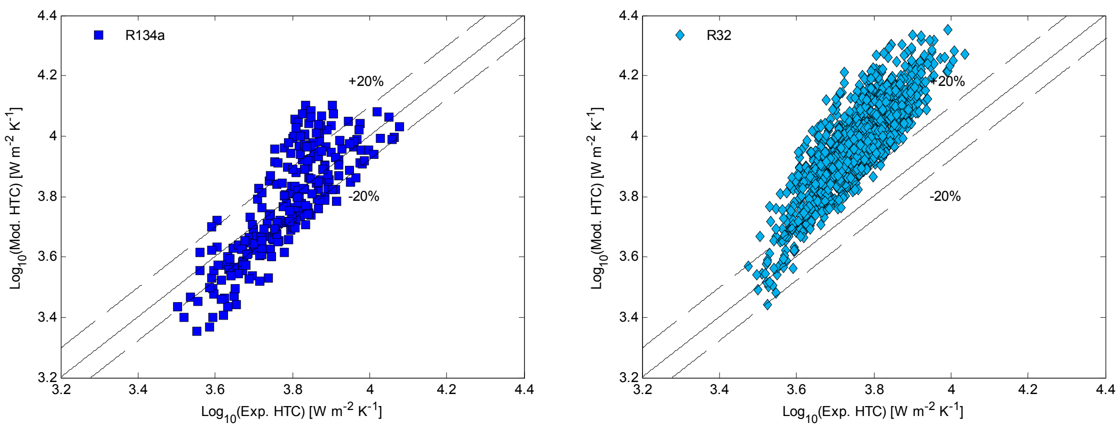

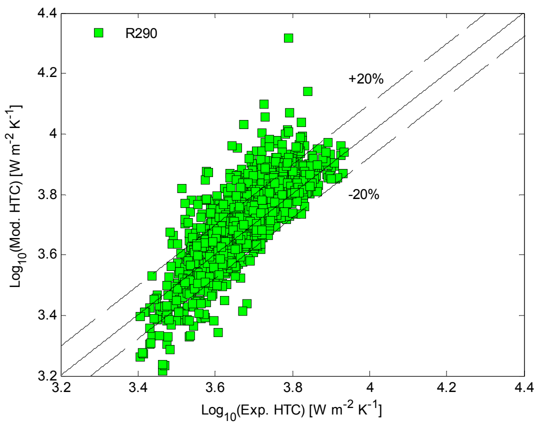

Figure 7.8. Bandhauer et al. prediction.

Table 7.1 shows the MARD and MRD values corresponding to the model considered above. They are provided for fluid separately and for the entire collection of experimental measurements.

The results show that there is no model able to predict experimental measurements for all the fluids, most of the models fail predicting one or two of them. Therefore a new adjustment proposal to a widely used HTC model is proposed in the following Chapter.

Table7.1. MARD and MRD values for heat transfer coefficient prediction models.

Author/Model	MRD					MARD				
	R134a	R32	R290	R1234yf	All Fluids	R134a	R32	R290	R1234yf	All Fluids
Dobson & Chato	47.66	148.7	54.9	51.9	88.1	49.5	148.7	55.5	51.9	88.4
Haraguchi et al.	167.9	327.2	161.1	177.8	225.3	167.9	327.2	161.1	177.8	225.3
Akers et al.	-32.1	11.59	-31.1	-33.1	-15.9	36.4	29.2	32.2	34.1	31.7
Koyama et al.	-0.9	-11.0	-14.5	-3.3	-10.2	18.9	16.1	17.7	12.2	16.2
Webb et al.	10.3	66.9	12.1	7.1	31.1	26.2	67.0	22.2	15.28	37.6
Cavallini et al.	10.1	64.4	6.87	3.1	27.4	25.1	83.9	33.2	14.2	47.6
Wang et al.	-7.7	5.5	-9.9	-13.5	-4.8	27.8	20.86	18.9	20.3	20.6
Bandhauer et al.	1.3	68.46	10.6	1.4	23.3	20.9	68.57	18.2	13.7	35.9

7.2 FRICTIONAL PRESSURE DROP

In this section the experimental frictional pressure drop measurements are compared with the results provided by some correlations presented in Chapter 3 under the same tested conditions. The correlations studied in this section are widely used to predict frictional pressure drop in macro and mini-channels. The correlations used in this section are the following: the Homogeneous model, Fridel [12], Müller-Steinhagen and Heck [13], Souza and Pimenta [14], Sun and Mishima [15], Zhang and Webb [16], Garimella et al. [17], Mishima and Hibiki [18], Cavallini et al. [19] and Kim and Mudawar [20] models.

Some of these correlations were developed to be used in macro-channels but can also be used to predict frictional pressure drop in reduced section tubes, other correlations cited in the following lines were developed specifically to be used in mini-channels. The experimental data are plotted sorted by author models and also by model type (macro or mini-channels). In each Figure, the prediction of each model for the four different fluids is depicted. The model comparisons are depicted in double logarithmic axis with measured values in X axis and predicted values in Y axis. A summarising table (Table 7.2) with mean absolute relative deviations “MARD” and mean relative deviations “MRD” is included after model comparison figures.

7.2.1 Models developed for macro-channels

In the following lines experimental frictional pressure drop is compared with several models developed for macro-channels. These models were originally developed to be used with macro-channels but several authors have reported the ability of these models to be used in mini-channel pressure drop prediction accurately. Some classical correlations are discussed below.

7.2.1.1 Homogeneous model

The homogeneous model considers the two-phase flow mixture as a single phase with mixture fluid properties in the tube. The behaviour of this model changes depending on the mixture fluid properties model considered. Quite high differences can be obtained with the different models proposed for two-phase flow viscosity. The model used for the evaluation of viscosity in the data represented in Fig. 7.9 corresponds to McAdams model. The homogeneous model captures the right tendency of all data but underestimates the measured values.

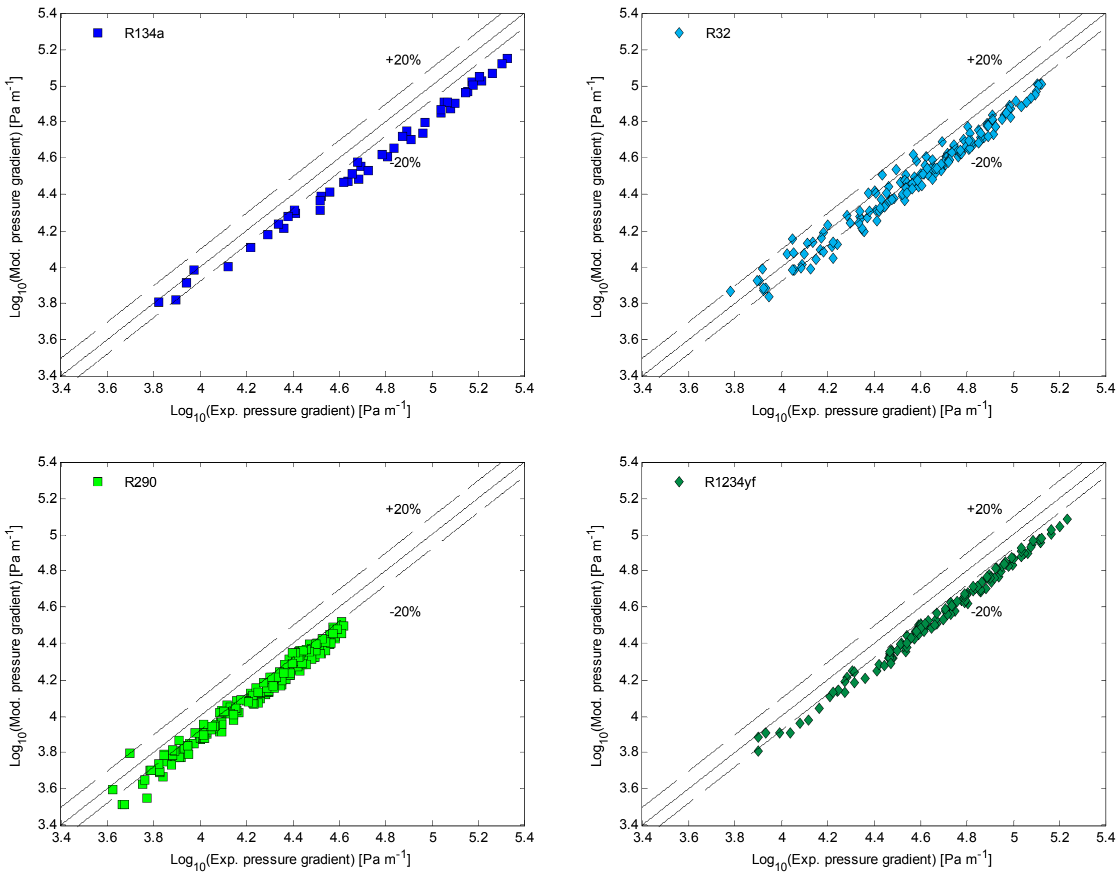

Figure 7.9. Homogeneous model prediction.

7.2.1.2 Friedel [12]

Friedel is the second model developed for macro-channels considered on this study. This model was adjusted from a database of 25000 experiments. The model takes into account the effects of gravity and surface tension. Friedel takes into account for this model different effects such as: surface tension to consider the forces relationship between bulk and surface of the liquid; Reynolds numbers of vapour and liquid phase to include the inertial to viscous forces of the fluid in relative motion to the surface; the ratios of viscous and density of both phases are also taken into account in order to capture how different vapour and liquid phases are. Other variables are also considered such as vapour quality, mass velocity and tube diameter.

As the previous model, Friedel model also captures the tendency of the data but overestimates pressure gradient measurements (Figure 7.10). It may overestimate the experimental measurements because the diameter range it was developed for tubes higher than 4 mm and the behaviour of fluid dynamics in much lower diameter is not sharply predicted.

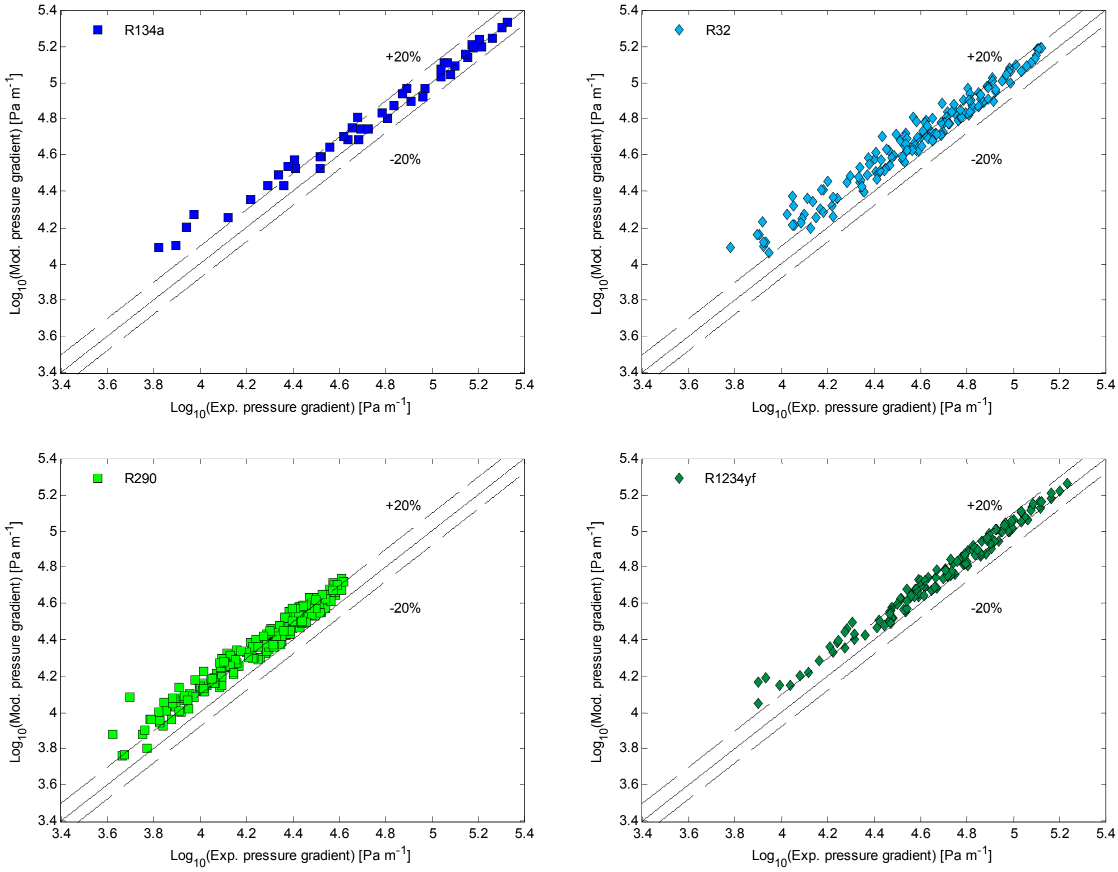

Figure 7.10. Friedel model prediction

7.2.1.3 Müller-Steinhagen and Heck [13]

Müller-Steinhagen and Heck model is essentially an empirical two-phase interpolation between all liquid and all vapour flow pressure drop. This model is able to predict with high accuracy the lowest values of frictional pressure drop. The authors observed that two-phase frictional pressure drop increases linearly until a value of quality around 0.7 then pressure drop decreases. This model does not consider the influence of the most common dimensionless groups used in other models to calculate two-phase frictional pressure drop. This latter point is very interesting if it is necessary to compare different refrigerants but it is possible to lose the refrigerant's properties effect on the pressure drop.

As is shown in Figure 7.11, this model tends to overestimate experimental measurements at high pressure gradient values. This is more accurate than Friedel´s one and this may be explained by the higher variety of fluids tested to obtain the correlation, much of them refrigerants.

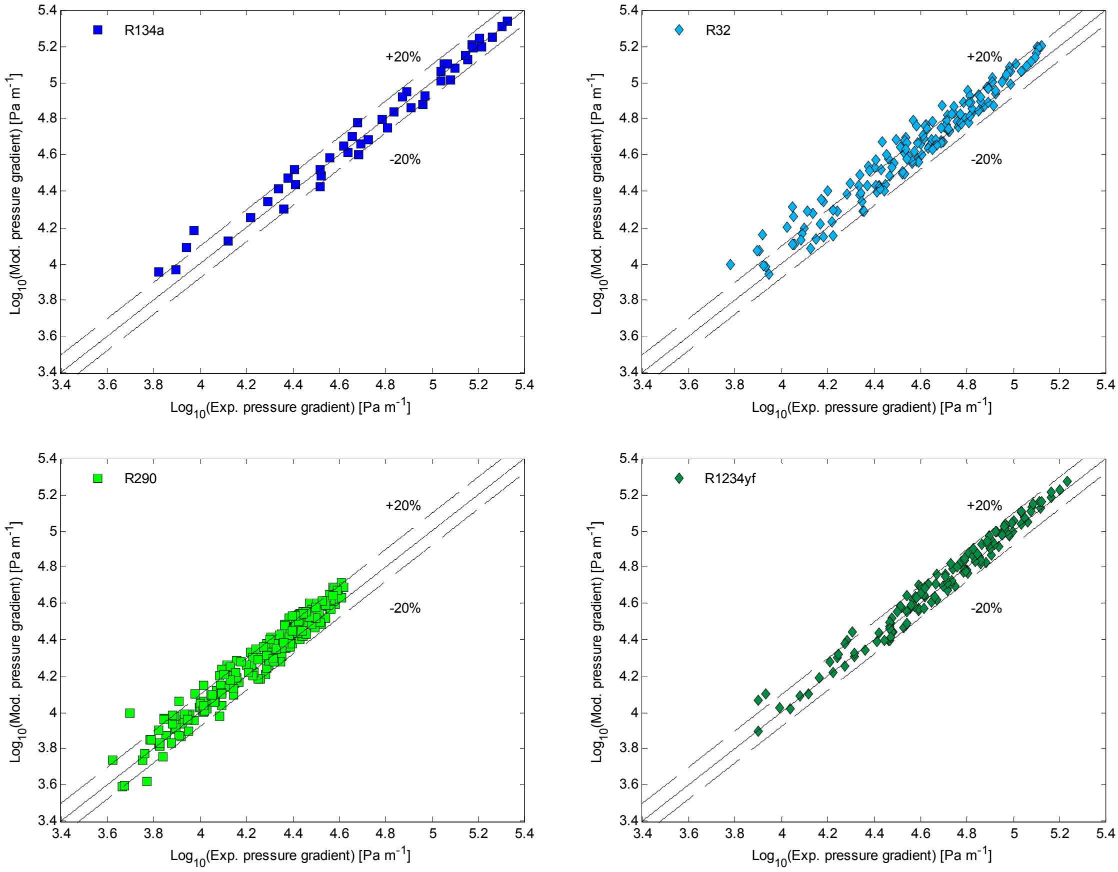

Figure 7.11. Müller-Steinhagen & Heck model prediction.

7.2.1.4 Souza and Pimenta [14]

The model of Souza and Pimienta correlates the Lockhart-Martinelli parameter and fluid physical properties to the liquid only two-phase flow multiplier. This model considers the ratios of liquid to vapour viscosities and densities to capture how different vapour and liquid phases are.

The model was derived by adjusting data from pure refrigerants (R-12, R22, and R134a) and mixtures (MP-39, R-32/125) and tube diameters of 7.75 and 10.92 mm in the range of saturation temperatures from -20 to 15ºC.

Experimental data prediction is accurate enough and tendency is correctly captured but the prediction given by this model is a bit more dispersed than previous models (Figure 7.12).

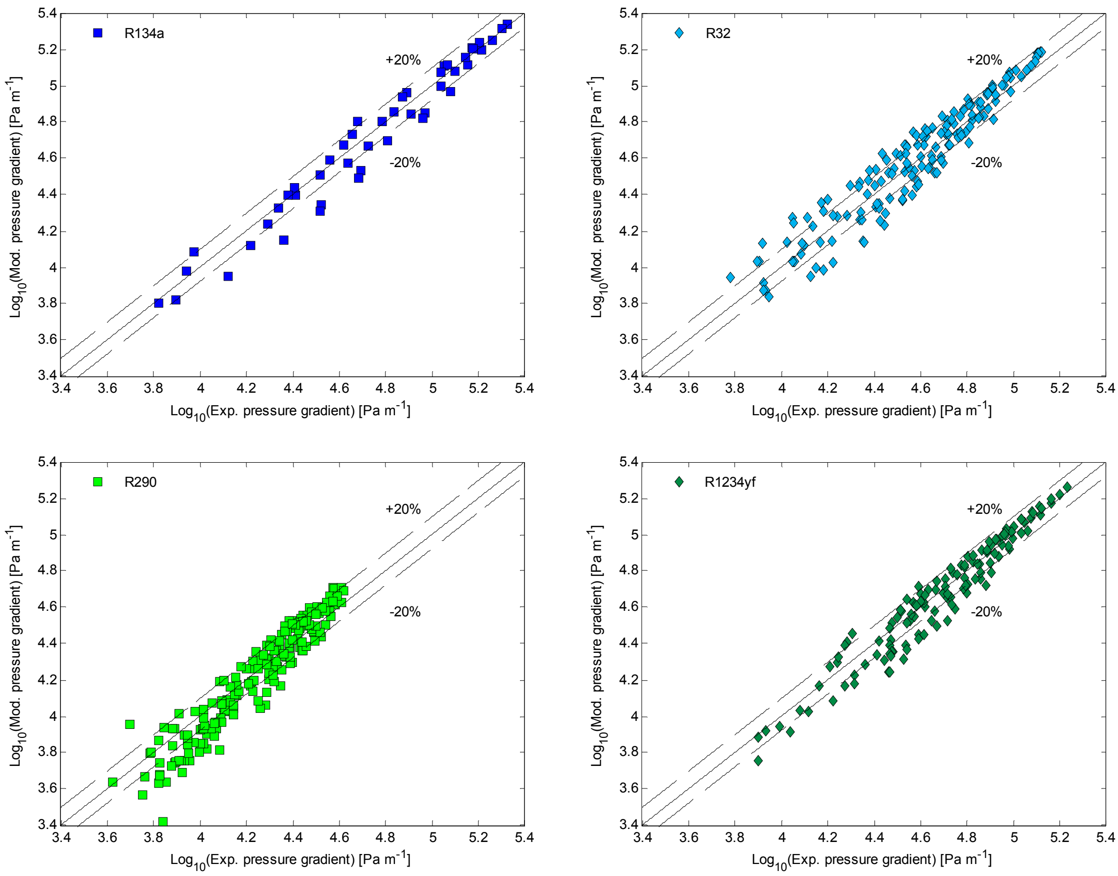

Figure 7.12. Souza and Pimenta model prediction.

7.2.2 Models developed for mini-channels

Several models have been developed to be used in mini-channels in the last decade due to the incorporation of mini-channels to industrial equipment. The different conditions for each model development are briefly described below. The prediction of each plotted model is also commented.

7.2.2.1. Sun and Mishima. [15]

Sun and Mishima model is based on 2092 experimental data points of R123, R134a, R22, R236ea, R245fa, R404A, R407C, R410A, R507, CO_2, water and air in 0.506–12 mm tubes. The model is enough accurate to predict experimental data. This behaviour may be explained thanks to the huge variety of refrigerants and conditions tested and the big range of diameters considered. The results represented in Figure 7.13 show that the predictions of this model are quite sharp and very small deviations can be observed.

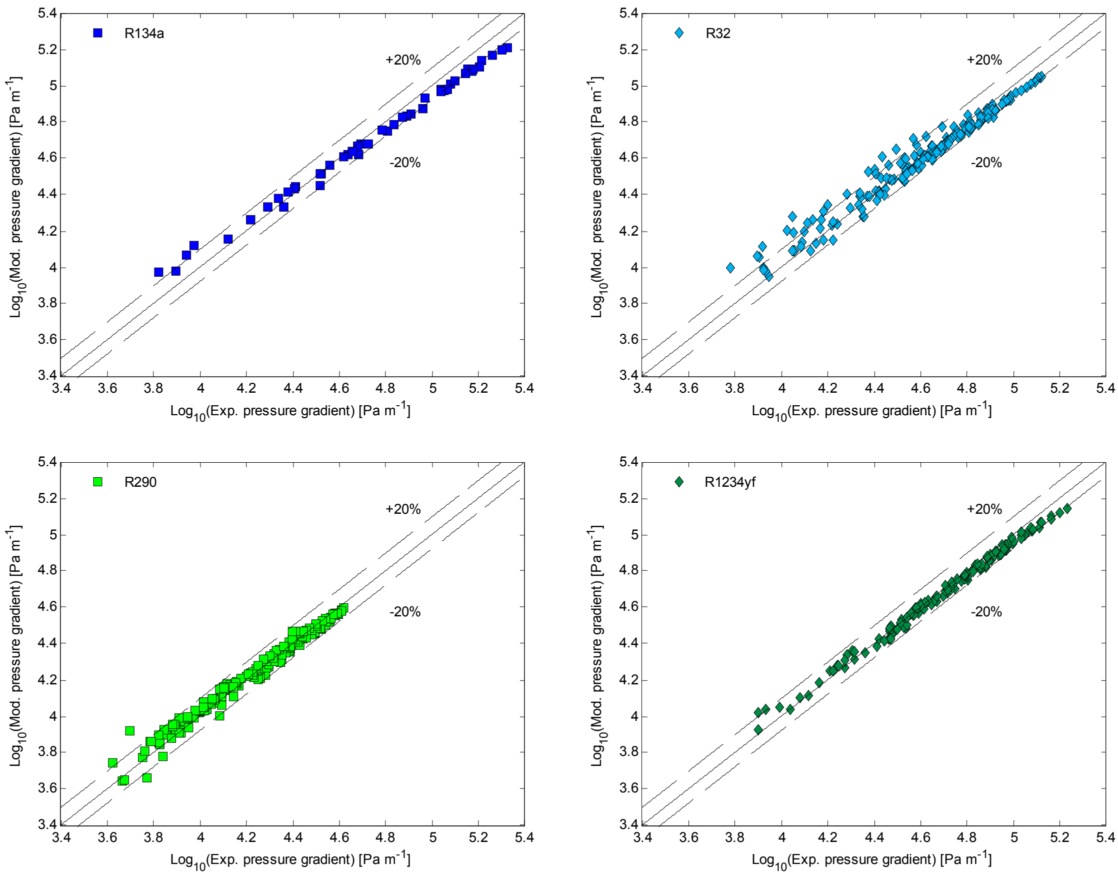

Figure 7.13. Sun & Mishima prediction.

7.2.2.2. Zhang and Webb. [16]

Zhang and Webb model was developed for adiabatic two-phase flows of R134a, R22 and R404A in a multiport tube of 2.13 mm and two copper tubes of 6.25 and 3.25 mm. The results displayed in Figure 7.14 show that this model is also quite accurate with little overestimations, lower than 30%, at high mass velocities ad vapour qualities. This model has been widely tested and validated by international researchers.

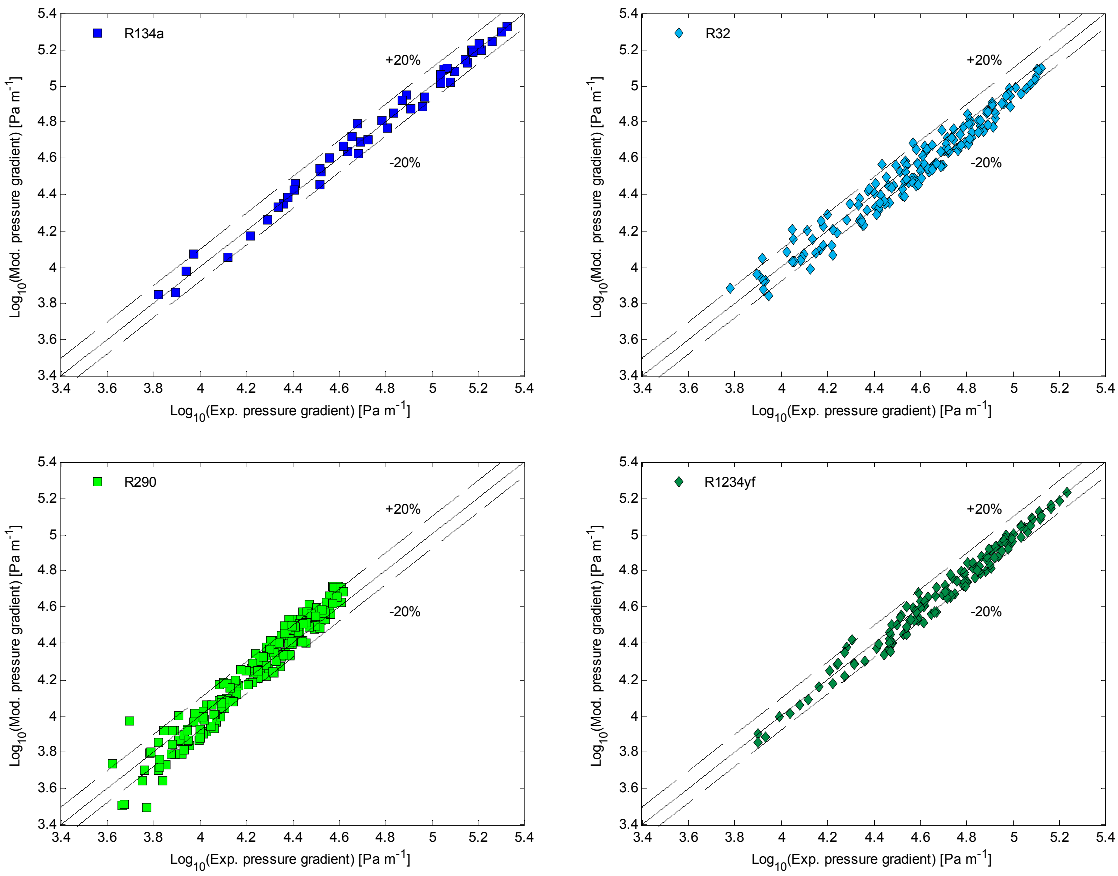

Figure 7.14. Zhang & Webb prediction.

7.2.2.3. Garimella et al. [17]

Garimella´s model was developed by means of R134a pressure drop measurements for intermittent flow. The model is based on flow pattern behaviour and different contributions by bubble size. It is a very accepted model to predict pressure drop. As shown in Figure 7.15, it overestimates frictional pressure drop at low pressure drop values and underestimates them at higher values. The predictions of R32 are not very sharp maybe because of very different fluid properties with its validation fluid. This model was developed with multi-port mini-channel tubes similar to the tube experimentally tested on this PhD.

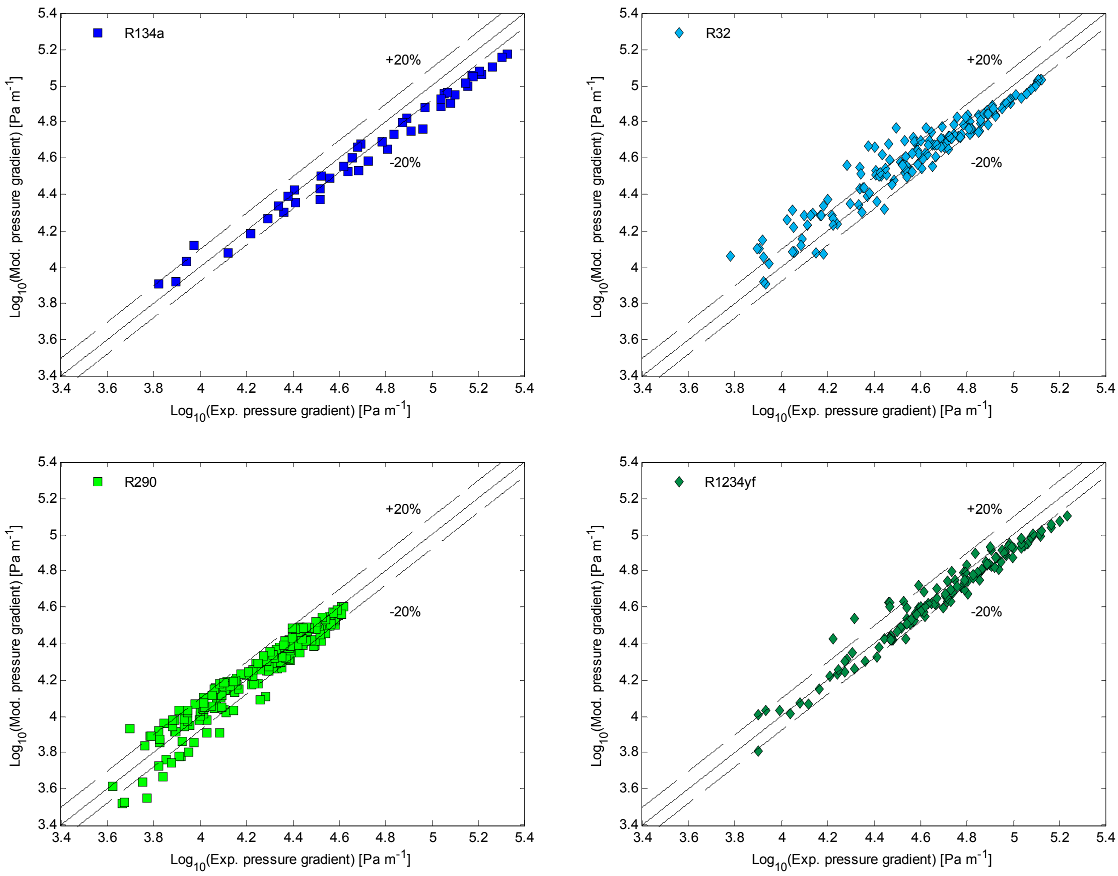

Figure 7.15. Garimella prediction.

7.2.2.4. Mishima and Hibiki. [18]

Mishima and Hibiki model is based on air-water flows in capillary tubes with inner diameter in the range from 1 to 4 mm. The model of pressure drop is performed by a new *"C"* Chisholm´s parameter as a function of inner diameter. This model is not able to predict experimental frictional pressure drop data correctly (Figure 7.16). This may be explained because the "Chisholm" two-phase flow multiplier depends only on the tube diameter, so no fluid properties can be taken into account. In that way as only one tube was experimentally tested, similar results were obtained for all refrigerants.

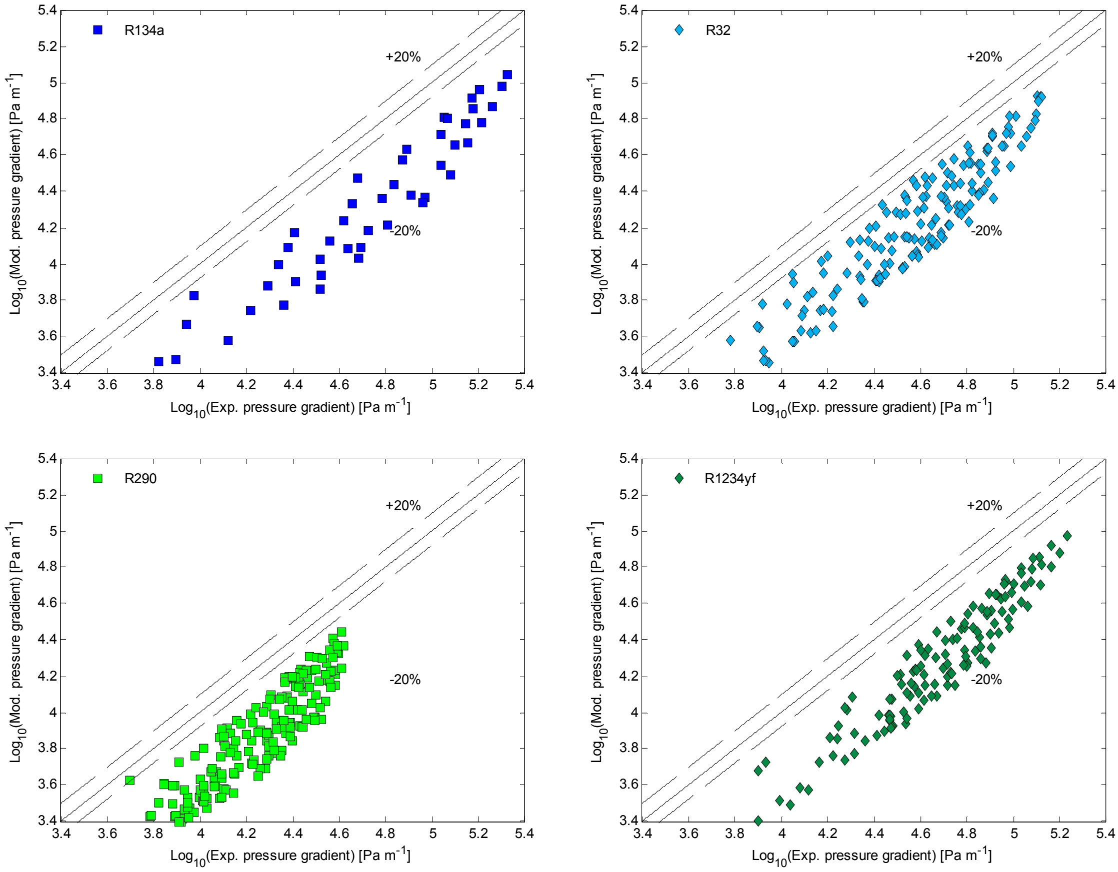

Figure 7.16. Mishima & Hibiki prediction.

7.2.2.5. Cavallini et al. [19]

Cavallini et al. model was developed for shear dominated flow regimes inside pipes, thus, annular, annular-mist and mist flow are well predicted with inner diameter from 0.5 to 3.2 mm for halogenated refrigerants. The results included in Figure 7.17 indicate that this is very accurate at high frictional pressure drop gradients but as mass velocity or vapour quality decreases, this model trends to overestimate pressure drop values. The maximum underestimation is around 20 %. The underestimation is a bit higher for the high pressure refrigerant, R32.

This model is based on liquid only two-phase flow multiplier models. The authors presented a new correlation for a two-phase flow multiplier for dimensionless gas velocities higher than 2.35. This multiplier uses the entrainment ratio of Paleev and Filipovic to consider the liquid bubbles that can be introduced in the tube. Since the dimensionless gas velocity higher than 2.35 usually correspond with annular or intermittent flow, this model also considers the gas core density in calculations. Other common relations such as gas to liquid density and viscosity ratios are introduced to evaluate the differences of liquid and vapour phase. Reduced pressure considers the variation of fluid properties with saturation temperature. Surface tension and all liquid friction factors are also introduced.

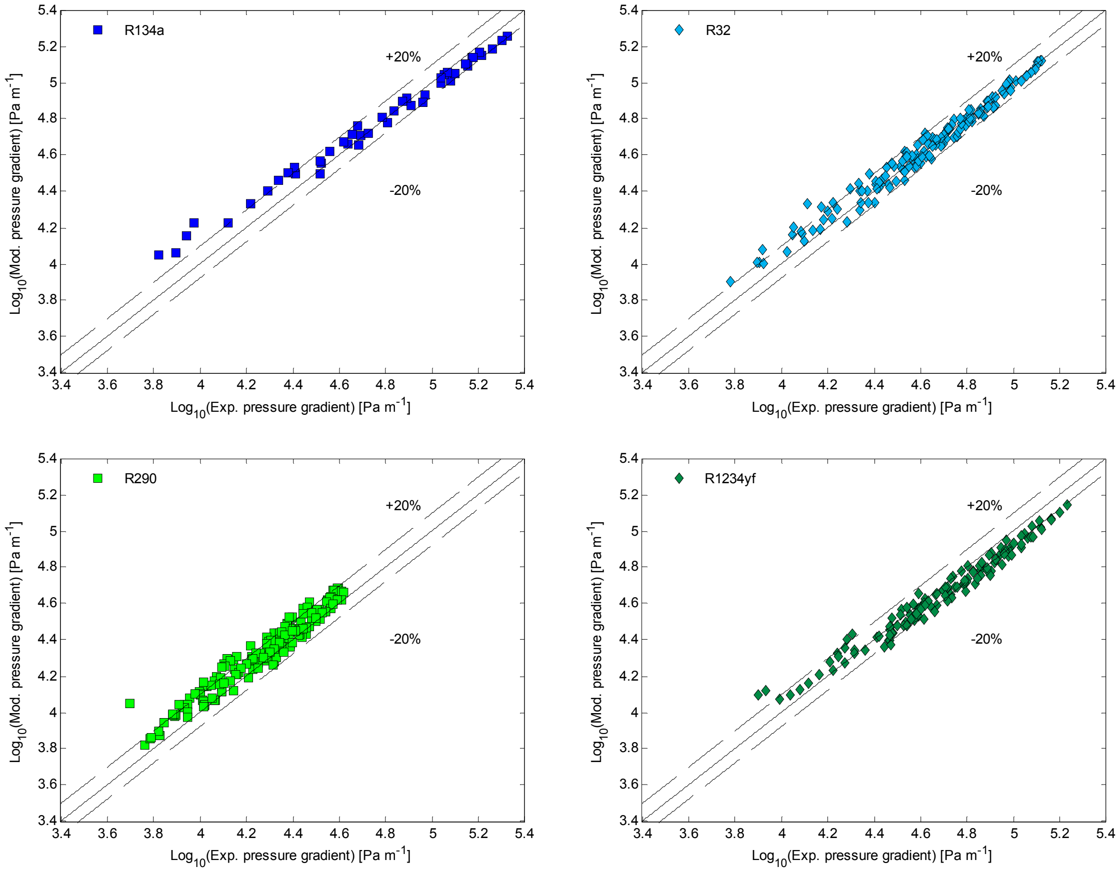

Figure 7.17. Cavallini et al. (2009) prediction.

7.2.2.6. Kim and Mudawar. [20]

Kim and Mudawar model is based on 7115 frictional pressure gradient data from 36 sources with 17 different fluids and diameters in the range from 0.0695 to 6.22 mm. Their model is accurate enough but trends to overestimate predictions at low frictional pressure drop values which correspond to low mass velocities and vapour qualities (Figure 7.18). At higher values the prediction matches with experimental values with differences lower than 20%.

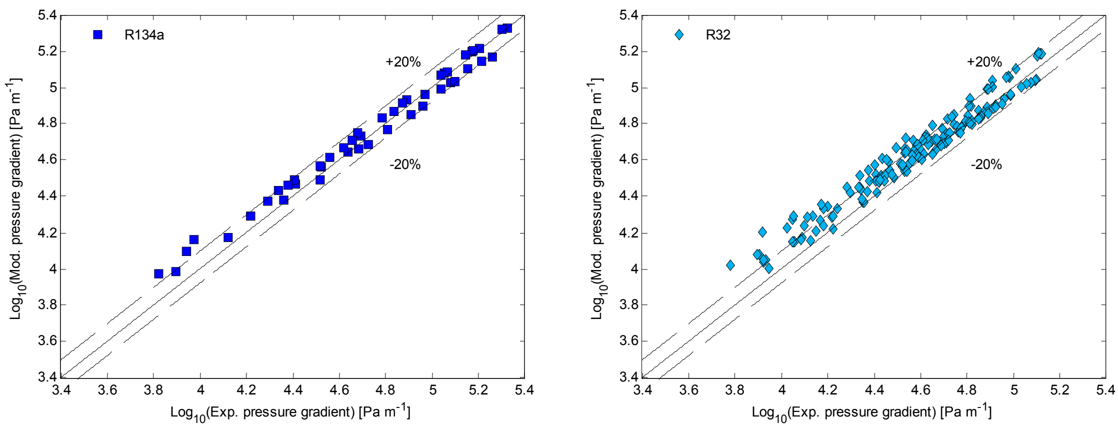

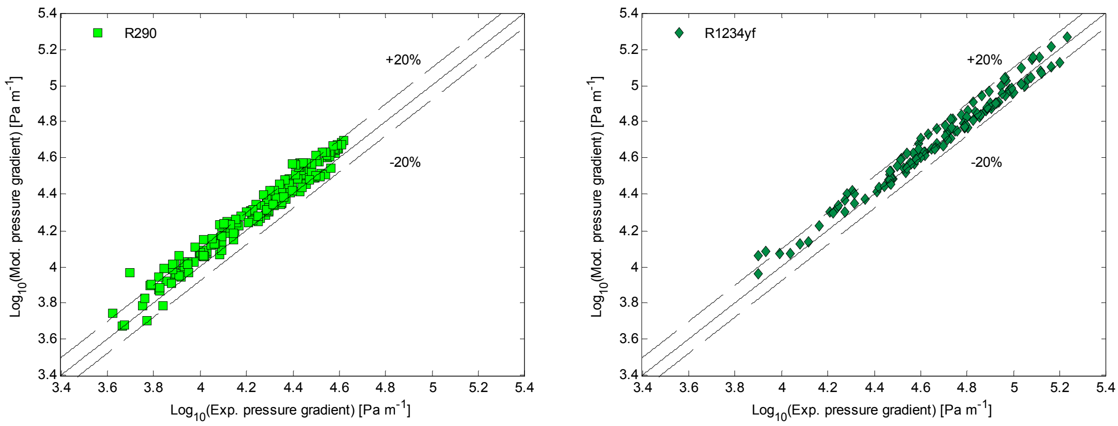

Figure 7.18. Kim & Mudawar prediction.

In Table 7.2, the MARD and MRD values for each model depending on the fluid and for the entire collection of experimental measurements are shown.

Table 7.2. MARD and MRD values for pressure drop prediction models.

Author/Model	MRD					MARD				
	R134a	R32	R290	R1234yf	All fluids	R134a	R32	R290	R1234yf	All fluids
Homogeneous	-103.1	-17.7	-23.8	-42.5	-22.8	103.2	19.9	24.1	42.5	23.6
Friedel	115.4	30.4	31.4	41.5	26.9	116.9	30.4	31.4	41.6	27.1
Müller-Steinhagen & Heck	34.7	17.89	10.5	13.9	11.1	54.1	19.8	14.4	20.7	15.1
Sun & Mishima	5.9	2.7	2.8	0.7	0.7	34.2	12.9	6.9	12.2	9.4
Zhang & Webb	-0.5	-7.5	3.8	-3.5	-1.7	48.3	14.3	15.1	17.7	12.8
Garimella et al.	-9.2	9.6	-0.3	-1.9	-0.1	55.2	19.9	11.9	23.3	15.5
Mishima & Hibiki	-237.5	-53.5	-56.9	-99.5	-56.6	237.5	53.5	56.9	99.5	56.6
Cavallini et al.	16.3	-4.9	4.19	-8.8	-1.2	84.2	18.7	26.1	28.8	20.8
Kim & Mudawar	60.1	17.8	16.8	19.8	13.8	67.5	19.9	17.4	23.8	16.1

7.3 CONCLUSIONS

In this chapter the prediction of the experimental measured values is presented with several models available in the literature. Several models correctly predict experimental values of HTC, most of them developed to be used in mini-channels. The experimental pressure drop is predicted accurately by more authors compared with HTC data. Some classical models do not fail in excess predicting experimental measurements of pressure drop.

Looking at the tables of deviations presented in this chapter, the best predicting models for our experimental data are Koyama et al for heat transfer coefficient and Sun and Mishima for pressure drop.

REFERENCES

[1] M.K. Dobson and J.C. Chato, Condensation in smooth horizontal tubes, Journal of Heat Transfer, 120 (1998) 193-213.

[2] J.C. Chato, Laminar condensation inside horizontal and inclined tubes, (1960).

[3] H. Haraguchi, S. Koyama, and T. Fujii, Condensation of refrigerants HCFC 22, HFC 134a and HCFC 123 in a horizontal smooth tube, Trans. JSME (B), 60 (1994) 245-252.

[4] D.P. Traviss, W.M. Rohsenow, and A.B. Baron, Forced Convection Condensation in tubes: A heat Transfer Correlation for condenser design, ASHRAE Transactions, 79 (1973) 157-165.

[5] W.W. Akers, H.A. Deans, and O.K. Crosser, Condensing heat transfer within horizontal tubes, Chem. Eng. Progr., 54 (1958).

[6] S. Koyama, K. Kuwahara, K. Nakashita, and K. Yamamoto, An experimental study on condensation of refrigerant R134a in a multi-port extruded tube, International Journal of Refrigeration, 26 (2003) 425-432.

[7] R. Webb, Prediction of Condensation and Evaporation in Micro-Fin and Micro-Channel Tubes, in: S. Kaka+º, A.E. Bergles, F. Mayinger, and H. Yünçü (Eds.), Heat Transfer Enhancement of Heat Exchangers*,* Springer Netherlands, 1999, pp. 529-550.

[8] A. Cavallini, D. Del Col, L. Doretti, M. Matkovic, L. Rossetto, and C. Zilio, Condensation Heat Transfer and Pressure Gradient Inside Multiport Minichannels, Heat Transfer Engineering, 26 (2005) 45-55.

[9] W.W. William Wang, T.D. Radcliff, and R.N. Christensen, A condensation heat transfer correlation for millimeter-scale tubing with flow regime transition, Experimental Thermal and Fluid Science, 26 (2002) 473-485.

[10] T.M. Bandhauer, A. Agarwal, and S. Garimella, Measurement and Modeling of Condensation Heat Transfer Coefficients in Circular Microchannels, Journal of Heat Transfer, 128 (2006) 1050-1059.

[11] S. Garimella, J.D. Killion, and J.W. Coleman, An Experimentally Validated Model for Two-Phase Pressure Drop in the Intermittent Flow Regime for Circular Microchannels, Journal of Fluids Engineering, 124 (2001) 205-214.

[12] L. Friedel, Improved Friction Pressure Drop Correlations for Horizontal and Vertical Two Phase Pipe Flow. European Two Phase Flow Group Meeting. Paper E 2. Ispra, Italy, 1979.

[13] H. Müller-Steinhagen and K. Heck, A simple friction pressure drop correlation for two-phase flow in pipes, Chemical Engineering and Processing: Process Intensification, 20 (1986) 297-308.

[14] A.L. de Souza and M.M. Pimenta, Prediction of pressure drop during horizontal two-phase flow of pure and MIXED refrigerents, Cavitation and Multiphase Flow, ASME., 210 (1995).

[15] L. Sun and K. Mishima, Evaluation analysis of prediction methods for two-phase flow pressure drop in mini-channels, International Journal of Multiphase Flow, 35 (2009) 47-54.

[16] M. Zhang and R.L. Webb, Correlation of two-phase friction for refrigerants in small-diameter tubes, Experimental Thermal and Fluid Science, 25 (2001) 131-139.

[17] S. Garimella, A. Agarwal, and J.D. Killion, Condensation Pressure Drop in Circular Microchannels, Heat Transfer Engineering, 26 (2006) 28-35.

[18] K. Mishima and T. Hibiki, Some characteristics of air-water two-phase flow in small diameter vertical tubes, International Journal of Multiphase Flow, 22 (1996) 703-712.

[19] A. Cavallini, D. Del Col, M. Matkovic, and L. Rossetto, Frictional pressure drop during vapour - liquid flow in minichannels: Modelling and experimental evaluation, International Journal of Heat and Fluid Flow, 30 (2009) 131-139.

[20] S.M. Kim and I. Mudawar, Universal approach to predicting two-phase frictional pressure drop for adiabatic and condensing mini/micro-channel flows, International Journal of Heat and Mass Transfer, 55 (2012) 3246-3261.

CHAPTER 8: Experimental Correlation and Correction Factor

In this chapter the experimental results are correlated to develop two models able to predict heat transfer coefficient and frictional pressure drop. The experimental data used in this task was obtained in the experimental installation built to do this PhD. thesis. Two different adjustments were made. The model for heat transfer coefficient was developed based on a previous existing model developed by Koyama et al. Updated coefficients were proposed to the previous model [1] developed by the author of this PhD thesis to predict frictional pressure drop inside mini-channel tubes in condensation tests.

8.1 TWO-PHASE FLOW HEAT TRANSFER COEFFICIENT MODEL ADJUSTMENT

As mentioned above, Koyama et al. correlation for condensation for heat transfer was derived in terms of Nusselt number. This is expressed as acombination of forced convection condensation and gravity controlled convection condensation terms. In what follows, the empirical constants of this model are optimised considering the new data obtained in the framework on this thesis:

$$Nu = \sqrt{Nu_F^2 + Nu_B^2} \tag{8.1}$$

where

$$Nu = \frac{\alpha D_h}{k} \tag{8.2}$$

The original forced condensation term is expressed as:

$$Nu_F = 0.0112 Pr_l^{1.37} \left(\frac{\phi_g}{X}\right) Re_l^{0.7} \tag{8.3}$$

Here, the two-phase multiplier factor is that of Mishima and Hibiki modified by Koyama et al.:

$$\phi_g = \sqrt{1 + 13.17 \left(\frac{\mu_l}{\mu_g}\right)^{0.17} \left(1 - e^{-0.6\sqrt{Bo}}\right) X + X^2} \tag{8.4}$$

where *Bo* is defined as:

$$Bo = \frac{D^2 g(\rho_l - \rho_g)}{\sigma} \tag{8.5}$$

and the Lockhart-Martinelli parameter as:

$$X = \left(\frac{1-x}{x}\right)^{0.9} \left(\frac{\rho_g}{\rho_l}\right)^{0.5} \left(\frac{\mu_g}{\mu_l}\right)^{0.1} \tag{8.6}$$

The liquid Reynolds number is given by:

$$Re_l = \frac{G(1-x)D}{\mu_l} \tag{8.7}$$

The gravity controlled convection, Nu_B is equal to zero because of horizontal configuration of the tube tested.

The forced condensation terms considered for optimisation is expressed in eq. 8.8.

$$Nu_F = a\, Pr_l^b \left(\frac{\phi_g}{X}\right)^c Re_l^d \tag{8.8}$$

where *a, b, c* and *d* are the constants considered in the process of best fitting.

The new model adjustment is presented in eq. 8.9.

$$Nu_F = 0.05997 Pr_l^{1.2235} \left(\frac{\phi_g}{X}\right)^{0.8121} Re_l^{0.8684} \tag{8.9}$$

Finally, in Fig. 8.1 experimental vs. Predicted HTC data graph is plotted for each refrigerant with the new adjustment. The model adjustment is able to predict the HTC data of R1234yf with a MARD of 11.7 % and MRD of -6.5 %. The MARD value for R134a is 14.7 % and MRD equal to -3.3 %. The model adjustment parameters show better prediction values and lower deviation than others compared with. The graphical results of the present database to this modified method for the horizontal multi-port mini-channel tube can be seen in Fig. 8.1.

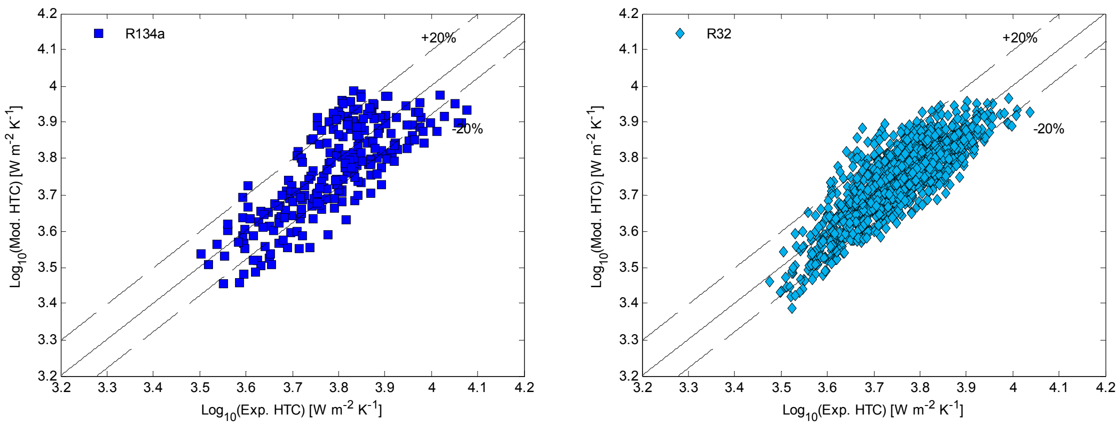

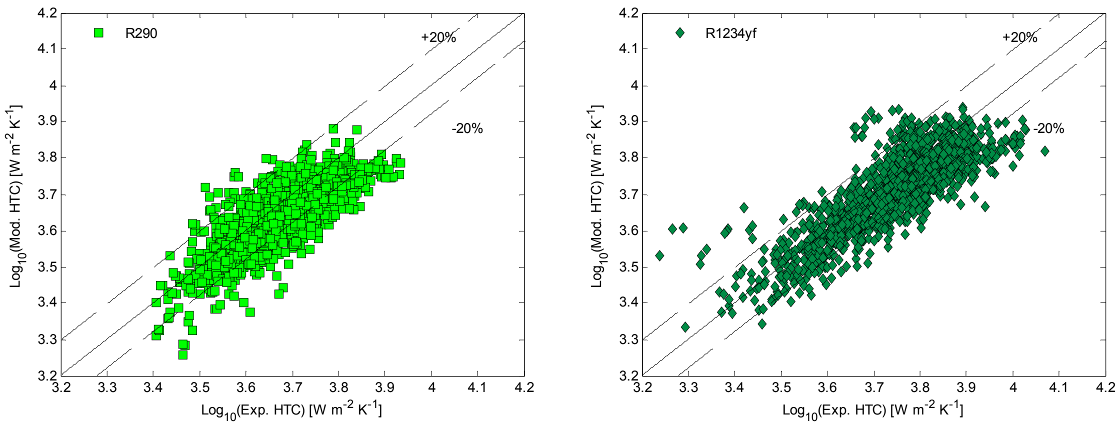

Figure 8.1. Koyama et al. HTC model readjustment.

Table 8.1. HTC MARD and MRD values of HTC model adjustment.

	R134a	R1234yf	R290	R32
MARD	14.7	11.7	12.8	11.1
MRD	-3.3	-6.5	-6.9	-1.93

8.2 TWO-PHASE FRICTIONAL PRESSURE GRADIENT MODEL DEVELOPMENT

A new pressure drop model was also developed during the realisation of this thesis.

As analysed in Chapter 7, all existing correlations show a slight over or under estimation of frictional pressure drop for condensing flows through mini-channels over the whole range of reduced pressures.

A correlation for "C" calculation is proposed. It is based on several dimensionless parameters that take into account the properties of the fluids and the differences between liquid and vapour phases. The ratio between inertial and viscous forces of the liquid phase and Martinelli parameter are also considered.

The correlation chosen is of the form

$$\left(\frac{dp}{dz}\right)_{tp} = \phi_l^2 \left(\frac{dp}{dz}\right)_l \tag{8.10}$$

with liquid flow multiplier defined by:

$$\phi_l^2 = 1 + \frac{C}{X} + \frac{1}{X^2} \tag{8.11}$$

where

$$\left(\frac{dp}{dz}\right)_l = \frac{G^2(1-x)^2}{2D\rho_{liq}} f_l \tag{8.12}$$

$$\left(\frac{dp}{dz}\right)_g = \frac{G^2x^2}{2D\rho_{gas}} f_g \tag{8.13}$$

and $f_l$and $f_g$are the single-phase frictional factors calculated by applying the liquid or gas phase properties and liquid or gas phase mass fluxes respectively to the following equations.

$$f = \frac{64}{Re} \; for \; Re \leq 2000 \tag{8.14}$$

$$f = 0.25\left[log\left(\frac{150.39}{Re^{0.98865}} - \frac{152.66}{Re}\right)\right]^{-2} \; for \; Re \geq 3000 \tag{8.15}$$

$$f = (1.1525Re + 895) \cdot 10^{-5} \; for \; 2000 < Re < 3000 \tag{8.16}$$

The previous equation for the friction factor in turbulent region (Eq. 8.15) was confirmed by Fang et al. [2,3] and Brkic [4] to be the very accurate single-phase friction factor equation flow in smooth tubes.

The equation for the transition zone (Eq. 8.16) was obtained by linear interpolation in Xu and Fang [5].

The Martinelli parameter, X, can be obtained as:

$$X = \sqrt{\left(\frac{dp}{dz}\right)_l \Big/ \left(\frac{dp}{dz}\right)_g} \tag{8.17}$$

Equations (8.14 to 8.16) were used for vapour and liquid phase in order to calculate vapour phase pressure gradient and afterwards the Martinelli parameter.

“C” was adjusted for best fitting experimental data by applying non-linear regression method to all the data points.

$$C = 0.05947\left(\frac{p}{p_{crit}}\right)^{-0.984} {Re_l}^{0.377}\left(\frac{\rho_l}{\rho_g}\right)^{0.0485} X^{-0.368} \tag{8.18}$$

which makes it valid for the experimental tests developed that cover the following ranges of variables

Vapour quality: x $= 0.083 - 0.8936$

Martinelli parameter: X $= 0.05 - 2.53$

Liquid Reynolds number:	$\mathrm{Re_l} = 528 - 8200$
Reduced pressure:	$\mathrm{p_{red}} = 0.183 - 0.603$
Density ratio:	$\rho_l/\rho_g = 7.03 - 32.92$

in a multi-port mini-channel tube with square ports and a hydraulic diameter of 1.16mm.

This equation was developed to minimise the error between the measured values and the prediction model. It takes into account the following terms: the reduced pressure was introduced to consider the variation of fluid properties with saturation temperature. The density ratio evaluates how different liquid and vapour phases are. Liquid Reynolds number considers the relative importance of inertial to viscous forces in the liquid flow condition. Finally the dimensionless Martinelli parameter includes the liquid fraction of the two-phase mixture flow.

Fig. 8.2 depicts the results obtained with new adjustment model. Modelled pressure gradient is plotted in X axis and experimental pressure gradient is plotted in Y axis. The new adjustment predicts the 94.20 % of the data in the range of ±20% and the 86.00 % in the range ±10%.

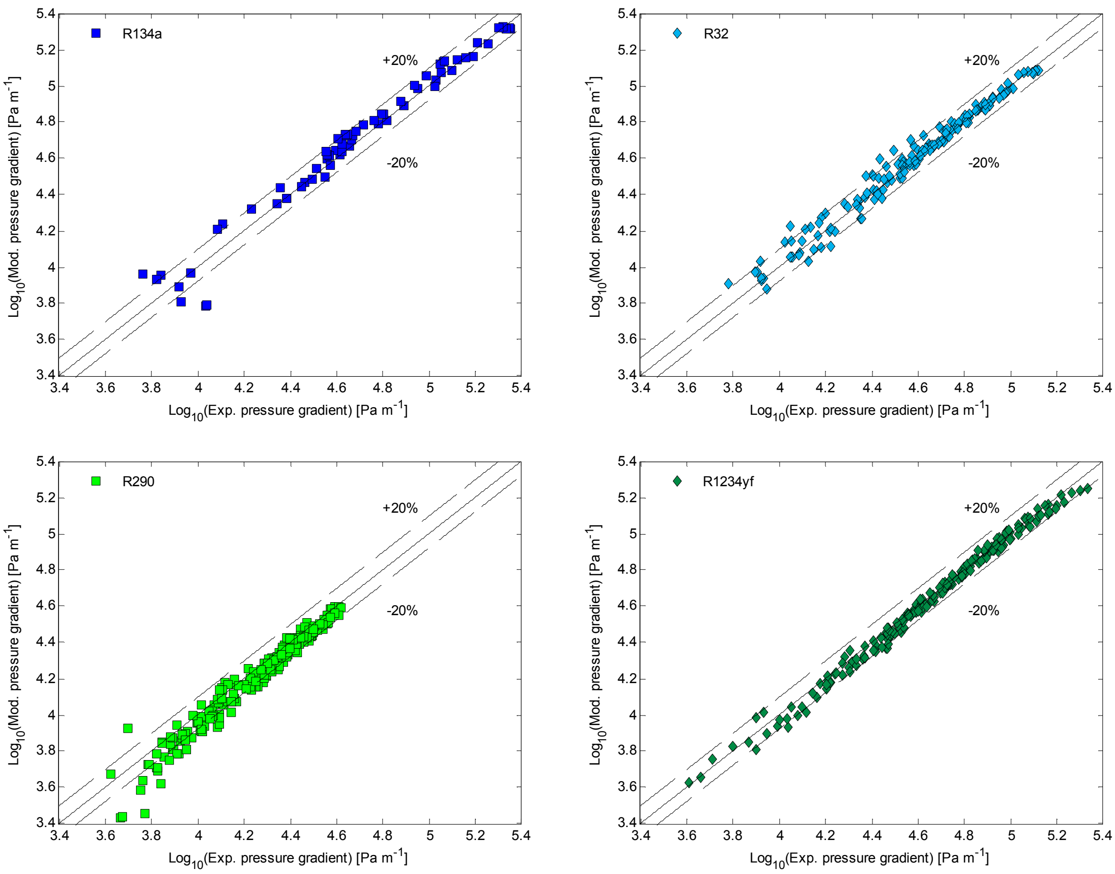

Figure 8.2. New frictional pressure drop model adjustment.

Table 8.2 shows the MARD and MRD values of the model proposed with the different fluids experimentally tested.

Table 8.2. HTC MARD and MRD values of frictional pressure drop model development.

	R134a	R1234yf	R290	R32
MARD	12.3	6.3	9.2	9.4
MRD	2.93	1.2	-3.2	7.1

8.3 CONCLUSIONS

In this chapter two new models have been proposed in order to try to improve the predicting accuracy of the models analysed in the previous chapter. The frictional pressure drop model is an update of the model described in [1] trying to improve its predicting accuracy including a new refrigerant to the database, R290.

Rather than developing an HTC model, a modification of the best predicting model found was made improving its accuracy to our data. Further investigation must be made in order to include new refrigerants and geometries to the frictional pressure drop model and to develop an HTC model.

REFERENCES

[1] A. López-Belchí, F. Illán-Gómez, F. Vera-García, and J.R. García-Cascales, Experimental condensing two-phase frictional pressure drop inside mini-channels. Comparisons and new model development, International Journal of Heat and Mass Transfer, 75 (2014) 581-591.

[2] X. Fang, Y. Xu, and Z. Zhou, New correlations of single-phase friction factor for turbulent pipe flow and evaluation of existing single-phase friction factor correlations, Nuclear Engineering and Design, 241 (2011) 897-902.

[3] X. Fang, H. Zhang, Y. Xu, and X. Su, Evaluation of using two-phase frictional pressure drop correlations for normal gravity to microgravity and reduced gravity, Advances in Space Research, 49 (2012) 351-364.

[4] D. Brkic, New explicit correlations for turbulent flow friction factor, Nuclear Engineering and Design, 241 (2011) 4055-4059.

[5] Y. Xu and X. Fang, A new correlation of two-phase frictional pressure drop for evaporating flow in pipes, International Journal of Refrigeration, 35 (2012) 2039-2050.

CHAPTER 9: Conclusions and Future Work

9.1 CONCLUSIONS

At present days the industry is manufacturing more equipment with multiport mini-channel tubes but using general correlations developed mostly with R134a to predict HTC and pressure gradient. The numerical models used in commercial software such as IMSTArt or EVAP-COND are highly dependent of the correlations programmed. Only a few publications were found dealing with natural flammable refrigerants such as R290 and R32. According to the state of the art presented, no publication of R290 or R32 was found in mini-channels multiport tubes, the vast majority of experimental investigation was made with R134a.

The author of this PhD thesis, aware of that, has measured experimentally two-phase condensing flows within a mini-channel multi-port tube with several fluids. These fluids were R134a firstly used to validate the system measurement; R1234yf, a recently developed refrigerant and potential substitute of R134a; R32, a medium Global Warming Potential (GWP) flammable refrigerant considered as potential substitute of R410A, was also experimentally tested. Finally, R290 was tested in the experimental installation. This latter fluid is a natural hydrocarbon with almost null GWP. This latter fluid was experimentally measured because its use can be widely extended in commercial systems due to the charge reduction obtained with compact systems using mini-channels.

Several condensation experiments have been carried out in a horizontal mini-channel multi-port tube with an inner hydraulic diameter of 1.16 mm at mass velocities ranging from 150 to 945 kg $m^{-2}s^{-1}$ and saturation temperatures of 30, 35, 40, 45 and 50 °C using the previously mentioned fluids. Experimental measurements of two-phase flow pressure gradient and heat transfer coefficient were recorded during the experimental campaign.

Regarding to what exposed in Chapter 4, it is primal to measure external tube wall temperature to be able to calculate refrigerant heat transfer coefficient. In that way, with local heat flux and wall temperatures, local heat transfer coefficients can be calculated along the test section. Assuming uniform heat flux in condensation test is not realistic because as the refrigerant condensates, the heat transfer coefficient of the fluid vary and so water heat transfer coefficient vary too.

The uncertainty of the measurements of interest such as HTC and pressure gradient is a bit higher because these variables are derived from multiple direct measured variables; the mathematical calculation process increases the combined uncertainty of them. Upgrading sensor elements with higher accuracies do not reduce final uncertainties significantly. The highest HTC uncertainty percentage comes from the uncertainty in the refrigerant to wall temperature difference measurement.

Concerning to experimental results, as R1234yf is a potential substitute of R134a, the fluid characteristics of both fluids are quite similar and these similarities allow comparing both fluid measurements directly. R410A should be compared with R32 but no experimental measurements of R410A in mini-channels have been already taken. R290 is a potential substitute of R22 but, in this case, there are no experimental measurements of R22 in multi-port mini-channel tubes in the specialised literature.

R134a, R1234yf and R32 densities are quite higher than R290 density. Since in a positive displacement pump the mass velocity is directly related to the fluid density and this parameter is substantially lower in the case of R290, mass velocities experimentally tested in the case of R134a, R1234yf and R32 are noticeably higher than in the case of R290. Only one value of mass velocity of 350 kg $m^{-2}s^{-1}$ was experimentally compared for all the four fluids. This value corresponds with the higher mass velocity tested for R290 and the lowest value tested for the rest of fluids. Therefore, the comparison of all fluids was made at this value of mass velocity.

According to what recorded at 350 kg $m^{-2}s^{-1}$, the heat transfer coefficient of all fluids is similar but there are relatively high differences with respect to frictional pressure gradient values. Regarding to frictional pressure gradient, the worst refrigerant is R290, followed by R134a, R1234yf and finally R32. This behaviour is completely explained by looking at the density and viscosity values of the fluids and consequently to Reynolds number. Higher Reynolds number lead to higher friction factors and frictional pressure gradients. The comparison of experimental measurements of R290 at mass velocities higher than 350 kg $m^{-2}s^{-1}$ is impossible due to the limitation of the installation.

For all the fluids tested, frictional pressure gradient values increase with increasing values of mass velocity, vapour quality and decreasing values of saturation temperature.

Since R32, R134a and R1234yf have similar density values, all the three fluids have been tested under a similar mass velocity range. R1234yf is the substitute of R134a in mobile systems, so they have been directly compared. According to the results obtained, R1234yf performs slightly better than R134a, since the pressure gradient is by 5-7 % lower in the whole range of mass velocities tested. These differences are explained by the differences of density and viscosity. Although R32 is not a substitute of R134a, the experimental measurements of R410A have not already been developed, so R32 results have been compared to R134a as reference fluid. As shown in previous Chapters, frictional pressure gradient of R32 is lower than that obtained for R134a and even lower than for R1234yf.

About heat transfer coefficient, R134a, R1234yf and R32 were compared at similar conditions under some restrictions due to uncertainty of measurements. Everything points that R32 has the highest values of HTC followed by R134a and R1234yf. This behaviour may be explained by the differences in liquid thermal conductivity between these three fluids. HTC differences between R134a and R1234yf go from 5 % at low mass flux and vapour quality values up to 25% at high values of both variables. A similar analysis is made with R290 at the mass velocity value of 350 kg $m^{-2}s^{-1}$; under these conditions R290 HTC is similar to R32 HTC. Not high differences were recorded due to the sensitive variation of HTC at low values of mass velocity.

The heat transfer coefficient behaviour recorded is similar to the theoretically expected. HTC increase with increasing mass velocity and vapour quality values and decreasing values of saturation pressure

Since the flow pattern in mini-channels is almost annular or intermittent, the liquid film around the gas core in the mini-channel increases the heat transfer in comparison with other flow patterns. So, higher liquid conductivities lead to higher HTC values in annular flows.

Regarding to what exposed in Chapter 7, most of the models developed for macro-channels fail predicting heat transfer coefficient in mini-channel tubes with deviations higher than 20 % in most cases. The models for macro-channels used to predict frictional pressure gradient in mini-channels perform better than the macro-channel models used for heat transfer coefficient prediction. Some classical models do not fail excessively predicting experimental measurements of pressure drop.

About the models specifically derived to be used in mini-channels, their ability to predict fluid behaviour depends on the process analysed. On one hand, these models usually capture the heat transfer coefficient correctly but some of them fail with the predictions of some very different fluids such as R32 and R290 compared with R134a. These fluids are pretty different to the most widely used refrigerant, R134a, and since most of the models for mini-channels were developed for this fluid, the very different fluid properties may make these models fail. R1234yf fluid properties are quite similar to R134a so the models predictions are similar in both cases. On the other hand, most of the models developed for mini-channels that consider fluid properties are able to correctly predict the experimental values of frictional pressure drop.

The best predicting models for the experimental data presented in this PhD. thesis are Koyama et al. for heat transfer coefficient and Sun and Mishima for frictional pressure drop.

Two new models have been proposed to predict frictional pressure drop and heat transfer coefficient. The frictional pressure drop model is an update of a previously developed model by the author of this PhD. thesis and co-workers. The update presented increases the database and includes a new refrigerant, R290.

Rather than developing a new HTC model, a modification of the best predicting model found was made improving its accuracy to our data. Further investigation must be made in order to include new refrigerants and geometries to the frictional pressure drop model and to develop an HTC model.

An important result of the effort made during this PhD can be observed as the publications and congress to which different communications were sent and accepted [1-8] and some of them under review process [9].

9.2 FUTURE WORK

As future work several recommendations must be made to continue researching in this area. First of all, refrigerants such as R410A and L41, Honeywell substitute for R410A should be experimentally tested and compared with the already tested R32. The comparison of L41 and R32 should be an interesting comparison because R32 is another potential substitute of R410A. Secondly, different tube geometries must be experimentally tested with the refrigerants already tested in this PhD thesis and the recommended L41 or R410A.

Further research must be done in that field because only with the effort of the whole community of researching groups and companies, the humanity can lead to a greener future with lower energy consumption systems and environmentally neutral to the ozone layer.

REFERENCES

[1] A. Lopez-Belchi, F. Vera-García, and J.R. Garcia-Cascales, Single and two-phase pressure drop in mini-channels using R134a as working fluid., *23rd IIR International Congress of Refrigeration. Refrigeration for Sustainable Developement. Prague. Czeck Republic.,* 2011.

[2] F. Vera-Garcia, J.R. Garcia-Cascales, A. Lopez-Belchi, and F.A. Ramirez-Rivera, Proceso Para La Obtencción De Los Coeficientes De Trasmisión De Calor Y Pérdida De Carga En Procesos De Evaporación Dentro De Tubos Multipuerto Con Minicanales. Conference Proceeding. VII Congreso Nacional de Ingeniería Termodinámica. Bilbao. Spain. 2011.

[3] A. Lopez-Belchi, F. Vera-Garcia, J.R. Garcia-Cascales, and D. Del Col, Two-phase pressure drop with non-uniform distribution, *3rd Refrigerant Charge Reduction In Refrigerant systems. Valencia. Spain.,* 2012.

[4] F. Vera-Garcia, J.R. Garcia-Cascales, A. Lopez-Belchi, and F.A. Ramirez-Rivera, Caída de presión en minicanales operando con R134a en monofásico y procesos de condensación. Conference Proceeding. VI Congreso Ibérico y V Congreso Iberoamericano de Ciencias y Técnicas del Frío. Madrid. Spain. 2012.

[5] A. Lopez-Belchi, F. Vera-Garcia, and J.R. Garcia-Cascales, Sistema de control de una instalación experimental de estudio de la caída de presión y del coeficiente de transferencia de calor en el interior de minicanales, 2012.

[6] A. Lopez-Belchi and F.A. Ramirez-Rivera, Transmisión de calor y caída de presión en procesos de condensación en minicanales, II Encuentro de máquinas y motores térmicos del sureste. Murcia. Spain. 2012.

[7] A. Lopez-Belchi, F.A. Ramirez-Rivera, J.R. Garcia-Cascales, F. Vera-Garcia, F. Illan-Gomez, and J.M. Cano-Izquierdo, Implementación de una red neuronal para la predicción de la caída de presión en minicanales, *VIII Congreso Nacional de Ingeniería Termodinámica,* Universidad de Burgos, 2013, pp. 607-614.

[8] A. López-Belchí, F. Illán-Gómez, F. Vera-García, and J.R. García-Cascales, Experimental condensing two-phase frictional pressure drop inside mini-channels. Comparisons and new model development, International Journal of Heat and Mass Transfer, 75 (2014) 581-591.

[9] Non-uniform condensation of refrigerant in mini-channel multiport tubes: two-phase pressure drop and HTC. A. Lopez-Belchi, F. Vera-Garcia, J.R. Garcia-Cascales. Applied Thermal Engineering. Article sent, under review process. ATE-2014-5958.

REFERENCES

- Abdelall, F.F., Hahn, G., Ghiaasiaan, S.M., Abdel-Khalik, S.I., Jeter, S.S., Yoda, M., and Sadowski, D.L., 2005. Pressure drop caused by abrupt flow area changes in small channels. Experimental Thermal and Fluid Science 29, 425-434. **Cited in Chapter 5 as [11].**
- Agarwal, A. and Garimella, S., 2008. Modeling of Pressure Drop During Condensation in Circular and Noncircular Microchannels. Journal of Fluids Engineering 131, 011302. **Cited in Chapter 2 as [101] and Chapter 3 as [39].**
- Agarwal, A., Bandhauer, T.M., and Garimella, S., 2010. Measurement and modeling of condensation heat transfer in non-circular microchannels. International Journal of Refrigeration 33, 1169-1179. **Cited in Chapter 2 as [38] and Chapter 4 as [3].**
- Agostini, B., Watel, B., Bontemps, A., and Thonon, B., 2002. Friction factor and heat transfer coefficient of R134a liquid flow in mini-channels. Applied Thermal Engineering 22, 1821-1834. **Cited in Chapter 2 as [71].**
- Ahmed, W.H., Ching, C.Y., and Shoukri, M., 2007. Pressure recovery of two-phase flow across sudden expansions. International Journal of Multiphase Flow 33, 575-594. **Cited in Chapter 5 as [15].**
- Akbar. M.K, Plummer. D.A, Ghiaasiaan. S.M, On gas–liquid two-phase flow regimes in microchannels.International Journal of Multiphase Flow, 29 (2003) 855 - 865. **Cited in Chapter 2 as [89].**
- Akers, W. W., Rosson, H. F. Condensation Inside a Horizontal Tube. Chemical Engineering Progress Symposium Series, 50 (1960). 145–149. **Cited in Chapter 3 as [25].**
- Akers, W.W., Deans, H.A., and Crosser, O.K., 1958. Condensing heat transfer within horizontal tubes. Chem.Eng.Progr. 54. **Cited in Chapter 2 as [5] and Chapter 7 as [5].**
- Al-Hajri, E., Shooshtari, A.H., Dessiatoun, S., and Ohadi, M.M., 2013. Performance characterization of R134a and R245fa in a high aspect ratio microchannel condenser. International Journal of Refrigeration 36, 588-600. **Cited in Chapter 2 as [58].**
- Baird, J.R., Fletcher, D.F., and Haynes, B.S., 2003. Local condensation heat transfer rates in fine passages. International Journal of Heat and Mass Transfer 46, 4453-4466. **Cited in Chapter 2 as [19].**
- Bandhauer, T.M., Agarwal, A., and Garimella, S., 2006. Measurement and Modeling of Condensation Heat Transfer Coefficients in Circular Microchannels. Journal of Heat Transfer 128, 1050-1059. **Cited in Chapter 2 as [25], Chapter 3 as [40] and Chapter 7 as [10].**
- Bankoff. S. G. A Variable Density Single-Fluid Model for Two-Phase FlowWith Particular Reference to Steam-Water Flow. *J. Heat Transfer* 82 (1960), 265-272. **Cited in Chapter 2 as [113].**
- Baroczy, C.J., 1966. A systematic correlation for two phase pressure drop. 62 ed., pp. 232-249. **Cited in Chapter 2 as [105] and Chapter 3 as [3].**

- Bohdal, T., Charun, H., and Sikora, M., 2011. Comparative investigations of the condensation of R134a and R404A refrigerants in pipe minichannels. International Journal of Heat and Mass Transfer 54, 1963-1974. **Cited in Chapter 2 as [41].**
- Bohdal, T., Charun, H., and Sikora, M., 2012. Pressure drop during condensation of refrigerants in pipe minichannels. Archives of Thermodynamics 33, 87-106. **Cited in Chapter 2 as [126].**
- Brkic, D., 2011. New explicit correlations for turbulent flow friction factor. Nuclear Engineering and Design 241, 4055-4059. **Cited in Chapter 5 as [5] and Chapter 8 as [4].**
- Cavallini, A., Censi, G., Del Col, D., Doretti, L., Longo, G.A., and Rossetto, L., 2001. Experimental investigation on condensation heat transfer and pressure drop of new HFC refrigerants (R134a, R125, R32, R410A, R236ea) in a horizontal smooth tube. International Journal of Refrigeration 24, 73-87. **Cited in Chapter 2 as [23].**
- Cavallini, A., Censi, G., Del Col, D., Doretti, L., Longo, G.A., Rossetto, L., and Zilio, C., 2003. Condensation inside and outside smooth and enhanced tubes – a review of recent research. International Journal of Refrigeration 26, 373-392. **Cited in Chapter 2 as [22].**
- Cavallini, A., Del Col, D., Doretti, L., Matkovic, M., Rossetto, L., and Zilio, C., 2004. Measurement of pressure gradient during two-phase flow inside multi-port mini-channels. 3rd Int. Symposium on Two-Phase Flow Modelling and Experimentation, Pisa, September 22–24, 2004. **Cited in Chapter 2 as [79], Chapter 3 as [18] and Chapter 7 as [8].**
- Cavallini, A., Del Col, D., Doretti, L., Matkovic, M., Rossetto, L., and Zilio, C., 2005. Two-phase frictional pressure gradient of R236ea, R134a and R410A inside multi-port mini-channels. Experimental Thermal and Fluid Science 29, 861-870. **Cited in Chapter 2 as [20] and Chapter 3 as [14].**
- Cavallini, A., Del Col, D., Doretti, L., Matkovic, M., Rossetto, L., and Zilio, C., 2005. Condensation Heat Transfer and Pressure Gradient Inside Multiport Minichannels. Heat Transfer Engineering, 26, 45-55. **Cited in Chapter 2 as [21], Chapter 3 as [33].**
- Cavallini, A., Del Col, D., Doretti, L., Matkovic, M., Rossetto, L., and Zilio, C., 2005. A model for condensation inside minichannels. ASME Summer Heat Transfer Conference. ASME Summer Heat Transfer Conference. **Cited in Chapter 3 as [35].**
- Cavallini, A., Doretti, L., Matkovic, M., and Rossetto, L., 2005. Update on condensation heat transfer and pressure drop inside minichannels. Heat Transfer Engineering 27, 74-87. **Cited in Chapter 2 as [2] and Chapter 3 as [15].**
- Cavallini, A., Bortolin, S., Del Col, D., Matkovic, M., and Rossetto, L., 2008. Condensation and vaporization of halogenated refrigerants inside a circular minichannel. **Cited in Chapter 2 as [30].**
- Cavallini, A., Del Col, D., Matkovic, M., and Rossetto, L., 2009. Frictional pressure drop during vapour – liquid flow in minichannels: Modelling and experimental evaluation. International Journal of Heat and Fluid Flow 30, 131-139. **Cited in Chapter 2 as [137]. Chapter 3 as [21] and Chapter 7 as [19].**
- Cavallini, A., Bortolin, S., Del Col, D., Matkovic, M., and Rossetto, L., 2011. Condensation Heat Transfer and Pressure Losses of High- and Low-Pressure Refrigerants Flowing in a Single Circular Minichannel. Heat Transfer Engineering 32, 90-98. **Cited in Chapter 2 as [50].**

- Cavallini, A., Del Col, D., Matkovic, M., and Rossetto, L., 2009. Pressure Drop During Two-Phase Flow of R134a and R32 in a Single Minichannel. Journal of Heat Transfer 131, 033107. **Cited in Chapter 2 as [34].**
- Chaobin. D, Hihara. E, In-tube cooling heat transfer of supercritical carbon dioxide. Part 1: Experimental measurement. International Journal of efrigeration, 27, (2004), 736-747. http://dx.doi.org/10.1016/j.ijrefrig.2004.04.018. **Cited in Chapter 2 as [48].**
- Charun, H., 2012. Thermal and flow characteristics of the condensation of R404A refrigerant in pipe minichannels. International Journal of Heat and Mass Transfer 55, 2692-2701. **Cited in Chapter 2 as [54].**
- Chato, J.C. Laminar condensation inside horizontal and inclined tubes, (1960). **Cited in Chapter 7 as [2].**
- Chen, J.J.J., 1986. A further examination of void fraction in annular two-phase flow. International Journal of Heat and Mass Transfer 29, 1760-1763. **Cited in Chapter 3 as [5].**
- Cheng, L., Ribatski, G., and Thome, J.R., 2008. New prediction methods for CO2 evaporation inside tubes: Part II - An updated general flow boiling heat transfer model based on flow patterns. International Journal of Heat and Mass Transfer 51, 125-135. **Cited in Chapter 2 as [96].**
- Cheng, L., Ribatski, G., Moreno Quibén, J.s., and Thome, J.R., 2008. New prediction methods for CO2 evaporation inside tubes: Part I - A two-phase flow pattern map and a flow pattern based phenomenological model for two-phase flow frictional pressure drops. International Journal of Heat and Mass Transfer 51, 111-124. **Cited in Chapter 2 as [33].**
- Chisholm, D., 1967. A theoretical basis for the Lockhart-Martinelli correlation for two-phase flow. International Journal of Heat and Mass Transfer 10, 1767-1778. **Cited in Chapter 2 as [84] and Chapter 3 as [4].**
- Choi, C.W., Yu, D.I., and Kim, M.H, 2011. Adiabatic two-phase flow in rectangular microchannels with different aspect ratios: Part I - Flow pattern, pressure drop and void fraction. International Journal of Heat and Mass Transfer 54, 616-624. **Cited in Chapter 2 as [116].**
- Choi, C. and Kim, M., 2011. Flow pattern based correlations of two-phase pressure drop in rectangular microchannels. International Journal of Heat and Fluid Flow 32, 1199-1207. **Cited in Chapter 2 as [117].**
- Choi, K.I., Pamitran, A.S., Oh, J.T., and Oh, H.K., 2005. Effect on boiling heat transfer of horizontal smooth minichannel for R-410A and R-407C. J Mech Sci Technol 19, 156-163. **Cited in Chapter 2 as [77].**
- Choi, K.I., Pamitran, A.S., Oh, C.Y., and Oh, J.T., 2008. Two-phase pressure drop of R-410A in horizontal smooth minichannels. International Journal of Refrigeration 31, 119-129. **Cited in Chapter 2 as [78].**
- Choi, K.I., Pamitran, A.S., Oh, J.T., and Saito, K., 2009. Pressure drop and heat transfer during two-phase flow vaporization of propane in horizontal smooth minichannels. International Journal of Refrigeration 32, 837-845. **Cited in Chapter 2 as [98].**
- Churchill, S.W., 1977. Friction-Factor Equation Spans All Fluid-Flow Regimes. Chem Eng (New York) 84, 91-92. **Cited in Chapter 3 as [13].**
- Cioncolini, A., Thome, J.R., and Lombardi, C., 2009. Unified macro-to-microscale method to predict two-phase frictional pressure drops of annular flows. International Journal of Multiphase Flow 35, 1138-1148. **Cited in Chapter 2 as [103].**

- Coleman. J. W., Flow Visualization and Pressure Drop for Refrigerant Phase Change and Air-Water Flow in Small Hydraulic Diameter Geometries, Ph.D. thesis, Iowa State University, Ames, Iowa, 2000. **Cited in Chapter 3 as [16].**
- Coleman, J.W. and Krause, P.E., 2004. Two phase pressure losses of R134a in microchannel tube headers with large free flow area ratios. Experimental Thermal and Fluid Science 28, 123-130. **Cited in Chapter 5 as [13].**
- Collier, J.G. and Thome, J.R., 1994. Convective boiling and condensation. Oxford University Press. **Cited in Chapter 5 as [17].**
- Copetti, J.B., Macagnan, M.H., and Zinani, F., 2013. Experimental study on R-600a boiling in 2.6-ámm tube. International Journal of Refrigeration 36, 325-334. **Cited in Chapter 2 as [134].**
- Dalkilic, A.S. and Wongwises, S., 2009. Intensive literature review of condensation inside smooth and enhanced tubes. International Journal of Heat and Mass Transfer 52, 3409-3426. **Cited in Chapter 5 as [8].**
- Dang, C., Haraguchi, N., Yamada, T., Li, M., and Hihara, E., 2013. Effect of lubricating oil on flow boiling heat transfer of carbon dioxide. International Journal of Refrigeration 36, 136-144. **Cited in Chapter 2 as [135].**
- De Souza, A.L. and Pimenta, M.M., 1995. Prediction of pressure drop during horizontal two-phase flow of pure and MIXED refrigerants. Cavitation and Multiphase Flow, ASME. 210. **Cited in Chapter 7 as [14].**
- Del Col, D., Torresin, D., and Cavallini, A., 2010. Heat transfer and pressure drop during condensation of the low GWP refrigerant R1234yf. International Journal of Refrigeration 33, 1307-1318. **Cited in Chapter 2 as [40] and Chapter 6 as [2].**
- Del Col, D., Bortolin, S., Cavallini, A., and Matkovic, M., 2011. Effect of cross sectional shape during condensation in a single square minichannel. International Journal of Heat and Mass Transfer 54, 3909-3920. **Cited in Chapter 2 as [46].**
- Del Col, D., Bisetto, A., Bortolato, M., Torresin, D., and Rossetto, L., 2013. Experiments and updated model for two phase frictional pressure drop inside minichannels. International Journal of Heat and Mass Transfer 67, 326-337. **Cited in Chapter 2 as [136].**
- Derby, M., Lee, H.J., Peles, Y., and Jensen, M.K., 2012. Condensation heat transfer in square, triangular, and semi-circular mini-channels. International Journal of Heat and Mass Transfer 55, 187-197. **Cited in Chapter 2 as [53].**
- Dittus. P. W., Boelter. L. M. K. Univ. Calif. Pub. Eng., Vol. 2, No. 13, pp. 443-461 (1930), reprinted in Int. Comm. Heat Mass Transfer, Vol. 12, pp. 3-22 (1985). **Cited in Chapter 3 as [29].**
- Dobson, M.K. and Chato, J.C., 1998. Condensation in smooth horizontal tubes. Journal of Heat Transfer 120, 193-213. **Cited in Chapter 2 as [16], Chapter 3 as [24] and Chapter 7 as [1].**
- Donaldson, A.A., Kirpalani, D.M., and Macchi, A., 2011. Single and two-phase pressure drop in serpentine mini-channels. Chemical Engineering and Processing: Process Intensification 50, 877-884. **Cited in Chapter 2 as [114].**
- Ducoulombier, M., Colasson, S.p., Bonjour, J., and Haberschill, P., 2011. Carbon dioxide flow boiling in a single microchannel – Part I: Pressure drops. Experimental Thermal and Fluid Science 35, 581-596. **Cited in Chapter 2 as [111].**
- English, N.J. and Kandlikar, S.G., 2006. An Experimental Investigation into the Effect of Surfactants on Air-Water Two-Phase Flow in Minichannels. Heat Transfer Engineering 27, 99-109. **Cited in Chapter 2 as [3].**

- Fang, X., Xu, Y., and Zhou, Z., 2011. New correlations of single-phase friction factor for turbulent pipe flow and evaluation of existing single-phase friction factor correlations. Nuclear Engineering and Design 241, 897-902. **Cited in Chapter 2 as [120], Chapter 5 as [3] and Chapter 8 as [2].**
- Fang, X., Zhang, H., Xu, Y., and Su, X., 2012. Evaluation of using two-phase frictional pressure drop correlations for normal gravity to microgravity and reduced gravity. Advances in Space Research 49, 351-364. **Cited in Chapter 5 as [4], Chapter 8 as [3].**
- Field, B.S. and Hrnjak, P., 2007. Adiabatic Two-Phase Pressure Drop of Refrigerants in Small Channels. Heat Transfer Engineering 28, 704-712. **Cited in Chapter 2 as [88].**
- Foroughi, H. and Kawaji, M., 2011. Viscous oil–water flows in a microchannel initially saturated with oil: Flow patterns and pressure drop characteristics. International Journal of Multiphase Flow 37, 1147-1155. **Cited in Chapter 2 as [118].**
- Friedel, L., 1979. Improved Friction Pressure Drop Correlations for Horizontal and Vertical Two Phase Pipe Flow. European Two Phase Flow Group Meeting. Paper E 2. Ispra, Italy. **Cited in Chapter 2 as [42], Chapter 3 as [7] and Chapter 7 as [12].**
- Garcia-Cascales, J.R., Vera-Garcia, F., Gonzalvez-Macia, J., Corberan-Salvador, J.M., Johnson, M.W., and Kohler, G.T., 2010. Compact heat exchangers modeling: Condensation. International Journal of Refrigeration 33, 135-147. **Cited in Chapter 2 as [39].**
- Garimella, S., Killion, J.D., and Coleman, J.W., 2001. An Experimentally Validated Model for Two-Phase Pressure Drop in the Intermittent Flow Regime for Circular Microchannels. Journal of Fluids Engineering 124, 205-214. **Cited in Chapter 2 as [74], Chapter 3 as [38] and Chapter 7 as [11].**
- Garimella, S., 2004. Condensation Flow Mechanisms in Microchannels: Basis for Pressure Drop and Heat Transfer Models. Heat Transfer Engineering 25, 104-116. **Cited in Chapter 2 as [75] and Chapter 3 as [37].**
- Garimella, S., 2004. Condensation flow mechanisms, pressure drop and heat transfer in microchannels. Microscale Heat Transfer 273-290. **Cited in Chapter 2 as [43]**
- Garimella, S., Agarwal, A., and Killion, 2006. Condensation Pressure Drop in Circular Microchannels. Heat Transfer Engineering 26, 28-35. **Cited in Chapter 2 as [26], Chapter 3 as [11] and Chapter 7 as [17].**
- Goss, J. and Passos, J.C., 2013. Heat transfer during the condensation of R134a inside eight parallel microchannels. International Journal of Heat and Mass Transfer 59, 9-19. **Cited in Chapter 2 as [56].**
- Grönnerud, R., 1972. "Investigation in Liquid Holdup, Flow Resistance and Heat Transfer in Circular Type Evaporators, Part IV: Two-Phase Resistance in Boiling Refrigerants", Bulletin de l'Inst.du Froid, Annexe 1972-1. **Cited in Chapter 2 as [93].**
- Hamdar, M., Zoughaib, A., and Clodic, D., 2010. Flow boiling heat transfer and pressure drop of pure HFC-152a in a horizontal mini-channel. International Journal of Refrigeration 33, 566-577. **Cited in Chapter 2 as [106].**
- Haraguchi, H., Koyama, S., and Fujii, T., 1994. Condensation of refrigerants HCFC 22, HFC 134a and HCFC 123 in a horizontal smooth tube. Trans.JSME (B) 60, 245-252. **Cited in Chapter 2 as [17], Chapter 3 as [24] and Chapter 7 as [3].**

- Harirchian, T. and Garimella, S.V., 2012. Flow regime-based modeling of heat transfer and pressure drop in microchannel flow boiling. International Journal of Heat and Mass Transfer 55, 1246-1260. **Cited in Chapter 2 as [129].**
- Heo, J., Park, H., and Yun, R., 2013. Condensation heat transfer and pressure drop characteristics of CO2 in a microchannel. International Journal of Refrigeration 36, 1657-1668. **Cited in Chapter 2 as [59].**
- Heo, J., Park, H., and Yun, R., 2013. Comparison of condensation heat transfer and pressure drop of CO2 in rectangular microchannels. International Journal of Heat and Mass Transfer 65, 719-726. **Cited in Chapter 2 as [60].**
- Hewitt, G.F. and Hall-Taylor, N.S., 1970. Annular two-phase flow Pergamon. **Cited in Chapter 3 as [20].**
- Hewitt, G.F., Shires, G.L., and Bott, T.R., 1994. Process heat transfer 113 ed. CRC press London. **Cited in Chapter 5 as [12].**
- Jang, Y., Park, C., Lee, Y., and Kim, Y., 2008. Flow boiling heat transfer coefficients and pressure drops of FC-72 in small channel heat sinks. International Journal of Refrigeration 31, 1033-1041. **Cited in Chapter 2 as [99].**
- Jassim, E.W., Newell, T.A., and Chato, J.C., 2006. Probabilistic Flow Regime Map Modeling of Two-Phase Flow. Air Conditioning and Refrigeration Center. University of Illinois at Urbana-Champaign. **Cited in Chapter 2 as [86].**
- Jige, D., Koyama, S., and Mino, M., 2011. An experimental study on condensation of pure refrigerants in horizontal rectangular mini-channels. **Cited in Chapter 2 as [52].**
- Ju Lee, H. and Yong Lee, S., 2001. Pressure drop correlations for two-phase flow within horizontal rectangular channels with small heights. International Journal of Multiphase Flow 27, 783-796. **Cited in Chapter 2 as [68] and Chapter 3 as [12].**
- Jung, D., Rademacher. R., Prediction of pressure drop during horizontal, annular flow boiling of pure and mixed refrigerants. International Journal of Heat and Mass Transfer 32 (1989) 24435-2446. **Cited in Chapter 2 as [94].**
- Kaew-On, J. and Wongwises, S., 2012. New proposed two-phase multiplier and evaporation heat transfer coefficient correlations for R134a flowing at low mass flux in a multiport minichannel. International Communications in Heat and Mass Transfer 39, 853-860. **Cited in Chapter 2 as [122].**
- Kawahara, A., Chung, P.M.Y., and Kawaji, M., 2002. Investigation of two-phase flow pattern, void fraction and pressure drop in a microchannel. International Journal of Multiphase Flow 28, 1411-1435. **Cited in Chapter 2 as [72].**
- Kays, W.M. and London, A.L., 1964. Compact heat exchangers. 2nd Edition. **Cited in Chapter 1 as [2].**
- Kays, W.M. and London, A.L., 1984. Compact heat exchangers. 3rd Edition. **Cited in Chapter 5 as [10].**
- Kim, M.H., Shin, J.S., Huh, C., Kim, T.J., and Seo, K.W., 2003. A study of condensation heat transfer in a single mini-tube and a review of Korean micro- and mini-channel studies. First International Conference on Microchannels and Minichannels. **Cited in Chapter 2 as [13].**
- Kim, S.M. and Mudawar, I., 2012. Universal approach to predicting two-phase frictional pressure drop for adiabatic and condensing mini/micro-channel flows. International Journal of Heat and Mass Transfer 55, 3246-3261. **Cited in Chapter 2 as [124], Chapter 3 as [23] and Chapter 7 as [20].**
- Kim, S.M. and Mudawar, I., 2012. Consolidated method to predicting pressure drop and heat transfer coefficient for both subcooled and saturated flow boiling in micro-

channel heat sinks. International Journal of Heat and Mass Transfer 55, 3720-3731. **Cited in Chapter 2 as [128].**

- Kim, S.M., Kim, J., and Mudawar, I., 2012. Flow condensation in parallel micro-channels: Part 1: Experimental results and assessment of pressure drop correlations. International Journal of Heat and Mass Transfer 55, 971-983. **Cited in Chapter 2 as [51].**
- Koyama, S., Kuwahara, K., and Nakashita, K., 2003. Condensation of refrigerant in a multi-port channel. First International Conference on Microchannels and Minichannels, First International Conference on Microchannels and Minichannels. Rochester. New York. USA. ed., pp. 193-205. **Cited in Chapter 2 as [14] and Chapter 3 as [32].**
- Koyama, S., Kuwahara, K., Nakashita, K., and Yamamoto, K., 2003. An experimental study on condensation of refrigerant R134a in a multi-port extruded tube. International Journal of Refrigeration 26, 425-432. **Cited in Chapter 2 as [15], Chapter 3 as [31], Chapter 4 as [2] and Chapter 7 as [6].**
- Kreutzer. M.T., Kapteijn. F., Moulijn. J. A., Kleijn C. R., Heiszwolf. J. J., Inertial and interfacial effects on pressure drop of Taylor flow in capillaries. AIChE Journal51 (2005), 2428-2440. **Cited in Chapter 2 as [115].**
- Lazarek, G.M. and Black, S.H., 1982. Evaporative heat transfer, pressure drop and critical heat flux in a small vertical tube with R-113. International Journal of Heat and Mass Transfer 25, 945-960. **Cited in Chapter 2 as [64].**
- Lemmon, E.W., Huber, M.L., and McLinden, M.O., 1999. NIST Standard ReferenceDatabase 23: Reference Fluid Thermodynamic and Transport Properties-REFPROP. 6.0. **Cited in Chapter 5 as [1].**
- Li, M., Dang, C., and Hihara, E., 2013. Flow boiling heat transfer of HFO1234yf and HFC32 refrigerant mixtures in a smooth horizontal tube: Part II. Prediction method. International Journal of Heat and Mass Transfer 64, 591-608. **Cited in Chapter 2 as [139].**
- Li, W. and Wu, Z., 2010. A general correlation for adiabatic two-phase pressure drop in micro/mini-channels. International Journal of Heat and Mass Transfer 53, 2732-2739. **Cited in Chapter 2 as [109].**
- Liu, N., Li, J.M., Sun, J., and Wang, H.S., 2013. Heat transfer and pressure drop during condensation of R152a in circular and square microchannels. Experimental Thermal and Fluid Science 47, 60-67. **Cited in Chapter 2 as [61].**
- Liu, Z. and Winterton, R.H.S., 1991. A general correlation for saturated and subcooled flow boiling in tubes and annuli, based on a nucleate pool boiling equation. International Journal of Heat and Mass Transfer 34, 2759-2766. **Cited in Chapter 2 as [131].**
- Lockhart, R.W. and Martinelli, R.C., 1949. Proposed correlation of data for isothermal two-phase, two-component flow in pipes. Chem.Eng.Prog 45, 39-48. **Cited in Chapter 2 as [73] and Chapter 3 as [6].**
- Lombardi. E, Pedrocchi. E, A pressure drop correlation in two-phase flow, Energy Nuclear.MiIan, 19 (1972) 91-99. **Cited in Chapter 2 as [104].**
- López-Belchí, A., Illán-Gómez, F., Vera-García, F., and García-Cascales, J.R., 2014. Experimental condensing two-phase frictional pressure drop inside mini-channels. Comparisons and new model development. International Journal of Heat and Mass Transfer 75, 581-591. **Cited in Chapter 6 as [3], Chapter 8 as [1] and Chapter 9 as [8].**

- Lopez-Belchi. A., Ramirez-Rivera. F.A., Garcia-Cascales. J.R., Vera-Garcia F., Illan-Gomez F., Cano-Izquierdo J.M., Implementación de una red neuronal para la predicción de la caída de presión en minicanales, *VIII Congreso Nacional de Ingeniería Termodinámica,* Universidad de Burgos, 2013, pp. 607-614. **Cited in Chapter 9 as [7].**
- Lopez-Belchi, A., Ramirez-Rivera F., Transmisión de calor y caída de presión en procesos de condensación en minicanales, 2012. II Encuentro de máquinas y motores térmicos del sureste. Murcia. Spain. **Cited in Chapter 9 as [6].**
- Lopez-Belchi, A., Vera-García, F., Garcia-Cascales, J.R., Single and two-phase pressure drop in mini-channels using R134a as working fluid. 23rd IIR International Congress of Refrigeration. Refrigeration for Sustainable Developement. Prague. Czeck Republic. 2011. **Cited in Chapter 9 as [1].**
- Lopez-Belchi. A., Vera-Garcia F., Garcia-Cascales J.R.. Non-uniform condensation of refrigerant in mini-channel multiport tubes: two-phase pressure drop and HTC.. Applied Thermal Engineering. ***Article sent, under review process. ATE-2014-5958.*** **Cited in Chapter 9 as [9].**
- Lopez-Belchi. A., Vera-Garcia. F., Garcia-Cascales, J.R., Sistema de control de una instalación experimental de estudio de la caída de presión y del coeficiente de transferencia de calor en el interior de minicanales, 2012. **Cited in Chapter 9 as [5].**
- Lopez-Belchi, A., Vera-Garcia, F., Garcia-Cascales J.R., Del Col, D., Two-phase pressure drop with non-uniform distribution, *3rd Refrigerant Charge Reduction In Refrigerant systems. Valencia. Spain.,* 2012. **Cited in Chapter 9 as [3].**
- Ma, Y., Ji, X., Wang, D., Fu, T., and Zhu, C., 2010. Measurement and Correlation of Pressure Drop for Gas-Liquid Two-phase Flow in Rectangular Microchannels. Chinese Journal of Chemical Engineering 18, 940-947. **Cited in Chapter 2 as [108].**
- Maqbool, M.H., Palm, B., and Khodabandeh, R., 2013. Investigation of two phase heat transfer and pressure drop of propane in a vertical circular minichannel. Experimental Thermal and Fluid Science 46, 120-130. **Cited in Chapter 2 as [140].**
- Matkovic, M., Cavallini, A., Bortolin, S., Del Col, D., and Rossetto, L., 2008. Heat transfer coefficient during condensation of a high pressure refrigerant inside a circular minichannel. 5th European Thermal-Sciences Conference, The Netherlands, 2008, 5th European Thermal-Sciences Conference, The Netherland ed. **Cited in Chapter 2 as [31].**
- Mercedes Benz España, S.A. 2013. Press release (09/08/2013): Mercedes-Benz considera que su evaluación de riesgos con respecto al uso del nuevo refrigerante R1234yf están confirmados. **Cited in Chapter 6 as [1].** http://www.mercedes.es/actualidad/noticias/news3.asp?NoNews=2276.
- Médéric, B., Lavieille, P., and Miscevic, M., 2006. Heat transfer analysis according to condensation flow structures in a minichannel. Experimental Thermal and Fluid Science 30, 785-793. **Cited in Chapter 2 as [29].**
- Mishima, K. and Hibiki, T., 1996. Some characteristics of air-water two-phase flow in small diameter vertical tubes. International Journal of Multiphase Flow 22, 703-712. **Cited in Chapter 2 as [18], Chapter 3 as [9] and Chapter 7 as [18].**
- Moreno-Quibén. J, Thome. .J R., Flow pattern based two-phase frictional pressure drop model for horizontal tubes, Part II: New phenomenological model. International Journal of Heat and Fluid Flow 28 (2007) 1060-1072. **Cited in Chapter 2 as [92].**

- Moser, K.W., Na, B., and Webb, R.L., 1998. A New Equivalent Reynolds Number Model for Condensation in Smooth Tubes. Journal of Heat Transfer 120, 410-417. **Cited in Chapter 2 as [9] and Chapter 3 as [27].**
- Müller-Steinhagen, H. and Heck, K., 1986. A simple friction pressure drop correlation for two-phase flow in pipes. Chemical Engineering and Processing: Process Intensification 20, 297-308. **Cited in Chapter 2 as [80], Chapter 3 as [8] and Chapter 7 as [13].**
- Oh, H.K. and Son, C.H., 2011. Condensation heat transfer characteristics of R-22, R-134a and R-410A in a single circular microtube. Experimental Thermal and Fluid Science 35, 706-716. **Cited in Chapter 2 as [44].**
- Paleev, I.I. and Filippovich, B.S., 1966. Phenomena of liquid transfer in two-phase dispersed annular flow. International Journal of Heat and Mass Transfer 9, 1089-1093. **Cited in Chapter 3 as [19].**
- Pamitran, A.S., Choi, K.I., Oh, J.T., and Oh, H.K., 2008. Two-phase pressure drop during CO2 vaporization in horizontal smooth minichannels. International Journal of Refrigeration 31, 1375-1383. **Cited in Chapter 2 as [97].**
- Pamitran, A.S., Choi, K.I., Oh, J.T., and Hrnjak, P., 2010. Characteristics of two-phase flow pattern transitions and pressure drop of five refrigerants in horizontal circular small tubes. International Journal of Refrigeration 33, 578-588. **Cited in Chapter 2 as [107].**
- Park, C.Y. and Hrnjak, P., 2009. CO_2 flow condensation heat transfer and pressure drop in multi-port microchannels at low temperatures. International Journal of Refrigeration 32, 1129-1139. **Cited in Chapter 2 as [36].**
- Park, C.Y., Jang, Y., Kim, B., and Kim, Y., 2012. Flow boiling heat transfer coefficients and pressure drop of FC-72 in microchannels. International Journal of Multiphase Flow 39, 45-54. **Cited in Chapter 2 as [121].**
- Park, J.E., Vakili-Farahani, F., Consolini, L., and Thome, J.R., 2011. Experimental study on condensation heat transfer in vertical minichannels for new refrigerant R1234ze(E) versus R134a and R236fa. Experimental Thermal and Fluid Science 35, 442-454. **Cited in Chapter 2 as [45] and Chapter 5 as [2].**
- Pehlivan, K., Hassan, I., and Vaillancourt, M., 2006. Experimental study on two-phase flow and pressure drop in millimeter-size channels. Applied Thermal Engineering 26, 1506-1514. **Cited in Chapter 2 as [83].**
- Pettersen, J., Rieberer, R., and Munkejord, S.T., 2000. Heat transfer and pressure drop characteristics of evaporating carbon dioxide in microchannels tubes. **Cited in Chapter 2 as [69].**
- Petukhov. B. S, Heat Transfer and Friction in Turbulent Pipe Flow with Variable Physical Properties. High Temperature Institute. Academy of Science of the USSR. Moscow. USSR. (1970). **Cited in Chapter 2 as [49].**
- Poggi, F., Macchi-Tejeda, H., Leducq, D., and Bontemps, A., 2008. Refrigerant charge in refrigerating systems and strategies of charge reduction. International Journal of Refrigeration 31, 353-370. **Cited in Chapter 1 as [1].**
- Qi, S.L., Zhang, P., Wang, R.Z., and Xu, L.X., 2007. Flow boiling of liquid nitrogen in micro-tubes: Part I – The onset of nucleate boiling, two-phase flow instability and two-phase flow pressure drop. International Journal of Heat and Mass Transfer 50, 4999-5016. **Cited in Chapter 2 as [90].**
- Revellin, R. and Thome, J.R., 2007. Adiabatic two-phase frictional pressure drops in microchannels. Experimental Thermal and Fluid Science 31, 673-685. **Cited in Chapter 2 as [87].**

- Ribatski, G., Wojtan, L., and Thome, J.R., 2006. An analysis of experimental data and prediction methods for two-phase frictional pressure drop and flow boiling heat transfer in micro-scale channels. Experimental Thermal and Fluid Science 31, 1-19. **Cited in Chapter 2 as [85].**
- Rosato, A., Mauro, A.W., Mastrullo, R., and Vanoli, G.P., 2009. Experiments during flow boiling of a R22 drop-in: R422D adiabatic pressure gradients. Energy Conversion and Management 50, 2613-2621. **Cited in Chapter 2 as [91].**
- Saisorn, S. and Wongwises, S., 2008. Flow pattern, void fraction and pressure drop of two-phase airΓÇôwater flow in a horizontal circular micro-channel. Experimental Thermal and Fluid Science 32, 748-760. **Cited in Chapter 2 as [100].**
- Saisorn, S., Kaew-On, J., and Wongwises, S., 2010. Flow pattern and heat transfer characteristics of R-134a refrigerant during flow boiling in a horizontal circular mini-channel. International Journal of Heat and Mass Transfer 53, 4023-4038. **Cited in Chapter 2 as [110].**
- Sakamatapan, K., Kaew-On, J., Dalkilic, A.S., Mahian, O., and Wongwises, S., 2013. Condensation heat transfer characteristics of R-134a flowing inside the multiport minichannels. International Journal of Heat and Mass Transfer 64, 976-985. **Cited in Chapter 2 as [62] and Chapter 4 as [4].**
- Saraceno, L., Celata, G.P., Furrer, M., Mariani, A., and Zummo, G., 2012. Flow boiling heat transfer of refrigerant FC-72 in microchannels. International Journal of Thermal Sciences 53, 35-41. **Cited in Chapter 2 as [130].**
- Schmidt, J. and Friedel, L., 1997. Two-phase pressure drop across sudden contractions in duct areas. International Journal of Multiphase Flow 23, 283-299. **Cited in Chapter 5 as [14].**
- Shah, R.K., 1978. Laminar Flow Forced Convection in Ducts. Advances in Heat Transfer. **Cited in Chapter 2 as [6].**
- Shah. M. M., “An Improved and Extended General Correlation for Heat Transfer during Condensation in Plain Tubes,” HVAC&R Research, 15(2009), pp. 889-913. **Cited in Chapter 2 as [53].**
- Smith, S.L., 1969. Void Fractions in Two-Phase Flow: A correlation Based upon an Equal Velocity Head Model. 184 ed., pp. 647-664. **Cited in Chapter 3 as [2].**
- Son, C.H. and Oh, H.K., 2012. Condensation pressure drop of R22, R134a and R410A in a single circular microtube. Heat Mass Transfer 48, 1437-1450. **Cited in Chapter 2 as [125].**
- Sun, L. and Mishima, K., 2009. Evaluation analysis of prediction methods for two-phase flow pressure drop in mini-channels. International Journal of Multiphase Flow 35, 47-54. **Cited in Chapter 2 as [102], Chapter 3 as [22] and Chapter 7 as [15].**
- Sur, A. and Liu, D., 2012. Adiabatic air/water two-phase flow in circular microchannels. International Journal of Thermal Sciences 53, 18-34. **Cited in Chapter 2 as [123].**
- Taylor, B.N., 2009. Guidelines for Evaluating and Expressing the Uncertainty of NIST Measurement Results. DIANE Publishing. 2009. **Cited in Chapter 5 as [18]**
- Thome, J.R., 1997, Refrigeration Heat Transfer, Course notes, GRETh/CEA, Grenoble, France.VDI, 1994, VDI-Wärmeatlas, Düsseldorf, Germany, VDIVerlag. **Cited in Chapter 2 as [70].**
- Thome, J.R., El Hajal, J., and Cavallini, A., 2003. Condensation in horizontal tubes, part 2: new heat transfer model based on flow regimes. International Journal of Heat and Mass Transfer 46, 3365-3387. **Cited in Chapter 2 as [35].**

- Tong, W., Bergles, A.E., and Jensen, M.K., 1997. Pressure drop with highly subcooled flow boiling in small-diameter tubes. Experimental Thermal and Fluid Science 15, 202-212. **Cited in Chapter 2 as [65].**
- Tran, T.N., Chyu, M.C., Wambsganss, M.W., and France, D.M., 2000. Two-phase pressure drop of refrigerants during flow boiling in small channels: an experimental investigation and correlation development. International Journal of Multiphase Flow 26, 1739-1754. **Cited in Chapter 2 as [67].**
- Traviss, D.P., Rohsenow, W.M., and Baron, A.B., 1973. Forced Convection Condensation in tubes: A heat Transfer Correlation for condenser design. ASHRAE Transactions 79, 157-165. **Cited in Chapter 2 as [27] and Chapter 7 as [3].**
- Trieu Phan, H., Caney, N., Marty, P., Colasson, S.p., and Gavillet, J. 2011. Flow boiling of water in a minichannel: The effects of surface wettability on two-phase pressure drop. Applied Thermal Engineering 31, 1894-1905. **Cited in Chapter 2 as [112].**
- Triplett, K.A., Ghiaasiaan, S.M., Abdel-Khalik, S.I., LeMouel, A., and McCord, B.N., 1999. Gas-liquid two-phase flow in microchannels: Part II: void fraction and pressure drop. International Journal of Multiphase Flow 25, 395-410. **Cited in Chapter 2 as [66].**
- Vakili-Farahani, F., Agostini, B., and Thome, J.R., 2013. Experimental study on flow boiling heat transfer of-ámultiport tubes with R245fa and R1234ze (E). International Journal of Refrigeration 36, 335-352. **Cited in Chapter 2 as [138].**
- Vera-Garcia. F., Garcia-Cascales J.R., Lopez-Belchi A., and F.A. Ramirez-Rivera, Proceso Para La Obtencción De Los Coeficientes De Trasmisión De Calor Y Pérdida De Carga En Procesos De Evaporación Dentro De Tubos Multipuerto Con Minicanales. Conference Proceeding. VII Congreso Nacional de Ingeniería Termodinámica. Bilbao. Spain. 2011. **Cited in Chapter 9 as [2].**
- Vera-Garcia F., Garcia-Cascales J.R., Lopez-Belchi A., Ramirez-Rivera F.A., Caída de presión en minicanales operando con R134a en monofásico y procesos de condensación, 2012. Conference Proceeding. VI Congreso Ibérico y V Congreso Iberoamericano de Ciencias y Técnicas del Frío. Madrid. Spain. **Cited in Chapter 9 as [4].**
- Wang, C.C., 2013. An overview for the heat transfer performance of HFO-1234yf. Renewable and Sustainable Energy Reviews 19, 444-453. **Cited in Chapter 2 as [63].**
- Webb, R.L., Zhang, M., and Narayanamurthy, R., 1998. Condensation heat transfer in small diameter tubes. Heat Transfer, 6 ed., pp. 403-408. **Cited in Chapter 2 as [8], Chapter 3 as [26].**
- Webb, R.L., Kemal, E., 2001. Effect of Hydraulic Diameter on Condensation of R-134A in Flat Extruded Aluminum Tubes. Journal of Enhanced Heat Transfer 8, 77-90. **Cited in Chapter 2 as [10].**
- Webb, R., 1999. Prediction of Condensation and Evaporation in Micro-Fin and Micro-Channel Tubes. in: Kakaç, S., Bergles, A.E., Mayinger, F., and Yüncü, H. (Eds.), Heat Transfer Enhancement of Heat Exchangers, 355 ed. Springer Netherlands, pp. 529-550. ISBN: 978-90-481-5190-5 (Print) 978-94-015-9159-1 (Online). **Cited in Chapter 7 as [7].**
- Wen, M.Y., Ho, C.Y., and Hsieh, J.M., 2006. Condensation heat transfer and pressure drop characteristics of R-290 (propane), R-600 (butane), and a mixture of R-290/R-600 in the serpentine small-tube bank. Applied Thermal Engineering 26, 2045-2053. **Cited in Chapter 2 as [28].**

- Wen, M.Y. and Ho, C.Y., 2009. Condensation heat-transfer and pressure drop characteristics of refrigerant R-290/R-600a oil mixtures in serpentine small-diameter U-tubes. Applied Thermal Engineering 29, 2460-2467. **Cited in Chapter 2 as [37].**
- William Wang, W.W., Radcliff, T.D., and Christensen, R.N., 2002. A condensation heat transfer correlation for millimeter-scale tubing with flow regime transition. Experimental Thermal and Fluid Science 26, 473-485. **Cited in Chapter 2 as [12], Chapter 3 as [28] and Chapter 7 as [9].**
- Winkler, J., Killion, J., Garimella, S., and Fronk, B.M., 2012. Void fractions for condensing refrigerant flow in small channels: Part I literature review. International Journal of Refrigeration 35, 219-245. **Cited in Chapter 5 as [9].**
- Wu, J., Koettig, T., Franke, C., Helmer, D., Eisel, T., Haug, F., and Bremer, J., 2011. Investigation of heat transfer and pressure drop of CO2 two-phase flow in a horizontal minichannel. International Journal of Heat and Mass Transfer 54, 2154-2162. **Cited in Chapter 2 as [119].**
- Xu, Y. and Fang, X., 2012. A new correlation of two-phase frictional pressure drop for evaporating flow in pipes. International Journal of Refrigeration 35, 2039-2050. **Cited in Chapter 2 as [132], Chapter 8 as [5].**
- Xu, Y., Fang, X., Su, X., Zhou, Z., and Chen, W., 2012. Evaluation of frictional pressure drop correlations for two-phase flow in pipes. Nuclear Engineering and Design 253, 86-97. **Cited in Chapter 2 as [127].**
- Xu, Y. and Fang, X., 2013. A new correlation of two-phase frictional pressure drop for condensing flow in pipes. Nuclear Engineering and Design 263, 87-96. **Cited in Chapter 2 as [141] and Chapter 5 as [6].**
- Yan, Y.Y. and Lin, 1999. Condensation heat transfer and pressure drop of refrigerant R-134a in a small pipe. International Journal of Heat and Mass Transfer 42, 697-708. **Cited in Chapter 2 as [11].**
- Yang, C.Y. and Webb, R.L., 1996. Condensation of R-12 in small hydraulic diameter extruded aluminum tubes with and without micro-fins. International Journal of Heat and Mass Transfer 39, 791-800. **Cited in Chapter 2 as [4].**
- Yang, C.Y., Webb, R.L. 1997. A Predictive Model for Condensation in Small Hydraulic Diameter Tubes Having Axial Micro-Fins. Journal of Heat Transfer 119, 776-782. **Cited in Chapter 2 as [7].**
- Yu, W., France, D.M., Wambsganss, M.W., and Hull, J.R., 2002. Two-phase pressure drop, boiling heat transfer, and critical heat flux to water in a small-diameter horizontal tube. International Journal of Multiphase Flow 28, 927-941. **Cited in Chapter 2 as [76].**
- Yue, J., Chen, G., and Yuan, Q., 2004. Pressure drops of single and two-phase flows through T-type microchannel mixers. Chemical Engineering Journal 102, 11-24. **Cited in Chapter 2 as [80].**
- Yun, R., Kim, Y., and Soo Kim, M., 2005. Flow boiling heat transfer of carbon dioxide in horizontal mini tubes. International Journal of Heat and Fluid Flow 26, 801-809. **Cited in Chapter 2 as [81].**
- Zhang. M., A New Equivalent Reynolds Number Model for Vapor shear controlled Condensation inside Smooth and Micro-Fin Tubes. Ph.D. thesis, The Pennsylvania State University, 1998. **Cited in Chapter 3 as [17].**
- Zhang, H.Y., Li, J.M., Liu, N., and Wang, B.X., 2012. Experimental investigation of condensation heat transfer and pressure drop of R22, R410A and R407C in mini-tubes. International Journal of Heat and Mass Transfer 55, 3522-3532. **Cited in Chapter 2 as [55].**

- Zhang, M. and Webb, R.L., 2001. Correlation of two-phase friction for refrigerants in small-diameter tubes. Experimental Thermal and Fluid Science 25, 131-139. **Cited in Chapter 2 as [24], Chapter 3 as [10], Chapter 4 as [1], Chapter 5 as [16] and Chapter 7 as [16].**
- Zhang, Z., Weng, Z.L., Li, T.X., Huang, Z.C., Sun, X.H., He, Z.H., van Es, J., Pauw, A., Laudi, E., and Battiston, R., 2013. CO2 condensation heat transfer coefficient and pressure drop in a mini-channel space condenser. Experimental Thermal and Fluid Science 44, 356-363. **Cited in Chapter 2 as [57].**
- Zhao, C.R., Jiang, P.X., and Zhang, Y.W., 2011. Flow and convection heat transfer characteristics of CO2 mixed with lubricating oil at super-critical pressures in small tube during cooling. International Journal of Refrigeration 34, 29-39. **Cited in Chapter 2 as [47].**
- Zhu, K., Xu, G.Q., Tao, Z., Deng, H.W., Ran, Z.H., and Zhang, C.B., 2013. Flow frictional resistance characteristics of kerosene RP-3 in horizontal circular tube at supercritical pressure. Experimental Thermal and Fluid Science 44, 245-252. **Cited in Chapter 2 as [133].**
- Zivi, S.M., 1964. Estimation of steady-state steam void-fraction by means of the principle of minimum entropy production. Journal of Heat Transfer 86, 247. **Cited in Chapter 3 as [1] and Chapter 5 as [7].**